KEM-11

Quality control for the publication of offline data by KNMI

October 2022

NORSAR

Contents

List of Tables

Project summary

Project leader:

5.1.2.e

Project team:

5.1.2.e

Staatstoezicht op de Mijnen contact person:

5.1.2.e

Project period:

01.01.2021-31.10.2022

Executive summary

The advent of induced seismicity in the Dutch gas fields required the development of a seismic network to enhance the seismic monitoring. Until 2010, borehole and accelerometer stations were run in triggered mode and only gradually changed to continuous mode. Until now, the triggered seismic event data were only available on request. Before publishing this data set, both KNMI (Dost et al., 2022) and NORSAR assessed its completeness and quality. Our findings can be summarised as follows:

1. Completeness of seismic event waveform data:
   (a) Apart from one event (see section 3.3.4 for details), both accelerometer and borehole waveform data are complete.
2. Metadata:
   (a) Accelerometer instrument responses and orientation angles are indicated correctly in the StationXML files. However, the orientation uncertainties as well as instrument response units are missing.
   (b) Apart from few minor elements (see section 3.3.4 for details), the borehole instrument responses and orientation angles are indicated correctly in the StationXML files.
3. Waveform data quality:
   (a) Orientation angles
      i. Although most of KNMI's results for the orientation of accelerometer components could be confirmed, a few are afflicted with large differences, which result from instabilities in the analysis. These uncertainties are not completely reflected by standard deviations stored in the StationXML files.
      ii. Both the orientations of vertical and horizontal components of borehole sensors are consistent with the values reported in the StationXML files. The only exceptions are station FSW1, for which components might be switched, as well as station PPB, for which a polarity flip is reported in Dost et al. (2022) between May 1995 and May 1998, but not included in the StationXML file.
   (b) Amplitudes
      i. No major issues were found concerning amplitude information of accelerometer records.
      ii. Amplitudes seem to be mostly recorded correctly despite occasional malfunctioning of sensors and components that have occurred throughout the recording period. Most of our and KNMI's findings overlap, but we detected a peculiar behaviour at station FSW in addition.
   (c) Timing

i. Since the correction and adaptation of QuakeML files were not part of the project, the cause of a few mismatches between event catalogue information and waveforms is difficult to assess for the accelerometer data. In addition, there is no information available on synchronicity of the AC-63 records (comprising 25% of the records).

ii. Only a few significant timing issues were detected in the borehole data, based on the assumption of one-sample accuracy in the DCF signal trace.

Throughout the report, we provide the interested reader with short summary statements (boxes highlighted in dark blue). In addition, we provide specific warnings on potential pitfalls (boxes highlighted in red), discussion items (boxes highlighted in orange), notes (boxes highlighted in grey) and obspy example code snippets (highlighted in light blue) targeted at future users of the data.

Introduction

The seismic network across the Netherlands developed in several stages. The first large induced earthquake in 1986 in Assen (M_L2.8) triggered the need for a better seismic monitoring of the Netherlands, particularly in the regions in which gas production takes place. Therefore, borehole and accelerometer stations were gradually deployed with the common purpose of complementing the existing network of broadband seismometers. The very first borehole station to be installed was FSW, close to the Groningen field, in 1991. Ten additional borehole stations were established in the period 1995-1998. The setup of accelerometers at the surface started approximately in the same period (10 stations by 1997) and the network was upgraded regularly until 2009 (26 stations). At that time, transferring large amounts of data in real-time was still challenging and constitutes one of the main reasons why operating in triggered mode was preferred. However, from 2010 on, both borehole and accelerometer stations were changed gradually to operate and send data in continuous mode. This replacement process was stretched over several years and was performed slightly later for the accelerometers. The continuous data are publicly available through the KNMI data portal. However, the triggered data were only available on request. For a more detailed description of the KNMI seismic network development over years, we refer the reader to previously published reports and articles on the subject (Dost, 2016; Dost et al., 2017; Dost et al., 2022; NORSAR, 2018).

In the framework of this project, KNMI made those triggered data publicly available. This implies conversion of the data and metadata into suitable formats for download through their web service. Whenever possible, KNMI provides a quality control and assessment of the data. The output of their work was summarised in a report (Dost et al., 2022), which will also be accessible to the public.

NORSAR's role in this project is to ensure that the newly available data and metadata are complete, to review KNMI's quality assurance tests and to perform independent tests. Seismic data quality is of particular importance when it comes to data timing and amplitude measurements. The work was carried out in two phases, firstly on an offline dataset provided to us directly by KNMI and secondly, on the same dataset retrieved through the FDSN web service.

The current report combines findings from both stages and is divided into four parts:

1. Waveform data completeness: Which data are included? Are the data correctly written? Is there any missing information?
2. Station metadata completeness: Is the metadata on instrument response and sensor orientation complete? Are potential changes over time well described and documented?
3. Waveform and metadata validity: How did KNMI quality control data and metadata? What can NORSAR add to their analyses and what are the main conclusions?
4. Online data retrieval and recommendations to KNMI.

Waveform data completeness

In this chapter, we briefly describe the waveform data we received from KNMI before assessing their completeness. We confirmed that the information contained in the miniSEED files is in agreement with the information described in KNMI's report (Dost et al., 2022).

All analyses were carried out using the Obspy python package (Beyreuther et al., 2010), except if specified otherwise.

1.1 Accelerometer waveform data

KNMI initially provided us with **81** miniSEED files containing the accelerometer **triggered** waveform data. The report (Dost et al., 2022) states that the analysis was performed for **82** local events occurring both in the Roswinkel and Groningen fields. The miniSEED files were named after the event origin times, hence we were able to retrieve event information itself from the KNMI FDSN web service and summarise the most important parameters in Table 1.1. The spatial distribution of the events is shown in Fig. 1.1.

TABLE 1.1: List of events recorded on accelerometers. Depth is expressed in km. Events whose ID is coloured in blue are located in the Roswinkel field while those in black are in the Groningen field.

ID	Origin time	Latitude	Longitude	Depth	M_L	ID	Origin time	Latitude	Longitude	Depth	M_L
1	1996-12-06 16:46:48.000	52.83490	7.053200	1.5	1.58	42	2007-01-26 00:20:09.100	53.35183	6.755000	3.0	2.33
2	1996-12-28 18:16:52.900	52.83430	7.043200	2.0	2.74	43	2007-05-14 12:19:24.020	53.33117	6.701667	3.0	1.99
3	1997-01-16 00:12:46.600	52.83500	7.045600	2.0	2.42	44	2007-06-09 20:07:33.630	53.35300	6.746666	3.0	2.07
4	1997-02-19 21:53:50.700	52.83230	7.038400	2.0	3.35	45	2008-05-18 13:23:46.140	53.37533	6.728333	2.8	2.17
5	1997-05-19 15:43:55.200	52.83583	7.053333	2.0	1.25	46	2008-10-30 05:54:29.080	53.33667	6.720000	3.0	3.22
6	1997-06-20 00:45:37.700	52.83133	7.055000	2.0	1.84	47	2008-11-07 16:40:01.270	53.38083	6.735000	3.0	2.16
7	1997-07-09 06:23:11.300	52.83300	7.053333	2.0	1.20	48	2008-12-15 20:41:17.080	53.33600	6.600000	3.0	1.54
8	1997-08-18 04:42:28.770	52.83433	7.050000	2.0	1.57	49	2009-01-01 16:54:46.910	53.36633	6.771667	3.0	1.73
9	1997-08-18 05:17:32.250	52.83417	7.050000	2.0	2.07	50	2009-01-08 01:17:01.760	53.34767	6.716667	3.0	1.66
10	1998-01-28 21:33:02.900	52.83267	7.041667	2.0	2.68	51	2009-01-09 20:16:58.440	53.34117	6.713333	3.0	1.88
11	1998-01-28 22:34:03.400	52.83317	7.036667	2.0	1.98	52	2009-02-01 04:23:24.160	53.35983	6.740000	3.0	2.23
12	1998-07-14 12:12:02.230	52.83250	7.053333	2.0	3.26	53	2009-04-14 21:05:25.880	53.34467	6.680000	3.0	2.62
13	1999-03-12 19:06:42.970	52.83280	7.051500	2.0	1.30	54	2009-05-08 05:23:11.950	53.35383	6.761667	3.0	3.00
14	1999-03-17 23:14:25.460	52.83200	7.051667	2.0	1.50	55	2009-07-05 10:42:46.260	53.30750	6.755000	3.0	1.79
15	1999-05-06 18:13:56.320	52.83567	7.055000	2.0	1.42	56	2009-12-04 04:12:32.140	53.28417	6.743333	3.0	2.34
16	1999-05-14 18:30:20.730	52.83433	7.051667	2.0	1.70	57	2010-02-19 23:12:51.580	53.28767	6.801667	3.0	1.80
17	1999-05-15 19:28:30.360	52.83433	7.051667	2.0	1.38	58	2010-05-03 09:26:16.070	53.38700	6.810000	3.0	2.31
18	1999-12-31 11:00:55.330	52.83517	7.048333	2.0	2.80	59	2010-06-09 19:19:22.460	53.18184	6.775000	3.0	2.02
19	2000-01-07 14:19:06.760	52.83417	7.043334	2.0	1.10	60	2010-08-14 07:43:20.250	53.40283	6.703333	3.0	2.50
20	2000-03-27 10:23:22.030	52.83517	7.045000	2.0	0.80	61	2010-11-15 11:42:45.950	53.34783	6.703333	3.0	1.40
21	2000-10-25 18:10:34.790	52.83183	7.051667	2.3	3.20	62	2011-01-19 19:39:31.660	53.31867	6.645000	3.0	2.43
22	2001-04-28 23:00:15.880	52.83317	7.053333	2.0	2.36	63	2011-03-26 20:45:54.340	53.33484	6.731667	3.0	1.50
23	2002-02-14 17:01:04.740	52.83150	7.035000	2.0	2.07	64	2011-05-12 16:44:29.830	53.19533	6.756667	3.0	1.79
24	2002-10-14 23:45:22.510	52.83400	7.045000	2.0	0.94	65	2011-06-23 09:14:46.290	53.32100	6.775000	3.0	1.71
25	2002-12-24 02:57:22.580	52.83250	7.041667	2.0	1.43	66	2011-06-27 15:48:09.710	53.30283	6.786667	3.0	3.23
26	2003-03-03 20:51:21.890	53.36033	6.661667	3.0	2.17	67	2011-07-29 22:48:33.630	53.33650	6.728333	3.0	1.82
27	2003-09-27 13:57:54.150	53.34783	6.696667	3.0	2.71	68	2011-08-31 06:23:57.160	53.44400	6.686666	3.0	2.54
28	2003-10-11 11:44:08.340	52.83533	7.055000	2.0	1.61	69	2011-09-06 21:48:10.980	53.33750	6.805000	3.0	2.54
29	2003-11-10 00:22:38.030	53.32533	6.690000	3.0	2.99	70	2011-09-25 12:59:01.280	53.36333	6.728333	3.0	1.96
30	2003-11-16 20:04:11.480	53.34367	6.701667	3.0	2.67	71	2011-12-30 06:20:12.690	53.35250	6.656667	3.0	2.17
31	2004-09-06 20:31:20.280	52.83400	7.048333	2.0	1.00	72	2012-05-24 15:52:39.810	53.35900	6.670000	3.0	1.49
32	2006-01-18 08:12:46.650	53.29033	6.765000	3.0	1.49	73	2012-08-15 19:17:36.490	53.35300	6.805000	3.0	2.44
33	2006-02-12 14:36:38.630	53.29683	6.795000	3.0	1.48	74	2012-08-16 20:30:33.280	53.34533	6.671667	3.0	3.60
34	2006-03-21 14:50:33.700	53.30200	6.755000	3.0	2.37	75	2013-01-19 20:10:06.480	53.28483	6.790000	3.0	2.40
35	2006-03-23 03:12:23.910	53.28350	6.778333	3.0	2.24	76	2013-02-07 22:31:58.380	53.37533	6.666667	3.0	2.68
36	2006-03-25 13:54:38.140	52.83417	7.045000	2.0	2.10	77	2013-02-07 23:19:08.970	53.38917	6.666667	3.0	3.23
37	2006-03-25 13:55:51.170	52.83383	7.043334	2.0	1.70	78	2013-02-09 05:26:10.050	53.36633	6.758333	3.0	2.69
38	2006-08-08 05:04:00.050	53.35033	6.696667	3.0	3.47	79	2013-07-02 23:03:55.500	53.29350	6.785000	3.0	3.03
39	2006-08-08 09:49:23.380	53.34950	6.706666	3.0	2.53	80	2013-09-04 01:33:32.170	53.34400	6.771667	3.0	2.77
40	2006-08-26 22:41:18.560	53.34317	6.711667	3.0	2.31	81	2013-10-02 20:24:26.870	53.31683	6.791667	3.0	1.90
41	2006-10-23 13:38:05.840	53.37233	6.738333	3.0	2.27	82	2014-02-13 02:13:14.320	53.35683	6.781667	3.0	3.01

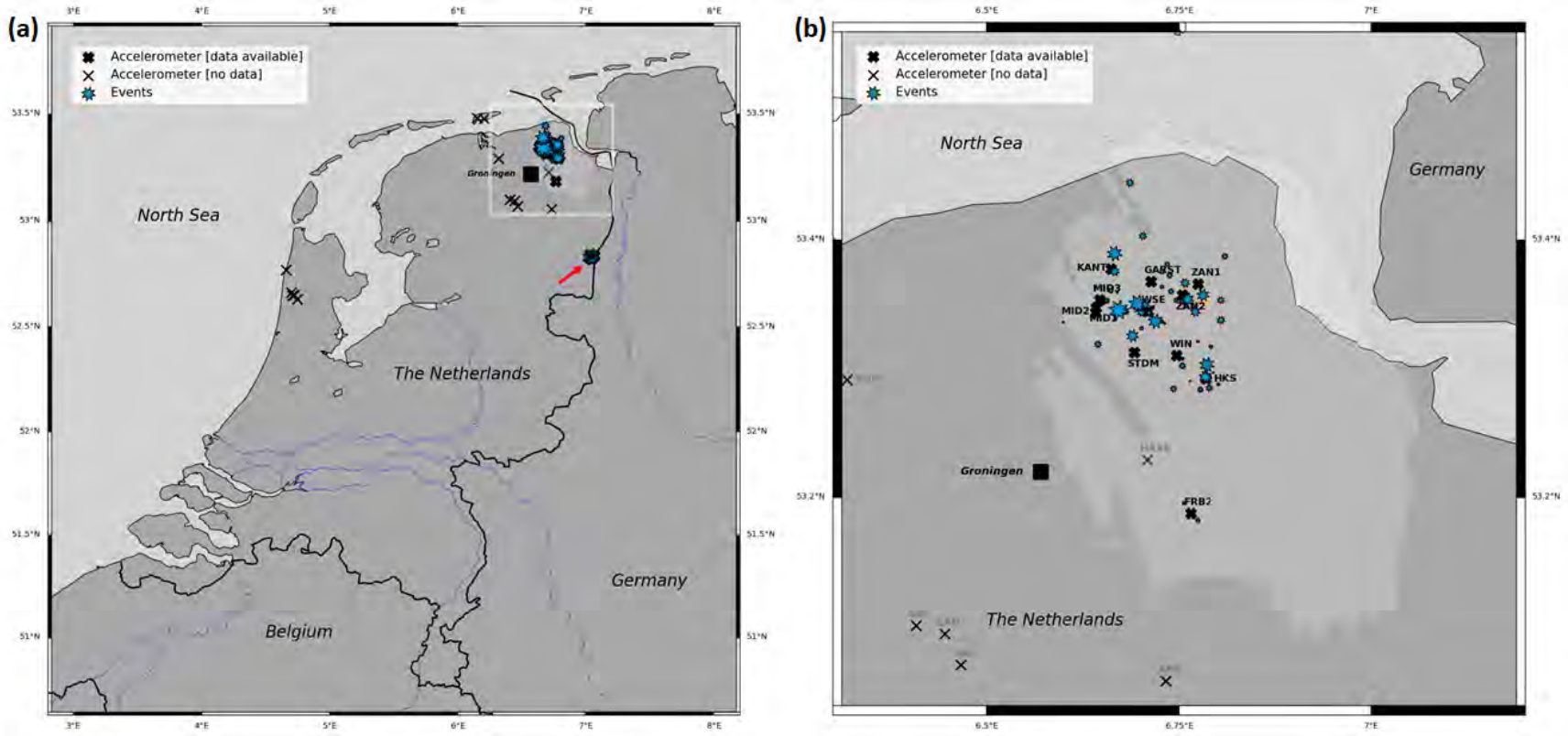

FIGURE 1.1: Maps showing the locations of KNMI accelerometers (black crosses) and available events (blue symbols) within (a) the Netherlands and (b) the Groningen field and surroundings. Note that we distinguish between accelerometers for which event data are available (bold crosses) or unavailable (thin crosses). The latter were not part of this review. The red arrow in (a) indicates the location of the Roswinkel field, where 5 stations were installed.

Note that the difference between the number of files and the number of events (81 vs. 82) is due to the fact that two events (#36 and #37, both occurring on 2006-03-25) were contained in the same file. To ease our work, we split them into two separate files. In addition, please note that since Roswinkel and Groningen fields are at some distance from each other, events in Roswinkel are typically only recorded by ROS* stations. For clarification, we coloured the events in **lighter blue** for Roswinkel and **black** for Groningen.

The histogram in Figure 1.2 shows the distribution of events over years. The numbers on top of each column correspond to the second column of Table 7 in KNMI's report (Dost et al., 2022).

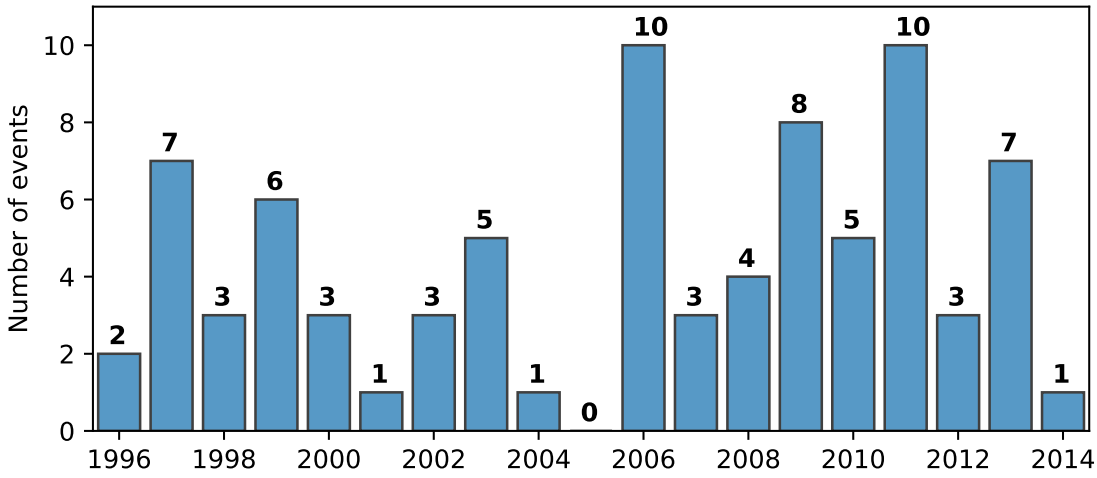

FIGURE 1.2: Histogram of the number of events per year recorded by one or several accelerometers (to be compared with the second column of Table 7 of KNMI's report by Dost et al., 2022).

Similarly, we confirmed that the content of the miniSEED files was in agreement with the report. For that purpose, we summarised the number of records at each station for each year in Table 1.2. This table is directly comparable with Table 7 in KNMI's report (Dost et al., 2022). Figure 1.3 represents the same information visually, providing more details with each cross representing a record for a given event at a given station. Note that the location flag (00, 01, etc.) was also considered, resulting in some stations appearing multiple times. Finally, the grey rectangles in the background show the time periods for which the stations (at a given location) were active. Note that all data are three-component (3C) and labelling was consistent throughout all the files.

All waveform data were recorded with a 200 Hz sampling rate. However, as illustrated in Fig. 1.4, the length of records varies. Although most records last approximately 15 s, in practice, there are 157 different record lengths for a total of 191 records.

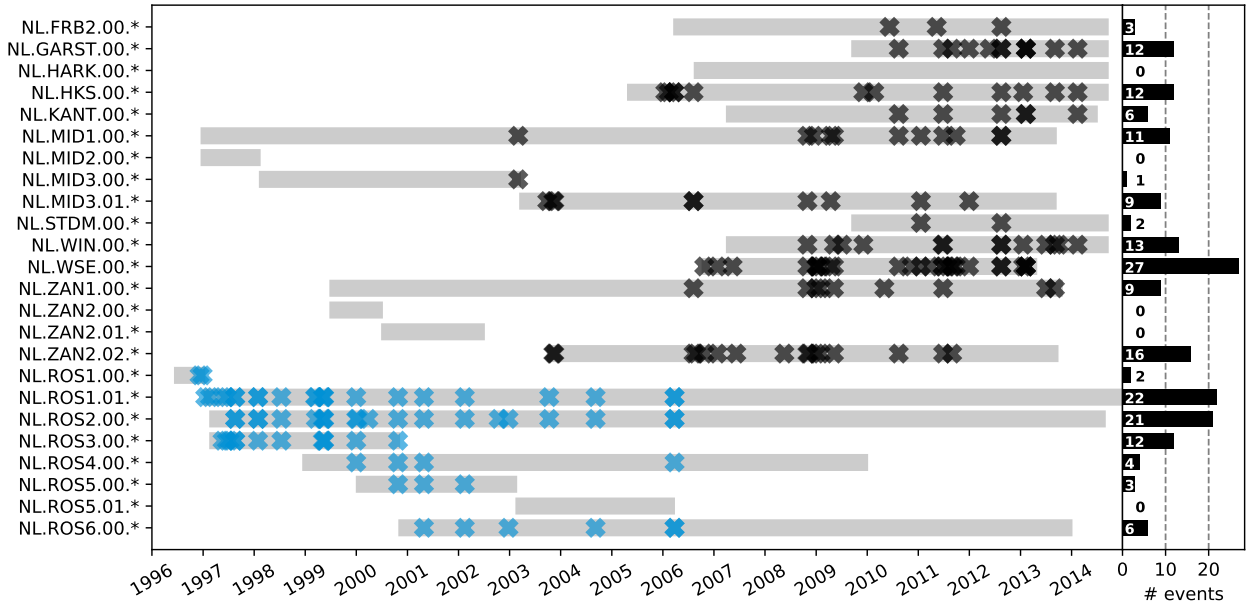

FIGURE 1.3: Overview of accelerometer triggered data. Grey rectangles represent the time span, in which stations were operational. Crosses symbolise events for which waveform data are available (blue: events outside of the Groningen field; black: within the field). The histogram on the right summarises the number of events recorded at each station (cp. to Dost et al., 2022). Note that we distinguished records by their full location, i.e. stations MID3, ROS1, ROS5 and ZAN2 have multiple entries.

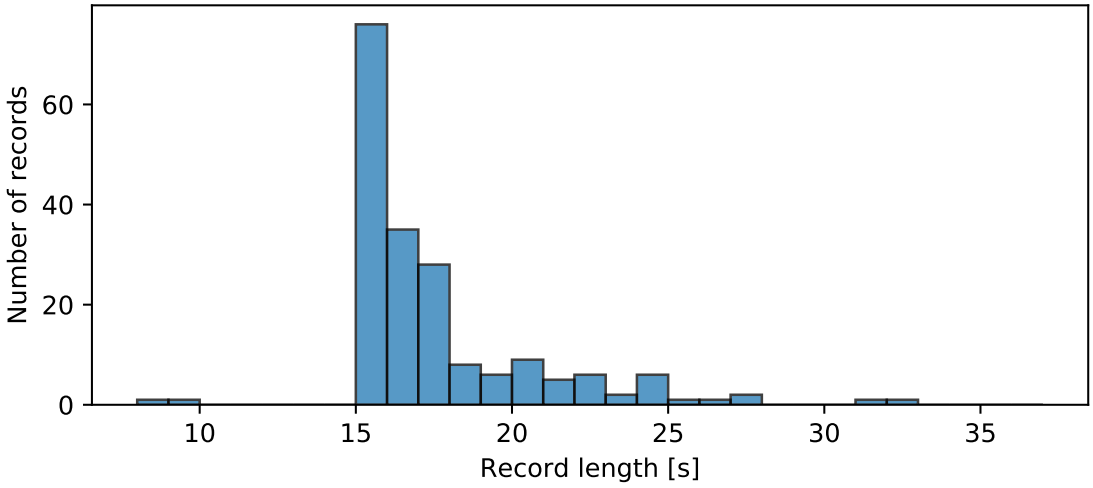

FIGURE 1.4: Distribution of the length of accelerometer records in seconds.

TABLE 1.2: Number of events per year recorded on each accelerometer (for comparison with Table 7 of KNMI report by Dost et al., 2022).

Year	FRB2	GARST	HKS	KANT	MID1	MID3	STDM	WIN	WSE	ZAN1	ZAN2	ROS1	ROS2	ROS3	ROS4	ROS5	ROS6
1996												2					
1997												6	2	5			
1998												3	3	2			
1999												6	5	4	1		
2000												1	3	1	1	1	
2001												1	1		1	1	1
2002												1	3			1	2
2003					1	4					2	1	1				
2004												1	1				1
2005																	
2006			5			2			1	1	3	2	2		1		2
2007									2		2						
2008					2	1		1	1	1	3						
2009			1		2	1		3	6	3	3						
2010	1	1	1	1	1				2	1	1						
2011	1	3	1	1	3	2	1	2	9	1	2						
2012	1	3	1	1	2		1	2	2								
2013		4	2	2				4	4	2							
2014		1	1	1				1									
Total	3	12	12	6	11	10	2	13	27	9	16	24	21	12	4	3	6

Finally, although it is difficult to assess the data completeness for triggered data, we represent the number of available stations in Figure 1.5 together with the number of stations that recorded the event. Please note that for Roswinkel, only ROS* stations were considered, whereas for Groningen, all

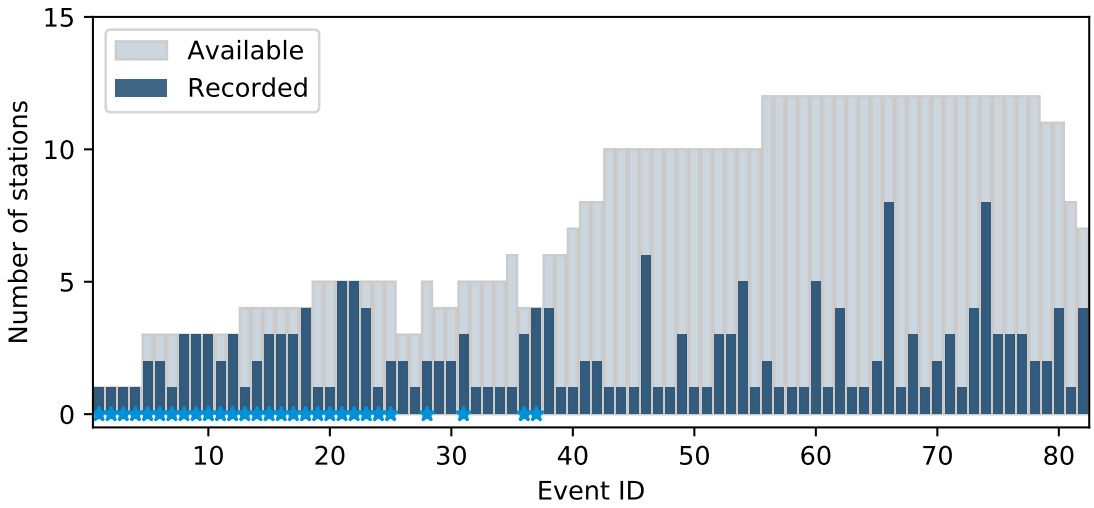

FIGURE 1.5: Histogram showing the number of operating stations (light grey) and the number of triggered stations, i.e. recording waveform data (dark blue) for each event. Events occurring in the Roswinkel field are marked by blue stars.

stations except ROS* were considered. This figure shows that in many cases, data are available only at a single station and the number of records rarely exceeds half of the number of operational stations (at least for the events occurring within the Groningen field). Of course, there is a strong relation between the number of stations that recorded the events and the event magnitudes, as illustrated in Figure 1.6.

Summary

Accelerometer waveform data are complete.

The content of the accelerometer waveform data can be summarised as follows. We verified that the information contained in the miniSEED files is correct in terms of trace ID (Network.StationName.LocationFlag.Channel), with respect to the events' origin times and the periods of operation of each station. No metadata are missing (records are always available for all three components and are correctly labelled, the sampling rate is always given and consistent). Note that of the 31 accelerometers listed in Table 5 of KNMI's report (Dost et al., 2022), data were available only for 18 stations, because the others were placed farther away from the Groningen field and were not triggered by low magnitude events (see Fig. 1.1a).

1.2 Borehole data

KNMI initially provided us with **584** miniSEED files containing the borehole **triggered** waveform data of **596** local events. The miniSEED files were named after the event origin times, hence we were able to retrieve the relevant event information from the KNMI FDSN web service and plot their locations on the maps in Fig. 1.8. Most events are located within or close to the Groningen field (Fig. 1.8b). Events are listed in Table B.1 in the appendix (p. 82).

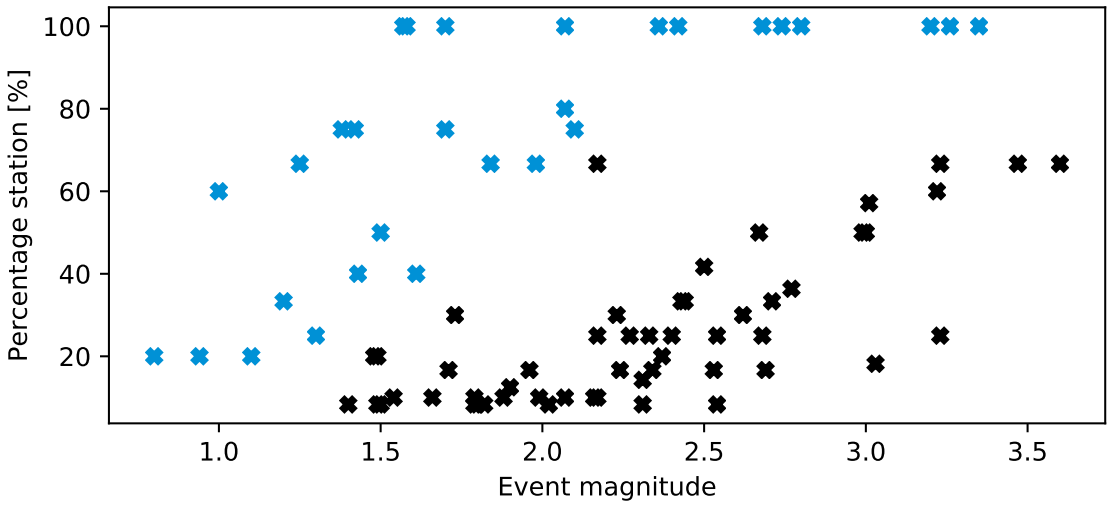

FIGURE 1.6: Percentage of stations recording waveforms for a certain event versus event magnitude (blue crosses: events outside the Groningen field, black crosses: within the field).

Similarly to the accelerometer data, the difference between number of files and number of events can be explained by consecutive events being recorded in a common file. Such events are listed in Table 1.3. The distribution of the number of events over time is shown in Fig. 1.7.

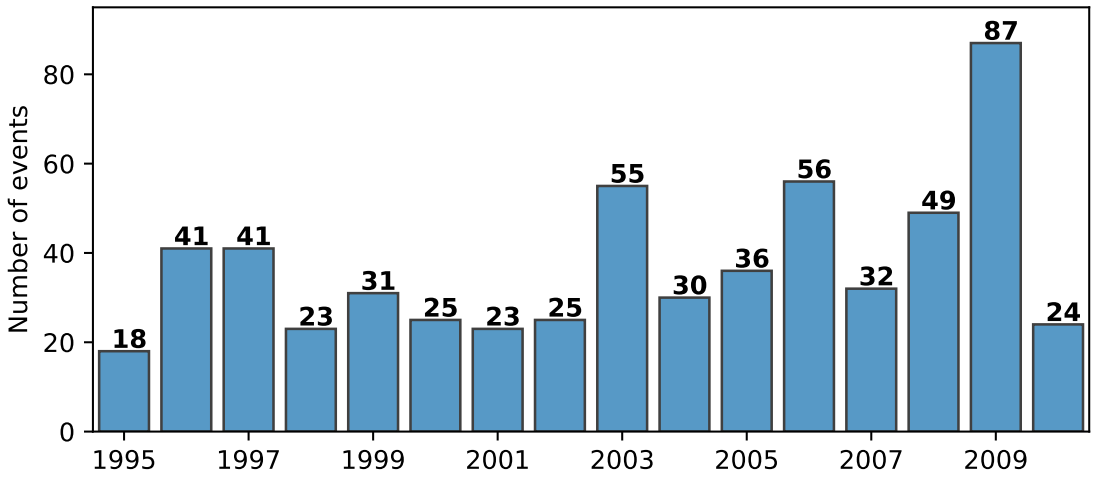

FIGURE 1.7: Histogram of the number of events per year that were recorded by one or several borehole stations.

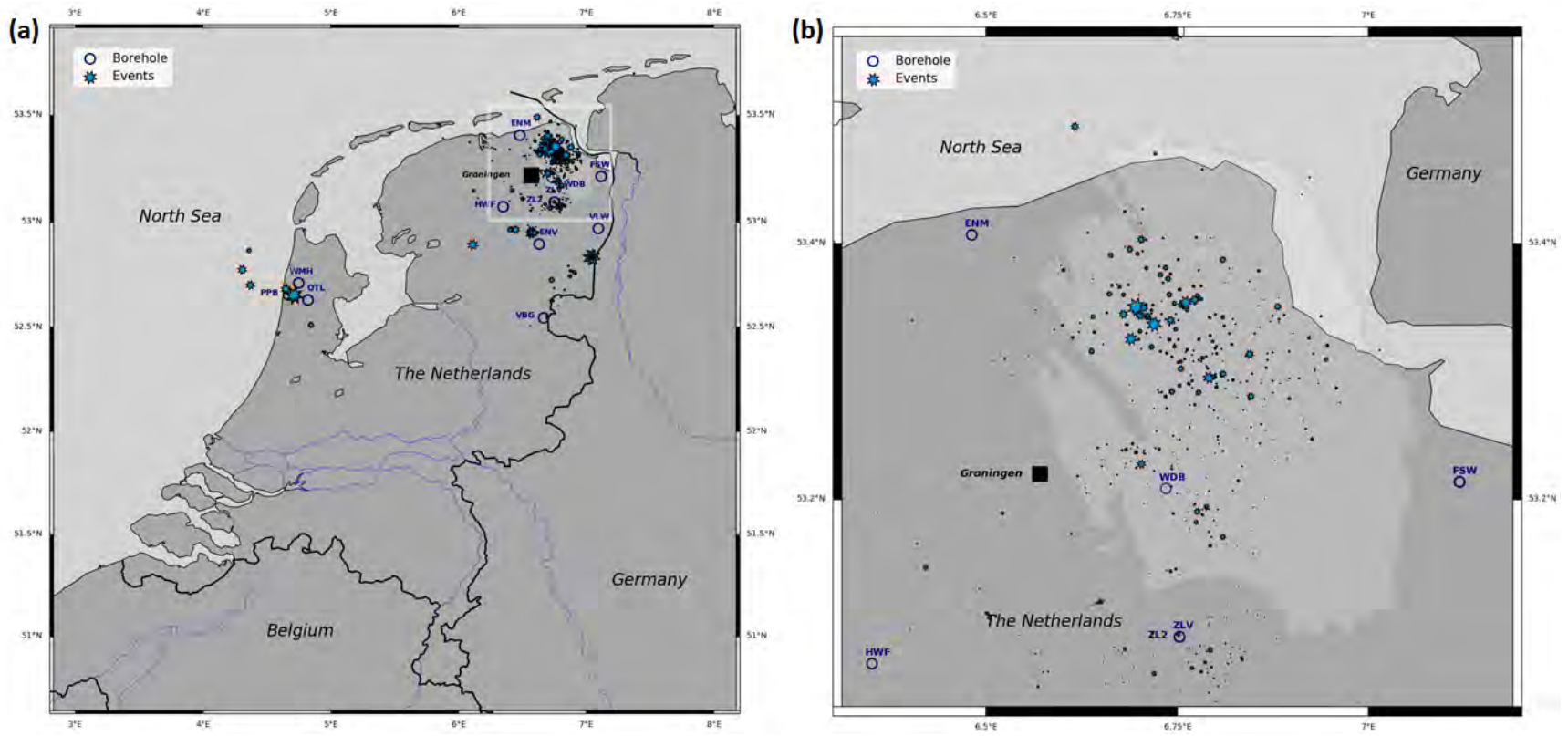

FIGURE 1.8: Maps showing the location of KNMI borehole stations (empty circles) and events for which borehole records are available (blue symbols) within (a) the Netherlands and (b) the Groningen field and surroundings. Event marker sizes are proportional to event magnitudes.

TABLE 1.3: List of events that occur close in time and may be contained in single files.

Event origin time	Magnitude
2001-04-28 10:00:08.290	1.54
2001-04-28 10:00:55.510	1.08
2001-10-10 14:06:43.350	0.99
2001-10-10 14:06:57.240	0.75
2001-12-04 19:08:31.060	0.19
2001-12-04 19:08:37.830	-0.01
2006-03-25 13:54:38.140	2.1
2006-03-25 13:55:51.170	1.7
2009-03-14 15:32:16.310	1.02
2009-03-14 15:32:27.700	0.98
2009-03-17 19:10:16.550	0.93
2009-03-17 19:10:33.600	0.93
2009-03-17 19:10:49.310	0.93
2009-03-17 19:11:12.380	1.01
2009-03-17 19:27:36.410	0.68
2009-03-17 19:28:41.320	0.68
2009-03-20 22:48:15.160	0.37
2009-03-20 22:49:29.960	0.45
2009-03-22 00:32:19.110	1.22
2009-03-22 00:34:53.490	0.61
2010-05-30 18:58:36.120	1.5
2010-05-30 18:58:57.990	1.2

Note that the number of events in Fig. 1.7 differs from Table 10 in KNMI's report (Dost et al., 2022), since we follow a different logic: KNMI counted all events in the induced seismicity catalogue for the time period of interest (610 events) and explained why for some of the events, records were not available, while we built the catalogue of events of interest to this specific project by associating files to events based on filenames.

The data availability at level 4 for all borehole stations is presented in Fig. 1.9. A number of stations (OTL, PPB and WMH) recorded only a few events as they are located farther away from the Groningen field in which most of the seismicity occurred (see Fig. 1.8a). Data availability plots for other borehole levels are placed in the appendix in Fig. B.1 to Fig. B.5 (pp. 90-92).

The distribution of event magnitudes (Fig. 1.10) shows that most events have a magnitude lower than 1.2. Many of them occur within the Groningen field (Fig. 1.8b) and therefore cannot be recorded by all borehole stations (e.g. PPB, WMH, OTL, VBG and in a lesser extent, ENV, VLW, HWF - see histogram on the right of Fig. 1.9).

Most data were acquired with a 120 Hz sampling rate, except at station FSW, which recorded data with a 121.12 Hz sampling rate until May 1996. Although the overwhelming majority of records are 128 s long (Fig. 1.11a), 80 records have shorter lengths (from 29.9 s to 115.2 s), while only a single record is longer (256 s) as demonstrated in Fig. 1.11b.

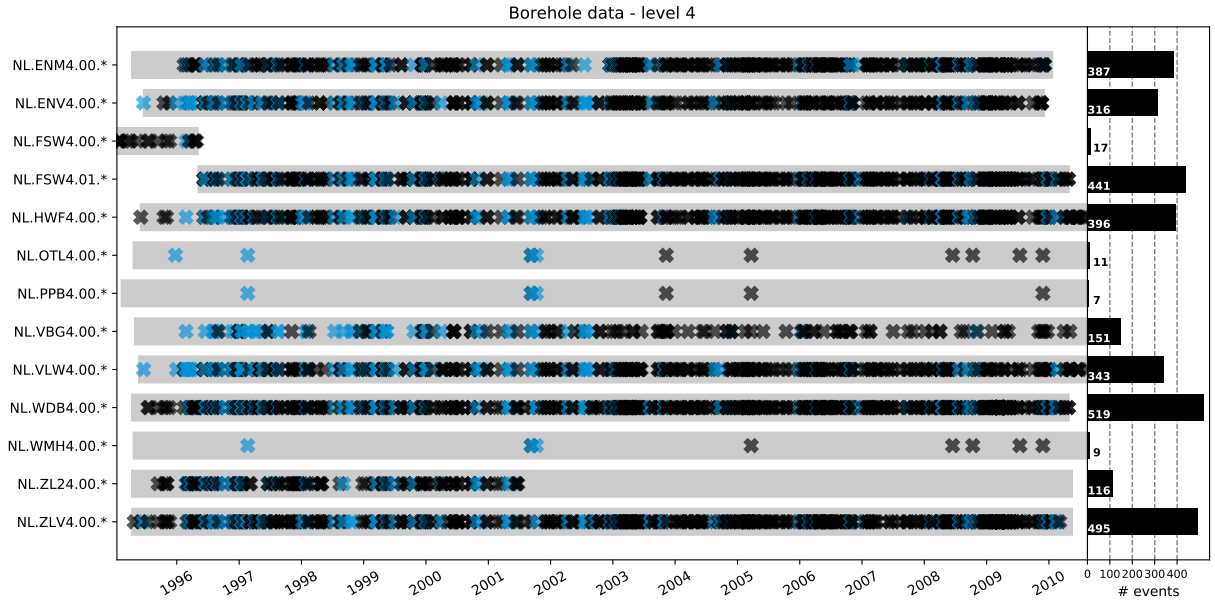

FIGURE 1.9: Overview of borehole triggered data (level 4 only). Grey rectangles represent the time span, in which stations were operational. Crosses symbolise events for which waveform data are available (blue: events outside the Groningen field, black: within the field). The histogram on the right summarises the number of events recorded at each station. Note that we distinguished stations by their full location, therefore FSW4 appears twice (locations '00' and '01').

Summary

Borehole waveform data are complete.

The content of the borehole waveform data can be summarised as follows. We verified that the information contained in the miniSEED files is correct in terms of trace ID (network name, station name, channel name), with respect to the events' origin times and the periods of operation of each station. No metadata are missing (records are always available for all three components and are correctly labelled, the sampling rate is always given and consistent).

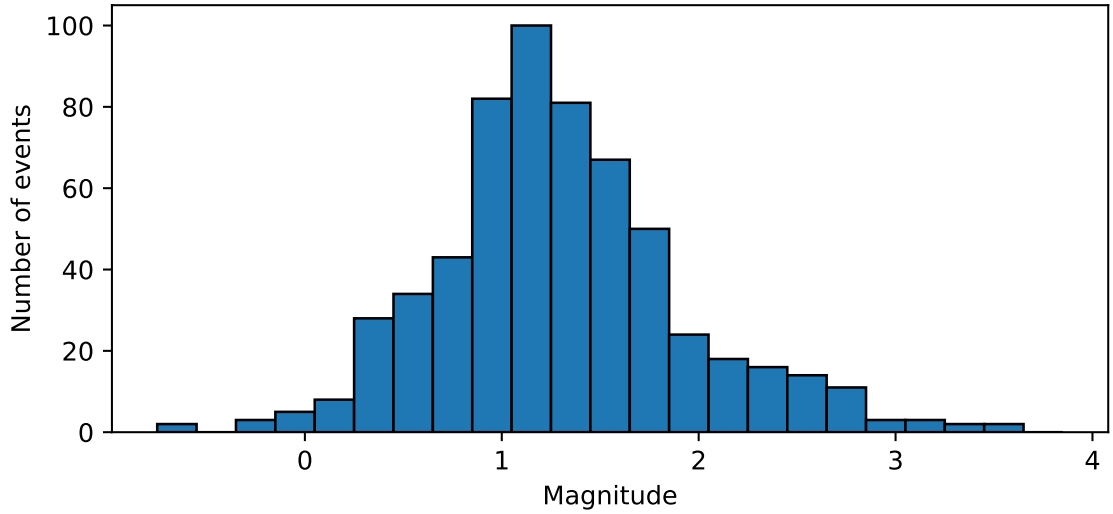

FIGURE 1.10: Distribution of local magnitudes for the events recorded by the borehole stations between January 1995 and August 2010.

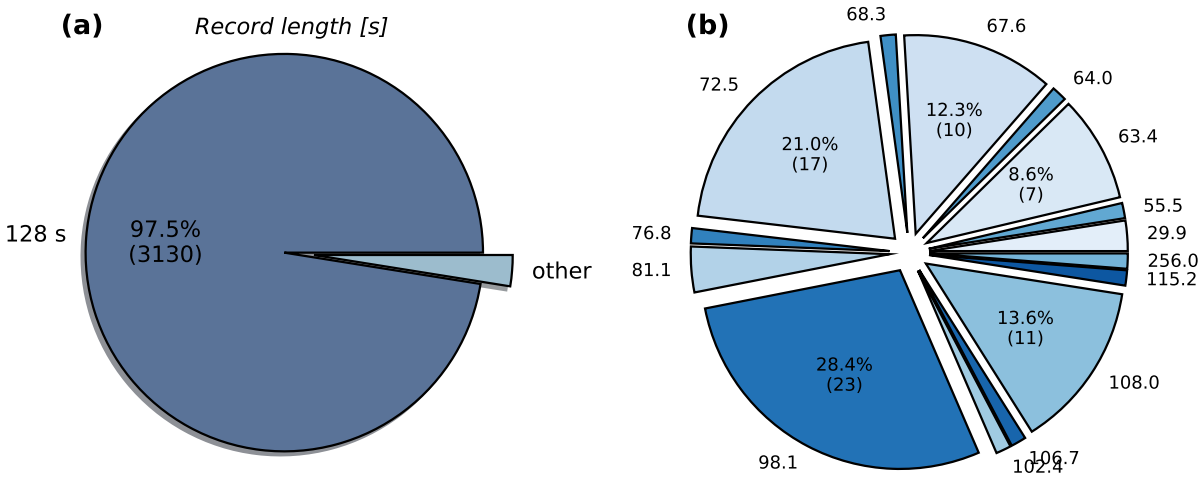

FIGURE 1.11: (a) Length of available borehole records in seconds. (b) Distribution of records with length differing from 128 s ("other"). Record lengths are given in seconds outside of the pie diagram. Proportions in % and number of records (in brackets) are indicated on pie slices exceeding 5%.

Metadata completeness

2.1 Introduction

In this chapter, we assess the completeness of the station metadata. We verified that the information stated in the FDSN StationXML files (installation date, instrument correction and orientation) matches the information reported by KNMI (Dost et al., 2022). Further, we revised that this information is consistent with the waveform data. In addition, we verified that time synchronisation errors were reported. All analyses were performed using the Obspy python package (Beyreuther et al., 2010), except if specified otherwise.

2.2 Accelerometer stations metadata

2.2.1 Data

KNMI initially provided 17 StationXML files, one for each of the stations that recorded at least one event. A summary of the information extracted from these files is shown in Table 2.1. We verified that the periods of installation and coordinates for each station are consistent with Table 5 in Dost et al. (2022). In addition, we checked that the information is coherent for all channels. The naming of the stations and channels corresponds to header information from the waveform data. The sampling rate of 200 Hz is assigned consistently.

2.2.2 Instrument response

Two different sets of accelerometers were installed in the network, both manufactured by GeoSig, but with distinct instrument response: the AC-23 sensor, which is combined with the SMACH-SM2 datalogger, and the AC-63 sensor combined with the GSR-18 datalogger. The sensor type is specified for each station in Table 2.1.

According to personal communication with KNMI, the instrument response of the AC-23 sensor was provided by the manufacturer. However, it is stated by KNMI in an earlier report (Dost and Haak, 2002) that this transfer function "slightly differs" from what was previously provided by the manufacturer. That report also notes that the gain of the transfer function is technically not used, since the output of the data is already in cm/s^2, such that no conversion to acceleration is required. Despite this, it is worth considering the reasons for any differences in the stated transfer function to understand the validity of the data. Neither the current report nor Dost and Haak (2002) explicitly states the unit of sensitivity for the transfer function, although it is implied in the former to be $V/m/s^2$. The output of the transfer function, however, is declared as acceleration in the current report, while it is stated as being displacement in Dost and Haak (2002), suggesting the unit of sensitivity is V/m. The different information provided by the manufacturer of the sensors accounts for these differences. The instrument response of the AC-63 sensor was provided by the manufacturer as well and outputs data in the unit g, therefore as well in acceleration.

Since for both types of sensors, the output data are already expressed in acceleration (cm/s^2 and g), the total gain merely corresponds to the conversion of these units to m/s^2. A schematic description of the different portions of the instrument response is shown in Fig. 2.1.

TABLE 2.1: Accelerometer metadata extracted from StationXML files. Fs is the sampling rate in Hz. Station orientations in the North, East, Z (up) coordinate system are specified by azimuth and dip angles in degrees. Note that no waveform data are associated with ZAN2.00, ZAN2.01 and ROS5.01.

Name	Code	Channel	Installation date	Removal date	Latitude	Longitude	Fs [Hz]	Type	Azimuth [°]	Dip [°]
FRB2	00	HGZ	2006-03-22	2014-09-17	53.1875	6.7655	200	AC-63	0	-90
	00	HG1	2006-03-22	2014-09-17	53.1875	6.7655	200	AC-63	30±30	0
	00	HG2	2006-03-22	2014-09-17	53.1875	6.7655	200	AC-63	300±30	0
GARST	00	HGZ	2009-09-15	2014-09-17	53.3677	6.7135	200	AC-63	0	-90
	00	HG1	2009-09-15	2014-09-17	53.3677	6.7135	200	AC-63	355±16	0
	00	HG2	2009-09-15	2014-09-17	53.3677	6.7135	200	AC-63	265±16	0
HKS	00	HGZ	2005-04-26	2014-09-17	53.2920	6.7850	200	AC-63	0	-90
	00	HG1	2005-04-26	2014-09-17	53.2920	6.7850	200	AC-63	358±19	0
	00	HG2	2005-04-26	2014-09-17	53.2920	6.7850	200	AC-63	268±19	0
KANT	00	HGZ	2007-04-03	2014-07-01	53.3772	6.6621	200	AC-63	0	-90
	00	HG1	2007-04-03	2014-07-01	53.3772	6.6621	200	AC-63	35±29	0
	00	HG2	2007-04-03	2014-07-01	53.3772	6.6621	200	AC-63	305±29	0
MID1	00	HGZ	1996-12-20	2013-09-11	53.3473	6.6423	200	AC-23	0	90
	00	HG1	1996-12-20	2013-09-11	53.3473	6.6423	200	AC-23	199±19	0
	00	HG2	1996-12-20	2013-09-11	53.3473	6.6423	200	AC-23	289±19	0
MID3	00	HGZ	1998-02-10	2003-03-17	53.3533	6.6472	200	AC-23	0	90
	00	HG1	1998-02-10	2003-03-17	53.3533	6.6472	200	AC-23	180	0
	00	HG2	1998-02-10	2003-03-17	53.3533	6.6472	200	AC-23	270	0
	01	HGZ	2003-03-17	2013-09-10	53.3533	6.6472	200	AC-23	0	90
	01	HG1	2003-03-17	2013-09-10	53.3533	6.6472	200	AC-23	132±16	0
	01	HG2	2003-03-17	2013-09-10	53.3533	6.6472	200	AC-23	222±16	0
STDM	00	HGZ	2009-09-15	2014-09-17	53.3123	6.6921	200	AC-63	0.0	-90
	00	HG1	2009-09-15	2014-09-17	53.3123	6.6921	200	AC-63	57±21	0
	00	HG2	2009-09-15	2014-09-17	53.3123	6.6921	200	AC-63	327±21	0
WIN	00	HGZ	2007-04-03	2014-09-17	53.3104	6.7471	200	AC-63	0.0	-90
	00	HG1	2007-04-03	2014-09-17	53.3104	6.7471	200	AC-63	343±39	0
	00	HG2	2007-04-03	2014-09-17	53.3104	6.7471	200	AC-63	253±39	0
WSE	00	HGZ	2006-10-11	2013-04-24	53.3444	6.7099	200	AC-23	0	90
	00	HG1	2006-10-11	2013-04-24	53.3444	6.7099	200	AC-23	199±22	0
	00	HG2	2006-10-11	2013-04-24	53.3444	6.7099	200	AC-23	289±22	0
ZAN1	00	HGZ	1999-06-29	2013-10-24	53.3657	6.7751	200	AC-23	0	90
	00	HG1	1999-06-29	2013-10-24	53.3657	6.7751	200	AC-23	88±17	0
	00	HG2	1999-06-29	2013-10-24	53.3657	6.7751	200	AC-23	178±17	0
ZAN2	00	HGZ	1999-06-29	2000-07-03	53.3568	6.7547	200	AC-23	0	90
	00	HG1	1999-06-29	2000-07-03	53.3568	6.7547	200	AC-23	180	0
	00	HG2	1999-06-29	2000-07-03	53.3568	6.7547	200	AC-23	270	0
	01	HGZ	2000-07-03	2002-07-02	53.3568	6.7547	200	AC-23	0	90
	01	HG1	2000-07-03	2002-07-02	53.3568	6.7547	200	AC-23	180	0
	01	HG2	2000-07-03	2002-07-02	53.3568	6.7547	200	AC-23	270	0
	02	HGZ	2003-09-30	2013-09-23	53.3568	6.7547	200	AC-23	0	90
	02	HG1	2003-09-30	2013-09-23	53.3568	6.7547	200	AC-23	210±15	0
	02	HG2	2003-09-30	2013-09-23	53.3568	6.7547	200	AC-23	300±15	0
ROS1	00	HGZ	1996-06-13	1997-01-10	52.8425	7.0327	200	AC-23	0	90
	00	HG1	1996-06-13	1997-01-10	52.8425	7.0327	200	AC-23	180	0
	00	HG2	1996-06-13	1997-01-10	52.8425	7.0327	200	AC-23	270	0
	01	HGZ	1997-01-10	2020-01-01	52.8425	7.0327	200	AC-23	0	90
	01	HG1	1997-01-10	2020-01-01	52.8425	7.0327	200	AC-23	172±8	0
	01	HG2	1997-01-10	2020-01-01	52.8425	7.0327	200	AC-23	262±8	0
ROS2	00	HGZ	1997-02-20	2014-08-27	52.8206	7.0465	200	AC-23	0	90
	00	HG1	1997-02-20	2014-08-27	52.8206	7.0465	200	AC-23	191±24	0
	00	HG2	1997-02-20	2014-08-27	52.8206	7.0465	200	AC-23	281±24	0
ROS3	00	HGZ	1997-02-20	2000-11-03	52.8365	7.0679	200	AC-23	0	90
	00	HG1	1997-02-20	2000-11-03	52.8365	7.0679	200	AC-23	163±4	0
	00	HG2	1997-02-20	2000-11-03	52.8365	7.0679	200	AC-23	253±4	0
ROS4	00	HGZ	1998-12-17	2010-01-01	52.8365	7.0679	200	AC-23	0	90
	00	HG1	1998-12-17	2010-01-01	52.8365	7.0679	200	AC-23	249±19	0
	00	HG2	1998-12-17	2010-01-01	52.8365	7.0679	200	AC-23	339±19	0
ROS5	00	HGZ	2000-01-04	2003-02-18	52.8336	7.0479	200	AC-23	0	90
	00	HG1	2000-01-04	2003-02-18	52.8336	7.0479	200	AC-23	141±21	0
	00	HG2	2000-01-04	2003-02-18	52.8336	7.0479	200	AC-23	231±21	0
	01	HGZ	2003-02-18	2006-03-22	52.8336	7.0479	200	AC-23	0	90
	01	HG1	2003-02-18	2006-03-22	52.8336	7.0479	200	AC-23	180	0
	01	HG2	2003-02-18	2006-03-22	52.8336	7.0479	200	AC-23	270	0
ROS6	00	HGZ	2000-11-03	2014-01-01	52.8275	7.0283	200	AC-23	0	90
	00	HG1	2000-11-03	2014-01-01	52.8275	7.0283	200	AC-23	146±21	0
	00	HG2	2000-11-03	2014-01-01	52.8275	7.0283	200	AC-23	236±21	0

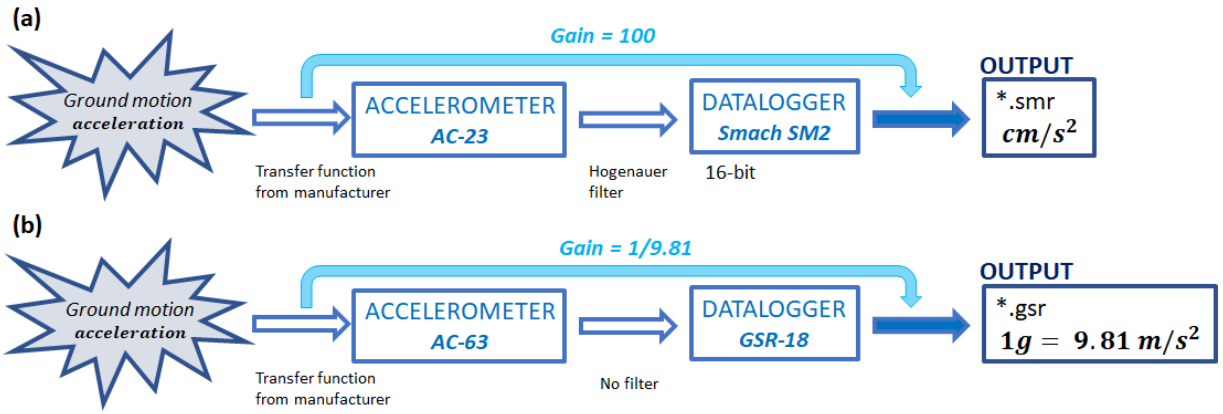

FIGURE 2.1: Summary of the instrument response for (a) AC-23 sensors combined with SMACH-SM2 dataloggers and (b) AC-63 sensors combined with GSR-18 dataloggers.

Accelerometer instrument responses can be retrieved from the StationXML files.

In Figures 2.2 and 2.3, we reproduced the response amplitude and phase plots shown in Dost et al. (2022, Figs. 4-6) based on the information available from the StationXML files for each station with a given sensor-datalogger combination. Since all curves plot on top of each other, the information contained in the StationXML files is correct and consistent. Moreover, the resulting plots visually correspond to the ones presented by Dost et al. (2022) (to ease the comparison, we use same axes scales and limits[1]).

In addition, units of input and output data are correctly labelled in the StationXML files.

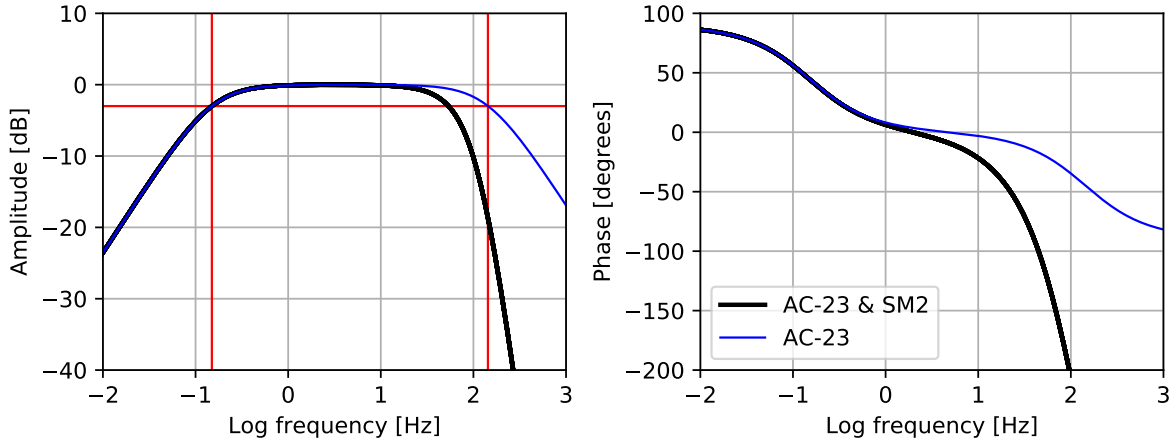

FIGURE 2.2: Response for the AC-23 sensor individually (blue curve) and combined with the SMACH-SM2 datalogger (black curve). The two vertical red lines symbolise the corner frequencies of the two poles of the AC-23 sensor's transfer function at 0.15 and 143.4 Hz, respectively. When taking the datalogger into account, i.e. the transfer function of the Hogenauer filter (Dost et al., 2022, Fig. 3), the corner frequency at 143.4 Hz is lowered (see horizontal red line at -3 dB).

[1]The decibel scale is defined as ten times the logarithm with base 10.

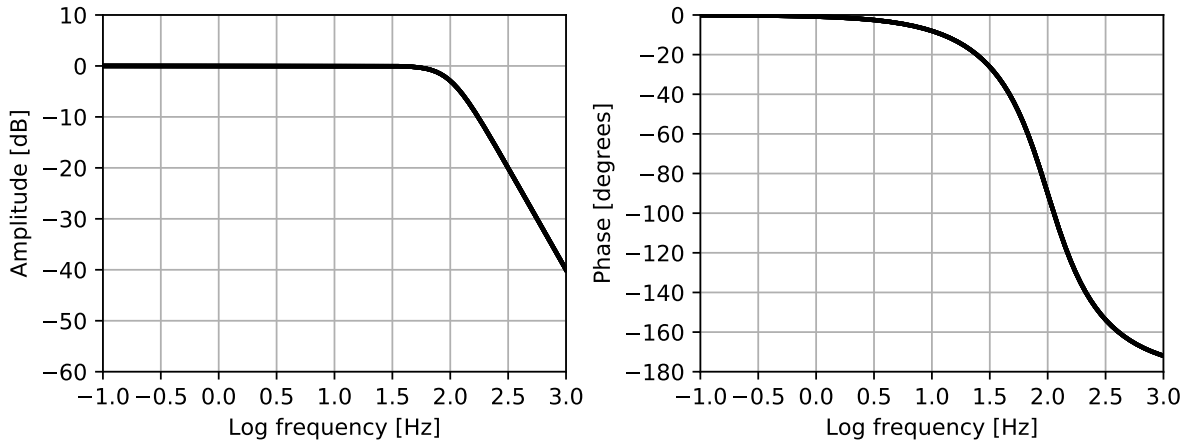

FIGURE 2.3: Response for the AC-63 sensor combined with the GSR-18 datalogger.

2.2.3 Sensor orientation

In their report (Dost et al., 2022), KNMI highlight that the sensors are oriented differently depending on the instrument type:

- AC-23: North, East, Z coordinates are all negative, i.e. the sensor is oriented in the South, West, Down system;
- AC-63: North, West, Z coordinates are positive.

The convention to store orientation angles in StationXML files is the North, East, Down system. Thus, we verified that the dip angle is given as 90° for the AC-23 sensors and as -90° for the AC-63 instruments in the StationXML files (Table 2.1).

In practice, the coordinate systems employed by KNMI mean that for the transition into the conventional North, East, Z (up) system, all components of the AC-23 sensors must be multiplied by -1, while for the AC-63 sensors, only the second horizontal component must be multiplied by -1.

Accelerometer orientations and their associated uncertainties can be retrieved from StationXML files.

To derive the horizontal components' orientations, KNMI tested two different methods, which are detailed in Dost et al. (2022). In this chapter, we merely verified that the azimuth angles given in the StationXML files[2] (column "Azimuth" in Table 2.1 of the present document) are consistent with the results in Table 8 by Dost et al. (2022, column #8)[3]

[2]Note that no orientation angles are given for a few specific location codes for the following stations: MID3.00, ZAN2.00, ZAN2.01, ROS1.00 and ROS5.01. Consequently, these stations were not oriented, but - being AC-23 sensors - assigned default values of 180° (South) and 270° (West) for the first and second horizontal components, respectively.

[3]These latter values need to be corrected according to the aforementioned rules to be comparable to the azimuth angles stored in the StationXML files, i.e. for the AC-23 sensors, 180° need to be added for the orientation of the first horizontal component and 90° for the second horizontal component, whereas for the AC-63 sensors, the orientation of the second horizontal component is obtained by subtracting 90°. Note that the angles are defined in the range [0°-360°].

NOTE

- Rotation to the N,E,D coordinate system can be achieved by using the angles stored in the StationXML files.
- Without use of the StationXML files, please be aware that the aforementioned corrections for the different types of sensors must be applied.

2.3 Borehole station metadata

2.3.1 Data

Furthermore, KNMI provided 12 StationXML files for the borehole instruments, one for each of the stations having recorded at least one event. Each borehole comprises four or more geophones at different depths and a few are complemented by a surface sensor. A short summary of the information extracted from these files is shown in Table 2.2 for station ENM and for the other stations in the appendix (Tables B.2 to B.10, pp. 92-95). The information is consistent for all stations and components at all depth levels. The station coordinates as well as start and end dates are in agreement with the ones displayed in Table 2 by Dost et al. (2022). Note that some of the surface sensors (e.g. HWF0, PPB0) were installed later than the corresponding sensors within the borehole, as reported in Table 4 by Dost et al. (2022).

TABLE 2.2: Metadata extracted from the XML file for borehole station ENM. Depth is measured from ground level. Fs is the sampling rate in Hz. The station orientations in the North, East, Z (up) coordinate system are specified by azimuth and dip angles in °.

Name	Channel	Installation date	Removal date	Latitude	Longitude	Depth [m]	Elevation [m]	Fs [Hz]	Azimuth [°]	Dip [°]
ENM1	HHN	1995-04-12	2010-01-22	53.4064	6.4817	50	1	120	122	0
	HHE	1995-04-12	2010-01-22	53.4064	6.4817	50	1	120	212	0
	HHZ	1995-04-12	2010-01-22	53.4064	6.4817	50	1	120	0	-90
ENM2	HHN	1995-04-12	2010-01-22	53.4064	6.4817	100	1	120	177	0
	HHE	1995-04-12	2010-01-22	53.4064	6.4817	100	1	120	267	0
	HHZ	1995-04-12	2010-01-22	53.4064	6.4817	100	1	120	0	-90
ENM3	HHN	1995-04-12	2010-01-22	53.4064	6.4817	150	1	120	164	0
	HHE	1995-04-12	2010-01-22	53.4064	6.4817	150	1	120	254	0
	HHZ	1995-04-12	2010-01-22	53.4064	6.4817	150	1	120	0	-90
ENM4	HHN	1995-04-12	2010-01-22	53.4064	6.4817	200	1	120	91	0
	HHE	1995-04-12	2010-01-22	53.4064	6.4817	200	1	120	181	0
	HHZ	1995-04-12	2010-01-22	53.4064	6.4817	200	1	120	0	-90

Different borehole layouts were tested as illustrated in Fig. 2.4. FSW is the deepest borehole equipped with five sensors with 75 m spacing reaching 300 m depth. Note that its surface sensor is labelled FSW**1** as opposed to all other borehole stations, where the surface sensor is assigned the suffix "0". PPB is the second deepest borehole, also composed of five sensors with 75 m spacing to 240 m depth. Note that the first borehole sensor is placed at 15 m compared to 75 m for FSW. The remaining boreholes have a more consistent setup and are composed of four sensors placed with 50 m spacing to approximately 200 m depth.

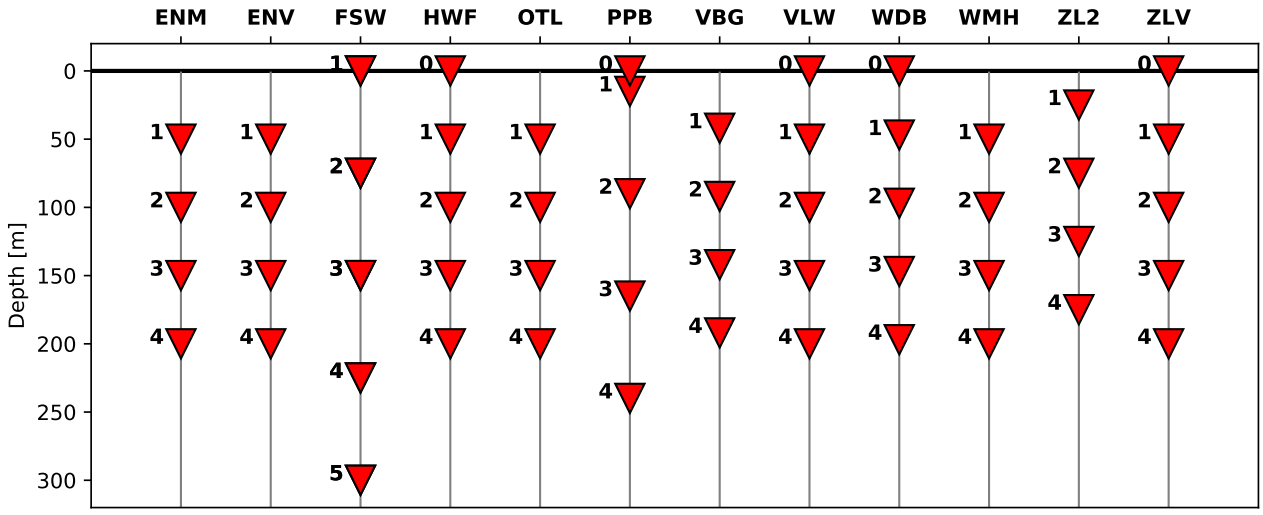

FIGURE 2.4: Borehole station layouts. Depth is measured from ground level.

COMMENT ON THE GAIN CHANGE REPORTED BY KNMI

KNMI discussed the issue about minimal gain setting changes for the borehole data during three different epochs. These minor changes were not properly documented, but the changes in the gain factors relate to values of only 0.003% in the beginning to a maximum of 2.3% in the end. None of these changes have an impact towards magnitude estimates, as the general uncertainties of magnitude estimates are at least one order of magnitude larger than the potential difference in gain settings. We therefore see no practical issue related to the documentation of gain settings.

2.3.2 Instrument response

All borehole sensors are of the same type (4.5 Hz SM6 geophones) and therefore have the same instrument response, except the FSW sensors before May 1996, when its datalogger was replaced. Details on how the response was obtained are described in Dost and Haak (2002) and are summarised schematically in Fig. 2.5. Please note that the specifications of poles and zeros indicated in the StationXML file slightly differs from the information given in Dost and Haak (2002), although according to Dost et al. (2022), this will not result in measurable changes in the response.

Borehole instrument responses can be retrieved from StationXML files.

The instrument response information could be retrieved properly from the StationXML files, all instrument responses plot consistently on top of each other in Fig. 2.6 and no discrepancies are observed compared to Figure 8 by Dost et al. (2022).

2.3.3 Sensor orientation

The sensor orientation information was extracted from the StationXML files and compared to the values reported by Dost et al. (2022, Table 7). No issues were found. All vertical components are oriented positive up, which, for the StationXML file convention (N-E-D), corresponds to dip angles of -90°.

Borehole sensor orientations can be retrieved from StationXML files.

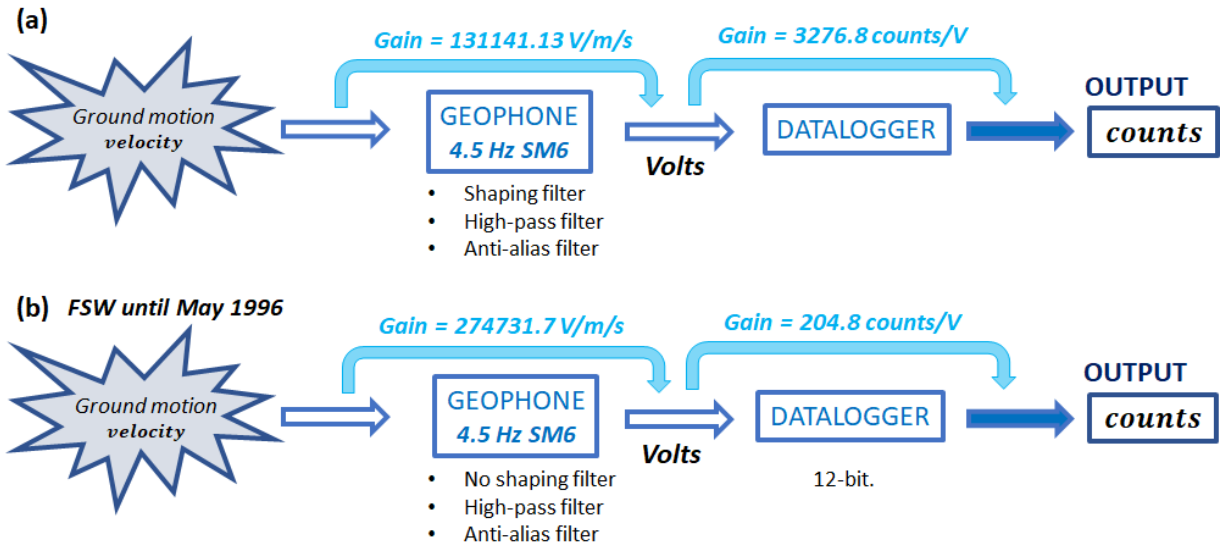

FIGURE 2.5: Summary of the instrument response for (a) all borehole geophones except (b) FSW from 1992 to May 1996.

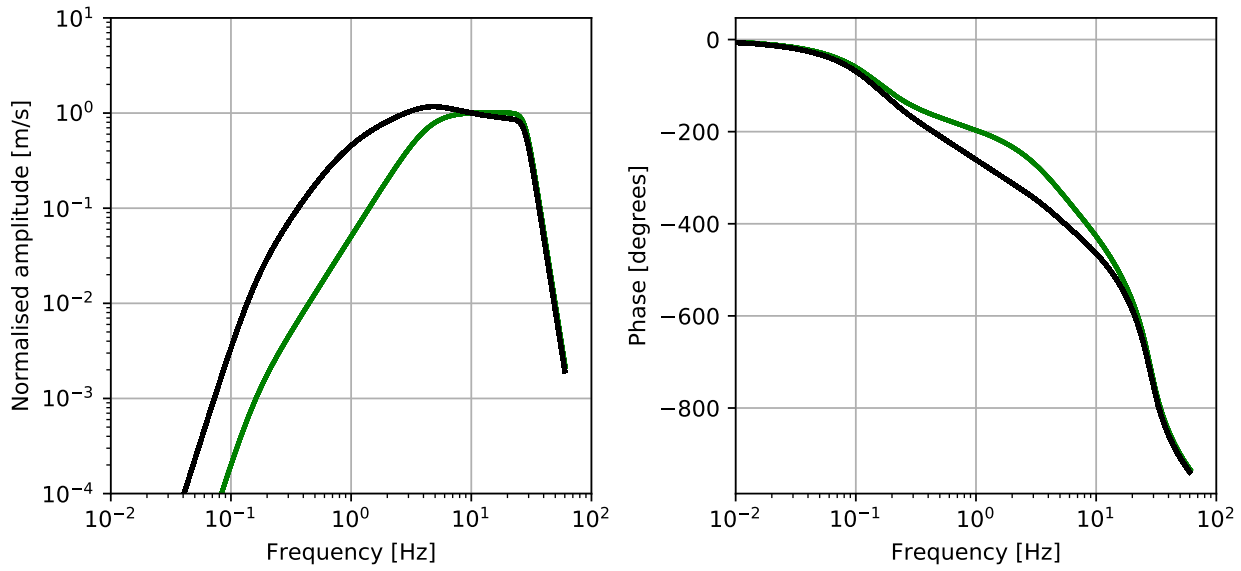

FIGURE 2.6: Amplitude (left) and phase (right) instrument response for all borehole sensors (black curves) as well as the first setup of station FSW (green curves).

WARNING!

Channel names for borehole stations are pseudo-North (HHN) and pseudo-East (HHE). In order for the rotation to be effective when using Obspy, the names of the components need to be specified as follows:

```
st.rotate(method="->ZNE", inventory=inv, components="ZNE")
```

instead of the default:

```
st.rotate(method="->ZNE", inventory=inv, components="Z12")
```

Waveform and metadata validity

3.1 Introduction

This chapter addresses the validity and accuracy of both the waveform and metadata for the newly available borehole and accelerometer data. We first reviewed the accelerometer data and subsequently the borehole data. For each data type, we employed quality assurance tests for sensor orientation, amplitude validity and data timing. For each of these aspects, we first appraised the quality assurance methods used by Dost et al. (2022). In a second step, we applied spot checks of the outlined methods to independently validate KNMI's results, before finally implementing our own quality assurance tests.

3.2 Accelerometer data

3.2.1 Sensor orientation

Vertical component

Unfortunately, no teleseismic earthquake data are available among the accelerometer triggered data. As a consequence, we did not verify the orientation of the vertical component using the same methodology as for the borehole sensors (see section 3.3.1). However, note that the vertical component could theoretically be oriented by analysing the particle motion and measuring the incidence angle (e.g. Oye and Ellsworth, 2005). This analysis was not carried out, though, as most particle motions turn out to be elliptical (see next section on the orientation of horizontal components, e.g. Fig. 3.3a) which would lead to large uncertainties.

Horizontal components

Regarding the orientation of the horizontal components, KNMI carried out two independent analyses, which are described in Dost et al. (2022): method 1 was applied automatically, while method 2 was performed manually. Both are based on the polarisation of P-waves. The data used to perform the analysis must be of sufficient quality, hence KNMI defined selection criteria based on a minimum event magnitude (to ensure a good signal-to-noise ratio) and a minimum event-station distance (to minimise the effect of location uncertainty). An additional threshold based on the absolute maximum amplitude recorded on the vertical component was defined as 0.1 cm/s^2. For stations outside the Roswinkel field, selection criteria on distance and magnitude were set to 2 km and M_L2.5. Within the Roswinkel field, due to better location accuracy, the distance criterion could be reduced to 1.5 km. Exceptions were made for stations ROS5 and ROS6, which otherwise could not have been oriented. KNMI provided a spreadsheet containing the individual orientation results of each analysed record. After checking that this list of records corresponds to the above criteria, we repeated the orientation analysis by implementing the automatic approach developed by KNMI (referred to as method 1) and compare the results.

Pre-processing consisted of the following work steps:

- bandpass-filter the data between 2 and 35 Hz;
- compute the STA/LTA function with a short-term average (STA) window of 0.01 s and a long-term average (LTA) window of 0.5 s;

- run an automatic detector on the STA/LTA trace with trigger-on and trigger-off thresholds set to 10 to determine the P-wave onset;
- cut the final analysis window 0.1 s before and 0.15 s after the trigger for AC-63 and 0.1 s before and 0.25 s after the trigger for AC-23 sensors[4].

During pre-processing, we found that multiple triggers were obtained in many instances using the STA/LTA algorithm as outlined. Manual adjustments were necessary to select the proper trigger. Hence, we cannot guarantee that the P-wave arrival times obtained in this way were identical to KNMI's during the following analysis, despite using the same processing parameters, frequency band and window lengths[5].

To perform the orientation analysis, the following steps were adopted:

- bandpass-filter the data between 2 and 30 Hz;
- consider the first component HG1 as pseudo-North and the second component HG2 as pseudo-East[6];
- rotate the waveforms into the radial-transverse-vertical (R-T-Z) system for all possible back-azimuth values from 0 to 360° with a 1° increment;
- for each rotation, compute the mean of the product of radial and vertical components (R·Z) as well as the energy on the tranverse component (|T|) as described in Jepsen and Kennett (1990);
- choose the back-azimuth angle which minimises |T| and maximises R·Z;
- correct this angle for the station-event back-azimuth;
- convert the resulting back-azimuth angle to azimuth (180° correction);
- compute the circular mean and standard deviation of the angles derived for each station analysing all recorded events. Note that KNMI used a different way of computing the mean and standard deviation. To ensure a fair comparison of their results with ours, we recomputed the circular mean and standard deviation for KNMI's results as well ($\bar{\theta}_K$ and $\bar{\sigma}_K$ in Table 3.1) and provide a comparison with the reported values ($\bar{\theta}_K$-$\bar{\theta}_R$ in Table 3.1). The differences are close to 0° and in all cases much below the uncertainty on the measurements confirming that the manner in which the mean was computed had no large impact.

Individual results are summarised in Fig. 3.1 and Table A.1 which can be found in the appendix (pp. 33 & 73).

The figure offers a direct comparison between NORSAR and KNMI results for each accelerometer. Most orientation measurements (dots, crosses and squares) are similar. However, some differ by

[4]In general, window lengths for polarisation analyses should be as short as possible. Here, window lengths were chosen by KNMI after carrying out several tests and to overcome the fact that some events show very weak signals on the horizontal components, particularly for larger magnitude and distant events (KNMI pers. comm.).

[5]In addition, the implementation of the STA/LTA algorithm may differ as well as the filter order and other details.

[6]Note that all components of AC-23 sensors need to be multiplied by -1 to be in the correct N, E, Z (up) system, whereas only the HG2 component needs to be multiplied by -1 for AC-63 sensors.

TABLE 3.1: Summary of the accelerometer orientation analysis using an automated approach. $\bar{\theta}$ is the circular mean of the azimuth angles found for all events at each station while σ_θ is the circular standard deviation. Subscript N stands for NORSAR results while K stands for KNMI results (method 1). Subscript R refers to KNMI reported results (first two columns of Table 8 in Dost et al., 2022) employing a different formula to compute angular mean and standard deviation. Note that KNMI automatically assigned a 30° standard deviation to stations for which only a single measurement was available.

Station	# events	$\bar{\theta}_K$[°]	σ_{θ_K}	$\bar{\theta}_K$-$\bar{\theta}_R$	$\bar{\theta}_N$[°]	σ_{θ_N}	$\bar{\theta}_N$-$\bar{\theta}_K$
FRB2	1	39	-	0	32	-	-7
GARST	7	351	24	0	351	28	0
HKS	4	353	26	1	357	25	4
KANT	1	80	-	0	69	-	-11
MID1	2	9	26	0	349	43	-20
MID3	6	308	21	1	310	22	2
STDM	1	54	-	0	71	-	17
WIN	7	2	54	-4	329	64	-33
WSE	6	19	35	1	167	177	148
ZAN1	3	268	22	0	311	71	43
ZAN2	5	30	19	0	76	59	46
ROS1	3	353	21	0	347	92	-6
ROS2	4	3	42	6	17	31	14
ROS3	4	345	4	1	253	141	-92
ROS4	2	65	40	0	67	17	2
ROS5	1	331	-	0	337	-	6
ROS6	1	322	-	0	330	-	8

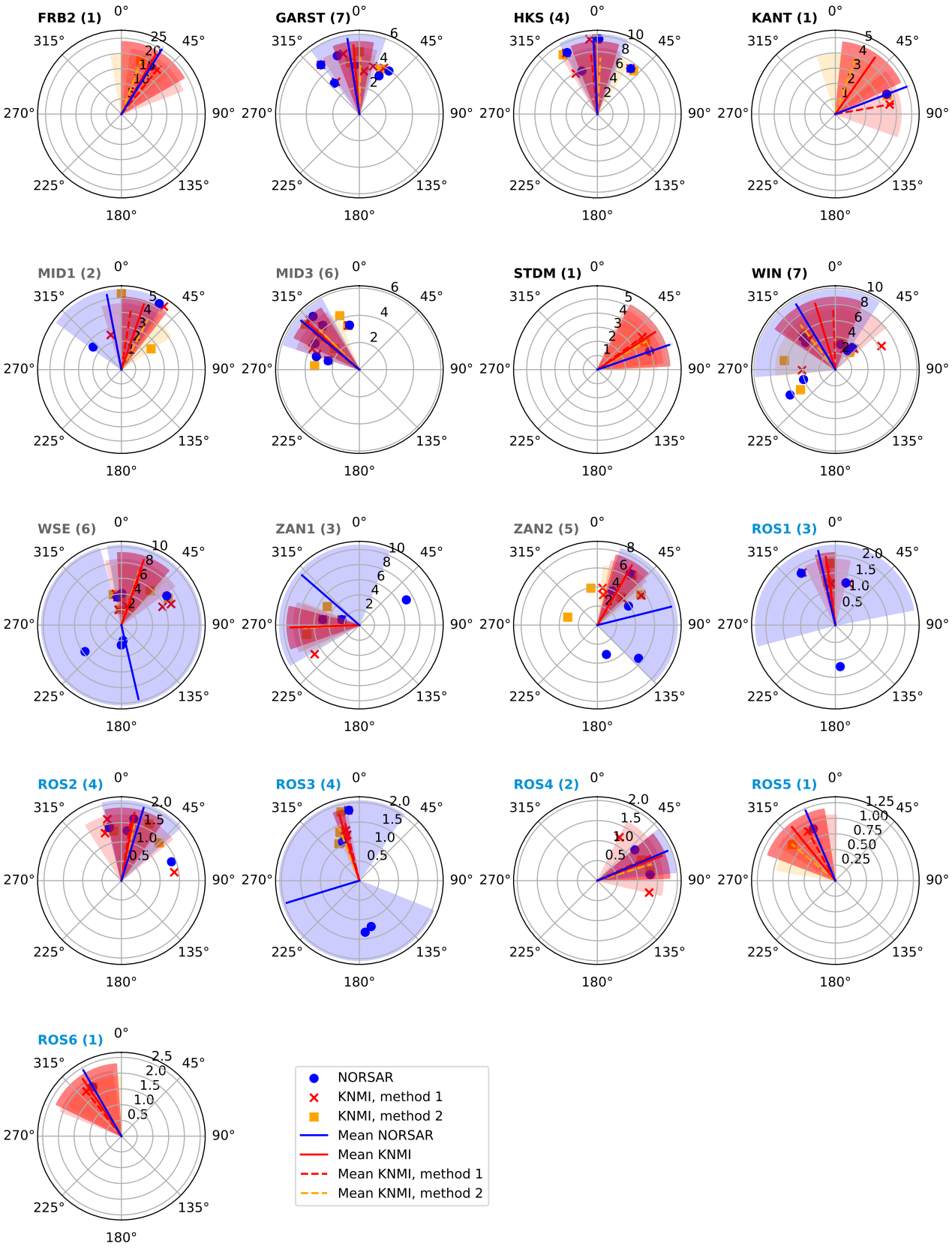

FIGURE 3.1: Comparison of orientation results for each station. The number of events employed for the analysis is indicated in parentheses together with the station name. Shaded areas represent the standard deviation for each series of measurements. The radial axis indicates the event-station distance [in km]. The results' dispersion is discussed in the text in more details.

180° leading to much higher standard deviations for our own computations compared to KNMI's (blue- and red-shaded areas in Fig. 3.1, respectively). The 180° ambiguity should have been handled by combining |T| and R·Z observations. However, the maximum of R·Z and the minimum of |T| do not always coincide.

This is illustrated in Fig. 3.2, in which the angular axis represents the angular difference between NORSAR and KNMI orientations, while the radial axis represents the offset angle between min(|T|) and max(R·Z). In addition, the circles' colour indicates the linearity of the particle motion in the horizontal

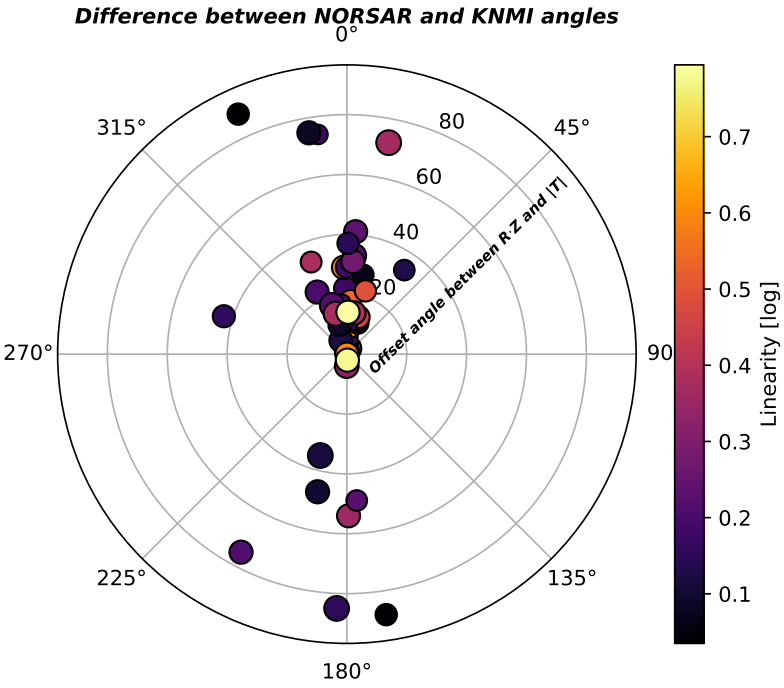

FIGURE 3.2: Angular difference between NORSAR's and KNMI's orientation results for accelerometers. The radial axis indicates the offset angle between R·Z and |T| measured in NORSAR's analysis. Circles are coloured by the linearity of the particle motion.

plane, which was obtained from its decomposition into eigenvectors and eigenvalues and defined as the ratio of the largest over the smallest eigenvalue. The more linear the motion, the more reliable the orientation should be. Fig. 3.2 shows that in general, NORSAR and KNMI obtained similar results if the offset angle was small (< 40°) and the particle motion linear (brighter colours). For all instances where the differences in orientation results are large, the offset angles are large (> 40°) and especially, the linearity is poor.

An example of the orientation analysis is displayed in Fig. 3.3 for an event recorded at station WSE. In this case, NORSAR's solution (234°) is approx. 180° different from KNMI's reported solution (66°), while the offset angle between min(|T|) and max(R·Z) is significant (47°). On the left of Fig. 3.3a, the waveforms recorded on radial as well as vertical (HGZ), pseudo-North (HG1) and pseudo-East (HG2) components are plotted for the considered analysis window. On the right, the particle motion in the vertical (top) and horizontal plane (bottom) are shown. On the lower right plot, blue lines symbolise the orientation axes from NORSAR's analysis, while black lines correspond to KNMI's result; the red

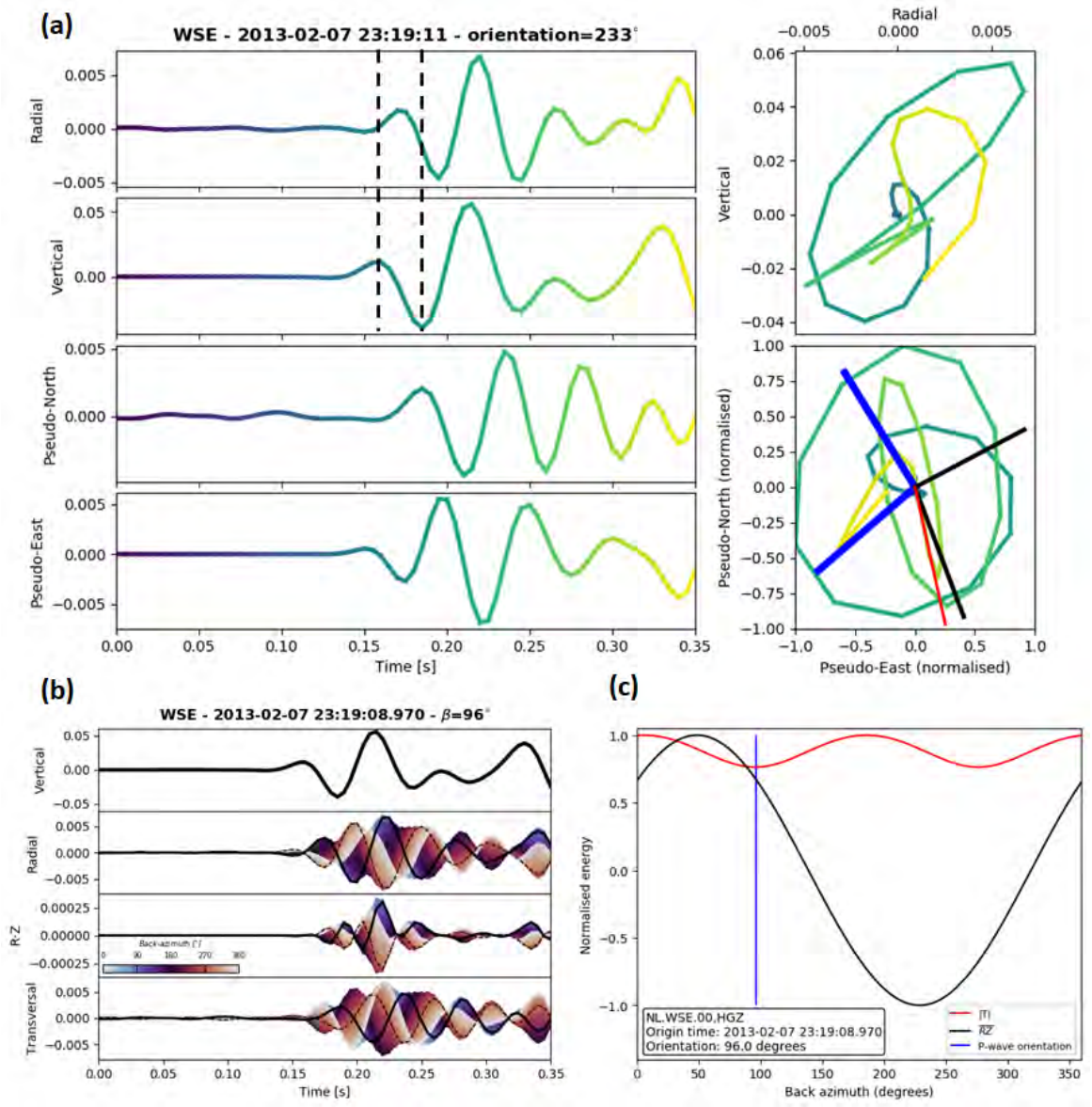

FIGURE 3.3: Orientation result example. (a) Waveforms and hodograms for radial, vertical, pseudo-north and pseudo-east component, dashed line highlights potential delay. (b)-(c) Minimum of |T| (red line) does not correspond to maximum of R·Z (black line). See text for details.

line corresponds to the principal direction obtained by decomposition of the particle motion[7]. Especially in the horizontal plane, the particle motion is more circular than linear. In Fig. 3.3b, vertical (Z), radial (R) and transverse (T) components are displayed for all possible back-azimuth angles together with the corresponding R·Z traces. The black lines represent waveforms for the best back-azimuth angle chosen from Fig. 3.3c and the dashed lines represent waveforms rotated with respect to the back-azimuth minimising |T|, but not maximising R·Z. Finally, in Fig. 3.3c, |T| and R·Z curves are plotted for each possible back-azimuth angle and the best compromise between max(R·Z) and min(|T|) is represented by the vertical blue line. According to KNMI (pers. comm.), the ≈180° difference results from the delay of a few milliseconds observed between the radial and vertical components as illustrated by the two vertical dashed lines in Fig. 3.3a. This is also discussed in their report (Dost et al., 2022), but as stated there, no systematic correction was applied, potentially implying that their results were fine-tuned manually. Because manual work is subjective and difficult to reproduce, we did not explore the matter further.

To conclude, regarding the orientation of the horizontal components of the accelerometers, we were able to reproduce most of KNMI's results by following the same automatic approach as described in Dost et al., 2022. However, some results display huge differences resulting in larger final uncertainties. These differences are potentially related to the time delay sometimes observed between the vertical and radial components. However, if such small delays have such a large impact on the results, it indicates that the analysis is unstable. Besides, it is worthwhile noting that the orientation analysis was carried out on less than 3 events for half of the accelerometers, which is too little to guarantee a stable statistical analysis. Therefore, the user must be warned and be cautious in using the sensor orientations. Although standard deviations are stored in the StationXML files, they do not reflect the full uncertainty, especially in case of a low number of analysed events. We therefore recommend that KNMI emphasises this situation in their report (Dost et al., 2022).

Although most of KNMI's orientation results could be confirmed, the remaining are afflicted with large differences, which result from instabilities in the analysis. These uncertainties are not completely reflected by standard deviations stored in the StationXML files. Therefore, users should be cautioned and be cautious in applying sensor orientations in their analyses.

[7] This method cannot resolve the 180° ambiguity.

DISCUSSION ON ORIENTATION ANGLES UNCERTAINTIES

KNMI computed uncertainties by using the weighted mean of the standard deviations of the two methods, where the weights correspond to the number of events, resulting in smaller combined uncertainties. However, such an approach is fully valid only if the two methods were independent, which is not the case. An alternative way would be to combine the results of the two methods and compute the resulting standard deviation. In this case, the uncertainties would reflect the dispersion of different observations; thus, they tend to be larger. However, the independence assumption in this approach is also violated. One must be aware of the poor statistical significance of the results (only a handful of observations at each accelerometer) and therefore use the orientation angles with caution.

3.2.2 Amplitude validity and gain irregularities

Assessment of the KNMI quality assurance tests

KNMI apraised the amplitudes of waveforms recorded on the accelerometers by computing event and station terms. These can be obtained if a ground-motion model is available, which is the case for the Groningen field (Bommer et al., 2019). A ground motion model (GMM) or ground-motion prediction equation (GMPE), as the name indicates, predicts the ground-motion amplitude resulting from an event (described in terms of its location and, more importantly, magnitude) at a specific distance. The station term is defined as the residual between observed and predicted amplitudes for a given event at a specific station, while the event term is defined as the average of the station terms for a specific event.

GMPEs are usually developed for larger magnitude events. For their analysis, KNMI selected a magnitude threshold of 2.5. Moreover, a minimum of 3 stations recording the event was required in order to compute the event term. Out of 82 events, only 20 events fit those criteria (Dost et al., 2022). Subsequently, the event terms obtained for the accelerometer data were compared to more recent events using both the current accelerometer and borehole networks (B- and G-networks, respectively). The analysis of both event and station terms led KNMI to conclude that despite the limitation of only few available events, no particular problem concerning the amplitudes of the accelerometer data could be identified. Instead of following their methodology, we conducted two independent analyses to verify the amplitudes of the accelerometer data.

Maximum amplitude vs distance

Firstly, we extracted the maximum amplitude of each component for each event-station pair. For that purpose, data were instrument-corrected (resulting in all amplitudes being expressed in m/s^2), rotated into the R-T-Z system and filtered using a butterworth band-pass filter from 2 to 35 Hz. Plotting these amplitudes as a function of event-station distance should highlight large discrepancies (Fig. 3.4). In general, we do not observe any particular issue: the amplitudes decrease as the distances increase. The largest amplitudes are observed at the Roswinkel stations for events with magnitude larger than 3 at very short distances (less than 2 km).

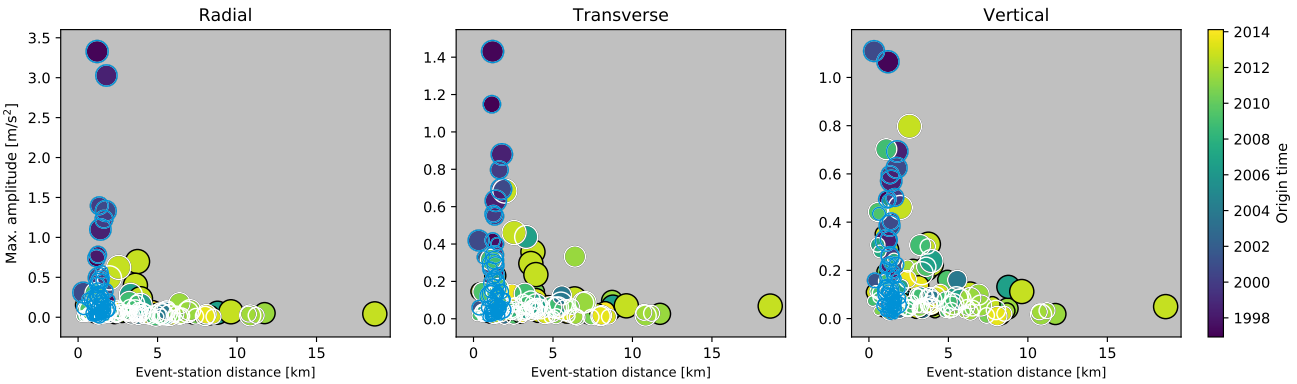

FIGURE 3.4: Maximum amplitude in m/s^2 as a function of distance for all records of (a) the radial, (b) the transverse and (c) the vertical components. Black-bordered circles represent AC-63 sensors, white-bordered circles AC-23 sensors and blue-bordered circles Roswinkel stations (ROS*). Circles are coloured by event origin time and their size is scaled by event magnitude.

RMS amplitude

Secondly, we extracted the RMS amplitude prior to the first arrival for each station to track potential changes with time. We define the RMS as the square root of the mean of the squared amplitudes. To obtain the first arrival, the same procedure as used for the orientation analysis was implemented. The RMS computation window starts at the beginning of the file and stops 0.1 s before the signal onset. Before analysis, waveform data were instrument-corrected and filtered between 2 and 35 Hz. An example is displayed in Fig. 3.5.

Since the record lengths vary (Fig. 1.4), the RMS window lengths vary as well (Fig. 3.6); most analysis windows have a length of approximately 5 s. In general, the longer the time window, the more stable the measurement.

Fig. 3.7 shows all RMS amplitudes per component over time. Similar plots are available for all stations individually in Figs. A.2 to A.4 in the appendix (pp. 74-76). Components, which have been reported as temporally malfunctioning by KNMI (Dost et al., 2022) are represented by red-bordered circles and listed in Table 3.2.

TABLE 3.2: List of files with erroneous amplitudes (red-bordered circles in Fig. 3.7).

Station	Event origin time	Comment
ROS1	1996-12-06 16:44:50.496	KNMI reported malfunctioning X(=H1) component
	1996-12-28 18:14:26.531	"
ROS6	2004-09-06 20:31:16.345	KNMI reported significant electronic noise
	2006-03-25 13:54:32.210	"
	2006-03-25 13:55:47.080	"

To conclude, if we exclude records reported as malfunctioning (Table 3.2), the RMS amplitudes do not exhibit any conspicuous changes over time. It is worthwhile noting that some stations display

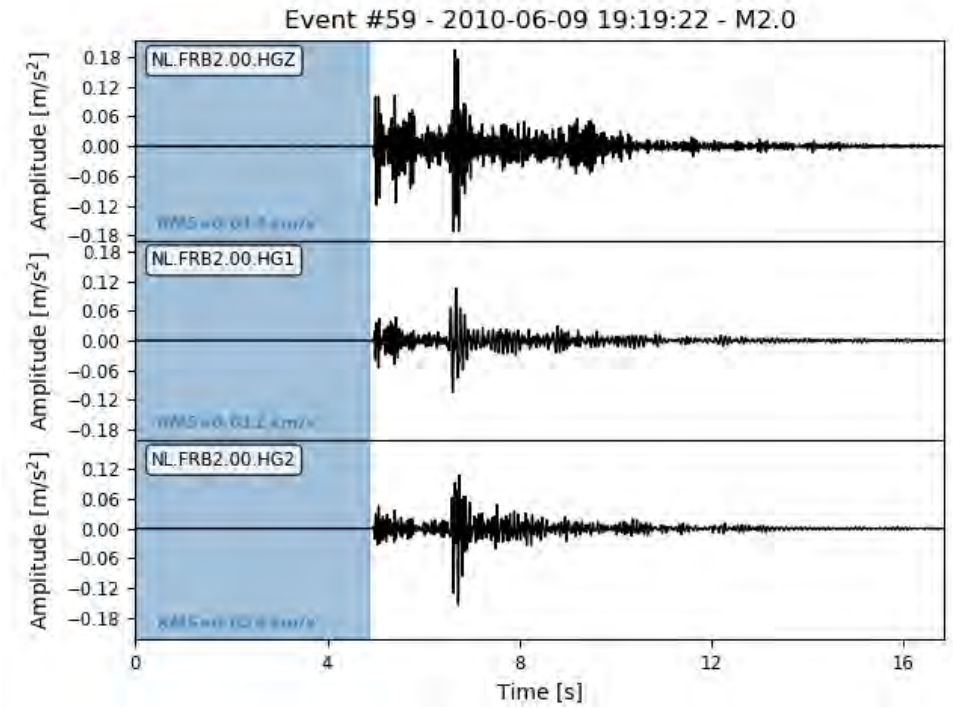

FIGURE 3.5: Three-component waveform records of the 9th June 2010 event recorded at FRB2. The blue-shaded area represents the RMS analysis window.

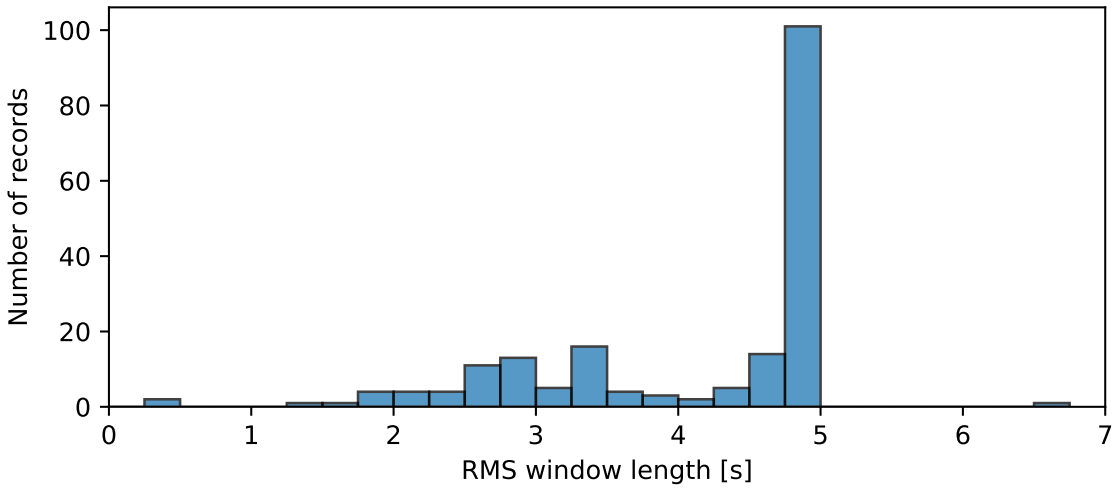

FIGURE 3.6: Distribution of the RMS window lengths in seconds for accelerometer data.

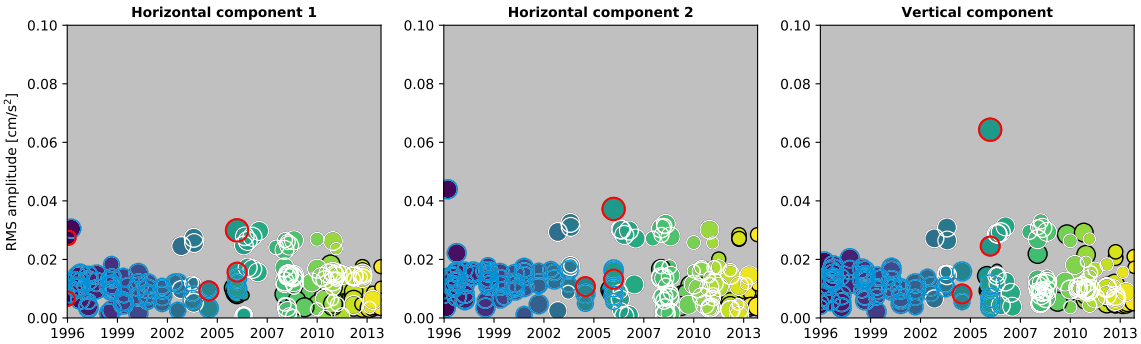

FIGURE 3.7: RMS amplitudes in cm/s^2 as a function of time. Black-bordered circles represent AC-63 sensors, white-bordered circles AC-23 sensors and blue-bordered circles Roswinkel stations (ROS*). Red-bordered circles correspond to components reported as malfunctioning by KNMI. Circles are coloured by event origin time and their size is scaled by the RMS window length.

slightly higher RMS amplitudes than others (e.g. WSE, ZAN2 and to a lesser extent ZAN1 and GARST, see Figs. A.2 to A.4), corresponding to accelerometers exhibiting a higher station term (cp. to Fig. 30, Dost et al., 2022). This behaviour may be attributed to higher seismic noise close to the stations in question.

Summary

We did not detect specific issues with accelerometer data amplitudes, but the amount of data available for the analysis is limited.

Similar to KNMI, we do not report any specific issues related to the accelerometer data amplitudes. It is worthwhile noting, however, that the limited amount of available data (both in terms of number of records and length of records) makes it difficult to conduct an exhaustive analysis.

3.2.3 Data timing

In this section, accelerometer data timing is evaluated. The timing quality is assessed via a flag in the header of the miniSEED files (Dost et al., 2022). KNMI assigned a value of 100 in case of synchronisation and 0 if there was clearly no synchronisation or if the synchronisation could not be determined.

Assessment of the KNMI quality assurance tests

As described by KNMI, time flags are stored in the blockette 1001 of each trace header in the miniSEED files. However, to get access to this information while reading the miniSEED file with ObsPy, the "details" option has to be set as True (see code snippet 3.1). Note that this information is currently not documented in the Obspy documentation of the "read" function, which makes it difficult to find for users. Moreover, this option is by default set as False and cannot be changed by the user when

calling the "get_waveforms" function[8] to download data from the server (more details in section 4.1). To assist potential future users of the data, we provide an exhaustive list of available accelerometer records together with their time flags in Table A.2 in appendix of this report (p. 77).

```
from obspy import read
# Read the miniSEED file and set the "details" option to True
st = read('200311162004.mseed', details=True)
# Loop over each trace and read the time flag in the blockette 1001
for tr in st:
    time_flag = tr.stats.mseed.blkt1001.timing_quality
    print(tr.id, time_flag)
```

CODE SNIPPET 3.1: Extracting time flags from accelerometer waveform data

Waveform plots

In order to review the timing of the records, we generated a series of waveform plots to which we added relevant information in the following manner:

- for AC-23 sensors: each synchronised record is coloured **black** and and each non-synchronised record is coloured in **light red**;
- similarly, for AC-63 sensors, each synchronised record is coloured **blue**, while non-synchronised records are coloured in **pink**. Note that information on time synchronisation was not possible to obtain for AC-63 sensors (Dost et al., 2022), thus by default, all records of stations FRB2, GARST, HKS, KANT, STDM and WIN were declared as non-synchronised.
- the event origin time is represented by an **orange** vertical dashed line.
- the P-wave arrival times that could be extracted from the event catalogue (QuakeML) are represented by **blue** vertical continuous lines.
- the theoretical P-wave arrival times estimated using an identical 1D velocity model both for Groningen and Roswinkel are represented by **blue** vertical dashed lines.

Different types of figures were generated displaying:

1. three-component waveforms for events aligned by the event origin time. This type of plot allows to spot obvious timing errors.
2. waveforms recorded on vertical components aligned by the event origin time and sorted by event-station distance. This type of plot allows to find smaller timing errors in addition. However, apparent timing errors may also be related to erroneous event locations.
3. three-component waveforms per station in order to identify stations with recurrent problems.

[8] An alternative way would have been to use the get_flag routine resulting in the flags being stored in an array. Presumably, each element of the array corresponds to a record in the miniSEED file. However, it turned out that the number of elements did not always correspond to the number of records, which made it impossible to associate the time flags with the data. After discussing with KNMI, it seems that the problem originates from the Obspy routine, which does not embed the information correctly if the miniSEED file contains multiple stations.

In this report, we only show the first type of plots for cases in which problems were identified. Please note that the information related to the event origin time, event location and event picks was extracted from the event catalogue. For the event-station distances, station coordinates were read from the StationXML files and the distances were computed in the lat/lon coordinate system before being converted to km. Although the theoretical travel-times were also computed using the event and station information from the respective QuakeML and StationXML files, we do not expect a perfect match to the data, since we may have employed a different velocity model than KNMI.

After having visually inspected the different plots, it resulted that:

- For most records, all available information match (e.g. Fig. 3.8a).
- For some records, timing errors are obvious and well reported by KNMI (e.g. Fig. 3.8b).
- For several events located in the Roswinkel field, the waveforms are delayed relatively to both the theoretical and manually determined arrival times, although the time flags indicate synchronicity (e.g. Figure 3.8c). KNMI (pers. comm.) explained this observation by a relocation carried out for these events.
- For other records, it is difficult to determine whether (1) the time was not synchronised, (2) if the origin time or location of the events was not well estimated or (3) if the velocity model employed to compute the theoretical P-wave arrival times was not adapted. An example is shown in Fig. 3.8d. None of the theoretical P-wave arrival times match the data even though timing issues were only reported at two stations: GARST and WIN (WIN records are outside the x-axis limits of the plot).
- In addition, some of the P-wave arrival times stored in the QuakeML files do not match the data (events #13 (ROS1), #53 (MID1), #66 (KANT), #74 (KANT, STDM), #75 (HKS), #80 (HKS)).

Time flags extracted for each record are reported in Table A.2 in the appendix (p. 77).

Summary

Assessing the absolute timing of the accelerometer triggered data is not simple. On many occasions, the information from the QuakeML event catalogue and the waveform data did not entirely match and it was difficult to conclude whether the problem is linked to a time synchronisation issue or to an issue in the event catalogue.

Since QuakeML files were not examined and corrected in this project, the cause of mismatches between event catalogue information and waveforms is difficult to assess.

3.2.4 Conclusion

Standard quality control methods cannot be applied for the analysis of the triggered accelerometer data. There is no information available on synchronicity of the AC-63 records (comprising 25% of the records). Ac-

Accelerometer data were analysed and evaluated. Due to both the limited amount of data and the shortness of the records, it is not

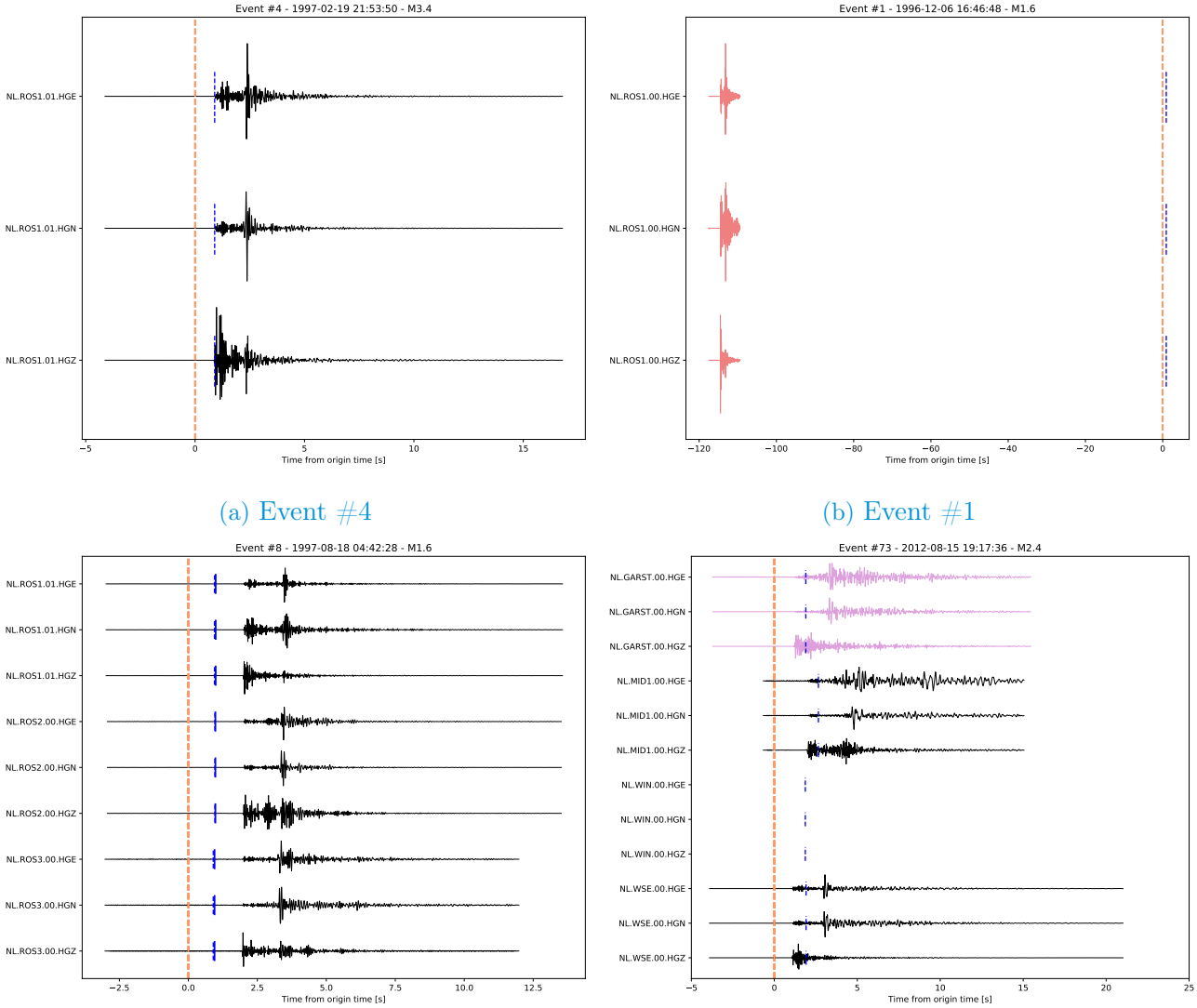

(a) Event #4

(b) Event #1

(c) Event #8

(d) Event #73

FIGURE 3.8: Examples of three-component accelerometer waveform data without (a) and with (b-d) timing issues. Description of individual examples in the text.

straightforward to apply standard quality control methods.

Timing information for AC-63 sensors could not be recovered, i.e. for at least 25% of the total number of records, it is unknown if they suffer from time synchronisation problems.

Sensor orientation results were partly unstable and results should be used with caution. Although uncertainties on orientation angles are stored in the metadata, they may not necessarily be representative of the real uncertainties due to the very limited number of events that could be analysed.

The analysis of amplitudes did not reveal any major issue.

3.3 Borehole data

3.3.1 Sensor orientation

Vertical component

Similar to KNMI (Dost et al., 2022), we used teleseismic events to check the polarity of the vertical components of the borehole stations. However, we did not compare the traces with broadband records, but employed the direct P phase or the PKP phase, which at an approximate distance of 145° has a large amplitude due to a focusing effect (Fig. 3.9). This test constitutes only a spot check, since the events chosen for the analysis do not cover the whole time period under analysis. We employed data from the events listed in Table 3.3 and displayed in Fig. 3.10.

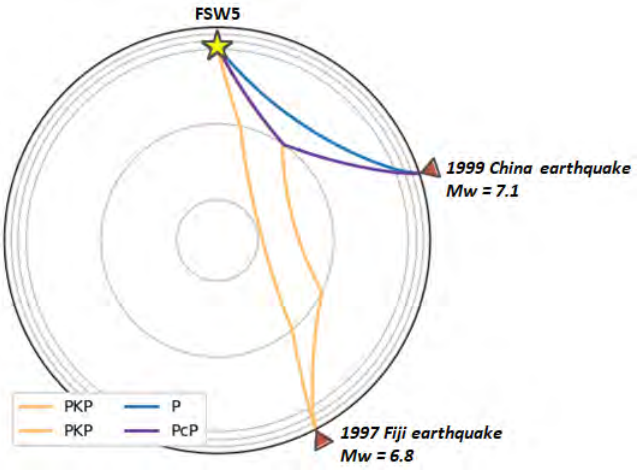

FIGURE 3.9: Illustration of the ray paths of the phases observed for the 1997 Fiji and 1999 China earthquakes.

TABLE 3.3: List of teleseismic earthquakes used to check the borehole instruments' orientation. Δ is the epicentral distance expressed in degrees.

Datetime	Latitude [°]	Longitude [°]	Depth [km]	Mw	Region	Δ [°]
1997-09-04 04:23:35.730	-26.4997	178.3193	608.0	6.8	Fiji	153
1998-03-29 19:48:12.970	-17.6585	-178.9897	499.6	7.1	Fiji	144
1999-04-08 13:10:34.130	43.609	130.413	564.1	7.1	China	72

Vertical component waveform data recorded at all levels of available borehole stations are displayed in Fig. 3.11 for the first earthquake and in the appendix for the two others (Figs. B.6 and B.7, p. 96). All waveforms were instrument-corrected to velocity, oriented in the geographical coordinate system using the information from StationXML files and filtered at low frequencies between 0.05 and 0.8 Hz.

Our observations are summarised below:

- for the 1997 Fiji earthquake (Fig. 3.11): polarities of the PKP-phases are consistent across the stations, but show a polarity reversal **at PPB level 2**. In addition, the vertical component of VBG level 4 seems to be malfunctioning, as well as the three components of ZL2 level 4 and ZLV levels 3 and 4.

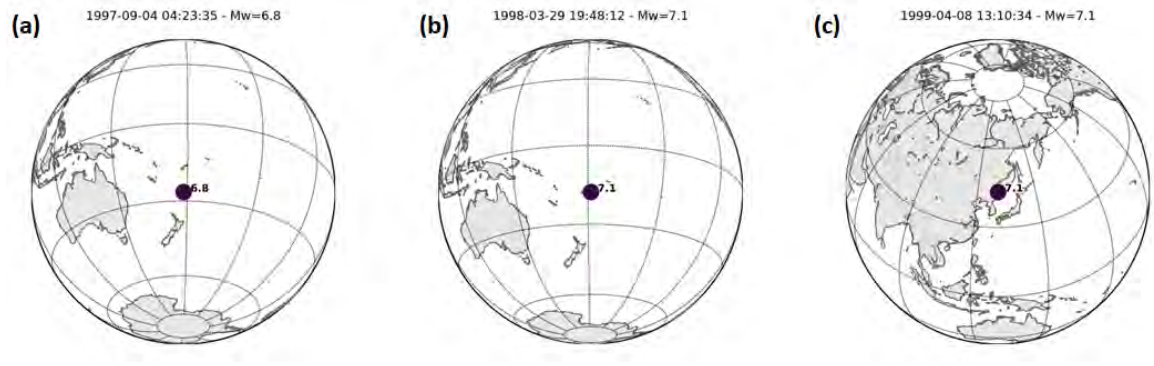

FIGURE 3.10: Location of the three teleseismic earthquakes employed to check the orientation of the borehole sensors.

- for the 1998 Fiji earthquake (Fig. B.6): polarities of the PKP-phases are consistent across the stations, but show a polarity reversal **at PPB level 2**. In addition, the vertical component of VBG level 4 seems to be malfunctioning and no data were available for ZL2. Also note that the data available at OTL span the time period just after the PKP-phase arrivals.
- for the 1999 China earthquake (Fig. B.7): polarities are consistent across the stations, including PPB level 2. Only the vertical component of VBG level 4 is malfunctioning.

To conclude, the orientation of the vertical component (positive up) of the borehole sensors is consistent. The observed polarity reversal at PPB2 between May 1995 and May 1998 is reported by KNMI (Dost et al., 2022), but not yet included in the StationXML file. The other malfunctioning components are also reported in Appendix B of KNMI's report. Only the orientation of the vertical component of VBG4 could not be assessed and, as indicated by KNMI, this component was never repaired.

Horizontal components

The orientation of the horizontal components of most borehole stations was determined using check shots as reported by Diephuis and Asmussen (1995) and later on, also explosions and local events (Ruigrok et al., 2019). The analysis of check shots cannot be repeated here and all the documents related to it were appended to KNMI's report (Dost et al., 2022). Dost et al. (2022) emphasised that the orientation of borehole sensors placed at the surface was more difficult to assess due to insufficient check shot data quality and that therefore most of them (except FSW1) were assigned default values of 0° and 90° for the first and second horizontal components, respectively.

The investigation presented in Dost et al. (2022) merely aims to resolve the 180° ambiguity by comparing the polarity of the vertical and radial components, not to assess the general orientation of horizontal components. As noted by KNMI, only the orientation for FSW, ENM, PPB and VBG remained the same as in previous documents; for all other stations, the orientation of the horizontal components was shifted by 180°. Orientations are verified by Dost et al. (2022) by showing event waveforms rotated into the R-T-Z system, in which radial and vertical components should be in phase and thus, exhibit the same polarity for the P-wave onsets.

It is also worthwhile noting that, contrary to the accelerometers, no uncertainties are assigned to

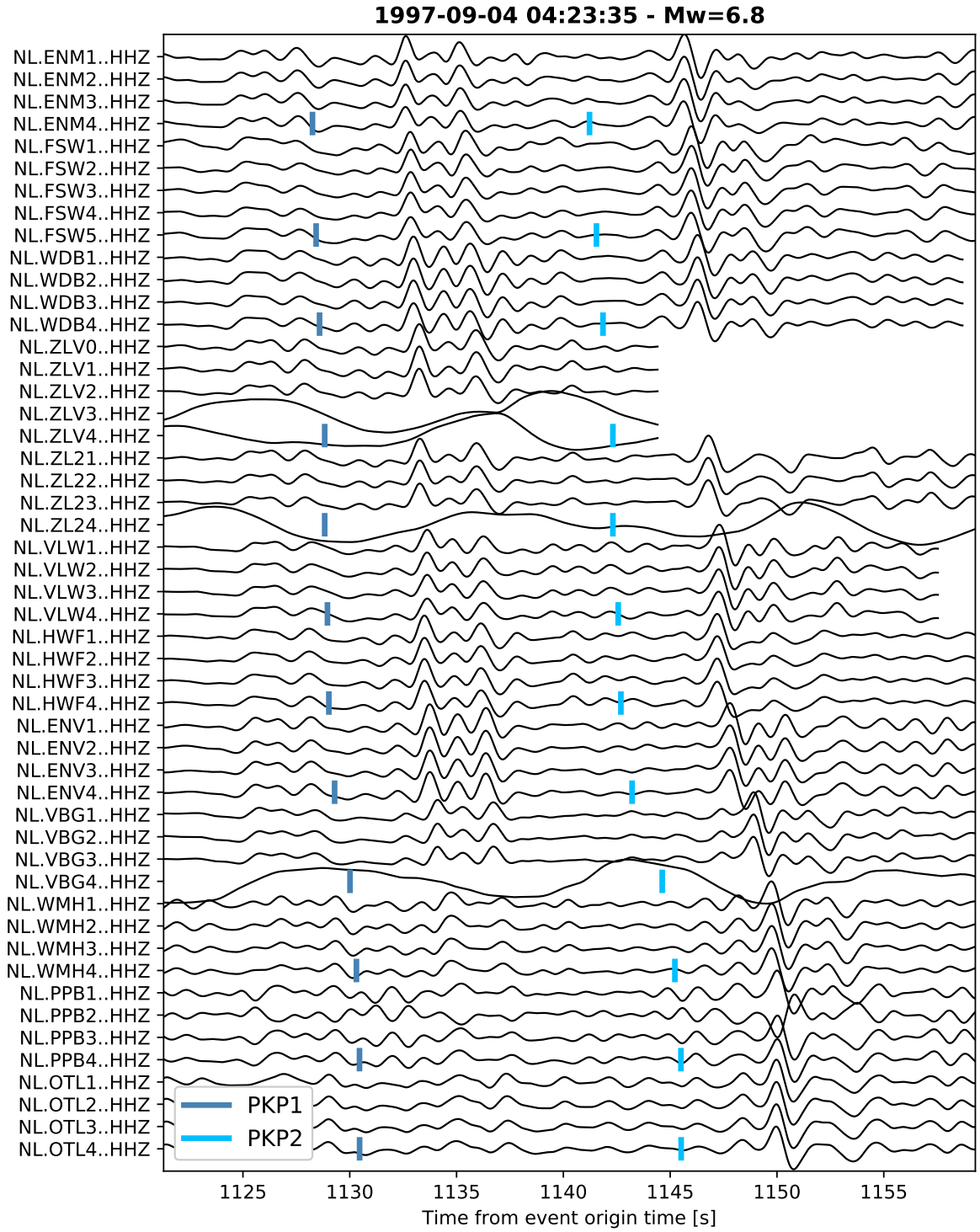

FIGURE 3.11: Vertical component waveforms recorded on each level of every borehole station for the 1997 M_w 6.8 Fiji earthquake and filtered between 0.05 and 0.8 Hz. Blue vertical bars represent the theoretical arrival times of the PKP-phases using the iasp91 1D velocity model (Kennett and Engdahl, 1991). Traces have been sorted by decreasing distance to the source from top to bottom.

orientation angles in the borehole StationXML files.

In order to assess the orientation of the horizontal components of the borehole sensors, we performed a semi-automated approach similar to the one implemented for the accelerometer data. Data selection and steps to obtain the final results are briefly described below:

- A first, rough selection based on the event catalogue was performed, keeping only records corresponding to events with local magnitude above 2.5 and event-station distance over 2 km. This resulted in 970 records.
- P-wave onsets were picked manually on instrument-corrected and bandpass-filtered data (2-35 Hz) recorded on the vertical component, whenever possible. This resulted in 823 records.
- A more strict selection of records was achieved based on a signal-to-noise ratio criterion ($\geq$25) computed on the vertical component only [9]. This resulted in 619 records.
- An automated orientation analysis was conducted (same as for the accelerometer data, see section 3.2) aiming to maximise R·Z and minimise |T|. For that purpose, we chose a time window starting 0.1 s before and reaching up to 0.25 to 0.35 s after the P-onset [10].
- Results were inspected visually (three-component waveforms in the analysis window and hodograms, see Fig. B.18, p. 106 for an example); following this, a number of records, for which the horizontal component data were extremely noisy, was rejected. This narrowed the selection to a total of 404 records, unequally split between the different levels of the 12 borehole stations.

Final results are presented in Fig. 3.12 and Figs. B.8 to B.17 (pp. 103-106) in the appendix for each borehole station.

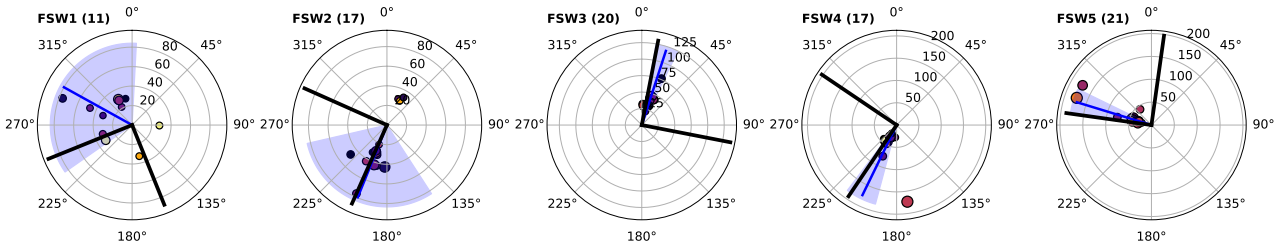

FIGURE 3.12: Orientation results for all levels of station FSW. The number of measurements contributing to the mean solution (blue line) is indicated in parentheses. Angles stored in the StationXML file are represented by the two black lines. Individual results are shown as circles with colour depending on the linearity of the particle motion in the horizontal plane (see Fig. 3.13) and size being proportional to event magnitude, plotted as function of the event-station distance in km (radial axis). Blue-shaded areas symbolise standard deviations.

[9] We defined the SNR as the maximum amplitude after the P-onset over the mean amplitude measured from the start of the record to 50 samples before the P-onset.

[10] For more distant earthquakes ($\geq$ 100 km), a longer time window was chosen. In practice, it would be better if the analysis window would be adapted manually for each record.

Individual results are summarised in Table B.13 (p. 98) and mean results in Table 3.4. Note that due to

TABLE 3.4: Summary of the borehole station orientation analysis. $\bar{\theta}$ is the circular mean of the azimuth angles found from all events at each station, while σ_θ is the circular standard deviation. θ_{XML} denotes angles assigned to the first horizontal component in the station XML files. Cells coloured in orange highlight differences over 30° and in red over 90°.

Station	# events	$\bar{\theta}$[°]	σ_θ[°]	θ_{XML}[°]	$\bar{\theta}$-θ_{XML}[°]
ENM1	6	140	52	122	18
ENM2	8	179	9	177	2
ENM3	10	197	82	164	33
ENM4	10	89	24	91	-2
ENV1	8	316	11	322	-6
ENV2	10	333	46	337	-4
ENV3	12	208	4	207	1
ENV4	11	301	6	311	-10
FSW1	11	299	64	158	141
FSW2	17	202	55	204	-2
FSW3	20	18	8	11	7
FSW4	17	206	11	214	-8
FSW5	21	287	9	278	9
HWF0*	2	162	11	0	162
HWF1	10	164	9	166	-2
HWF2	11	261	13	257	4
HWF3	13	342	12	342	0
HWF4	14	200	11	199	1
OTL1	1	80	0	89	-9
OTL2	2	192	8	191	1
OTL3	1	344	0	325	19
OTL4	2	105	2	115	-10
VBG1	3	297	78	340	-43
VBG2	4	283	3	294	-11
VBG3	9	97	41	104	-7
VBG4	3	74	12	90	-16
VLW0*	2	321	30	0	-39
VLW1	7	156	100	202	-46
VLW2	7	249	12	252	-3
VLW3	5	123	3	123	0
VLW4	9	77	6	89	-12
WDB0*	5	174	70	0	174
WDB1	8	85	42	94	-9
WDB2	11	220	26	232	-12
WDB3	2	192	20	131	61
WDB4	11	240	23	250	-10
WMH2	1	350	0	9	-19
WMH3	1	282	0	280	2
WMH4	1	221	0	210	11
ZL21	2	96	120	25	71
ZL22	4	356	5	350	6
ZL23	6	166	7	160	6
ZL24	2	43	13	44	-1
ZLV0*	10	185	23	0	-175
ZLV1	14	76	61	64	12
ZLV2	20	134	79	133	1
ZLV3	20	226	30	222	4
ZLV4	20	131	10	130	1

the selection criteria, no results could be obtained for PPB (all levels) and WMH1. Orientation angles of levels WMH2-4 resulted from a single measurement each. The same is true for OTL1-4.

The resulting mean angles are mostly in good agreement (within 20°) with the ones stored in the StationXML files. As expected, uncertainties (i.e. scattering of individual results) are usually larger for sensors placed closer to the surface (e.g. Fig. 3.12), despite the contrary behaviour is observed as well (e.g. ENM3 is less constrained than ENM2, see Fig. B.8, p. 103). Because the results were too scattered, borehole sensors placed at the surface were not oriented previously, except FSW1. Our results for this latter sensor, despite a few outliers, seem to be consistent and give a direction of 300°. This value is rather different from the one reported by KNMI (leftmost plot in Fig. 3.12), which can be

explained by differences both in the data used for the analysis and in the method employed, since KNMI used S-waves (Dost et al., 2022). For other surface sensors, either records are too sparse (HWF0, VLW0) or results are too dispersed (WDB0) to draw a final conclusion. Furthermore, in Table 3.4, it appears that results that show medium discrepancies ($30° \leq \bar{\theta}\text{-}\theta_{XML} \leq 90°$, marked in orange) and are not related to borehole sensors placed at the surface correspond to either a low number of measurements (≤ 3) or are affected by larger uncertainties. However, for ZLV0, all ten measurements are relatively consistent (see Fig. B.17, p. 106).

A selection of good quality results is visible in the appendix in Figs. B.18 to B.28 (pp. 106-111) for a selected sensor within each borehole. Results are considered to be of good quality if waveforms have a sufficient SNR and the particle motion is linear in both the horizontal and the radial-vertical planes. Such high-quality results always agree within $\pm 20°$ with the orientation angles given in the StationXML file (black lines). Note that the angle that results from the decomposition into eigenvectors and eigenvalues of the particle motion in the horizontal plane (red line) is often, but not always, consistent with the orientation found by employing the method by Jepsen and Kennett (1990).

Finally, as for the accelerometer data, angles deviating from the mean solution by close to 180° can occasionally be explained by a delay between radial and vertical components (Fig. 3.13). However, in

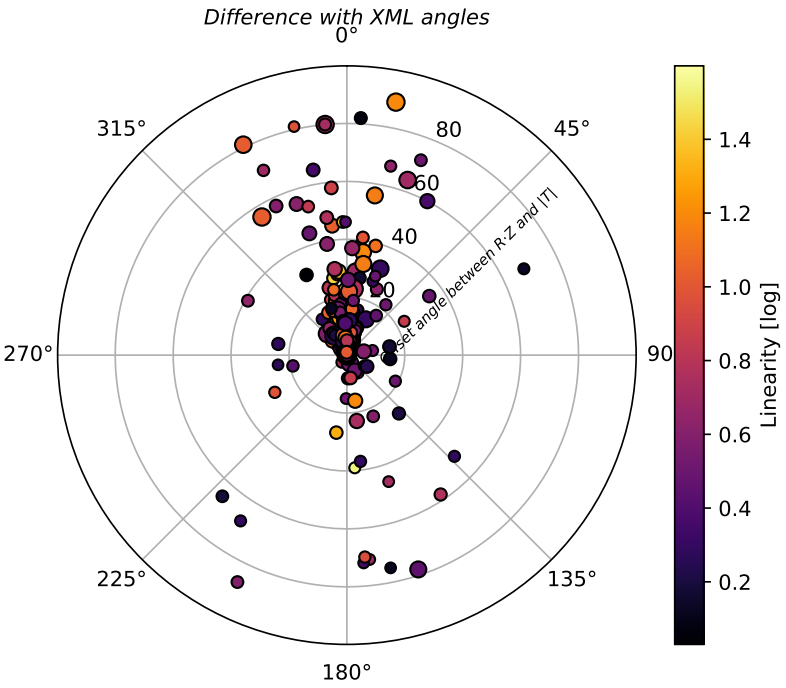

FIGURE 3.13: Angular difference between our results and angles stored in borehole StationXML files. Non-oriented surface sensors (HWF0, VLW0, WDB0 and ZLV0) are removed from this plot. The radial axis indicates the offset angle between R·Z and |T| measured in our analysis. Circles are coloured by the linearity of the particle motion.

the case of the surface sensor FSW1, such delay is not observed (see Fig. B.29, p. 112).

DISCUSSION ON ORIENTATION ANGLES UNCERTAINTIES

Uncertainties of orientation angles for individual borehole levels are not provided in the StationXML files, but are considered to be low (<10° according to Dost et al., 2022). They were computed using weighted standard deviation (Ruigrok et al., 2019; KNMI, 2019), namely using the inverse-variance weighting scheme (*Wikipedia*, last accessed 14/09/2022). However, we find that this way of computing uncertainties is not particularly suited to this case, where the uncertainties should be representative of the dispersion of the observations. Instead, it returns the smallest variance, which explains why the uncertainty decreases if the number of observations increases. However, in our opinion, the weighted uncertainty defined for the accelerometers (see our previous comment in section 3.2) would be more suitable here, especially since in this case, the independence assumption is not violated, because the observations result from different data sets, such as check shots, local explosions and local seismicity.

Summary

Both the orientation of the vertical and horizontal components of borehole sensors is consistent with the values in the StationXML files. The only exception is FSW1, where components might be switched.

The polarity of the vertical components of borehole sensors was checked using teleseismic earthquake records and showed that they are consistently oriented upwards (i.e., the dip is -90°), with only one exception as described in Dost et al. (2022). The orientation of horizontal components was verified by taking advantage of the locally induced seismic events and agrees well with the orientations previously obtained from check shots. In addition, orientation angles of surface sensors that could hitherto not be analysed could be evaluated now, although the results should be employed only cautiously.

3.3.2 Amplitude validity and gain irregularities

Assessment of the KNMI quality assurance tests

KNMI carried out a relative comparison of amplitudes recorded at different borehole levels, which helps spotting issues at a specific level for a specific component. For that purpose, the maximum amplitudes of a given event recorded by a certain component at a specific borehole are normalised by the average over all levels, based on the assumption that it is very unlikely that several geophones experience a similar problem simultaneously. For example, if a record presents a significantly lower amplitude than average (KNMI detects an anomaly below a threshold of 0.4), it may indicate a problem. However, the shallower the geophone, the higher the amplitude due to amplification in the shallow layers. Thus, the ratio tends to increase significantly for sensors located closer to the surface.

The analysis was performed for raw (i.e. not corrected for instrument response) and unfiltered data. Note that only deep levels were considered, except in the case of FSW where the surface geophone FSW1 was also included. This means that no information on the validity of amplitudes recorded on the surface sensors co-located with the boreholes is given by KNMI. Dost et al. (2022) provide figures for each borehole station together with descriptions of the identified anomalies. The method constitutes

a good approach to track problems sporadically affecting a component or a geophone at a specific level, but will not be able to identify, for example, if a borehole station experiences higher noise conditions at all levels.

Maximum amplitudes vs distance

We apply the same approach as for the accelerometer data. Data were instrument-corrected (amplitudes expressed in m/s) and rotated into the ray system using the sensor orientation from the StationXML files and the back-azimuth angles computed from the event location. Data were filtered using a butterworth band-pass filter from 2 to 50 Hz. Results are presented in Fig. 3.14. Malfunction-

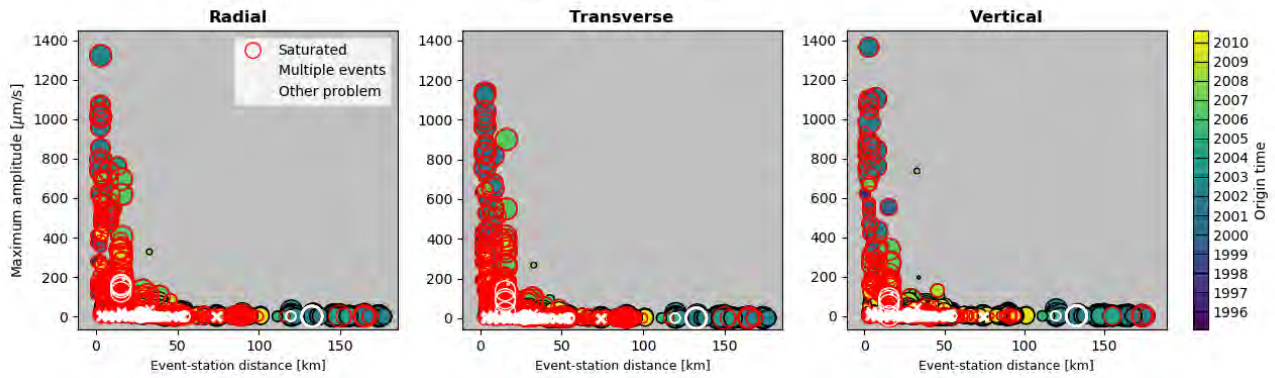

FIGURE 3.14: Maximum amplitudes in μm/s as a function of distance for all records on (a) the radial, (b) the transverse and (c) the vertical components. Circles are coloured by event origin time and their size is scaled by event magnitude. Red-bordered circles symbolise saturated records reported by KNMI, white-bordered circles erroneous records reported by KNMI and white crosses records that contain more than one event.

ing components and saturated records collected by KNMI in their report (tables 12-15 in section 5.2.4 and appendix G in Dost et al., 2022) are highlighted. The information is also summarised visually in appendix B.5 (p. 112). In addition, we marked the events, which belong to records containing multiple events, by white crosses (see Table 1.3, p. 19). In these cases, only the maximum amplitude of the largest event in the file was measured.

In Fig. 3.14, it appears that a large number of records at small distances are reported as saturated by KNMI. Therefore, Fig. B.54 (p. 132) in the appendix shows the results without saturated and malfunctioning records. No erroneous amplitudes could be identified. Individual results by stations and levels are available in the appendix B.6 in Figs. B.42 to B.53 (pp. 120-131).

RMS amplitudes

Subsequently, we applied a similar approach as for the accelerometer data. Data were instrument-corrected (amplitudes expressed in m/s) and filtered using a butterworth band-pass filter from 2 to 50 Hz. Similar to KNMI, we did not rotate the data, hence the horizontal components are pseudo-North and pseudo-East. The noise window was chosen from the start of the record to 0.1 s before the theoretical P-wave arrival time. In most cases, this is sufficient to ensure that the window does not include signals due to either mismodelling of the velocity model, event location inaccuracies or

minor time synchronisation errors. However, if major timing errors occur, the approach is defective. As shown in Fig. 3.15, there is a large variability in the RMS window lengths with a quasi-uniform distribution from 10 to 128 s.

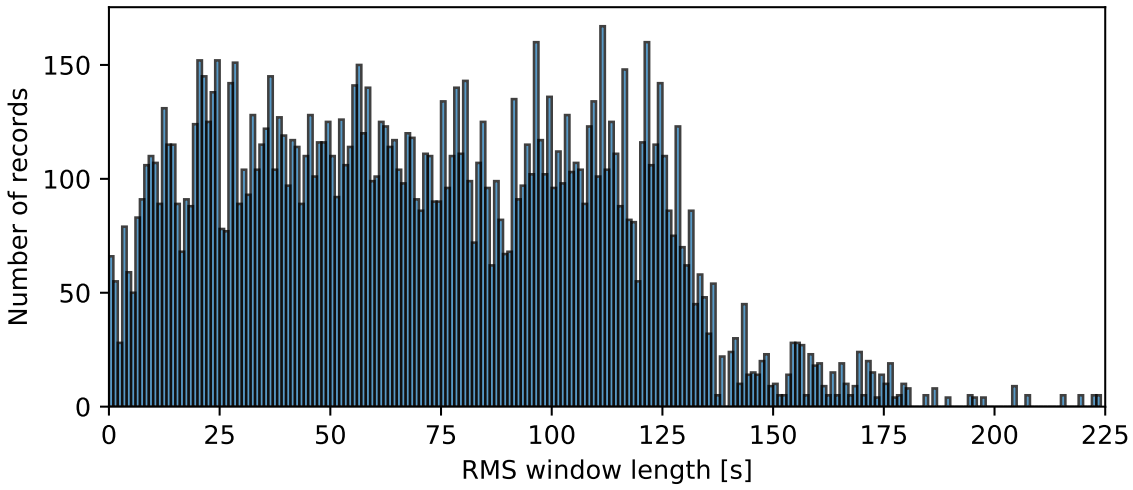

FIGURE 3.15: Distribution of the RMS window length in seconds for borehole data.

Results are presented in Fig. 3.16. There seems to be a slight increase in amplitude levels after the

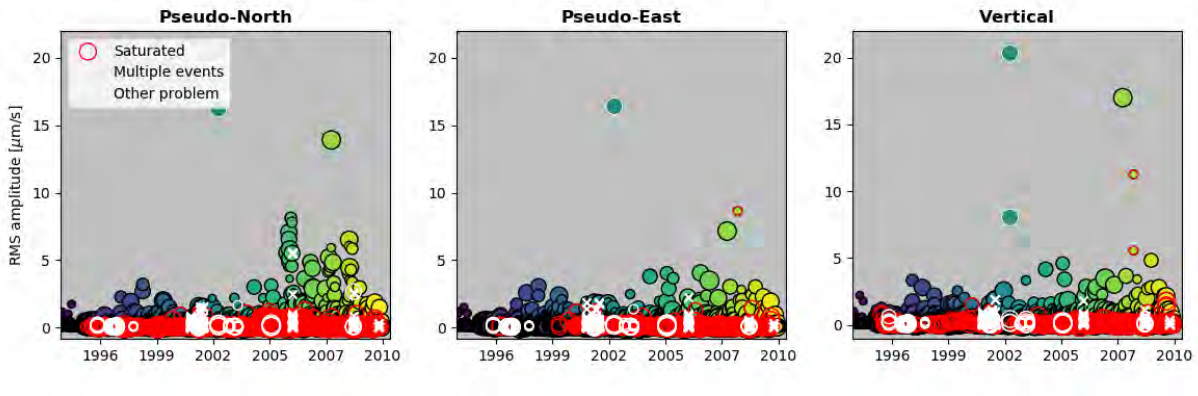

FIGURE 3.16: RMS amplitudes in μm/s as a function of time for all records on the (a) pseudo-North, (b) pseudo-East and (c) vertical components. Circles are coloured by event origin time and their size is scaled by RMS window lengths. Red-bordered circles symbolise saturated records and white-bordered circles erroneous records reported by KNMI and white crosses indicate records that contain multiple events.

year 2005. However, the individual results for each station and level have to be assessed before an interpretation (appendix B.7, Figs. B.55 to B.66, pp. 133-144). Note that all records which clearly display anomalous RMS amplitudes in Fig. 3.16 correspond to records reported as problematic by KNMI, with the exception of the 2008-02-19 15:44:51 event recorded on VLW, for which the noise window seems to include a local spurious signal (Fig. B.67, p. 145).

For each station, we manually reviewed the records corresponding to abnormally high amplitudes. We defined an outlier as a record with an RMS amplitude higher than the 95th percentile of all records

for a given station, level and component. Note that we excluded PPB, OTL and WMH, since too little data was available for these stations. In general, we found that most anomalies were due to either:

- local noise conditions or electronic noise affecting the records (e.g. Fig. B.67, Fig. B.68, Fig. B.69 and Fig. B.70, pp. 145-pp. 146), or
- the noise window containing the event (e.g. Fig. B.71,p. 147);

Note that many of these outliers were already flagged by KNMI in their report. We also noticed that records featuring abnormally low amplitudes correspond to smaller noise windows, i.e. the noise sample is not representative.

We are not only interested in individual records, but also in longer-term changes. Therefore, in Fig. B.72 and Figs. B.73 to B.81 (pp. 147-156), we present the same results without outliers. We summarise our observations in the following:

- **EMN** (Fig. B.55, p. 133 & Fig. B.73, p. 148): RMS amplitudes seem to steadily increase over time. From 2008 on, amplitudes do not exceed 0.15 μm/s on the pseudo-East component of ENM1.
- **ENV** (Fig. B.56, p. 134 & Fig. B.74, p. 149): RMS amplitudes seem to steadily increase over time. The most striking change is observed on the pseudo-North component of ENV4 on which RMS amplitudes are sporadically abnormally high from November 2005 on. Two examples of such records are shown in Fig. B.83 (p.158).
- **FSW** (Fig. B.57, p. 135 & Fig. B.75, p. 150): beginning in year 2005, amplitudes recorded on all three components and all depth levels (i.e. except FSW1 at the surface) are significantly increased. A decrease towards lower values (but not to the original level) is visible from 2009 on. Examples are shown in Fig. B.84 (p. 158). Nevertheless, this behaviour tends to disappear if the data are not filtered, meaning that it seems to be restricted to a certain frequency band (see Fig. B.82, p. 157).
- **VBG** (Fig. B.61, p. 139 & Fig. B.77, p. 152): RMS amplitudes decrease on the pseudo-East component of VBG1 starting from mid-2003 on (e.g. Fig. B.85a, p. 159). Lower amplitudes are also observed on the vertical component of VBG4 from 1996 to late 1999 (e.g. Fig. B.85b, p. 159).
- **VLW** (Fig. B.62, p. 140 & Fig. B.78, p. 153): from 2008 on, VLW0 has very low amplitudes on all three components (e.g. Fig. B.86, p. 159). From 2001 until late 2004, the pseudo-East component of VLW3 exhibits higher amplitudes (e.g. Fig. B.87, p. 160).
- **WDB** (Fig. B.63, p. 141 & Fig. B.79, p. 154): abnormally low amplitudes on the pseudo-North component of WDB3 are observed from 1996 to the end of 1998, and on its vertical component from 2004 on (e.g. Fig. B.88a, p. 160). Finally, the vertical and pseudo-North components of WDB0 show low amplitudes from 2010 on (e.g. Fig. B.88b, p. 160).
- **ZL2** (Fig. B.65, p. 143 & Fig. B.80, p. 155): Around the year 2000, the vertical component of ZL24 records higher amplitudes, as was also reported by KNMI (e.g. Fig. B.89, p. 161).
- **ZLV** (Fig. B.66, p. 144 & Fig. B.81, p. 156): from 2006 on, low amplitudes are observed on the pseudo-East component of ZLV0 (e.g. Fig. B.90a, p. 161). On the vertical component, there are

two episodes featuring low amplitudes: from 2002 to 2004 and 2007 to 2009 (e.g. Fig. B.90, p. 161). The pseudo-North component of ZLV1 went through an episode of significantly higher amplitudes from 2004 to late 2006 (e.g. Fig. B.91, p. 162). Lastly, ZLV4 amplitudes seem to increase over time on the pseudo-East component, especially from mid-2004 on.

Also note that noise levels generally increase closer to the surface and are slightly higher on the vertical component than on the two horizontal components.

Summary

The analysis of RMS amplitudes is especially suitable to identify anomalous amplitude levels. Most of our and KNMI's findings overlap, but we detected a peculiar behaviour at station FSW in addition.

In general, we did not find any major issues regarding the amplitudes recorded on borehole sensors. The analysis of RMS amplitudes is very suited to identify patterns and led to similar findings as by KNMI. Most of the problematic cases are records that KNMI reported as well, either as observations in Dost et al. (section 5.2.4 of 2022) or as component malfunctions (appendix F & G of the same report). A few outliers were due to issues caused by the automatic implementation (most notably, the noise window selection). The only instance that we found in addition concerns the FSW stations showing an increase in noise level from 2006 on for all components and levels, except on the surface sensor. Due to this exemption, an increase in ambient seismic noise level is improbable. In addition, we observed that this behaviour was hardly identifiable on unfiltered data (Fig. B.82, p. 157). According to KNMI (pers. comm.), the effect could be due to ageing of the equipment.

3.3.3 Data timing

DCF signal

As opposed to AC-23/SM2 accelerometer stations, the borehole timing was achieved by recording the DCF signal simultaneously as separate channel. The DCF is a German long-wave time signal with the sender located close to Frankfurt, Germany, being received in large parts of Europe. Short-term disconnections of under two minutes may occur due to service interruptions, while longer lasting interruptions may be due to strong winds, freezing rain or snow-induced antenna movement (https://en.wikipedia.org/wiki/DCF77). The carrier signal has a frequency of 77.5 kHz generated from local atomic clocks linked with the German master clocks. In addition, the signal carries an amplitude-modulated, pulse-width coded 1 bit/s signal and a phase modulation. These carry information on the current date and time, leap second warnings, an announcement of the change to and from summer time, abnormal transmitter operation identification as well as parity bits. Since 2003, it also carries a civil defence emergency signal and since 2006, a civil protection and weather forecast signal.

The knowledge on how to decode the amplitude and phase modulation of the DCF signal seems to have been lost within the seismological community and we strongly encourage KNMI to collect this information and publish it along with the data.

The DCF77 signal marks seconds by reducing carrier power; the rising zero-crossings occur on the second, and the last second of every minute is marked by no carrier power reduction. Below, we analyse the recordings searching for these zero-crossings. More information is available by

decoding the amplitude or phase modulation. Due to the rise of the Global Positioning System (GPS), which is used to achieve timing at seismic stations nowadays, the knowledge of how to decode the signal seems to have been lost within the seismological community. While it was not feasible for us to recover it during the short period of this review, we strongly encourage KNMI to collect this information and publish it along with the data.

Although no DCF decoder was available and thus, not all information could be recovered, we endeavour to analyse the DCF signals available for each record with the aim of **automatically** assigning flags reflecting the reliability and quality of timing. The steps that we used are described as follows:

1. find the position of the pulses;
2. check if the first pulse corresponds to a second: if yes, assign a flag on the second mark that is 0; otherwise, the flag is equal to the number of samples that separates the pulse from the nearest second;
3. compute the theoretical position of the pulses and compare them with the position of the recorded pulses;
4. keep only the pulses that do NOT match with the theoretical pulses;
5. check if the missing pulses correspond to the last second pulse before a minute: if this is the case, assign a flag on the minute mark that is 0; else, the flag is equal to the number of samples that separates the pulse from its theoretical position;
6. check if there are still pulses, which do not correspond to either second or minute marks. These pulses are called spurious. If the pulses on second marks are irregular, they will count as spurious as well.

In short, our analysis returns three flags for each record: one for the second mark, one for the minute mark (both giving the number of samples of difference between the observed pulse and the theoretical pulse) and one for spurious marks in-between (only ”true”/”false”). Please note that FSW had different DCF settings[11] from 1992 to May 1995: for that reason, all events recorded at this station within this time period were not part of our analysis. Also note that a downside of our analysis is that it is mostly based on the positioning of the very first pulse. In the following, we consider a one-sample difference with respect to theoretical marks as acceptable and not as evidence of a timing error.

WARNING!

The results presented in this section are based on the automatic analysis of the DCF signals and are only indicative. Although they constitute a general overview, it happens on rare occasions that well-synchronised records are wrongly flagged, and vice-versa. We therefore recommend that the users manually review the DCF signals of the records they are interested in.

Fig. 3.17 displays examples of DCF signals corresponding to the following situations:

[11] Only the minute marks, and not the second marks, are recorded.

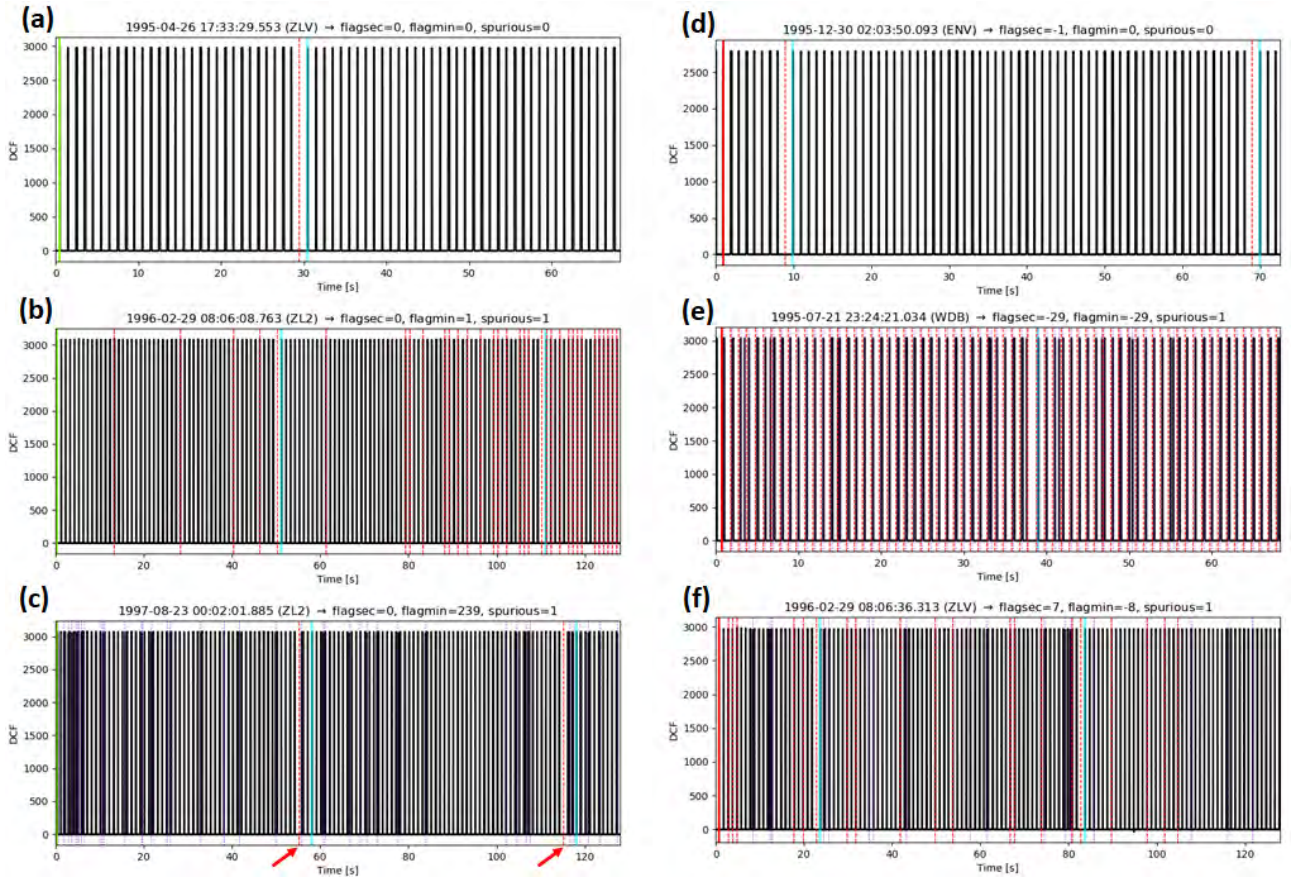

FIGURE 3.17: Example for DCF signals. Minute marks based on data time vector are represented by the vertical cyan lines. Green lines indicate a correct first second-pulse whereas red lines correspond to incorrect second-pulses. Detailed description available in the text.

(a) example of a signal without timing problem. All flags are set to 0. The first pulse corresponds exactly to a second mark (vertical green line). The vertical dashed red line symbolises a missing second mark and occurs exactly 1 s before the minute mark (in cyan).

(b) example of a signal where the first pulse corresponds exactly to a second mark (green), but the minute mark is delayed by one sample. Although this is hardly visible with the naked eye, other pulses also do not exactly match the theoretical second marks (vertical dashed red lines) and the flag for spurious pulses is therefore set to 1.

(c) example of a signal where the first pulse corresponds exactly to a second mark (green), but the minute mark is delayed by 239 samples (i.e., almost 2 s). The erroneous minute marks are visible by eye and highlighted by the red arrows. Irregularities within the DCF signal are also noticeable (vertical dotted purple lines) and the flag for spurious pulses is therefore set to 1.

(d) example of a signal where the first pulse is delayed by one sample with respect to the second (vertical red line), whereas the minute marks match exactly the minute.

(e) example of a signal where both second and minute marks are consistently delayed by the same number of samples (29). Further irregularities are visible in addition.

(f) similar to (e).

An overview of our analysis is presented in Fig. 3.18 as pie diagrams. They indicate that:

(a) A large majority (>75%) of the first second-pulses coincides with a second. For the remaining cases, the histogram on the right demonstrates that most first pulses are only shifted by a single or a few (2-3) samples.

(b) In contrast, a vast majority (>85%) of the minute marks does not coincide with a minute. However, similar to the previous point, the histogram shows that the differences are in general on the order of one or a few samples.

(c) Half of the DCF signals contain irregular pulses.

To conclude, even if we consider, as written earlier, that a shift of a single sample of second or minute marks is not indicative of a timing issue, our analysis still reveals a few timing issues regarding the borehole data. These are summarised in Table B.14 in the appendix (p. 162). Moreover, in Fig. 3.19, DCF signal irregularities are represented as a function of time for each borehole station. For instance, it appears that ENM and FSW underwent several perturbations from 2005 on, while HWF or ZLV show erroneous signals in the period 1996 to 2002.

Waveform plots

In this section, we review the waveform data timing differently, namely by plotting the waveforms in a similar fashion as for the accelerometer data. To this end, we take advantage of the flags defined via the analysis of the DCF signals in the previous section and define a colour code related to the absolute values of those flags:

- **black**: minute and second flags both ≤ 1, i.e. no time synchronisation issue;

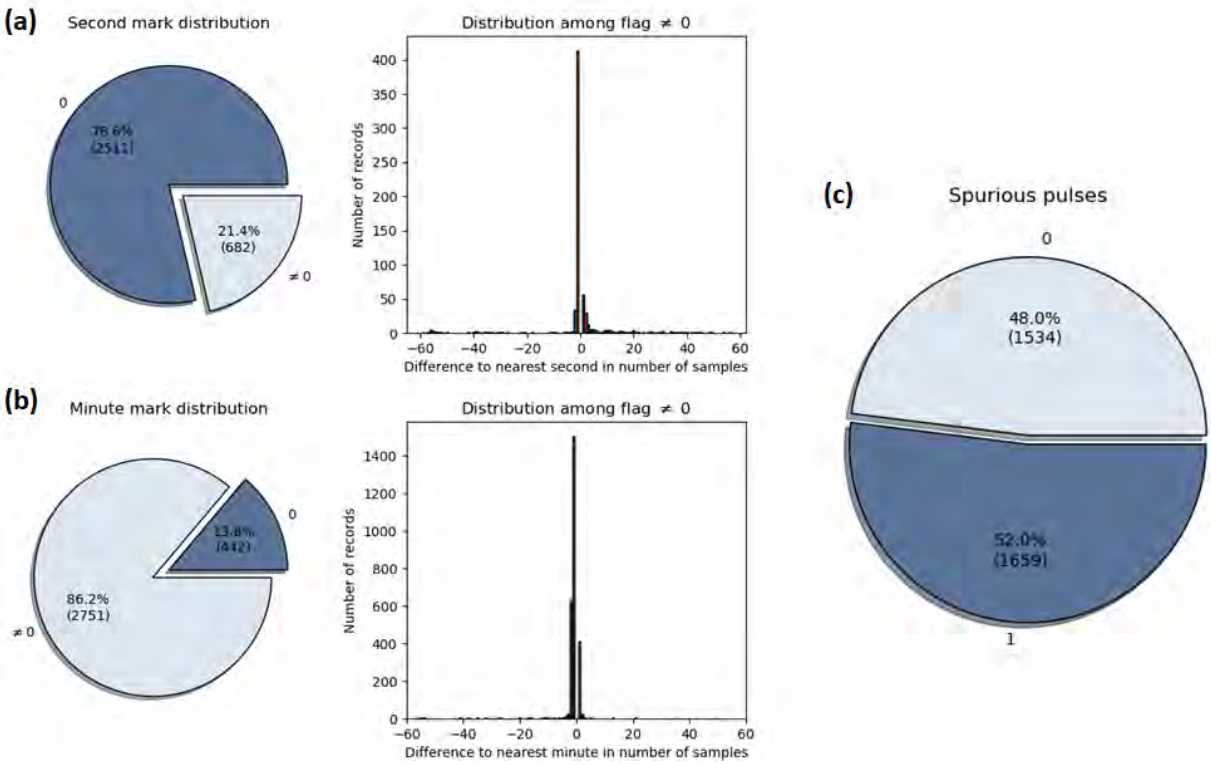

FIGURE 3.18: Statistics of DCF signal analysis: (a) second marks, (b) minute marks and (c) presence of "spurious" pulses. For (a) and (b), histograms showing the distribution of pulse shifts in terms of number of samples are provided in addition (NB: 60 samples are equivalent to 0.5 s). Percentages as well as absolute numbers of records (in brackets) are indicated.

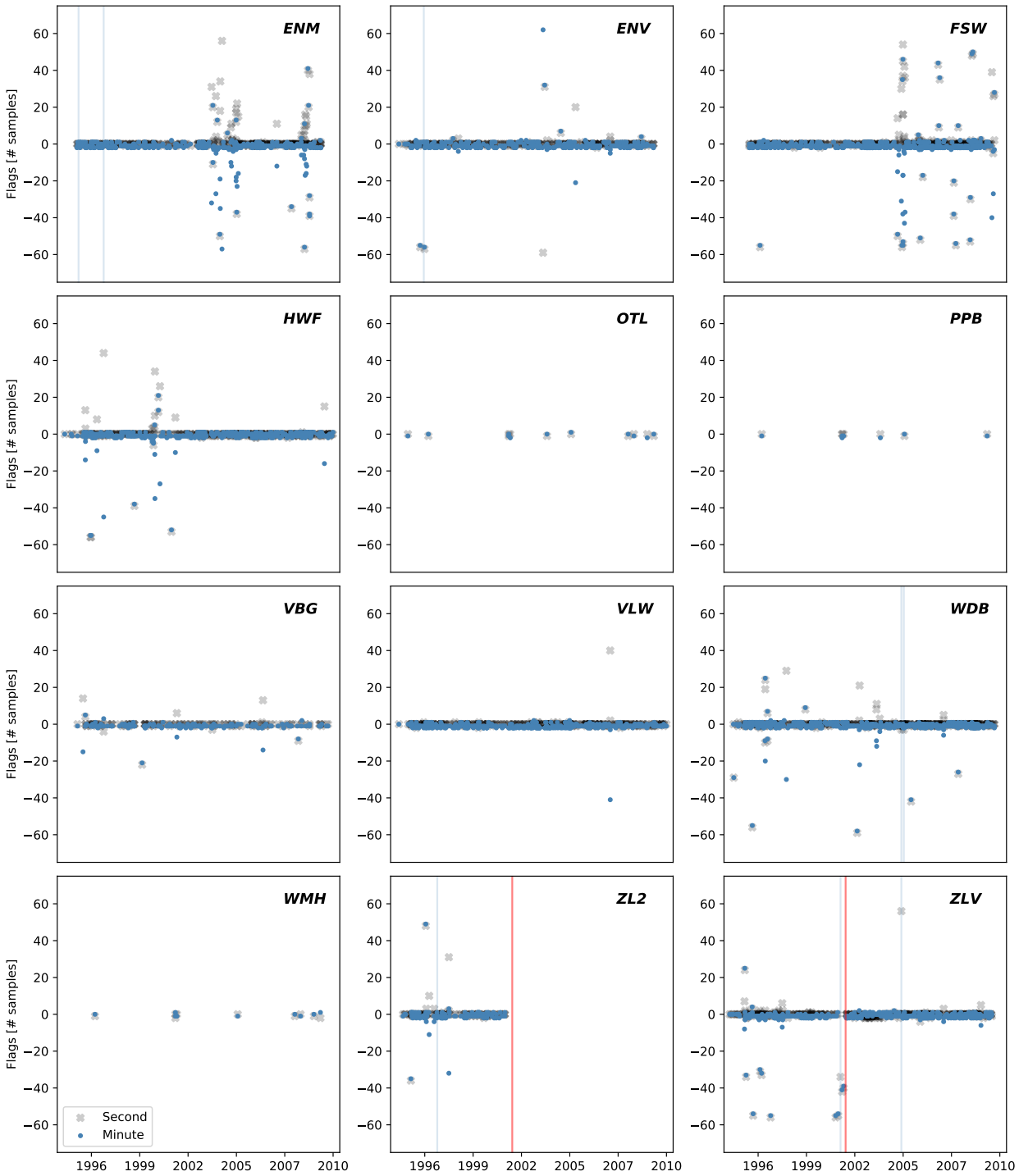

FIGURE 3.19: Second and minute flags (expressed in number of aberrant samples) over time for all borehole stations. Since the y-axis is limited to ±75 samples, larger differences are represented by vertical blue lines. Red vertical lines for ZL2 and ZLV correspond to the damage of the DCF receiver reported in appendix F of Dost et al., 2022.

- **purple**: second flag ≤ 1 and $1 <$ minute flag ≤ 10;
- **grey**: consistent delay of second and minute flags & (second flag > 1);
- **blue**: $1 <$ second flag ≤ 10 and minute flag ≤ 1;
- **seagreen**: $1 <$ both second and minute flags ≤ 10;
- **light red**: both second and minute flags > 10, i.e. significant timing issue;
- **light orange** for FSW records before the 5th of May, 1996.

In addition, station names are written in white on light grey background if the spurious flag is 0; white on dark grey background if it is 1 and black on light grey if the flag has no value assigned.

By visually inspecting the waveform plots, we found that most records did not exhibit discernible timing issues (e.g. Fig. 3.20) or put differently, the potential timing issues detected while analysing the DCF signal are not easily recognisable in a waveform plot. This is particularly visible for the records corresponding to DCF examples (c) & (e) in Fig. 3.17, shown in Figs. B.92 and B.93 in the appendix (pp. 165). Since in both cases, only one additional borehole station detected the event, the precise event origin time cannot be deducted, meaning it may be highly uncertain.

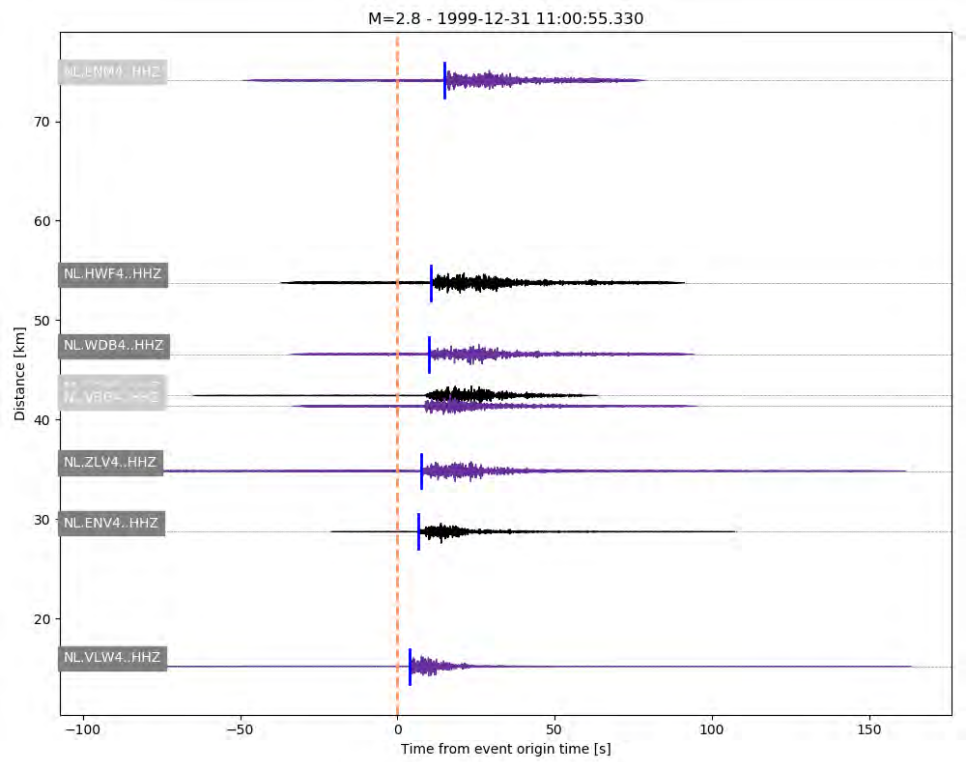

FIGURE 3.20: Vertical component waveforms for the 31st January, 1999 event recorded on the 4th borehole level sorted according to the event-station distances. Data have been instrument-corrected and filtered between 2 and 50 Hz. The event origin time is symbolised by the vertical orange dashed line. P-wave arrival times (if available) are plotted as vertical blue bars. Traces are coloured following the colour code described in the text.

Nevertheless, three types of issues could be determined:

- waveforms are clearly offset from the event origin time (occurs only for a single event, see Fig. 3.21a);
- picks from QuakeML not matching the waveforms (affects six events, see example in Fig. 3.21b);
- event origin time coinciding with the signal onset (affects three events, see example in Fig. 3.22); according to KNMI (pers. comm.), these events, located in the Roswinkel field, have been relocated, but the database was not yet updated accordingly.

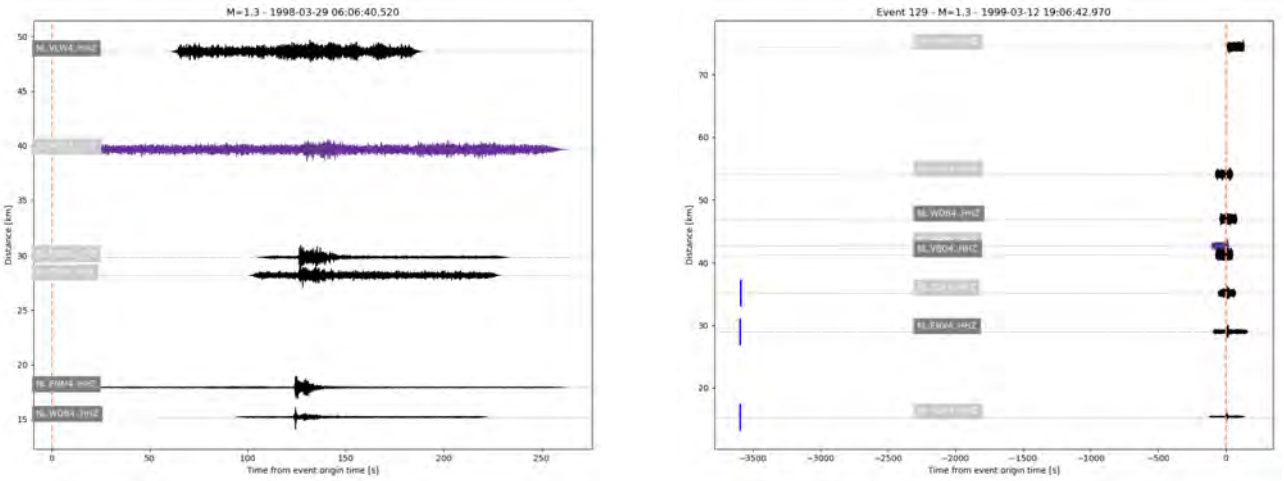

(a) 29th March, 1998 event. (b) 12th March, 1999 event.

FIGURE 3.21: Vertical component waveforms recorded on the 4th borehole level sorted according to the event-station distances. See caption of Fig. 3.20 for a detailed description.

Only two events were identified as having significant time synchronisation issues:

- 2001-08-07 17:09:01 at ZLV (see Fig. 3.23);
- 2003-08-20 08:46:14 at ENV (see Fig. 3.24); in this example, however, the event is not even visible on the record, so it may be of lesser importance.

Summary

In our analysis, we disregarded shifts of second and minute marks of the DCF signal if they just comprised one sample. However, we found a few instances of timing issues of the data recorded on borehole stations. Not all potential DCF timing disruptions are readily detectable from seismogram sections and users should review the DCF signal before using the data, especially if dealing with arrival-time sensitive methods such as event location. A further problem is that the knowledge on how to decode the amplitude and phase modulation of the DCF signal seems to have been lost within the seismological community.

> Although assuming that a shift of just one sample in DCF signal second or minute marks is negligible, we detect a few significant timing issues. Users should check the DCF trace before using the data for arrival-time dependent analyses.

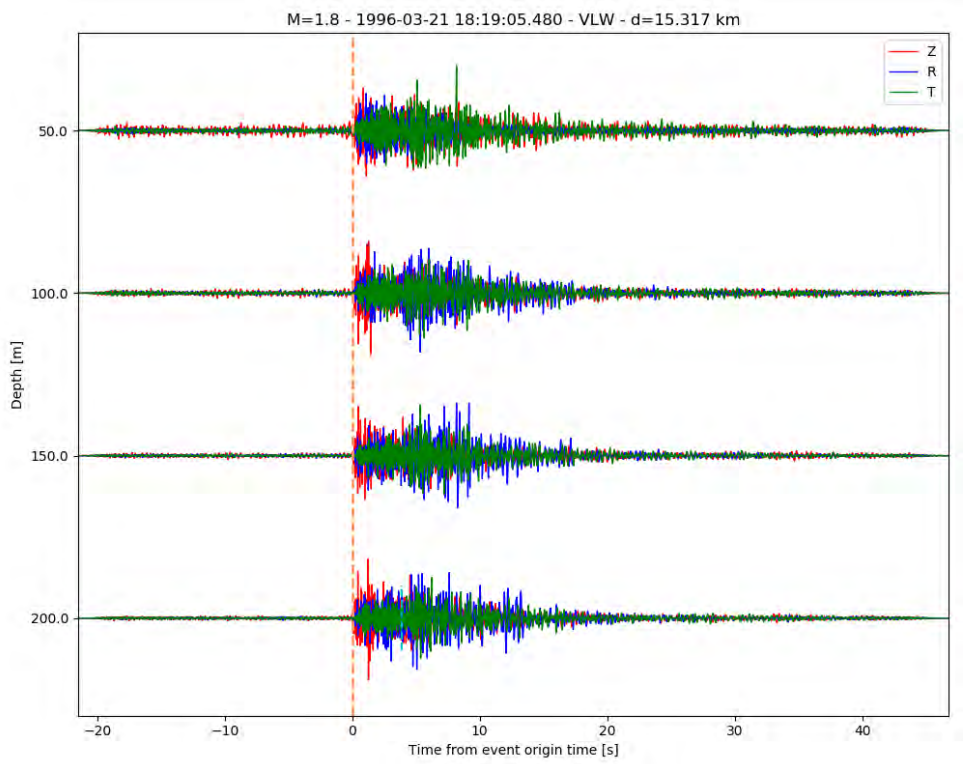

FIGURE 3.22: VLW borehole three-component records for the 21st March, 1996 event. Data have been instrument-corrected and filtered between 2 and 50 Hz. Event origin time is symbolised by the vertical orange dashed line.

3.3.4 Conclusion

Borehole triggered data, due to the larger number of records, is partly easier to quality control than the accelerometer data.

Sensor orientation, for example, was the subject of a careful analysis in the past and the continuity of data acquisition until today allowed for a comparison to more recent borehole installations such as the G-network. The full analysis could not be repeated here, since we did not possess e.g. records of check shots. Instead, we demonstrate a simple approach to test the polarity of vertical components, which - if more records of teleseismic events are available - can also be used to track temporal changes.

Amplitudes seem to be mostly recorded correctly despite occasional malfunctioning of sensors and components that have occurred throughout the recording period. Together with KNMI's analysis (Dost et al., 2022), we demonstrate multiple ways of reviewing amplitudes and highlight periods in which measurements appear to be anomalous.

Finally, data timing does not seem to be problematic. However, the precise interpretation (and decoding) of DCF signals would help confirming this statement.

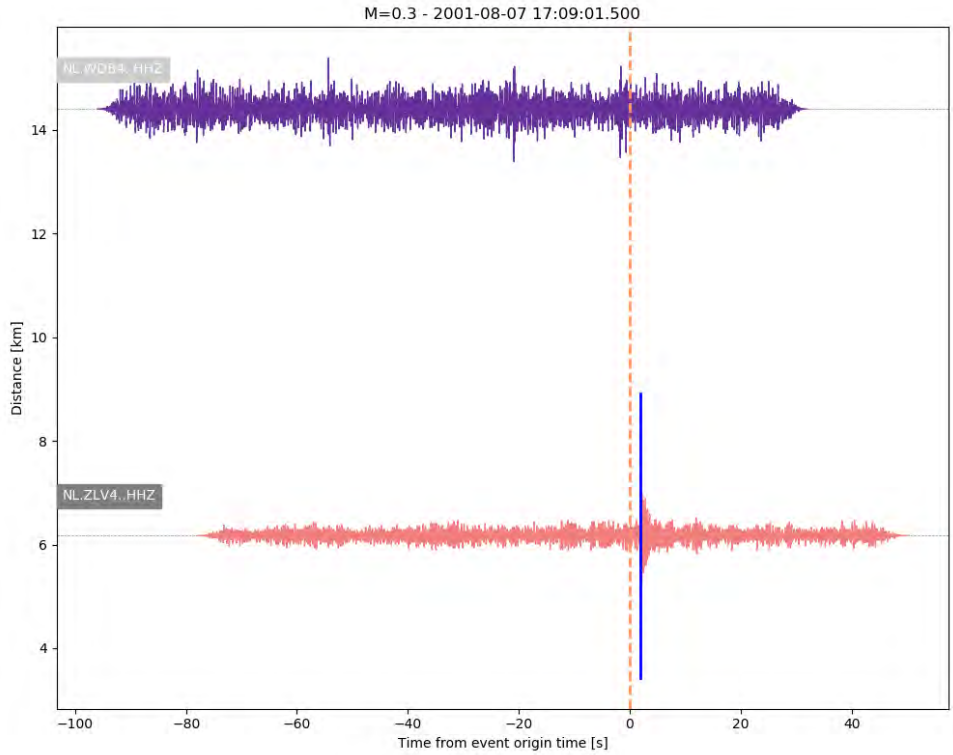

(a) Vertical component waveforms for the 7th August, 2001 event at 17:09:01 recorded on the 4th borehole level sorted according to the event-station distances.

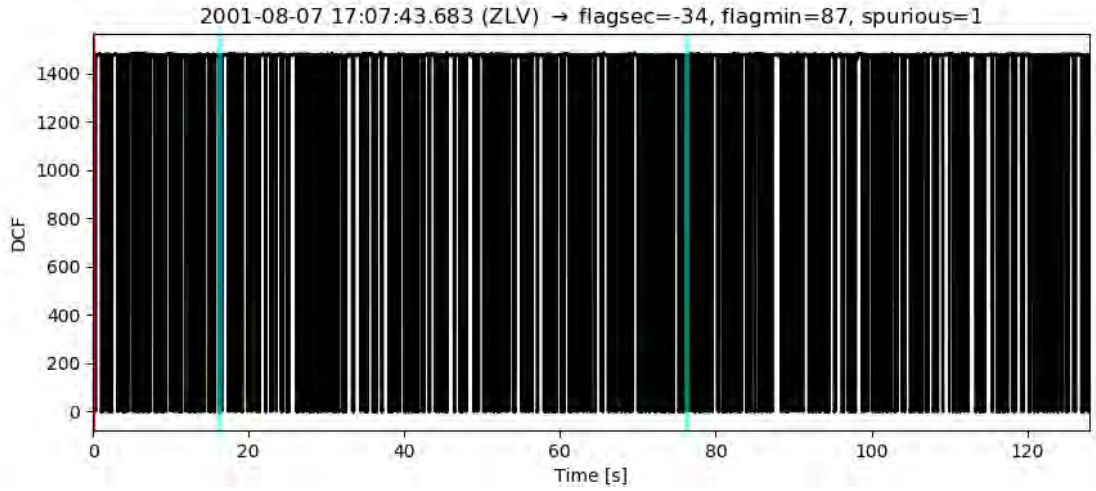

(b) DCF signal for ZLV.

FIGURE 3.23: Significant timing error identified for ZLV.

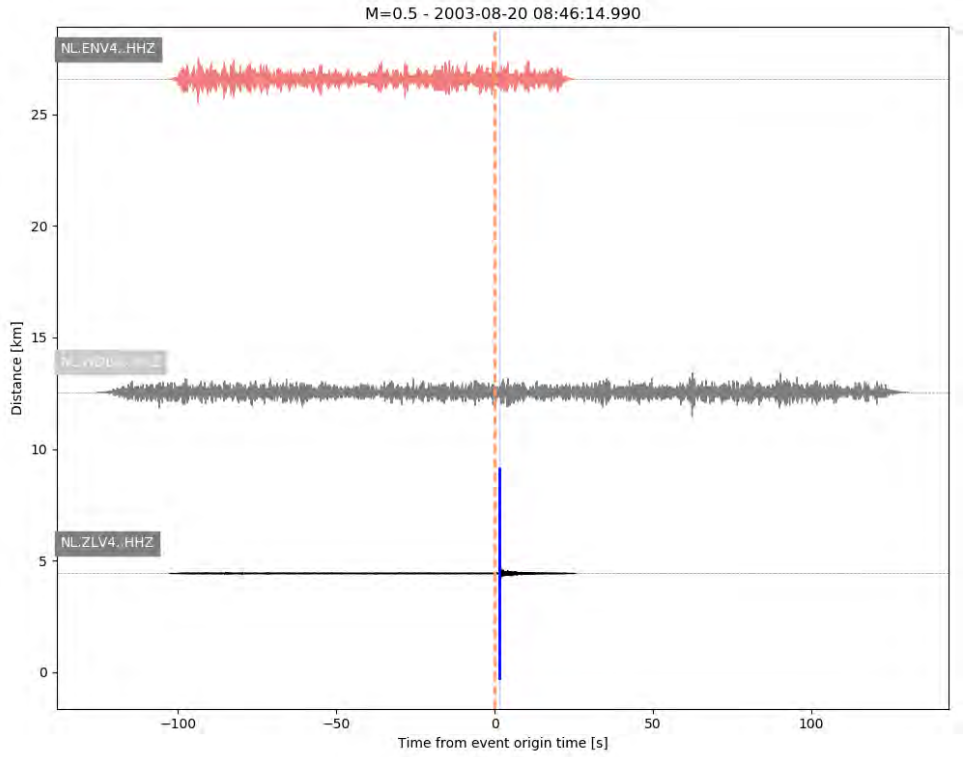

(a) Vertical component waveforms for the 20th August, 2003 event at 08:46:14 recorded on the 4th borehole level sorted according to the event-station distances.

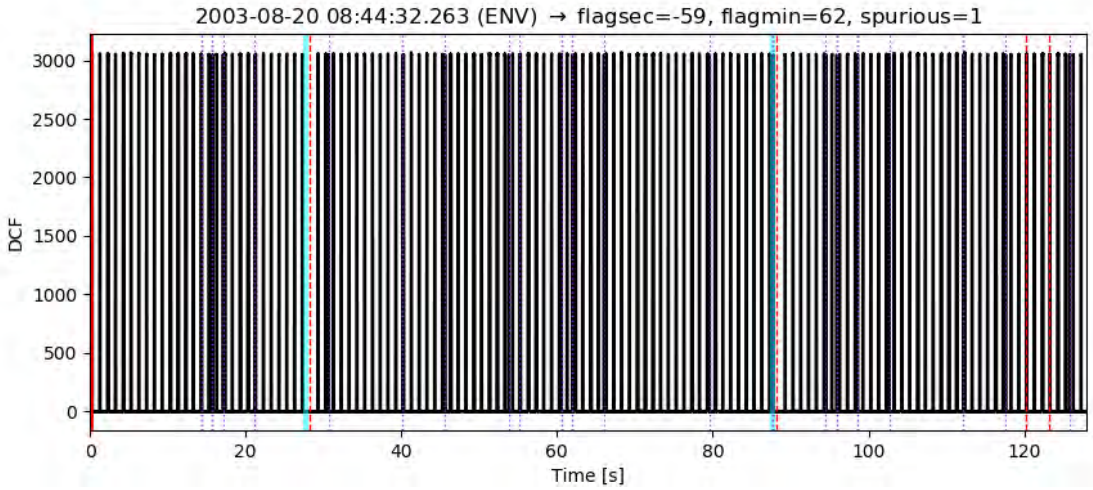

(b) DCF signal for ENV.

FIGURE 3.24: Significant timing error identified for ENV.

Public data availability and accessibility

As mentioned in the introduction, NORSAR's work was carried out in two phases, firstly on an offline dataset provided directly by KNMI and secondly, on the same dataset retrieved through the FDSN web service. All findings and figures presented in the previous sections are based on the online data set. Thus, all data used in the previous sections were downloaded from the KNMI FDSN server (`http://rdsa.knmi.nl/`, last accessed 19/08/2022) via ObsPy (Beyreuther et al., 2010). Waveform data, event data and station metadata could successfully be retrieved both for accelerometer and borehole stations. We provide related Python code snippets in the sections 4.1 and 4.2.

Below, we summarise findings related to accessibility and completeness of the online data that can be fixed by KNMI by the time this report is published. Corrections are partly necessary in KNMI's report and partly in the publicly available files:

1. **Accelerometer data**:
    - Waveform data (miniSEED files)
        > Time flags cannot be extracted. Since there is no easy solution (other than maybe contacting the Obspy developers), we provided some tips throughout this report.
    - Station metadata (StationXML files)
        > Orientation uncertainties are not stored.
        > Instrument response units are wrong / not set.
    - Event catalogue (QuakeML files)
        > OK; occasionally, P-wave picks do not match the waveforms (see 4.2 and Fig. A.1).
2. **Borehole data**:
    - Waveform data (miniSEED files)
        > Waveform data could not be downloaded for event #500 (2009-02-26 01:22).
        > DCF channels for FSW until 1996-05-05 are missing.
        > Channels are named "N", "E", "Z" which is different from KNMI's naming in their report ("1", "2", "Z").
        > WDB records for events #512, #513 and #518 have gaps and do not coincide with the timing of the DCF channel.
        > no records for ZLV0 before 1996 could be downloaded (see also station metadata).
    - Station metadata (StationXML files)
        > FSW1 instrument response is wrong from 1996-05-05 to 2010-04.
        > PPB polarity flip is not reported in the corresponding StationXML station file.

> ZL2 end time is different in the online data (2009-04-10) as compared to the offline data that were first provided by KNMI and what is reported by Dost et al. (2022) (2010-05-18).

> ZLV0 start time is different in the online data (1996-02-15) as compared to the offline data that were first provided by KNMI (1995-04-12); data could not be downloaded for that period.

- Event catalogue (QuakeML files): KNMI (pers. comm., see email 14-Jul-2022) identified three events with origin time issues

  > event #6: 1995-04-26 (ZLV), origin time should be 17:33:49.

  > event #415: 2007-03-11 (WDB ENM FSW ZLV), origin time is too late.

  > event #485: 2008-12-24 (ZLV HWF ENV WDB VLW ENM FSW), origin time is ca. 27 s too early.

4.1 How to access the accelerometer data

```
# 1. READ CATALOGUE OF EVENTS
from obspy.core.event import read_events
cat = read_events("KNMI_catalogue_acc.xml") # catalogue name has to be adapted; could also be a text file based for example on Table 1 or Table A.2 of this report.

# 2. DEFINE STATION LIST (here, for accelerometers)
list_acc = ["FRB2", "GARST", "HARK", "HKS", "KANT", "MID1", "MID2", "MID3", "STDM", "WIN", "WSE", "ZAN1", "ZAN2", "ROS1", "ROS2", "ROS3", "ROS4", "ROS5", "ROS6"]
list_sta_query = ",".join(list_acc)

# 3. CONNECT TO SERVER
from obspy.clients.fdsn import Client
client = Client("http://rdsa.knmi.nl")

# 4. LOOP OVER EVENTS AND GET WAVEFORM DATA
import numpy as np
for ev in cat:
    tstart = ev.origins[0].time
    try:
        # Fetching data: search for available data +/- 500 s around the event origin time
        st = client.get_waveforms("NL", list_sta_query, "*", "HG*", tstart-500, tstart+500)
        st.merge(method=1, fill_value=np.nan) # just in case, but not necessary in principle
        st.write("%s.mseed"%(tstart.strftime("%Y%m%d%H%M")), format="MSEED")
    except:
        continue
```

CODE SNIPPET 4.1: Fetching accelerometer waveform data

WARNING!

For accelerometer data, time flags are stored in the blockette 1001 of the miniSEED trace headers. The header is accessible only if the option "details" is set to True when reading a file. By default, this option is set to False, and cannot be changed through the entry parameters of "get_waveforms" (line 22 of the code snippet). We modified the source code manually (line 850 in the ObsPy "client.py" function) such that the option is always set to True, thus enabling us to access the time flags. Time flags of individual records are also available in Table A.2, p. 77 of this report.

NOTE

We chose a sufficiently long time window around the event origin time to ensure that non-synchronised data are included. However, note that two events (#36 and #37) occur within a short period (73 s) on the same day (2006-03-25) and that the records from station ROS4 belong to event #37.

```
# 1. DEFINE STATION LIST
list_acc = ["FRB2", "GARST", "HARK", "HKS", "KANT", "MID1", "MID2", "MID3", "STDM",
    "WIN", "WSE", "ZAN1", "ZAN2", "ROS1", "ROS2", "ROS3", "ROS4", "ROS5", "ROS6"]

# 2. CONNECT TO SERVER
from obspy.clients.fdsn import Client
client = Client("http://rdsa.knmi.nl")

# 3. LOOP OVER STATIONS AND STORE XML FILES
# To store the instrument response, set level to "response"
for sta in list_acc:
    client.get_stations(network="NL", station=sta, filename="%s.%s.xml"%(net,sta),
    level="response")
```

CODE SNIPPET 4.2: Fetching accelerometer StationXML files

4.2 How to access the borehole data

```
# 1. READ CATALOGUE OF EVENTS: see Table B.1 of this report (p. 76-83).
import pandas as pd
df = pd.read_csv("list_events.csv")

# 2. DEFINE STATION LIST
list_bor = ["FSW*", "ENM*", "WDB*", "ZLV*", "ZL2*", "ENV*", "VLW*", "VBG*", "HWF*", "
    OTL*", "PPB*", "WMH*"]
list_sta_query = ",".join(list_bor)

# 3. CONNECT TO SERVER
from obspy.clients.fdsn import Client
client = Client("http://rdsa.knmi.nl")

# 4. LOOP OVER EVENTS, GET WAVEFORM DATA AND FILL IN QUAKEML CATALOGUE
```

```
from obspy import UTCDateTime, Catalog
CAT = Catalog()
for iev, ev in df.iterrows():
    torig = UTCDateTime(ev.Origin_time)
    tstart = torig - ev.Left
    tend = torig + ev.Right
    try:
        st = client.get_waveforms("NL", list_sta_query, "*", "H*", tstart, tend)
        st.write("%s.mseed"%(torig.strftime("%Y%m%d%H%M")), format="MSEED")
        CAT = CAT + client.get_events(starttime=torig-120, endtime=torig+120,
    includeallorigins=True, includearrivals=True, includepicks=True)
    except:
        continue
CAT.write("catalogue_borehole_events.xml", format="QUAKEML")
```

CODE SNIPPET 4.3: Fetching borehole waveform data and event catalogue

Recommendations

Apart from the recommendations mentioned in the previous chapters, we would like to propose an additional analysis to be performed.

5.1 QuakeML - event catalogue

Updating the QuakeML event files containing event metadata (i.e. source parameters as well as P- and S-wave picks, time residuals, etc.) was not part of the current project. However, it turned out in multiple occasions during our work that this information cannot be easily distinguished from the waveform data if they are released to the public.

Time synchronisation issues, for example, were sometimes difficult to assess as they could also be related to erroneous event origin times. We consider it crucial to update this information to ensure that end-users employ the most up-to-date and reliable event catalogue. In addition, we noticed that the information in the QuakeML database is not always stored in a consistent manner. The example in Fig. A.1 (p. 72) is a good illustration of this problem: it shows accelerometer data for which - although the records are not synchronised in time (**pink** traces) - (1) the P-wave arrival times (vertical blue lines) are consistent with waveform timing at FRB2 and HKS, but (2) not consistent for KANT and STDM.

Other issues concerning the QuakeML catalogue are related to epicentral distances that are not consistent with event and station locations when recomputed independently. After several exchanges with KNMI on that subject, it appears to us that they use a different database internally than the one publicly available.

Finally, a number of events occurs close in time and therefore, they are combined in a single file (see Table 1.3, p. 19). Metadata for these events must be correct in order for the end-user to be able to properly identify the individual events.

For all the aforementioned reasons, we strongly recommend that KNMI obtains a separate project by SodM to enable them to solve these issues and update the QuakeML files of all events (wherever necessary) to ensure consistency, at least with regard to event origin time and location.

5.2 Publication

We strongly encourage a publication of the analyses in a scientific paper, once that the QuakeML files have been corrected as well. To this end, KNMI's and NORSAR's approaches could be combined to

- promote the publication of this new, carefully evaluated data set for the Groningen field, potentially enabling users to extend their analyses in time;
- propose newly developed approaches to test historical (or partly also more recent) data sets.

References

Beyreuther, M., R. Barsch, L. Krischer, T. Megies, Y. Behr, and J. Wassermann (2010). "ObsPy: a Python toolbox for seismology". In: Seismological Research Letters 81.3, p. 530.

Bommer, J.J., B. Edwards, P.P. Kruiver, A. Rodriguez-Marek, P.J. Stafford, B. Dost, M. Ntinalexis, E. Ruigrok, and Spetzler J. (Dec. 2019). V6 Ground Motion Model (GMM) for induced seismicity in the Groningen field. NAM Report. Nederlandse Aardolie Maatschappij BV.

Diephuis, G. and U. Asmussen (1995). KNMI arrays in Groningen and Drenthe. NAM Report.

Dost, B. (2016). Evolution of the Groningen earthquake monitoring network and event catalogue. Mmax Expert Workshop, 8 - 10 March 2016, World Trade Centre, Schiphol Airport, the Netherlands.

Dost, B. and H. Haak (2002). A comprehensive description of the KNMI seismological instrumentation. Tech. rep. KNMI.

Dost, B., E. Ruigrok, and J. Spetzler (2017). "Development of seismicity and probabilistic hazard assessment for the Groningen gas field". In: Netherlands Journal of Geosciences 96.5, s235–s245.

Dost, B., W. Zhou, and E. Ruigrok (2022). Quality assurance and publication of the KNMI 1995-2013 induced seismic data. Tech. rep. KNMI.

Jepsen, D.C. and B.L.N. Kennett (1990). "Three-component analysis of regional seismograms". In: Bulletin of the Seismological Society of America 80.6, pp. 2032–2052.

Kennett, B.L.N. and E.R. Engdahl (1991). "Traveltimes for global earthquake location and phase identification". In: Geophysical Journal International 105.2, pp. 429–465.

KNMI (2019). Sensor orientation. Tech. rep. KNMI.

NORSAR (June 2018). Review of the public KNMI induced earthquake catalogue from the Groningen gas field (report project phase 1, WP1: Catalogue review). KEM-11 Improving the earthquake catalogue in the Groningen region: WP1 18-004. NORSAR. DOI: 10.21348/p.2018.0001.

Oye, V. and W.L. Ellsworth (2005). "Orientation of Three-Component Geophones in the San Andreas Fault Observatory at Depth Pilot Hole, Parkfield, California". In: Bulletin of the Seismological Society of America 95.2, pp. 751–758.

Ruigrok, E., J. Domingo-Ballesta, G.-J. van den Hazel, B. Dost, and L. Evers (2019). "Groningen explosion database". In: First Break 37.8, pp. 37–41.

Appendix: Additional figures

A.1 Accelerometer waveform plots

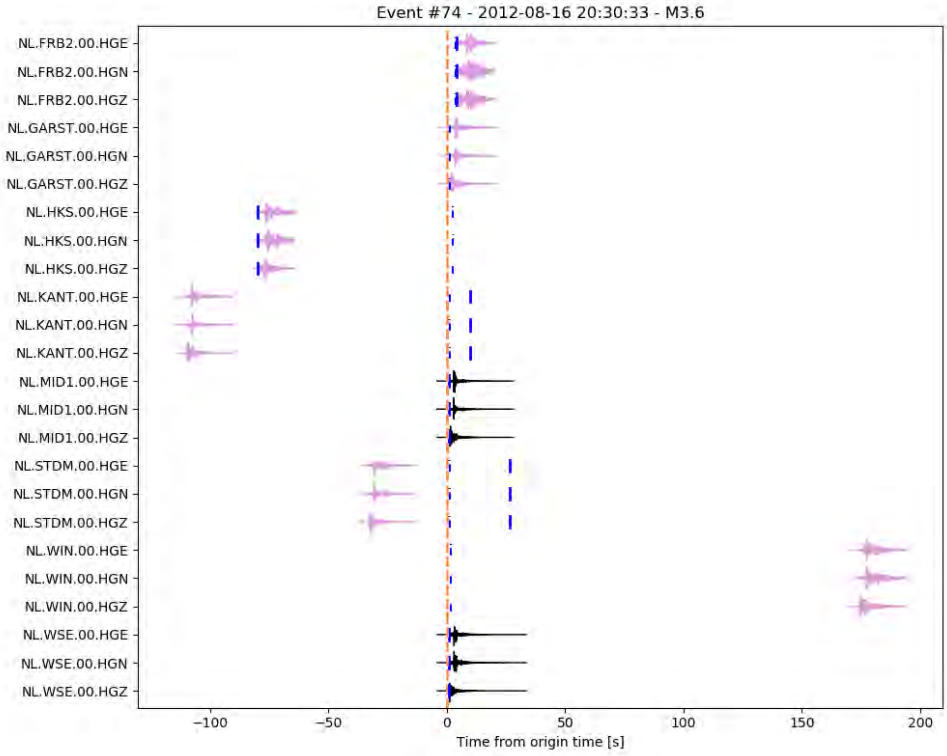

FIGURE A.1: Accelerometer records for event #74: records which are not time synchronised are coloured pink. P-wave arrival times extracted from QuakeML are partly in agreement with the waveforms, even though not synchronised, partly not.

A.2 Accelerometer orientation results

TABLE A.1: Individual orientation results. M_L is the event magnitude. d is the event-station distance. β is the back-azimuth. KNMI 1 and KNMI 2 are KNMI's orientation results for methods 1 and 2, respectively. The offset angle is measured between max(R·Z) and min(|T|). The last column indicates the particle motion linearity. Cells coloured in blue highlight records for which there are large discrepancies between results by NORSAR and KNMI using method 1 results. Red cells highlight records for which the offset angle is important ($> 25°$).

Station	Origin time	M_L	d [km]	β [°]	KNMI 1 [°]	KNMI 2 [°]	NORSAR [°]	Offset [°]	Linearity
FRB2	2012-08-16 20:30:33.280	3.6	18.7	160	39	20	32	14	6.0
GARST	2011-06-27 15:48:09.710	3.2	8.7	326	337	350	342	2	2.1
	2012-08-16 20:30:33.280	3.6	3.7	48	376	385	356	2	3.1
	2013-02-07 22:31:58.380	2.7	3.2	105	366	-	27	32	2.4
	2013-02-07 23:19:08.970	3.2	3.9	127	388	350	34	18	2.7
	2013-02-09 05:26:10.050	2.7	3.0	273	324	-	321	1	10.2
	2013-09-04 01:33:32.170	2.8	4.7	304	345	-	339	13	5.0
	2014-02-13 02:13:14.320	3.0	4.7	285	322	360	322	9	6.7
HKS	2006-08-08 05:04:00.050	3.5	8.8	138	333	330	334	13	4.9
	2012-08-16 20:30:33.280	3.6	9.6	128	354	0	1	4	9.4
	2013-09-04 01:33:32.170	2.8	5.9	171	332	-	340	15	1.8
	2014-02-13 02:13:14.320	3.0	7.2	178	396	40	36	2	8.5
KANT	2012-08-16 20:30:33.280	3.6	3.6	350	80	70	69	73	2.3
MID1	2008-10-30 05:54:29.080	3.2	5.3	283	34	0	30	40	1.7
	2009-04-14 21:05:25.880	2.6	2.5	277	343	55	309	35	1.3
MID3	2003-09-27 13:57:54.150	2.7	3.4	280	346	345	347	4	2.3
	2003-11-10 00:22:38.030	3.0	4.2	318	319	340	321	21	1.5
	2003-11-16 20:04:11.480	2.7	3.8	286	294	310	300	1	1.8
	2006-08-08 05:04:00.050	3.5	3.3	276	290	275	287	3	2.6
	2008-10-30 05:54:29.080	3.2	5.2	291	315	310	319	7	1.4
	2009-04-14 21:05:25.880	2.6	2.4	294	287	310	286	5	1.5
STDM	2012-08-16 20:30:33.280	3.6	3.9	160	54	60	71	18	1.6
WIN	2008-10-30 05:54:29.080	3.2	3.4	148	42	370	38	30	1.9
	2009-05-08 05:23:11.950	3.0	4.9	191	322	240	312	11	8.2
	2011-06-27 15:48:09.710	3.2	2.8	288	23	40	33	75	1.2
	2012-08-16 20:30:33.280	3.6	6.4	128	63	280	241	83	1.4
	2013-07-02 23:03:55.500	3.0	3.2	307	29	-	12	11	2.8
	2013-09-04 01:33:32.170	2.8	4.1	204	269	-	253	25	3.1
	2014-02-13 02:13:14.320	3.0	5.7	204	316	320	315	15	3.8
WSE	2009-04-14 21:05:25.880	2.6	2.0	91	350	355	174	50	1.7
	2009-05-08 05:23:11.950	3.0	3.6	253	352	0	352	12	1.6
	2011-06-27 15:48:09.710	3.2	6.9	312	67	60	57	14	2.4
	2012-08-16 20:30:33.280	3.6	2.6	92	15	25	180	34	1.3
	2013-02-07 23:19:08.970	3.2	5.8	150	66	40	234	48	1.3
	2013-02-09 05:26:10.050	2.7	4.0	233	350	345	1	10	2.8
ZAN1	2008-10-30 05:54:29.080	3.2	4.9	49	279	300	279	1	4.0
	2011-06-27 15:48:09.710	3.2	7.0	354	237	260	62	2	6.0
	2013-09-04 01:33:32.170	2.8	2.4	5	288	-	287	35	1.4
ZAN2	2003-11-10 00:22:38.030	3.0	5.6	51	56	55	129	42	1.4
	2003-11-16 20:04:11.480	2.7	3.8	68	43	40	59	11	1.2
	2006-08-08 05:04:00.050	3.5	3.9	79	8	350	23	13	2.4
	2008-10-30 05:54:29.080	3.2	3.2	46	11	285	163	76	1.6
	2011-06-27 15:48:09.710	3.2	6.4	340	34	35	32	14	17.1
ROS1	1997-02-19 21:53:50.810	3.4	1.2	341	354	354	173	4	2.1
	1998-01-28 21:33:03.840	2.7	1.3	331	378	350	14	20	3.5
	1998-07-14 12:12:02.230	3.3	1.8	309	328	355	327	13	4.0
ROS2	1998-01-28 21:33:03.840	2.7	1.4	166	81	45	69	29	1.2
	1998-07-14 12:12:02.230	3.3	1.4	199	345	348	347	29	4.0
	1999-12-31 11:00:55.330	2.8	1.6	184	347	26	11	89	1.1
	2000-10-25 18:10:34.790	3.2	1.3	196	341	351	7	23	1.6
ROS3	1998-01-28 21:33:03.840	2.7	1.8	76	351	345	351	27	1.5
	1998-07-14 12:12:02.230	3.3	1.1	66	341	331	337	35	1.7
	1999-12-31 11:00:55.330	2.8	1.3	84	345	338	174	89	1.1
	2000-10-25 18:10:34.790	3.2	1.2	65	345	343	166	55	2.3
ROS4	1999-12-31 11:00:55.330	2.8	1.3	84	103	80	84	13	1.1
	2000-10-25 18:10:34.790	3.2	1.2	65	27	65	51	9	1.3
ROS5	2002-02-14 17:01:04.740	2.1	0.9	75	331	310	337	17	1.6
ROS6	2001-04-28 23:00:15.880	2.4	1.8	250	322	330	330	76	1.5

A.3 Accelerometer RMS amplitudes per station

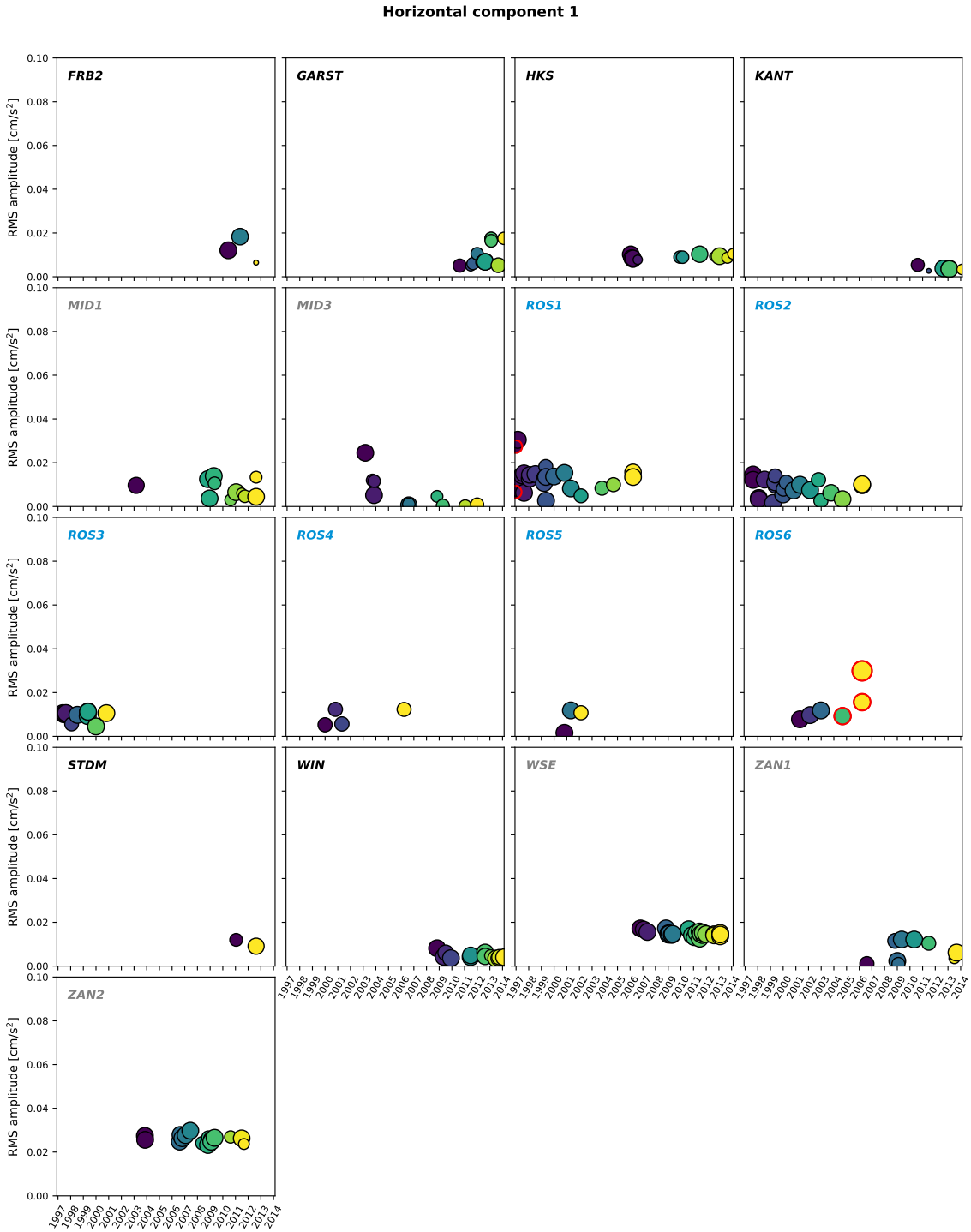

FIGURE A.2: RMS amplitudes in cm/s^2 measured on the first horizontal component as a function of time for each station. Station names are coloured black for AC-63 sensors, grey for AC-23 sensors and blue for Roswinkel stations. Red-bordered circles correspond to components reported as malfunctioning (see Table 3.2). Circles are coloured by event origin time and their size is scaled by the RMS window length. Y-axes limits are the same for all plots in order to ease the comparison.

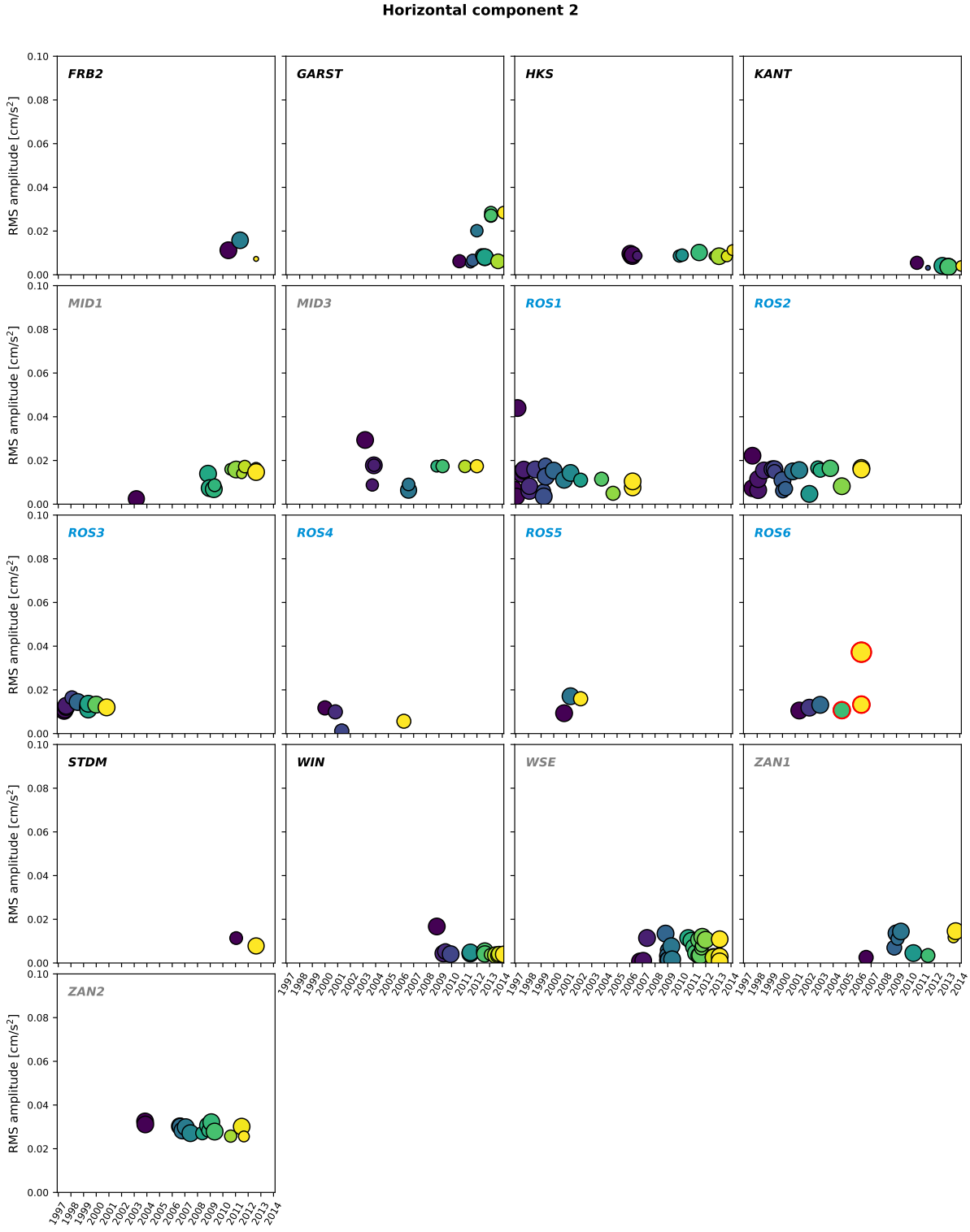

FIGURE A.3: Same as Fig. A.2 for the second horizontal component.

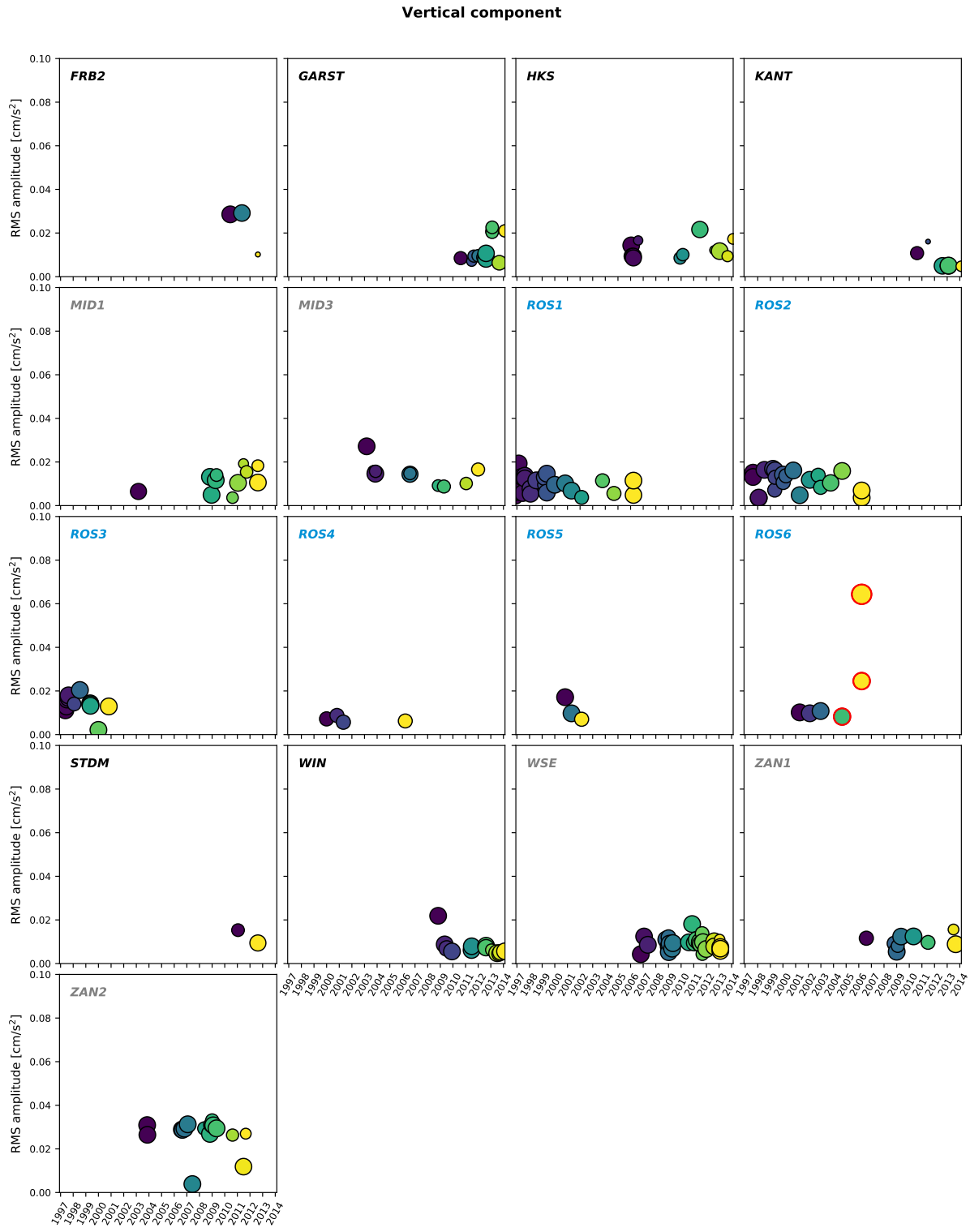

FIGURE A.4: Same as Fig. A.2 for the vertical component.

A.4 Accelerometer time flags

TABLE A.2: List of accelerometer records available for each event. Start and end record times are given as well as time flags. A time flag of 100 indicates a synchronised record while 0 indicates a non-synchronised record or an unknown state of synchronisation.

Event ID	Station	Start time	End time	Time flag
1	ROS1	1996-12-06 16:44:50.496	1996-12-06 16:44:58.596	0
2	ROS1	1996-12-28 18:14:26.531	1996-12-28 18:14:35.631	0
3	ROS1	1997-01-16 00:12:42.420	1997-01-16 00:12:59.415	100
4	ROS1	1997-02-19 21:53:46.695	1997-02-19 21:54:07.600	100
5	ROS1	1997-05-19 15:43:52.260	1997-05-19 15:44:08.735	100
	ROS3	1997-05-19 15:43:52.180	1997-05-19 15:44:07.180	100
6	ROS1	1997-06-20 00:45:34.650	1997-06-20 00:45:51.225	100
	ROS3	1997-06-20 00:45:34.445	1997-06-20 00:45:50.815	100
7	ROS3	1997-07-09 06:23:08.005	1997-07-09 06:23:23.000	100
8	ROS2	1997-08-18 04:42:25.835	1997-08-18 04:42:42.285	100
	ROS3	1997-08-18 04:42:25.750	1997-08-18 04:42:40.750	100
	ROS1	1997-08-18 04:42:25.790	1997-08-18 04:42:42.330	100
9	ROS1	1997-08-18 05:17:29.250	1997-08-18 05:17:46.320	100
	ROS2	1997-08-18 05:17:29.250	1997-08-18 05:17:47.385	100
	ROS3	1997-08-18 05:17:29.215	1997-08-18 05:17:45.605	100
10	ROS1	1998-01-28 21:32:59.770	1998-01-28 21:33:18.750	100
	ROS2	1998-01-28 21:32:59.805	1998-01-28 21:33:18.135	100
	ROS3	1998-01-28 21:33:01.580	1998-01-28 21:33:16.980	100
11	ROS1	1998-01-28 22:34:00.340	1998-01-28 22:34:17.040	100
	ROS2	1998-01-28 22:34:00.360	1998-01-28 22:34:17.835	100
12	ROS2	1998-07-14 12:11:59.220	1998-07-14 12:12:19.115	100
	ROS1	1998-07-14 12:11:59.310	1998-07-14 12:12:21.360	100
	ROS3	1998-07-14 12:11:59.170	1998-07-14 12:12:18.205	100
13	ROS1	1999-03-12 19:06:41.500	1999-03-12 19:06:56.585	100
14	ROS1	1999-03-17 23:14:22.520	1999-03-17 23:14:39.165	100
	ROS2	1999-03-17 23:14:22.420	1999-03-17 23:14:38.810	100
15	ROS1	1999-05-06 18:13:54.925	1999-05-06 18:14:09.980	100
	ROS2	1999-05-06 18:13:54.870	1999-05-06 18:14:09.970	100
	ROS3	1999-05-06 18:13:53.250	1999-05-06 18:14:08.255	100
16	ROS1	1999-05-14 18:30:17.775	1999-05-14 18:30:34.380	100
	ROS2	1999-05-14 18:30:17.805	1999-05-14 18:30:34.270	100
	ROS3	1999-05-14 18:30:17.675	1999-05-14 18:30:32.685	100
17	ROS1	1999-05-15 19:28:27.400	1999-05-15 19:28:43.925	100
	ROS2	1999-05-15 19:28:28.860	1999-05-15 19:28:43.855	100
	ROS3	1999-05-15 19:28:27.320	1999-05-15 19:28:42.315	100
18	ROS4	1999-12-31 11:00:52.650	1999-12-31 11:01:07.965	100
	ROS3	1999-12-31 11:00:51.320	1999-12-31 11:01:15.065	100
	ROS1	1999-12-31 11:00:51.315	1999-12-31 11:01:09.850	100

Continued on next page

Event ID	Station	Start time	End time	Time flag
	ROS2	1999-12-31 11:00:51.340	1999-12-31 11:01:16.305	100
19	ROS2	2000-01-07 14:19:04.105	2000-01-07 14:19:19.370	100
20	ROS2	2000-03-27 10:23:19.470	2000-03-27 10:23:34.585	100
21	ROS1	2000-10-25 18:10:30.830	2000-10-25 18:10:50.100	100
	ROS2	2000-10-25 18:10:30.725	2000-10-25 18:10:57.285	100
	ROS3	2000-10-25 18:10:30.760	2000-10-25 18:10:53.880	100
	ROS4	2000-10-25 18:10:32.145	2000-10-25 18:10:47.340	100
	ROS5	2000-10-25 18:10:30.630	2000-10-25 18:10:47.965	100
22	ROS6	2001-04-28 23:00:11.970	2001-04-28 23:00:32.320	100
	ROS5	2001-04-28 23:00:11.775	2001-04-28 23:00:28.090	100
	ROS4	2001-04-28 23:00:13.160	2001-04-28 23:00:28.210	100
	ROS2	2001-04-28 23:00:11.925	2001-04-28 23:00:33.155	100
	ROS1	2001-04-28 23:00:12.030	2001-04-28 23:00:28.545	100
23	ROS1	2002-02-14 17:01:02.055	2002-02-14 17:01:17.515	100
	ROS2	2002-02-14 17:01:00.690	2002-02-14 17:01:20.580	100
	ROS5	2002-02-14 17:01:02.030	2002-02-14 17:01:17.030	100
	ROS6	2002-02-14 17:01:00.535	2002-02-14 17:01:21.150	100
24	ROS2	2002-10-14 23:45:19.915	2002-10-14 23:45:35.035	100
25	ROS2	2002-12-24 02:57:19.900	2002-12-24 02:57:35.560	100
	ROS6	2002-12-24 02:56:41.461	2002-12-24 02:56:58.581	0
26	MID1	2003-03-03 20:51:19.490	2003-03-03 20:51:34.490	100
	MID3	2003-03-03 20:51:18.750	2003-03-03 20:51:35.780	0
27	MID3	2003-09-27 13:57:53.300	2003-09-27 13:58:08.365	0
28	ROS1	2003-10-11 11:44:05.910	2003-10-11 11:44:20.905	100
	ROS2	2003-10-11 11:44:04.660	2003-10-11 11:44:22.435	100
29	MID3	2003-11-10 00:22:34.335	2003-11-10 00:22:51.540	100
	ZAN2	2003-11-10 00:22:34.511	2003-11-10 00:22:52.241	0
30	MID3	2003-11-16 20:04:09.895	2003-11-16 20:04:24.905	100
	ZAN2	2003-11-16 20:04:08.500	2003-11-16 20:04:25.700	0
31	ROS1	2004-09-06 20:31:17.740	2004-09-06 20:31:32.775	100
	ROS2	2004-09-06 20:31:16.325	2004-09-06 20:31:32.805	100
	ROS6	2004-09-06 20:31:16.345	2004-09-06 20:31:32.750	100
32	HKS	2006-01-18 08:12:42.704	2006-01-18 08:12:58.294	0
33	HKS	2006-02-12 14:36:35.019	2006-02-12 14:36:50.109	0
34	HKS	2006-03-21 14:50:30.209	2006-03-21 14:50:45.699	0
35	HKS	2006-03-23 03:12:20.274	2006-03-23 03:12:35.464	0
36	ROS1	2006-03-25 13:54:34.115	2006-03-25 13:54:51.115	100
	ROS2	2006-03-25 13:54:34.175	2006-03-25 13:54:53.900	100
	ROS6	2006-03-25 13:54:32.210	2006-03-25 13:55:09.650	100
37	ROS1	2006-03-25 13:55:47.175	2006-03-25 13:56:03.635	100
	ROS2	2006-03-25 13:55:47.195	2006-03-25 13:56:04.530	100
	ROS4	2006-03-25 14:00:35.500	2006-03-25 14:00:50.525	0
	ROS6	2006-03-25 13:55:47.080	2006-03-25 13:56:04.990	100
38	ZAN1	2006-08-08 05:03:58.250	2006-08-08 05:04:15.465	100

Continued on next page

Event ID	Station	Start time	End time	Time flag
	ZAN2	2006-08-08 05:03:57.308	2006-08-08 05:04:19.568	0
	HKS	2006-08-08 05:04:01.094	2006-08-08 05:04:16.684	0
	MID3	2006-08-08 05:03:56.755	2006-08-08 05:04:17.230	100
39	MID3	2006-08-08 09:49:21.875	2006-08-08 09:49:36.890	100
40	ZAN2	2006-08-26 22:41:14.885	2006-08-26 22:41:31.845	100
41	WSE	2006-10-23 13:38:02.175	2006-10-23 13:38:19.585	0
	ZAN2	2006-10-23 13:38:02.168	2006-10-23 13:38:19.028	0
42	WSE	2007-01-26 00:20:05.336	2007-01-26 00:20:26.551	0
	ZAN2	2007-01-26 00:20:01.539	2007-01-26 00:20:18.344	0
43	WSE	2007-05-14 12:19:19.760	2007-05-14 12:19:36.950	100
44	ZAN2	2007-06-09 20:07:30.636	2007-06-09 20:07:47.411	0
45	ZAN2	2008-05-18 13:23:44.270	2008-05-18 13:23:59.330	100
46	ZAN1	2008-10-30 05:54:26.760	2008-10-30 05:54:43.480	100
	ZAN2	2008-10-30 05:54:25.191	2008-10-30 05:54:45.321	0
	WSE	2008-10-30 05:54:25.761	2008-10-30 05:54:53.476	0
	MID3	2008-10-30 05:54:28.165	2008-10-30 05:54:43.350	100
	WIN	2008-10-30 06:01:31.904	2008-10-30 06:01:46.909	0
	MID1	2008-10-30 05:54:26.597	2008-10-30 05:54:48.307	0
47	ZAN2	2008-11-07 16:39:59.225	2008-11-07 16:40:14.265	100
48	MID1	2008-12-15 20:41:13.055	2008-12-15 20:41:28.100	100
49	WSE	2009-01-01 16:54:44.511	2009-01-01 16:54:59.511	0
	ZAN1	2009-01-01 16:54:42.830	2009-01-01 16:54:57.830	100
	ZAN2	2009-01-01 16:54:43.690	2009-01-01 16:54:58.705	0
50	WSE	2009-01-08 01:16:57.589	2009-01-08 01:17:14.399	0
51	WSE	2009-01-09 20:16:54.336	2009-01-09 20:17:11.201	0
52	ZAN2	2009-02-01 04:23:20.220	2009-02-01 04:23:37.005	100
	ZAN1	2009-02-01 04:23:22.405	2009-02-01 04:23:37.580	100
	WSE	2009-02-01 04:23:20.382	2009-02-01 04:23:39.092	0
53	MID1	2009-04-14 21:05:21.905	2009-04-14 21:05:42.480	100
	MID3	2009-04-14 21:05:23.775	2009-04-14 21:05:38.900	100
	WSE	2009-04-14 21:05:22.535	2009-04-14 21:05:45.025	0
54	MID1	2009-05-08 05:23:11.465	2009-05-08 05:23:27.610	100
	WIN	2009-05-08 05:23:20.684	2009-05-08 05:23:38.289	0
	WSE	2009-05-08 05:23:08.281	2009-05-08 05:23:32.401	0
	ZAN1	2009-05-08 05:23:08.415	2009-05-08 05:23:26.675	100
	ZAN2	2009-05-08 05:23:08.773	2009-05-08 05:23:26.828	0
55	WIN	2009-07-05 10:43:38.704	2009-07-05 10:43:53.774	0
56	WIN	2009-12-04 04:15:21.864	2009-12-04 04:15:37.684	0
	HKS	2009-12-04 04:12:30.719	2009-12-04 04:12:46.009	0
57	HKS	2010-02-19 23:12:49.729	2010-02-19 23:13:04.819	0
58	ZAN1	2010-05-03 09:26:12.395	2010-05-03 09:26:29.275	100
59	FRB2	2010-06-09 19:19:18.374	2010-06-09 19:19:35.209	0
60	GARST	2010-08-14 07:43:17.089	2010-08-14 07:43:32.309	0
	KANT	2010-08-14 07:43:21.754	2010-08-14 07:43:36.939	0

Continued on next page

Event ID	Station	Start time	End time	Time flag
	MID1	2010-08-14 07:43:19.265	2010-08-14 07:43:34.290	100
	WSE	2010-08-14 07:43:16.575	2010-08-14 07:43:33.760	100
	ZAN2	2010-08-14 07:43:18.820	2010-08-14 07:43:33.840	100
61	WSE	2010-11-15 11:42:42.080	2010-11-15 11:42:58.865	100
62	MID1	2011-01-19 19:39:27.960	2011-01-19 19:39:45.170	100
	MID3	2011-01-19 19:39:30.210	2011-01-19 19:39:45.215	100
	STDM	2011-01-19 19:39:30.014	2011-01-19 19:39:45.319	0
	WSE	2011-01-19 19:39:28.825	2011-01-19 19:39:45.860	100
63	WSE	2011-03-26 20:45:50.335	2011-03-26 20:46:05.380	100
64	FRB2	2011-05-12 16:44:25.709	2011-05-12 16:44:40.709	0
65	WIN	2011-06-23 09:19:08.034	2011-06-23 09:19:23.179	0
	WSE	2011-06-23 09:14:42.995	2011-06-23 09:15:00.295	100
66	ZAN1	2011-06-27 15:48:08.210	2011-06-27 15:48:29.175	100
	ZAN2	2011-06-27 15:48:06.645	2011-06-27 15:48:28.990	100
	WSE	2011-06-27 15:48:06.825	2011-06-27 15:48:38.000	100
	WIN	2011-06-27 15:52:34.834	2011-06-27 15:52:57.344	0
	MID1	2011-06-27 15:48:10.700	2011-06-27 15:48:31.110	100
	KANT	2011-06-27 15:46:28.869	2011-06-27 15:46:44.044	0
	HKS	2011-06-27 15:47:41.249	2011-06-27 15:48:08.739	0
	GARST	2011-06-27 15:48:10.079	2011-06-27 15:48:26.464	0
67	WSE	2011-07-29 22:48:29.575	2011-07-29 22:48:46.450	100
68	GARST	2011-08-31 06:23:56.704	2011-08-31 06:24:11.714	0
	WSE	2011-08-31 06:23:56.645	2011-08-31 06:24:14.335	100
	ZAN2	2011-08-31 06:23:57.670	2011-08-31 06:24:12.715	100
69	WSE	2011-09-06 21:48:09.250	2011-09-06 21:48:24.320	100
70	MID1	2011-09-25 12:59:00.045	2011-09-25 12:59:15.125	100
	WSE	2011-09-25 12:58:57.485	2011-09-25 12:59:13.210	100
71	WSE	2011-12-30 06:20:08.805	2011-12-30 06:20:25.940	100
	GARST	2011-12-30 06:20:11.214	2011-12-30 06:20:26.219	0
	MID3	2011-12-30 06:20:10.485	2011-12-30 06:20:25.495	100
72	GARST	2012-05-24 15:52:37.844	2012-05-24 15:52:52.854	0
73	GARST	2012-08-15 19:17:32.779	2012-08-15 19:17:51.944	0
	MID1	2012-08-15 19:17:35.830	2012-08-15 19:17:51.535	100
	WIN	2012-08-15 19:20:24.469	2012-08-15 19:20:41.719	0
	WSE	2012-08-15 19:17:32.585	2012-08-15 19:17:57.505	100
74	STDM	2012-08-16 20:29:55.434	2012-08-16 20:30:20.374	0
	WSE	2012-08-16 20:30:29.220	2012-08-16 20:31:06.920	100
	WIN	2012-08-16 20:33:22.674	2012-08-16 20:33:47.259	0
	KANT	2012-08-16 20:28:38.394	2012-08-16 20:29:03.129	0
	HKS	2012-08-16 20:29:12.159	2012-08-16 20:29:28.849	0
	GARST	2012-08-16 20:30:29.599	2012-08-16 20:30:54.729	0
	FRB2	2012-08-16 20:30:36.864	2012-08-16 20:30:53.449	0
	MID1	2012-08-16 20:30:29.150	2012-08-16 20:31:01.605	100
75	HKS	2013-01-19 20:06:17.464	2013-01-19 20:06:34.754	0

Continued on next page

Event ID	Station	Start time	End time	Time flag
	WIN	2013-01-19 20:10:07.379	2013-01-19 20:10:22.379	0
	WSE	2013-01-19 20:10:06.965	2013-01-19 20:10:21.965	100
76	WSE	2013-02-07 22:31:55.125	2013-02-07 22:32:12.795	100
	GARST	2013-02-07 22:31:56.929	2013-02-07 22:32:12.154	0
	KANT	2013-02-07 22:29:14.594	2013-02-07 22:29:31.574	0
77	WSE	2013-02-07 23:19:06.496	2013-02-07 23:19:28.871	0
	GARST	2013-02-07 23:19:07.424	2013-02-07 23:19:22.784	0
	KANT	2013-02-07 23:16:25.084	2013-02-07 23:16:46.949	0
78	GARST	2013-02-09 05:26:08.534	2013-02-09 05:26:23.999	0
	WSE	2013-02-09 05:26:06.575	2013-02-09 05:26:28.235	100
79	ZAN1	2013-07-02 23:03:58.480	2013-07-02 23:04:13.675	0
	WIN	2013-07-02 23:04:10.799	2013-07-02 23:04:30.924	0
80	HKS	2013-09-04 01:28:51.494	2013-09-04 01:29:06.984	0
	WIN	2013-09-04 01:34:39.754	2013-09-04 01:34:56.564	0
	GARST	2013-09-04 01:33:29.899	2013-09-04 01:33:47.354	0
	ZAN1	2013-09-04 01:33:29.390	2013-09-04 01:33:46.830	0
81	WIN	2013-10-02 20:25:57.616	2013-10-02 20:26:12.651	0
82	HKS	2014-02-13 02:11:27.829	2014-02-13 02:11:43.219	0
	KANT	2014-02-13 02:12:27.079	2014-02-13 02:12:42.109	0
	GARST	2014-02-13 02:13:13.114	2014-02-13 02:13:28.824	0
	WIN	2014-02-13 02:16:22.409	2014-02-13 02:16:40.814	0

B.1 Borehole event catalogue

TABLE B.1: List of events recorded on borehole instruments. The last two columns indicate the length of the time window to consider before (left) and after (right) the event origin time to fully retrieve the waveform data. In the "Stations" column, only triggered stations are listed. From 2009 on, the triggered mode was progressively replaced by a continuous mode, i.e. more records than presented in this work may be available for the events occurring in this time period

ID	Origin time	Latitude	Longitude	Depth [km]	Magnitude	Stations	Left [s]	Right [s]
1	1995-01-24 09:38:39.190	53.3155	6.8967	3.0	1.26	FSW	9	55
2	1995-01-31 19:47:55.620	53.0632	6.7200	3.0	2.04	FSW	7	61
3	1995-02-01 00:31:32.000	53.0787	6.7750	3.0	1.20	FSW	7	58
4	1995-03-21 16:37:44.340	53.4378	6.9133	3.0	1.07	FSW	8	61
5	1995-04-06 08:03:43.450	53.3597	6.6800	3.0	1.99	FSW	8	60
6	1995-04-26 17:35:49.640	53.0840	6.6683	3.0	0.69	ZLV	141	72
7	1995-05-15 09:52:39.350	53.3090	6.9450	3.0	1.83	FSW	10	54
8	1995-06-03 22:06:38.200	53.1898	6.3583	3.0	0.86	HWF,ZLV	21	56
9	1995-06-20 08:59:40.120	52.8320	7.0298	2.0	2.71	ENV,VLW,ZLV	19	57
10	1995-07-15 16:05:39.140	53.2065	6.8233	3.0	1.03	FSW,WDB,ZLV	22	58
11	1995-07-21 23:24:40.480	53.2755	6.9633	3.0	1.10	FSW,WDB	20	56
12	1995-09-13 21:34:36.830	53.3348	6.7283	3.0	1.09	FSW,ZLV,WDB,ZL2	19	60
13	1995-10-18 00:34:27.360	53.1293	6.4917	3.0	1.27	HWF,ZLV,WDB,ZL2,ENV	23	63
14	1995-11-02 01:07:00.710	53.3517	6.7183	3.0	1.64	WDB,ZLV,ZL2,HWF,FSW	21	60
15	1995-11-04 05:50:43.210	53.4698	6.7217	3.0	1.78	ZLV,ZL2	15	55
16	1995-11-20 02:20:54.730	53.3150	6.7617	3.0	1.13	WDB,ZLV,ENV,FSW	19	60
17	1995-12-24 13:26:34.160	52.5108	4.8467	3.0	2.26	OTL	22	52
18	1995-12-30 02:04:08.940	52.8453	7.0483	3.0	1.19	ENV,VLW	19	54
19	1996-02-12 14:02:24.240	53.2558	6.7667	3.0	0.91	ENM,VLW,WDB	68	61
20	1996-02-24 03:31:07.560	52.7605	6.9083	3.0	1.77	HWF,VLW,ENV,VBG,FSW,ZL2,ENM	33	141
21	1996-02-25 13:55:09.300	52.8380	7.0620	1.5	0.88	VLW	19	50
22	1996-02-29 08:07:34.420	53.3425	6.6400	3.0	2.03	ENM,ZL2,ZLV	86	70
23	1996-03-06 09:20:50.200	52.8380	7.0620	1.5	1.56	ZLV,VLW	112	145
24	1996-03-12 00:51:44.670	53.0637	6.7900	3.0	1.14	ZLV,WDB,ZL2,ENV	37	100
25	1996-03-12 12:13:48.170	52.8376	7.0594	2.0	2.58	ENM,ZLV,VLW,WDB,ZL2,FSW,ENV	73	128
26	1996-03-12 18:34:12.680	53.0723	6.6533	3.0	0.75	ZL2,ZLV	74	107
27	1996-03-14 22:23:58.300	52.8377	7.0641	2.0	1.09	ZLV,VLW,ENV	42	132
28	1996-03-16 04:16:32.770	53.2980	6.8483	3.0	1.36	ENM,WDB,ZLV,ZL2,FSW	38	95
29	1996-03-21 18:19:05.480	52.8332	7.0540	2.0	1.82	ZLV,WDB,ZL2,ENV,VLW	59	106
30	1996-04-01 18:53:45.190	52.9395	6.6083	3.0	0.62	ZLV,WDB,ZL2,ENV,VLW	89	95
31	1996-04-01 23:28:18.390	53.0673	6.7900	3.0	0.13	ZLV,WDB,ZL2	50	101
32	1996-04-09 13:58:34.430	53.0595	6.7983	3.0	1.10	ZLV,WDB,ZL2	41	114
33	1996-04-15 03:41:31.200	53.2893	6.6883	3.0	0.86	WDB,ZLV,ENM,FSW	111	60
34	1996-04-17 19:05:12.180	53.3573	6.8833	3.0	0.93	WDB,ZL2,ENM,FSW	110	87
35	1996-04-21 21:36:02.320	53.3758	6.5950	3.0	0.50	ZLV,WDB,ENM	93	126
36	1996-04-25 23:22:20.440	53.3558	6.8633	3.0	0.88	ENM,ZL2,FSW	110	91
37	1996-06-07 04:20:56.640	53.0850	6.7800	3.0	1.15	ENM,ZL2,ZLV,WDB,VLW,ENV,FSW	62	129
38	1996-06-07 08:34:07.010	53.3088	6.7783	3.0	1.29	ZLV,VLW,ENV,WDB,HWF,FSW	113	130
39	1996-06-07 14:59:10.820	53.0823	6.8317	3.0	0.70	ZL2,WDB,ZLV	77	84
40	1996-06-16 02:53:27.880	52.9467	6.5683	3.0	1.65	ZL2,ZLV,VBG,ENV,WDB,HWF,FSW,VLW,ENM	44	103
41	1996-07-03 21:40:07.160	53.0528	6.8033	3.0	0.84	ZL2,ENV,HWF,WDB,ZLV	116	107
42	1996-08-04 00:42:17.830	52.7243	6.7383	3.0	1.61	ENM,FSW,VBG,VLW,HWF,ZL2,ENV,WDB,ZLV	109	159
43	1996-08-06 13:38:27.760	52.7555	6.9167	3.0	1.62	ZLV,HWF,FSW,VBG,ENV,WDB,VLW	113	109
44	1996-08-09 02:31:45.710	53.0572	6.6883	3.0	0.28	ZLV,ENV,WDB,FSW,HWF,ZL2	61	126
45	1996-08-09 06:38:47.140	53.2868	6.9583	3.0	1.64	HWF,VLW,ZL2,WDB,ENV,FSW,ENM	151	141
46	1996-08-11 01:10:16.250	52.6010	6.7817	3.0	0.65	VBG,VLW,ZLV,ENV,HWF	124	142
47	1996-08-25 22:24:11.140	52.9453	6.5700	3.0	1.71	FSW,ZLV,ZL2,VBG,VLW,ENV,WDB,HWF,ENM	113	156
48	1996-09-02 05:20:51.920	53.1467	6.4217	3.0	2.10	ZLV,ENV,FSW,VBG,VLW,ZL2,WDB,ENM	124	158
49	1996-10-16 05:09:00.100	52.9415	6.6100	3.0	1.26	WDB,ZL2,VLW,ZLV,ENM,ENV,HWF	105	122
50	1996-11-16 03:33:49.870	53.3550	6.7550	3.0	1.32	VLW,HWF,ENV,ENM,ZL2,WDB,ZLV,FSW	151	113
51	1996-11-17 04:59:52.050	52.7243	6.7317	3.0	2.24	HWF,VBG,WDB,ZL2,ZLV,ENM,VLW,FSW,ENV	84	146
52	1996-11-30 20:26:57.950	53.1652	6.4100	3.0	1.04	ENV,HWF,WDB,ZLV,ENM	117	140
53	1996-12-06 16:46:48.000	52.8349	7.0532	1.5	1.58	HWF,ENV,VLW,FSW,VBG,WDB,ZLV	113	117
54	1996-12-16 16:01:15.160	53.0718	6.8150	3.0	0.53	VLW,ZLV,ZL2,HWF,ENV,FSW,WDB	102	126
55	1996-12-16 16:06:50.210	53.0777	6.8217	3.0	-0.06	WDB,VLW,ZLV,ZL2,ENV	82	124
56	1996-12-26 19:52:05.570	53.2612	6.7650	3.0	-0.17	WDB	28	101
57	1996-12-28 00:54:08.570	53.1070	6.5050	3.0	1.94	ZL2,ENM,VBG,ENV,VLW,WDB,ZLV,FSW,HWF	53	104
58	1996-12-28 18:16:52.900	52.8343	7.0432	2.0	2.74	FSW,VBG,HWF,WDB,ZL2,VLW,ZLV,ENV,ENM	105	183
59	1996-12-28 23:39:46.900	53.1105	6.5017	3.0	1.83	WDB,ZL2,VLW,ZLV,ENV,ENM,FSW,VBG,HWF	121	144
60	1997-01-08 01:20:54.490	53.3378	6.7133	3.0	1.50	ENM,ZL2,ZLV,WDB,VLW,ENV,HWF,FSW,VBG	122	144
61	1997-01-14 21:13:40.620	52.9430	6.5767	3.0	0.74	ENV,VBG,HWF,WDB,VLW,ZL2,ZLV	117	125
62	1997-01-16 00:12:46.600	52.8350	7.0456	2.0	2.42	ENV,VLW,ZLV,FSW,HWF,ENM,VBG,ZL2,WDB	120	153
63	1997-01-24 04:00:04.540	53.0793	6.6783	3.0	0.64	ENV,ZL2,ZLV,WDB,FSW,HWF	65	76

Continued on next page

ID	Origin time	Latitude	Longitude	Depth [km]	Magnitude	Stations	Left [s]	Right [s]
64	1997-02-17 07:20:55.230	53.3872	6.7517	3.0	1.60	ENM,HWF,WDB,ENV,ZLV,FSW	121	136
65	1997-02-17 11:16:00.470	52.9475	6.5683	3.0	1.15	ENV,HWF,ZLV,FSW	109	130
66	1997-02-19 21:53:50.700	52.8323	7.0384	2.0	3.35	ZLV,VLW,ENV,OTL,WDB,VBG,ENM,PPB,WMH,FSW	124	208
67	1997-02-26 19:31:22.430	52.6415	6.8033	3.0	1.20	VBG,FSW,WDB,ZLV,VLW,ENV	90	127
68	1997-03-02 15:25:32.540	53.2882	6.2667	3.0	1.30	ZLV,HWF,ENV,ZL2,ENM,FSW,WDB,VLW	120	147
69	1997-03-08 14:29:04.280	53.1065	6.8150	3.0	-0.75	WDB,ZLV,HWF,ZL2	80	100
70	1997-03-25 00:13:07.740	53.2515	6.7483	3.0	-0.18	WDB,ZLV	14	115
71	1997-04-01 00:34:19.040	52.7683	6.8733	3.0	1.40	HWF,FSW,VLW,VBG,ENV,WDB,ZLV	101	125
72	1997-04-09 22:21:43.970	53.2003	6.8650	3.0	0.47	ZLV,HWF,ENM,FSW,WDB	115	121
73	1997-04-17 20:28:02.900	52.8340	7.0530	2.0	0.82	VLW,VBG	75	96
74	1997-04-29 18:16:46.340	53.2490	6.8033	3.0	1.40	FSW,ENM,WDB,ZLV,VLW	82	125
75	1997-05-04 02:42:39.740	53.3002	6.9300	3.0	1.09	WDB,ENM,VLW,FSW,ZLV	42	113
76	1997-05-04 04:29:09.850	53.1442	6.7367	3.0	0.79	ENM,FSW,ENV,HWF,WDB,ZLV,VLW	132	171
77	1997-05-19 15:43:55.200	52.8358	7.0533	2.0	1.25	ZLV,FSW,WDB,ENV,VLW,VBG	84	173
78	1997-06-06 19:39:18.880	53.2925	6.8750	3.0	1.22	WDB,HWF,FSW,ENM,ZLV	105	106
79	1997-06-19 23:19:25.560	53.3638	6.7533	3.0	1.83	HWF,VLW,WDB,VBG,FSW,ZLV,ZL2,ENM	109	157
80	1997-06-20 00:45:37.700	52.8313	7.0550	2.0	1.84	WDB,VLW,VBG,ENM,ZLV,ENV,ZL2,FSW,HWF	86	113
81	1997-06-21 00:30:33.080	53.0940	6.7517	3.5	1.88	HWF,ENM,ZL2,VBG,VLW,ENV,WDB,ZLV,FSW	88	103
82	1997-07-17 02:56:29.710	53.0607	6.7167	3.0	-0.72	ZLV,ENV,WDB,FSW,ZL2	89	118
83	1997-07-23 06:44:36.040	53.2467	6.7533	3.0	1.22	FSW,VLW,WDB,ZLV,HWF,ENM	111	146
84	1997-08-18 04:42:28.770	52.8343	7.0500	2.0	1.57	FSW,ZL2,VBG,VLW,ENM,WDB,ENV,HWF	118	139
85	1997-08-18 05:17:32.250	52.8342	7.0500	2.0	2.07	FSW,VBG,ZL2,VLW,ENM,WDB,ENV,HWF	45	151
86	1997-08-22 10:27:08.850	53.0632	6.8133	3.0	0.21	ZLV,WDB,ZL2	36	114
87	1997-08-23 00:01:56.530	53.0632	6.8133	3.0	0.55	ZLV,ZL2	112	134
88	1997-08-23 19:39:35.040	53.2390	6.6833	3.0	1.63	HWF,ENV,WDB,VLW,FSW,ENM	120	137
89	1997-09-13 21:30:41.020	53.3380	6.7467	3.0	1.08	ENM,HWF,FSW,WDB,ZLV	122	135
90	1997-09-14 19:39:02.590	53.0455	6.7400	3.0	0.40	ZLV,ZL2	101	156
91	1997-11-01 22:56:25.870	53.4267	6.7050	3.0	1.36	WDB,VLW,FSW,HWF,ZLV,ENV,ENM	113	144
92	1997-11-03 18:12:48.770	53.1080	6.5133	3.0	1.41	WDB,VLW,FSW,ZL2,ENV,HWF,ENM	119	138
93	1997-11-04 19:55:01.940	53.3278	6.7933	3.0	1.65	WDB,ZLV,FSW,VLW,VBG,HWF,ZL2,ENV,ENM	108	132
94	1997-11-15 16:22:32.140	53.1042	6.8217	3.0	0.31	ZL2,ZLV	54	93
95	1997-11-20 17:35:21.040	53.2063	6.7917	3.0	1.15	ENV,ZL2,ENM,WDB,VLW,ZLV,FSW,HWF	69	128
96	1997-11-26 02:35:37.010	53.2543	6.7650	3.0	0.17	ZL2,WDB,FSW	125	134
97	1997-12-03 14:47:19.710	53.2787	6.8967	3.0	1.78	ZLV,WDB,ENM,HWF,ZL2,FSW,ENV	120	146
98	1997-12-03 15:01:03.650	53.2437	6.8583	3.0	1.31	HWF,VLW,ZL2,FSW,ZLV,ENV,WDB,ENM	103	115
99	1997-12-07 07:02:44.490	53.0748	6.7017	3.0	0.33	WDB,ZL2,FSW,ZLV	114	101
100	1997-12-23 06:21:32.110	53.3165	7.0150	3.0	1.25	ENM,ZL2,VLW,FSW,WDB	118	141
101	1998-01-08 08:11:45.260	52.9372	6.5967	3.0	1.20	HWF,ZLV,ENV	126	131
102	1998-01-22 10:31:55.150	52.9840	6.5467	3.5	1.08	ENV	28	101
103	1998-01-28 21:33:02.900	52.8327	7.0417	2.0	2.68	VLW,FSW,ZL2,ZLV,ENM,HWF,ENV,WDB,VBG	193	162
104	1998-01-28 22:34:03.400	52.8332	7.0367	2.0	1.98	ENV,WDB,VBG,FSW,ZL2,ZLV,VLW,ENM,HWF	96	161
105	1998-01-31 08:39:39.260	53.2365	6.7450	3.0	0.72	WDB,ENM,FSW,ZL2	112	130
106	1998-02-05 21:11:49.340	53.2905	6.9350	3.0	1.09	ENM,ZLV,WDB,VLW,FSW	99	75
107	1998-02-15 07:24:16.420	53.3558	6.7733	3.0	2.64	WDB,ZLV,VBG,FSW,ENV,HWF,ZL2,ENM,VLW	123	134
108	1998-03-29 06:06:40.520	53.3447	6.7300	3.0	1.31	ENM,HWF,VLW,WDB,ZLV,FSW	7	263
109	1998-04-19 08:00:12.080	53.3388	6.7233	3.0	1.54	ENV,ZL2,HWF,WDB,FSW,ZLV,ENM	128	129
110	1998-04-19 15:32:35.720	53.4245	6.6817	3.0	1.62	ENM,WDB,FSW,ZL2,ENV,ZLV,HWF	77	140
111	1998-04-28 02:02:25.270	53.1073	6.8650	3.0	0.41	ZLV,ZL2	50	112
112	1998-04-30 01:08:41.720	53.1967	6.7067	3.0	0.85	ZLV,FSW,HWF,ENM,ZL2,WDB	30	103
113	1998-05-18 22:03:42.460	53.4038	6.7317	3.0	1.34	VLW,ENM,HWF,ZLV,FSW,WDB	138	146
114	1998-05-30 09:43:15.140	53.2035	6.7767	3.0	0.91	ENV,HWF,FSW,ZLV,WDB,ENM	122	156
115	1998-07-14 12:12:02.230	52.8325	7.0533	2.0	3.26	WDB,HWF,ZLV,VBG,ENM,ENV,FSW,VLW	113	144
116	1998-08-14 19:25:16.890	53.1920	6.8033	3.0	1.12	ZLV,ZL2,FSW,WDB,ENV,ENM,VLW,HWF	103	115
117	1998-08-24 04:28:58.000	53.2978	6.8100	3.0	2.44	ENM,FSW,ENV,ZLV,VLW,HWF	67	133
118	1998-09-05 20:36:11.240	52.7422	6.8750	3.0	1.91	ZL2,WDB,ZLV,VBG,ENV,HWF,ENM,VLW,FSW	97	119
119	1998-10-04 03:28:32.970	53.3528	6.7483	3.0	0.95	WDB,FSW,ENV,ENM	102	118
120	1998-10-20 21:32:05.000	52.9740	6.6067	3.0	0.83	VBG,WDB,ENV,FSW,HWF,ZLV,ENM,VLW	100	76
121	1998-11-01 17:48:29.500	52.9545	6.5717	3.0	1.30	ENV,WDB,VLW,ZLV,ENM,FSW,HWF,VBG	121	140
122	1998-12-12 07:51:39.520	53.3917	6.6983	3.0	1.95	HWF,ENV,VBG,WDB,VLW,FSW,ENM	117	140
123	1998-12-26 23:48:02.190	53.2145	6.8300	3.0	1.60	HWF,ENV,ZL2,WDB,ZLV,ENM,FSW,VLW	83	123
124	1999-01-11 09:36:09.100	52.8370	7.0570	2.0	1.14	HWF,WDB,ENV,VLW,VBG	108	149
125	1999-01-13 19:36:37.030	53.3590	6.7767	3.0	2.09	VLW,ZL2,WDB,ENM,ZLV,ENV,HWF,VBG	103	194
126	1999-01-31 04:53:00.590	53.2550	6.8250	3.0	0.44	HWF,ENV,ENM,VBG,WDB,ZLV,FSW	123	134
127	1999-03-05 19:00:40.230	53.1013	6.7917	3.0	1.01	ZL2,ENV,HWF,ZLV,WDB,VLW,FSW	120	143
128	1999-03-06 05:56:39.960	53.3247	6.7783	3.0	1.60	VBG,VLW,ENM,HWF,ENV,WDB,ZLV,ZL2,FSW	108	149
129	1999-03-12 19:06:42.970	52.8328	7.0515	2.0	1.30	VLW,FSW,ENV,HWF,VBG,ZLV,WDB,ENM	120	162
130	1999-03-17 23:14:25.460	52.8320	7.0517	2.0	1.50	ZLV,VBG,HWF,WDB,FSW,VLW,ZL2,ENM,ENV	120	152
131	1999-04-21 10:59:56.440	53.3120	6.8400	3.0	1.38	HWF,ZLV,VLW,FSW,ENV,ENM,ZL2,WDB	86	171
132	1999-04-22 22:58:02.900	53.1115	6.1517	3.0	1.04	VBG,VLW,FSW,ENM,ZL2,HWF,ZLV,WDB,ENV	123	139
133	1999-05-06 18:13:56.320	52.8357	7.0550	2.0	1.42	FSW,WDB,VBG,VLW,ENV	102	103
134	1999-05-08 20:40:18.930	53.3250	6.7000	3.0	1.56	VLW,ENV,ENM,FSW,ZLV,WDB,HWF,ZL2	110	147
135	1999-05-14 18:30:20.730	52.8343	7.0517	2.0	1.70	VLW,ENV,ENM,FSW,ZL2,VBG,HWF,ZLV,WDB	118	142
136	1999-05-15 19:28:30.360	52.8343	7.0517	2.0	1.38	ZLV,ZL2,VBG,ENV,VLW,FSW,WDB,HWF,ENM	116	141
137	1999-05-21 00:09:38.860	53.1645	6.8150	3.0	0.68	FSW,ENV,ZL2,ZLV,VLW,HWF,WDB	71	100
138	1999-06-07 20:20:31.380	53.0973	6.4017	3.0	1.05	ZLV,ENM,HWF,WDB,ENV	118	202
139	1999-07-07 09:03:11.360	52.9503	6.6267	3.0	1.30	ZL2,HWF,VLW,ENV,ZLV,WDB	58	126
140	1999-08-10 23:24:18.310	53.3818	6.7267	3.0	1.40	WDB,ZLV,FSW,ENM,ZL2	122	135
141	1999-08-11 01:18:00.960	53.3462	6.7017	3.0	0.71	ENM,WDB,ZLV,FSW	76	181

Continued on next page

ID	Origin time	Latitude	Longitude	Depth [km]	Magnitude	Stations	Left [s]	Right [s]
142	1999-09-07 17:16:23.540	53.0682	6.7950	3.0	1.53	FSW,ENV,ZLV,VLW,HWF,ZL2,WDB	149	161
143	1999-09-07 19:47:51.090	53.0572	6.8133	3.0	0.47	WDB,FSW,ENV,ZLV,VLW,HWF,ZL2	182	136
144	1999-10-18 18:56:09.540	53.0775	6.7183	3.0	0.41	WDB,HWF,ENV,ZLV,VLW,ZL2,FSW	141	152
145	1999-10-18 18:57:55.400	53.0605	6.6783	3.0	0.31	ZL2,FSW,WDB,HWF,ENV,ZLV,VLW	169	138
146	1999-10-22 13:19:16.770	52.9410	6.5917	3.0	1.71	ENV,ZLV,VLW,ZL2,FSW,ENM,HWF,VBG,WDB	116	141
147	1999-12-08 05:39:28.470	53.1792	6.8017	3.0	0.28	ZL2,WDB,FSW,HWF,ZLV,VLW	77	126
148	1999-12-09 09:38:00.050	53.2465	6.8033	3.0	1.12	WDB,ENM,ZL2,FSW,ENV	125	155
149	1999-12-09 09:52:12.960	53.1833	6.7983	3.0	1.01	ENV,WDB,ENM,ZLV,FSW	128	129
150	1999-12-10 06:13:32.010	53.1745	6.7917	3.0	1.40	ENV,ZLV,HWF,FSW,WDB,VBG,ZL2,ENM,VLW	120	149
151	1999-12-20 12:29:29.690	53.3523	6.7100	3.0	1.47	VBG,ENM,FSW,WDB,HWF,ENV,VLW,ZLV	180	142
152	1999-12-21 04:52:37.740	53.1900	6.7650	3.0	0.98	ENM,VBG,HWF,FSW,VLW,ZLV,ENV,WDB	137	130
153	1999-12-24 23:52:41.120	53.3200	6.9467	3.0	1.81	ENV,HWF,ZL2,VBG,VLW,ZLV,ENM,FSW,WDB	119	141
154	1999-12-31 11:00:55.330	52.8352	7.0483	2.0	2.80	ZLV,VLW,FSW,ENM,HWF,WDB,VBG,ENV	95	164
155	2000-01-07 14:19:06.760	52.8342	7.0433	2.0	1.10	VBG,ENV,ZLV,VLW,FSW	93	66
156	2000-01-10 04:18:07.460	53.0770	6.6550	3.0	0.60	HWF,FSW,WDB,ENV,ZLV,ZL2	91	128
157	2000-02-12 19:48:10.610	53.3210	6.8217	3.5	1.67	ZLV,VLW,ZL2,ENM,ENV,WDB,HWF,FSW,VBG	91	135
158	2000-03-19 16:13:36.080	53.3428	6.6983	3.0	1.56	ENM,WDB,ZLV,ZL2,FSW	103	127
159	2000-04-01 03:13:51.380	52.6847	6.7500	3.0	1.30	ZL2,ENV,VLW,FSW,VBG,ZLV	117	144
160	2000-04-08 11:07:29.680	53.2047	6.6317	3.0	1.17	FSW,ZL2,VLW,HWF,WDB,ENM	98	94
161	2000-04-08 21:13:17.800	53.3702	6.8450	3.0	1.12	FSW,ZL2,VLW,HWF,WDB,ENM	95	96
162	2000-04-14 23:07:47.790	53.3077	6.7717	3.0	1.21	ENM,FSW,ZL2,VLW	117	140
163	2000-05-16 01:11:14.730	53.3805	6.7100	3.0	1.89	ZLV,WDB,ENM,FSW,HWF	54	83
164	2000-06-09 17:03:47.280	53.0868	6.8133	3.0	1.07	HWF,VLW,ENV,FSW,ZLV,WDB,ENM,VBG,ZL2	129	128
165	2000-06-11 04:12:20.130	53.3480	6.7633	3.0	2.03	ZL2,WDB,HWF,ENV,ENM,VBG,VLW,FSW,ZLV	108	151
166	2000-06-12 15:48:23.010	53.3398	6.7417	3.0	2.55	WDB,ENM,VBG,ZL2,HWF,FSW,VLW,ENV,ZLV	112	145
167	2000-06-15 01:42:24.950	53.2803	6.8467	3.0	2.45	ENV,WDB,ZLV,VBG,ENM,VLW,ZL2,FSW,HWF	5	135
168	2000-07-06 23:09:56.720	53.3398	6.7517	3.0	1.19	ZLV,WDB,ENM,HWF,FSW,VLW	106	240
169	2000-07-10 15:05:49.120	53.0643	6.5750	3.0	1.04	ZLV,ZL2,HWF,ENV	111	150
170	2000-07-13 08:41:52.430	53.0788	6.5650	3.0	1.12	HWF,WDB,ENV,ZL2,ZLV	124	133
171	2000-07-16 01:34:12.000	53.3665	6.7817	3.0	1.54	ENM,HWF,FSW,WDB,ZLV,VLW	24	108
172	2000-09-22 17:05:16.770	53.0757	6.8200	3.0	0.98	WDB,FSW,ENV,ZL2,ZLV,VLW	93	132
173	2000-09-22 20:52:06.400	53.0817	6.7933	3.0	2.16	FSW,ENM,ENV,HWF,ZL2,ZLV,VLW,WDB,VBG	105	152
174	2000-09-23 03:47:47.430	53.0807	6.7883	2.7	0.96	ENV,WDB,ENM,ZL2,ZLV,VBG,HWF,VLW,FSW	111	121
175	2000-10-25 18:10:34.790	52.8318	7.0517	2.3	3.20	ZL2,ENM,ENV,FSW,VLW,ZLV,WDB,VBG,HWF	112	200
176	2000-11-12 02:16:36.270	52.9773	6.6083	3.0	0.31	HWF,ZL2,ENV,VLW	9	124
177	2000-11-29 16:06:48.390	52.6257	6.7417	3.0	1.63	ENV,VLW,VBG,ZLV	106	127
178	2000-12-23 05:20:06.170	53.1080	6.8117	3.0	0.36	HWF,ENV,ENM,WDB,ZLV,ZL2,FSW,VLW	129	218
179	2000-12-26 16:33:57.640	53.2943	6.9100	3.0	1.38	ZL2,ZLV,HWF,ENV,WDB,ENM,VLW,FSW,VBG	122	179
180	2001-02-26 11:39:07.310	53.0723	6.8217	3.0	0.77	ZLV,WDB,ZL2	87	114
181	2001-03-18 04:14:20.680	53.2433	6.6917	3.0	1.61	ZLV,HWF,ENM,ENV,ZL2,VBG,VLW,WDB,FSW	151	106
182	2001-04-28 10:00:08.290	52.9482	6.5667	3.0	1.54	ENV,VLW,WDB,FSW,ENM,ZL2,HWF,ZLV	46	213
183	2001-04-28 10:00:55.510	52.9590	6.5750	3.0	1.08	ENV,VLW,WDB,FSW,ENM,ZL2,HWF,ZLV	93	166
184	2001-04-28 23:00:15.880	52.8332	7.0533	2.0	2.36	VBG,HWF,ZLV,FSW,VLW,WDB,ENV,ENM	107	212
185	2001-05-17 07:48:15.470	53.1730	6.6117	3.0	1.41	ZL2,VLW,ZLV,VBG,WDB,FSW,ENM,ENV	110	149
186	2001-06-10 03:35:33.200	53.0490	6.7533	3.0	0.48	HWF,WDB,ZLV,ENV,ZL2	155	121
187	2001-06-19 06:49:55.570	53.0788	6.8200	3.0	0.97	ZLV,ZL2,WDB	133	124
188	2001-06-21 03:50:49.050	53.2953	6.8000	3.0	1.73	ENM,FSW,ENV,VBG,ZL2,WDB,HWF,VLW	116	141
189	2001-08-07 17:09:01.500	53.0970	6.8450	3.0	0.32	WDB,ZLV	96	51
190	2001-09-09 06:58:12.520	52.6510	4.7133	2.0	3.48	OTL,VBG,ENV,ENM,HWF,VLW,WMH,PPB,WDB,FSW,ZLV	86	168
191	2001-09-10 04:30:15.430	52.6526	4.7118	2.0	3.20	OTL,FSW,VBG,PPB,ENV,WMH,ENM,HWF,VLW	111	201
192	2001-10-10 06:41:09.360	52.6818	4.6483	2.9	2.70	VLW,ENV,WMH,OTL,VBG,WDB,FSW,PPB,HWF,ENM	175	187
193	2001-10-10 14:06:43.350	53.2390	6.7633	3.0	0.99	ZLV,ENV,HWF,VLW,WDB,FSW	156	178
194	2001-10-10 14:06:57.240	53.2397	6.7633	3.0	0.75	ZLV,ENV,HWF,VLW,WDB,FSW	170	164
195	2001-11-12 14:33:15.370	53.6945	7.3767	3.0	1.36	VLW,FSW,WDB,HWF,ENV,ENM	129	129
196	2001-12-04 19:08:31.060	53.2042	6.7850	3.0	0.19	FSW,VLW,HWF,ZLV,ENM,WDB,VBG,ENV	133	126
197	2001-12-04 19:08:37.830	53.2042	6.7850	3.0	-0.01	FSW,VLW,HWF,ZLV,ENM,WDB,VBG,ENV	140	120
198	2001-12-04 22:33:37.960	53.2098	6.7433	3.0	1.02	VLW,HWF,ZLV,ENM,WDB,VBG,ENV,FSW	150	142
199	2001-12-11 15:17:17.620	53.2167	6.7883	3.0	0.71	WDB	21	108
200	2001-12-20 01:25:42.980	53.0805	6.8383	3.0	0.47	ZLV	25	104
201	2001-12-25 23:28:11.710	53.3972	6.6817	3.0	1.14	VLW,ENM,FSW,WDB,ZLV,VBG,ENV	92	100
202	2001-12-26 12:36:53.070	53.0565	6.8050	3.0	-0.21	WDB,ZLV,ENV,FSW,VLW,ENM	123	134
203	2002-02-05 10:30:39.740	53.3190	6.7167	3.0	2.21	VBG,ENV,WDB,ENM,HWF,VLW,FSW,ZLV	94	113
204	2002-02-14 17:01:04.740	52.8315	7.0350	2.0	2.07	HWF,WDB,VBG,FSW,ZLV,VLW,ENV	125	156
205	2002-02-27 03:52:14.030	53.3370	6.8267	3.0	1.14	WDB,ENM,FSW,ZLV	114	146
206	2002-03-17 02:16:27.900	53.0933	6.5433	3.0	0.43	FSW,ENM,ZLV,VLW,HWF,WDB,ENV	128	137
207	2002-04-14 01:11:44.490	53.0718	6.7867	3.0	1.73	WDB,VLW,FSW,HWF,ZLV,ENM,VBG,ENV	84	54
208	2002-05-10 10:33:48.950	53.3783	6.8567	3.0	1.67	HWF,VLW,FSW,ZLV,ENM,WDB	120	137
209	2002-05-11 10:07:23.220	52.9432	6.5800	3.0	1.48	HWF,ENV,VLW,ZLV,WDB,FSW	118	139
210	2002-05-22 13:38:13.040	52.9560	6.5850	3.0	0.96	ZLV,ENV,HWF,VBG	18	123
211	2002-06-28 03:06:47.380	52.9680	6.4500	3.0	1.80	WDB,ZLV,FSW,HWF,VLW,VBG	75	56
212	2002-07-18 05:31:16.830	53.1878	6.7833	3.0	1.64	HWF,ZLV,FSW,WDB,VLW,ENM,ENV,VBG	115	184
213	2002-07-27 15:01:08.630	52.9470	6.5650	3.0	1.62	FSW,ENV,VLW,VBG,ZLV,WDB,HWF	168	165
214	2002-08-05 19:28:10.160	53.0552	6.6567	3.0	0.86	ENV,VLW,WDB,HWF,ZLV,FSW	124	133
215	2002-08-29 21:13:22.740	53.2468	6.7467	3.0	0.01	FSW,ZLV,WDB	116	146
216	2002-09-05 00:00:21.450	52.5075	6.5633	3.0	0.89	ENV,VLW,VBG	26	107
217	2002-09-06 06:07:05.500	53.1123	6.8417	3.0	0.60	ZLV,WDB	113	118
218	2002-09-22 07:13:33.430	53.0562	6.6800	3.0	0.58	WDB,ZLV	98	127
219	2002-09-22 07:30:13.810	53.0348	6.6383	3.0	0.47	ZLV	107	22

Continued on next page

ID	Origin time	Latitude	Longitude	Depth [km]	Magnitude	Stations	Left [s]	Right [s]
220	2002-10-12 02:32:13.630	53.1065	6.8150	3.0	0.86	HWF,ENV,WDB,ZLV	50	83
221	2002-10-14 23:45:22.510	52.8340	7.0450	2.0	0.94	ENV,ZLV,VLW,FSW,VBG	150	107
222	2002-10-19 18:03:39.430	53.0678	6.7683	1.8	1.28	FSW,ZLV,WDB,HWF,VBG,VLW	120	137
223	2002-12-14 00:13:24.620	52.6765	6.8317	3.0	1.38	WDB,FSW,HWF,ENM,VLW,ZLV,ENV	41	91
224	2002-12-16 12:23:39.090	53.0917	6.7183	3.0	1.38	FSW,ENV,VLW,WDB,ZLV,HWF	100	129
225	2002-12-17 00:23:18.740	53.2908	6.8600	3.0	0.88	FSW,ENV,HWF,ZLV,ENM,VLW,WDB	124	138
226	2002-12-18 20:31:09.150	53.1753	6.8467	3.0	0.77	HWF,WDB,ZLV,ENM,ENV,FSW	111	146
227	2002-12-24 02:57:22.580	52.8325	7.0417	2.0	1.43	VBG,WDB,VLW,ZLV,ENV	23	108
228	2003-01-01 19:16:15.310	53.3375	6.7433	3.0	0.96	ENM,WDB,HWF,ZLV,ENV,FSW	103	154
229	2003-01-13 02:45:45.500	52.9708	6.4133	3.0	1.66	VLW,FSW,ZLV,HWF,VBG,ENM,ENV,WDB	94	38
230	2003-01-18 18:12:43.320	53.2872	6.7700	3.0	1.05	VLW,ZLV,FSW,WDB,ENM,HWF	166	172
231	2003-01-23 07:46:16.660	53.3070	6.7517	3.0	1.65	ENV,WDB,VLW,HWF,ZLV,FSW,ENM	154	124
232	2003-01-30 01:27:30.240	53.3417	6.7933	3.0	1.51	ENM,WDB,VLW,HWF,ZLV	7	126
233	2003-01-31 15:20:47.780	53.2322	6.7817	3.0	0.32	ZLV,WDB,HWF	46	118
234	2003-02-02 09:32:23.690	52.9502	6.5883	3.0	1.96	ENV,WDB,VLW,VBG,ENM,ZLV,FSW,HWF	153	127
235	2003-02-06 19:25:24.910	53.2593	6.7683	3.0	0.32	WDB,HWF,ENM,ZLV,FSW	121	138
236	2003-02-11 19:29:49.560	53.3525	6.7733	3.0	1.35	FSW,HWF,ENV,ENM,VLW,ZLV,WDB	119	150
237	2003-02-12 06:22:20.020	53.2622	6.8117	3.0	0.80	FSW,ZLV,HWF,ENM,WDB	115	158
238	2003-02-14 06:54:24.140	53.1458	6.1217	3.0	1.82	ENM,VLW,ENV,WDB,ZLV,HWF,FSW	106	151
239	2003-02-28 21:54:18.190	53.3548	6.7300	3.0	0.70	WDB,HWF,FSW,ENM,ZLV	92	86
240	2003-03-03 20:51:21.890	53.3603	6.6617	3.0	2.17	HWF,ENV,VBG,ENM,FSW,VLW,ZLV,WDB	118	155
241	2003-03-06 20:15:18.670	53.1408	6.7533	3.0	0.94	ENV,FSW,ENM,VLW,WDB,ZLV,HWF	149	146
242	2003-03-09 05:31:26.700	53.3718	6.6400	3.0	1.06	WDB,FSW,ENM,HWF	65	91
243	2003-03-23 16:00:03.100	53.4573	6.7833	3.0	1.48	WDB,HWF,ZLV,FSW,VLW,ENM,ENV	82	175
244	2003-03-29 21:09:01.440	53.2375	6.6817	3.0	0.42	FSW,ZLV,WDB,HWF	103	79
245	2003-04-01 00:25:52.090	53.3637	6.8517	3.0	0.35	ZLV,FSW,WDB	20	110
246	2003-04-02 20:19:48.740	53.3398	6.7183	3.0	1.90	VLW,FSW,ENV,ZLV,WDB,HWF	101	88
247	2003-04-05 16:49:48.330	53.2092	6.6300	3.0	0.33	FSW,WDB,ENM	153	134
248	2003-04-06 00:07:50.700	53.2715	6.7950	3.0	0.07	ENM,FSW,WDB	91	41
249	2003-04-06 00:57:27.900	53.2045	6.7500	3.0	1.03	ENV,VLW,ENM,FSW,WDB,HWF	124	136
250	2003-04-06 23:02:04.370	53.2060	6.7633	3.0	0.71	VLW,ENM,ENV,ZLV,WDB,HWF	108	187
251	2003-04-16 16:20:42.530	53.2813	6.7750	3.0	0.68	WDB,ZLV,ENM,FSW,VLW	168	131
252	2003-04-18 23:59:55.000	53.2382	6.7533	3.0	0.00	ZLV,ENM,FSW,WDB	79	133
253	2003-04-20 00:19:39.190	53.2465	6.7500	3.0	0.10	WDB,FSW,ZLV,ENM	31	101
254	2003-04-28 21:56:11.330	53.2835	6.7267	3.0	1.00	ZLV,ENV,WDB,HWF,ENM,FSW,VBG,VLW	103	156
255	2003-04-29 02:55:04.920	53.2837	6.7300	3.0	1.28	HWF,ENV,WDB,ENM,FSW,VBG,VLW,ZLV	13	119
256	2003-05-14 20:52:15.910	53.2537	6.8650	3.0	0.76	FSW,ZLV,ENV,HWF,ENM,WDB,VLW	140	152
257	2003-05-14 22:23:46.520	53.2565	6.8467	3.0	0.77	WDB,VLW,FSW,ENV,ZLV,HWF,ENM	168	131
258	2003-05-21 04:57:09.240	53.0717	6.7650	3.0	1.11	ZLV,ENM,ENV,FSW,WDB,HWF	116	156
259	2003-05-23 02:59:50.860	53.0842	6.8233	3.0	0.56	ZLV,WDB,FSW	171	89
260	2003-05-31 23:12:25.730	53.2468	6.8750	3.0	0.77	ZLV,ENM,FSW,WDB	120	137
261	2003-06-03 16:15:38.910	53.3365	6.6833	3.0	1.45	ZLV,FSW,WDB,HWF,ENM	121	161
262	2003-06-06 14:27:16.470	53.2250	6.6817	3.0	0.68	VLW,ENM,ZLV,FSW,HWF,WDB	57	119
263	2003-06-08 05:30:47.240	53.1918	6.7883	3.0	1.02	FSW,VLW,ENV,ENM,HWF,WDB,ZLV	121	149
264	2003-06-08 08:14:16.550	53.2708	6.7367	3.0	1.47	WDB,ZLV,FSW,VLW,ENV,ENM,HWF	101	110
265	2003-06-16 00:44:17.120	52.9630	6.4067	2.6	2.26	ENV,WDB,ZLV,VLW,FSW,VBG,ENM	102	159
266	2003-08-05 18:45:08.490	52.9747	6.5583	3.0	1.11	ENV	77	52
267	2003-08-07 08:24:21.120	53.3495	6.7583	3.0	1.66	ENM,FSW,WDB,ZLV	115	142
268	2003-08-07 10:56:39.850	53.3447	6.7483	3.0	1.30	WDB,ZLV,ENM,FSW	77	109
269	2003-08-20 08:46:14.990	53.1063	6.8150	3.0	0.50	WDB,ENV,ZLV	126	131
270	2003-08-25 04:24:55.000	53.1077	6.7917	3.0	0.71	WDB,ZLV	25	124
271	2003-08-25 10:05:35.890	53.1077	6.7950	3.0	0.90	WDB,ZLV	114	35
272	2003-09-22 17:50:11.500	53.3952	6.6883	3.0	2.36	WDB,FSW,ZLV,ENV,VLW,HWF,VBG	114	145
273	2003-09-27 13:57:54.150	53.3478	6.6967	3.0	2.71	VBG,FSW,WDB,VLW,HWF,ZLV,ENM	124	160
274	2003-10-11 11:44:08.340	52.8353	7.0550	2.0	1.61	FSW,ENV,VLW,VBG,ZLV	124	140
275	2003-10-24 01:52:41.160	53.2950	6.7917	3.0	2.95	ENM,ENV,VBG,WDB,ZLV,VLW,HWF,FSW	118	150
276	2003-10-26 09:17:00.140	53.3040	6.7883	3.0	1.22	FSW,ENM,VLW,HWF,ZLV,WDB	118	164
277	2003-10-29 14:30:09.260	53.1917	6.7833	3.0	0.98	ZLV,ENM,FSW,VLW,HWF,WDB	76	120
278	2003-11-10 00:22:38.030	53.3253	6.6900	3.0	2.99	VLW,HWF,FSW,OTL,VBG,ENM,WDB,PPB,ENV	83	178
279	2003-11-10 02:40:55.010	53.3492	6.7100	3.0	1.43	ENM,VLW,HWF,WDB,ENV,FSW,VBG	113	157
280	2003-11-16 20:04:11.480	53.3437	6.7017	3.0	2.67	ZLV,HWF,VLW,FSW,WDB,ENM,VBG,ENV	203	173
281	2003-12-26 10:09:58.930	53.3197	6.8017	3.0	1.41	HWF,VLW,WDB,FSW,VBG,ENV,ENM	122	135
282	2003-12-29 13:09:59.310	53.3428	6.9383	3.0	1.47	WDB,VLW,ZLV,FSW,ENM	107	159
283	2004-01-12 01:05:47.910	53.1887	6.7450	3.0	1.58	ZLV,VLW,ENV,FSW,WDB,HWF,ENM	112	147
284	2004-01-24 13:53:44.540	53.2710	6.7200	3.0	0.95	WDB,ENM,FSW,HWF,ZLV,VLW	114	96
285	2004-01-30 11:47:40.990	53.3138	6.8683	3.0	1.17	ZLV,WDB,FSW,VLW,ENM	157	119
286	2004-03-07 07:18:30.450	53.1028	6.8450	3.0	0.16	WDB,ZLV	37	95
287	2004-03-08 01:41:16.410	53.2925	6.8950	3.0	0.44	ZLV,FSW,WDB,VLW,ENM	63	117
288	2004-03-16 23:49:41.240	53.0903	6.8800	3.0	0.96	FSW,ZLV,ENV,HWF,ENM,VBG,VLW,WDB	163	178
289	2004-03-21 17:05:44.580	53.2550	6.9183	3.0	1.44	WDB,FSW,ZLV,ENV,HWF,ENM,VLW	111	147
290	2004-03-26 02:32:45.520	53.2727	6.8617	3.0	0.48	FSW,ENM,ZLV,WDB	81	50
291	2004-04-15 04:50:23.620	53.0412	6.8000	3.0	0.99	WDB,ENV,ZLV	144	113
292	2004-04-30 22:12:43.890	53.2298	6.7117	3.0	0.51	WDB,ZLV,ENM,HWF,FSW,VLW	116	156
293	2004-05-24 05:03:13.440	53.3097	6.5250	3.0	1.36	VLW,WDB,ZLV,HWF,FSW,ENV,ENM	84	109
294	2004-05-29 21:06:42.270	53.3080	6.5083	3.0	0.84	FSW,HWF,ENM,WDB,ZLV	86	146
295	2004-05-31 00:59:19.960	53.3128	6.5183	3.0	0.28	WDB,ENM,HWF,FSW,ZLV	108	152
296	2004-06-10 01:13:26.720	53.3905	6.6633	3.0	2.15	ZLV,ENV,HWF,ENM,FSW,VBG,VLW,WDB	59	74
297	2004-06-21 23:32:02.760	52.9440	6.5683	3.0	2.78	ENV,ENM,WDB,HWF,VBG,FSW,ZLV,VLW	102	217

Continued on next page

ID	Origin time	Latitude	Longitude	Depth [km]	Magnitude	Stations	Left [s]	Right [s]
298	2004-07-27 22:49:45.940	53.3433	6.8750	3.0	1.16	ENM,FSW,HWF,WDB,ENV,VLW	120	137
299	2004-08-21 01:06:32.820	53.1635	6.7933	3.0	1.80	WDB,ENM,VBG,ZLV,FSW,VLW,ENV,HWF	29	103
300	2004-08-22 02:56:01.130	52.9460	6.5850	3.0	0.99	ZLV,ENV,HWF,VLW	69	63
301	2004-09-10 01:56:44.910	53.0638	6.6700	3.0	0.43	WDB,ZLV	97	34
302	2004-09-18 03:33:12.380	53.4157	6.7033	3.0	1.18	WDB,ZLV,ENM,FSW	125	155
303	2004-09-22 12:44:33.000	53.3113	6.7433	3.0	1.54	FSW,ENM,VLW,ZLV,WDB,HWF	120	137
304	2004-10-08 13:23:42.720	53.0760	6.8333	2.5	1.27	FSW,ZLV,ENV,HWF	137	120
305	2004-10-30 11:40:52.880	53.3562	6.7783	3.0	1.36	HWF,FSW,ENM,VBG,ENV,ZLV,WDB	124	236
306	2004-10-31 17:27:21.880	52.9523	6.6333	3.0	0.86	ENV,VBG,ZLV,WDB,HWF,FSW,ENM	137	175
307	2004-11-13 12:15:57.320	53.2905	6.8017	3.0	1.17	ENM,VLW,ZLV,HWF,WDB,ENV	156	171
308	2004-11-23 22:13:10.360	53.1162	6.8200	3.0	0.31	ZLV,VLW,ENV,WDB	120	143
309	2004-11-24 18:18:57.950	53.2888	6.7533	3.0	1.86	HWF,VBG,ENM,FSW,WDB,ENV,ZLV,VLW	110	176
310	2004-11-25 14:25:54.430	53.1945	6.7717	3.0	0.65	ZLV,VLW,HWF,FSW,VBG,ENM,ENV,WDB	118	185
311	2004-11-26 06:58:01.520	53.3142	6.7367	3.0	1.61	ZLV,VBG,WDB,FSW,ENV,HWF,ENM,VLW	126	143
312	2004-12-16 21:14:30.200	53.2308	6.6517	3.0	0.78	HWF,ENM,ZLV,ENV,FSW,VLW,WDB	150	152
313	2005-01-09 23:59:38.530	53.3233	6.7967	3.0	1.69	VLW,ENM,HWF,ENV,FSW,ZLV,WDB	98	150
314	2005-01-17 00:00:55.580	53.3173	6.8083	3.0	1.10	WDB,VLW,ZLV,FSW,ENM	60	71
315	2005-01-30 02:31:34.040	53.2768	6.6917	3.0	1.03	ENV,VLW,FSW,WDB,ZLV,ENM	137	147
316	2005-02-08 13:20:33.860	53.3157	6.6383	3.0	2.25	HWF,ENV,WDB,ZLV,ENM,VLW,FSW	139	140
317	2005-02-15 19:21:11.010	52.9553	6.6050	3.0	0.95	ZLV,WDB,VBG,ENV,VLW,HWF	113	160
318	2005-02-16 10:46:17.860	53.4040	6.7933	3.0	1.26	HWF,WDB,ENM,FSW	123	134
319	2005-02-18 11:26:29.870	53.0810	6.6733	3.0	0.63	ENV,WDB,ENM,VLW,HWF,FSW,ZLV	129	128
320	2005-02-18 12:55:46.580	53.3405	6.7350	3.0	1.34	ENV,VLW,ENM,HWF,FSW,WDB,ZLV	110	147
321	2005-02-18 18:49:25.650	53.2312	6.7500	3.0	0.54	WDB,ZLV,FSW,ENM,ENV,VLW,HWF	112	152
322	2005-02-18 22:05:52.170	53.2392	6.7267	3.0	1.63	WDB,ZLV,FSW,ENV,VLW,HWF,ENM	123	165
323	2005-02-20 06:03:24.650	53.1762	6.7950	3.0	0.02	WDB,HWF,ENV,FSW,ZLV	174	90
324	2005-02-25 03:46:09.860	53.3355	6.8117	3.0	1.58	WDB,ENM,ZLV,HWF	133	135
325	2005-03-01 16:31:59.410	53.3258	6.9217	3.0	1.23	VLW,ZLV,FSW,WDB,ENM	114	143
326	2005-03-08 23:00:58.530	53.2615	6.9150	3.0	0.86	ZLV,ENM,VLW,WDB,FSW	88	199
327	2005-03-10 02:04:39.780	53.3422	6.8100	3.0	1.95	ENM,HWF,WDB,VLW,FSW,ENV,ZLV	152	105
328	2005-03-21 10:58:33.930	53.2568	6.7667	3.0	0.93	FSW,HWF,ENM,VLW,ENV,ZLV,WDB	160	147
329	2005-03-21 23:21:19.980	53.4573	5.8500	3.0	1.76	HWF,WMH,VBG,PPB,WDB,VLW,ENV,OTL,ZLV,FSW,ENM	143	192
330	2005-04-02 23:21:08.740	53.2695	6.7983	3.0	1.21	ENV,HWF,ZLV,WDB,FSW,ENM	92	112
331	2005-04-18 19:11:16.590	53.2637	6.8033	3.0	1.03	VLW,WDB,FSW,HWF,ZLV,ENM	118	142
332	2005-04-21 20:49:21.640	53.2905	6.8850	3.0	0.90	VLW,WDB,FSW,HWF,ZLV,ENM	117	181
333	2005-04-22 00:14:49.670	53.3345	6.8583	3.0	0.82	HWF,WDB,FSW,ENM,VLW,ZLV	126	134
334	2005-04-30 19:28:02.720	53.3595	6.7000	3.0	0.97	HWF,WDB,ZLV,FSW,ENM	59	105
335	2005-05-17 08:50:14.190	53.2318	6.8933	3.0	1.00	WDB,VLW,ZLV,ENM,FSW	131	152
336	2005-05-25 21:33:46.220	53.1937	6.8500	3.0	1.06	FSW,VLW,ENV,HWF,ZLV,ENM	119	138
337	2005-05-28 19:57:57.640	53.3740	6.0883	3.0	1.43	FSW,WDB,HWF,ENM	104	96
338	2005-05-30 15:36:45.870	53.3425	6.7100	3.0	2.29	ENV,WDB,HWF,ENM,VBG,VLW,FSW,ZLV	178	140
339	2005-06-22 16:02:02.050	53.3295	6.8183	3.0	1.51	ENM,HWF,ZLV,FSW,VLW,WDB,ENV	118	150
340	2005-07-09 17:01:37.490	53.2383	6.6850	3.0	1.11	ENM,WDB,FSW,ZLV	117	140
341	2005-07-17 18:07:07.830	53.3192	6.7467	3.0	1.82	VLW,FSW,ENM,ZLV,HWF,WDB,ENV	139	150
342	2005-07-25 03:21:58.980	53.2118	6.7117	3.0	0.82	ENM,WDB,ZLV,HWF,FSW	107	71
343	2005-08-05 19:23:02.020	53.1703	6.8100	3.0	2.22	ENV,VLW,WDB,ENM,HWF,ZLV,FSW	90	133
344	2005-09-10 02:05:11.670	53.3162	6.7717	3.0	1.23	ZLV,WDB,ENM,FSW,VLW,HWF	92	40
345	2005-10-05 09:16:02.950	53.3307	6.6417	3.0	1.70	HWF,ZLV,ENM,FSW,WDB	127	154
346	2005-10-12 16:06:42.530	52.9628	6.4500	3.0	2.54	VBG,ZLV,ENV,VLW,WDB,ENM,FSW,HWF	148	190
347	2005-10-23 17:03:38.080	53.3658	6.6750	3.0	1.88	HWF,ZLV,ENM,WDB,FSW	96	124
348	2005-11-11 17:02:29.540	53.2243	6.6967	3.0	1.36	WDB,VLW,ENM,ENV,FSW,HWF,ZLV	127	143
349	2006-01-02 12:00:45.670	53.2358	6.6950	3.0	1.07	HWF,ENM,ZLV,VLW,FSW,WDB	111	167
350	2006-01-10 23:41:06.140	52.9560	6.5717	3.0	2.60	ENV,VLW,FSW,VBG,WDB,ENM,HWF,ZLV	131	166
351	2006-01-14 22:29:54.760	53.1767	6.7667	3.0	0.33	WDB,HWF,ZLV,FSW	123	158
352	2006-01-18 08:12:46.650	53.2903	6.7650	3.0	1.49	ZLV,FSW,ENM,VLW,HWF,VBG,WDB,ENV	176	112
353	2006-01-18 22:08:15.790	53.2738	6.7733	3.0	1.60	WDB,FSW,VBG,ENM,HWF,ZLV,VLW,ENV	222	192
354	2006-01-20 20:22:50.100	53.3362	6.7400	3.0	1.35	FSW,ENM,WDB,HWF,ZLV	92	99
355	2006-01-23 11:17:39.960	53.2367	6.6967	3.0	1.91	ENM,WDB,HWF,ENV,VLW,ZLV,VBG,FSW	99	188
356	2006-01-28 03:00:42.030	53.3802	6.8183	3.0	1.13	ENV,FSW,VBG,HWF,ENM,WDB,VLW,ZLV	95	38
357	2006-01-29 18:26:53.140	52.9518	6.5800	3.0	1.13	ZLV,HWF,VLW,ENV,WDB,FSW,ENM	119	151
358	2006-02-11 20:01:35.920	53.2562	6.8467	3.0	1.26	WDB,FSW,ENM,ZLV,HWF,VLW,ENV	94	127
359	2006-02-12 14:36:38.630	53.2968	6.7950	3.0	1.48	VLW,ENV,WDB,FSW,ENM,ZLV,HWF	124	133
360	2006-02-24 04:50:30.030	53.3115	6.7883	3.0	1.33	ZLV,FSW,ENM	99	103
361	2006-03-04 04:32:33.960	53.1435	6.7417	3.0	1.77	ZLV,ENM,FSW,VLW,WDB,HWF,ENV	147	137
362	2006-03-21 14:50:33.700	53.3020	6.7550	3.0	2.37	ENM,ZLV,FSW,VLW,HWF,ENV,WDB	122	183
363	2006-03-23 03:12:23.910	53.2835	6.7783	3.0	2.24	HWF,FSW,VLW,ENV,VBG,WDB,ENM,ZLV	29	104
364	2006-03-25 13:54:38.140	52.8342	7.0450	2.0	2.10	ENM,VBG,ZLV,FSW,HWF,VLW,ENV,WDB	97	210
365	2006-03-25 13:55:51.170	52.8338	7.0433	2.0	1.70	ENM,VBG,ZLV,FSW,HWF,VLW,ENV,WDB	170	137
366	2006-04-05 01:41:09.760	53.3438	6.8900	3.0	1.44	ENM,ZLV,HWF,FSW,VLW,WDB	58	75
367	2006-04-12 05:20:29.140	53.2697	6.8367	3.0	1.19	HWF,VLW,ENM,ZLV,WDB,FSW	153	143
368	2006-04-13 07:38:51.890	53.2402	6.6467	3.0	1.53	VLW,WDB,FSW,HWF,ZLV,ENM	107	150
369	2006-04-16 13:51:52.500	53.3105	6.7833	3.0	1.92	FSW,ENM,ZLV,VLW,WDB,HWF	120	161
370	2006-04-16 18:44:54.420	53.3128	6.7700	3.0	1.12	ZLV,VLW,WDB,HWF,FSW,ENM	112	159
371	2006-04-19 17:39:15.340	53.3363	6.6850	3.0	1.59	HWF,WDB,FSW,ENM,ZLV,VLW	90	129
372	2006-04-22 03:41:54.260	53.3248	6.7517	3.0	1.48	ZLV,WDB,ENV,HWF,VLW,FSW	39	134
373	2006-04-22 17:03:13.410	53.3823	6.5983	3.0	0.36	HWF,WDB,FSW,ENM,ZLV	104	99
374	2006-04-23 01:18:18.280	53.3383	6.8833	3.0	0.88	ENM,ZLV,FSW,HWF,WDB	95	162
375	2006-04-23 15:02:07.760	53.3887	6.5367	3.0	1.11	HWF,WDB,FSW,ENM,ZLV	134	140

Continued on next page

ID	Origin time	Latitude	Longitude	Depth [km]	Magnitude	Stations	Left [s]	Right [s]
376	2006-05-02 16:52:01.310	53.3137	6.7967	3.0	1.03	ZLV,VLW,HWF,ENM,WDB,FSW	130	140
377	2006-05-03 19:16:37.310	53.2898	6.7667	3.0	1.23	ENM,WDB,FSW,ZLV,VLW,HWF	116	141
378	2006-05-07 16:11:32.060	53.3452	6.7167	3.0	1.35	VLW,HWF,ENM,FSW,WDB,ZLV	122	135
379	2006-05-22 20:23:40.850	53.2408	6.6983	3.0	0.87	HWF,ENM,VBG,ENV,WDB,ZLV,VLW,FSW	158	137
380	2006-06-06 03:17:34.010	53.2377	6.8100	3.0	1.35	ENV,FSW,WDB,VLW,ENM,ZLV	95	82
381	2006-06-08 23:31:06.380	53.2398	6.6900	3.0	0.75	HWF,ENM,FSW,ENV,ZLV,WDB,VLW	87	116
382	2006-06-16 21:06:46.760	53.2925	6.7700	3.0	1.61	ENM,ENV,FSW,ZLV,WDB	129	147
383	2006-06-17 02:43:08.640	53.2970	6.7683	3.0	1.18	FSW,ZLV,ENV,WDB,ENM	65	67
384	2006-06-17 13:16:21.580	53.3295	6.8517	3.0	1.44	ZLV,WDB,ENM,ENV,FSW	122	135
385	2006-06-23 22:35:43.140	53.3168	6.7633	3.0	1.68	VLW,ENM,HWF,WDB,FSW,ZLV	148	110
386	2006-06-24 16:42:19.500	53.3407	6.8233	3.0	1.25	ENM,HWF,WDB,FSW,ZLV	139	139
387	2006-07-12 00:13:56.330	53.3693	6.8133	3.0	0.86	FSW,HWF,ENM,WDB,ZLV	72	60
388	2006-07-12 22:56:23.840	53.3088	6.8683	3.0	1.30	ZLV,WDB,ENM,FSW	101	73
389	2006-07-16 08:10:39.150	53.3028	6.8667	3.0	1.48	WDB,FSW,HWF,ENM,ZLV	91	127
390	2006-08-08 05:04:00.050	53.3503	6.6967	3.0	3.47	FSW,VBG,VLW,ENV,HWF,ENM,WDB,ZLV	111	169
391	2006-08-08 09:49:23.380	53.3495	6.7067	3.0	2.53	ENM,VBG,WDB,HWF,ENV,FSW,VLW,ZLV	95	104
392	2006-08-11 06:21:23.030	53.2190	6.6717	3.0	1.11	ENM,WDB,ZLV,FSW	124	133
393	2006-08-26 22:41:18.560	53.3432	6.7117	3.0	2.31	HWF,FSW,VLW,WDB,ENM,ZLV,VBG,ENV	159	164
394	2006-09-06 01:37:32.170	53.1888	6.5217	3.0	1.77	ZLV,VLW,ENV,HWF,ENM,WDB,FSW,VBG	96	35
395	2006-09-27 23:30:44.280	53.3675	6.6867	3.0	1.62	WDB,FSW,ENV,HWF,ZLV,ENM,VLW	85	128
396	2006-10-06 00:10:28.980	53.3022	6.7900	3.0	1.56	VLW,ZLV,WDB,ENM,HWF,FSW	121	138
397	2006-10-15 20:18:00.950	52.7675	6.8850	3.0	1.62	ZLV,FSW,VBG,VLW,WDB,ENV,HWF	125	138
398	2006-10-23 13:38:05.840	53.3723	6.7383	3.0	2.27	ENM,VLW,ZLV,WDB,ENV,HWF,FSW	178	146
399	2006-10-25 09:45:41.930	53.3255	6.9233	3.0	1.38	ZLV,VLW,HWF,VBG,ENV,WDB,ENM,FSW	171	140
400	2006-10-26 02:57:47.240	52.6422	6.8033	3.0	0.76	ENM,VBG,ENV,ZLV,HWF,VLW,WDB	174	98
401	2006-10-26 13:59:37.830	53.3937	6.7050	3.0	1.37	ENV,WDB,ZLV,HWF,ENM,FSW,VLW	125	144
402	2006-11-04 21:04:48.480	52.9342	6.5783	3.0	1.27	WDB,VLW,ENV,ZLV,FSW,HWF	117	130
403	2006-11-05 15:00:25.430	53.2727	6.7917	3.0	1.18	VLW,FSW,ENV,ZLV,HWF,WDB	98	118
404	2006-12-25 04:57:18.510	53.3400	6.4033	3.0	1.26	FSW,HWF,WDB,ENM	100	157
405	2007-01-10 18:36:28.540	53.3405	6.8833	3.0	1.46	ZLV,HWF,WDB,FSW,VLW	125	132
406	2007-01-18 22:29:44.290	53.2737	6.7667	3.0	0.89	FSW,WDB,ZLV	83	84
407	2007-01-26 00:20:09.100	53.3518	6.7550	3.0	2.33	VLW,ENV,HWF,ZLV,FSW,WDB,VBG,ENM	61	197
408	2007-01-31 01:03:35.870	53.3680	6.6717	3.0	1.19	ENM,FSW,ZLV,HWF,WDB	109	152
409	2007-02-04 04:47:35.160	53.3463	6.6583	3.0	0.64	ENM,WDB,FSW	105	92
410	2007-02-16 11:14:09.060	53.2285	6.7017	3.0	1.46	ZLV,VLW,ENV,ENM,VBG,HWF,WDB,FSW	109	172
411	2007-02-17 01:41:14.010	53.2273	6.7033	3.0	2.58	ENV,VBG,ENM,WDB,FSW,HWF,ZLV,VLW	62	198
412	2007-02-17 02:21:08.020	53.2278	6.6833	3.0	0.92	ENM,FSW,WDB,HWF,ZLV	23	108
413	2007-02-17 19:58:01.450	53.3510	6.8567	3.0	0.89	HWF,WDB,ZLV,FSW	113	164
414	2007-03-03 06:43:33.490	53.2353	6.7083	3.0	1.09	HWF,ENM,VLW,FSW,ZLV,WDB	116	141
415	2007-03-11 01:08:14.360	53.3257	6.7800	3.0	1.12	WDB,ENM,ZLV,FSW	2	130
416	2007-03-21 23:04:36.360	53.2400	6.7217	3.0	1.21	ENM,ENV,FSW,HWF,WDB,VLW,ZLV	116	141
417	2007-03-29 20:28:14.250	53.0678	6.6933	3.0	0.74	ZLV	70	58
418	2007-03-30 16:25:05.670	53.2360	6.7067	3.0	1.24	WDB,ENM,HWF,ENV,VLW,FSW	110	105
419	2007-04-01 15:42:37.310	53.2295	6.6900	3.0	0.66	ENM,WDB,ENV,VLW,FSW,HWF	118	139
420	2007-04-13 14:57:28.170	53.2262	6.7433	3.0	1.21	HWF,FSW,ENM,WDB,VLW	142	147
421	2007-05-14 12:19:24.020	53.3312	6.7017	3.0	1.99	ENM,ENV,WDB,FSW,VLW,HWF	125	132
422	2007-05-19 05:33:22.590	53.1630	6.8283	3.0	0.44	FSW,WDB	127	130
423	2007-06-09 20:07:33.630	53.3530	6.7467	3.0	2.07	ENV,VLW,ENM,HWF,WDB,FSW	127	168
424	2007-06-10 17:27:40.310	53.3262	6.6133	3.0	1.70	WDB,ZLV,VLW,ENM,HWF,FSW,ENV	109	160
425	2007-06-11 02:18:12.250	53.3210	6.6533	3.0	1.05	FSW,WDB,ZLV,ENM	108	156
426	2007-06-23 02:01:45.220	53.3173	6.7033	3.0	1.23	FSW,HWF,WDB,ENM	140	118
427	2007-07-02 20:57:03.350	52.7673	6.8750	3.0	1.43	ZLV,VLW,FSW,HWF,VBG,ENV,WDB	130	224
428	2007-08-15 05:49:24.240	53.3690	6.7317	3.0	1.46	WDB,FSW,ENV,HWF,ZLV,VLW,ENM	119	138
429	2007-09-17 05:01:20.880	53.3443	6.8000	3.0	1.55	VLW,ENM,HWF,FSW,WDB,ZLV,ENV	142	136
430	2007-09-18 06:16:33.810	53.2360	6.8000	3.0	0.88	FSW,ZLV,ENM,WDB	129	128
431	2007-09-28 05:26:40.030	53.3378	6.6233	3.0	1.22	HWF,WDB,ENM	170	115
432	2007-09-30 14:17:35.630	53.1942	6.7883	3.0	2.07	ENM,ENV,VLW,ZLV,WDB,FSW,HWF,VBG	168	200
433	2007-10-27 01:57:51.450	53.3328	6.7483	3.0	1.99	ENV,ENM,WDB,HWF,VLW,FSW,VBG,ZLV	36	96
434	2007-11-13 10:26:05.830	53.2932	6.8233	3.0	1.67	ENV,FSW,WDB,ZLV,VLW,ENM	114	143
435	2007-11-30 21:37:45.840	53.0530	6.5683	3.0	1.47	HWF,ENM,WDB,VLW,FSW,ZLV,ENV	122	182
436	2007-12-10 03:59:13.850	53.2972	6.5350	3.0	0.69	ENM,WDB	23	110
437	2008-01-02 03:36:15.850	52.9388	6.5600	3.0	1.40	HWF,VLW,ENV,FSW,WDB,ENM,ZLV	53	80
438	2008-01-05 20:31:49.730	53.0647	6.7817	3.0	1.74	WDB,ENM,HWF,FSW,VBG,ENV,ZLV,VLW	172	130
439	2008-01-07 21:53:16.800	53.2428	6.6583	3.0	1.15	ZLV,VLW,WDB,ENM,HWF,FSW,ENV	107	113
440	2008-01-24 19:21:01.700	53.1962	6.7733	3.0	1.52	WDB,FSW,ZLV,HWF,VLW,ENM	102	98
441	2008-02-12 02:48:49.960	53.3108	6.7833	3.0	0.91	HWF,ZLV,FSW,WDB,ENM	6	125
442	2008-02-17 16:35:15.190	53.0823	6.6817	3.0	1.80	FSW,VLW,ENM,ZLV,WDB,VBG,HWF,ENV	116	141
443	2008-02-19 15:44:51.340	53.1830	6.7617	3.0	0.92	VLW,ZLV,HWF,WDB,ENV,FSW,ENM	131	134
444	2008-03-19 17:02:10.020	53.3480	6.5650	3.0	1.16	HWF,ENV,ENM,WDB,FSW	131	126
445	2008-03-29 16:57:22.030	53.2922	6.8417	3.0	1.42	FSW,WDB,VLW,ENM,ZLV	122	150
446	2008-03-31 07:06:02.500	53.3463	6.7000	3.0	1.23	ENM,FSW,HWF,WDB	197	132
447	2008-04-02 01:15:31.700	52.9462	6.5917	3.0	1.93	FSW,ZLV,HWF,VBG,ENM,ENV,VLW,WDB	56	77
448	2008-04-02 01:28:37.190	52.9467	6.5950	3.0	2.47	FSW,ZLV,HWF,VBG,ENM,ENV,VLW,WDB	74	59
449	2008-04-07 04:32:22.730	53.2943	6.8967	3.0	1.22	FSW,ENM,WDB	137	120
450	2008-04-11 22:51:26.220	53.2832	6.8750	3.0	1.12	FSW,ENM,WDB,ZLV	102	115
451	2008-04-15 04:54:03.210	53.3122	6.5567	3.0	0.90	FSW,ENM,HWF,WDB	129	128
452	2008-04-22 11:46:02.530	53.0675	6.7700	3.0	1.84	HWF,ENM,FSW,VLW,WDB,ENV,ZLV	117	140
453	2008-04-28 02:47:01.090	53.2585	6.8600	3.0	1.30	FSW,VLW,WDB,ZLV,ENM,HWF	42	91

Continued on next page

ID	Origin time	Latitude	Longitude	Depth [km]	Magnitude	Stations	Left [s]	Right [s]
454	2008-05-05 19:56:08.310	53.3325	6.5900	3.0	1.01	WDB,ENM,ZLV,HWF,FSW	78	91
455	2008-05-09 21:33:03.070	53.2857	6.7250	3.0	1.32	VLW,WDB,ZLV,FSW,ENV,HWF	123	142
456	2008-05-10 23:20:35.310	53.3265	6.7283	3.0	1.22	ENV,WDB,ZLV,ENM,FSW,HWF,VLW	166	146
457	2008-05-18 13:23:46.140	53.3753	6.7283	2.8	2.17	HWF,ENM,ENV,VLW,WDB,ZLV,FSW	98	119
458	2008-05-19 15:07:29.550	53.3247	6.7400	3.0	1.85	WDB,ZLV,FSW,HWF,ENM,VLW,ENV	106	106
459	2008-05-30 14:48:08.510	53.4080	6.6333	3.0	1.33	ZLV,FSW,WDB,ENM,HWF	52	88
460	2008-06-01 11:00:58.770	53.3078	6.7817	3.0	1.32	ENM,WDB,VLW,ENV,FSW,ZLV,HWF	117	172
461	2008-06-10 20:51:05.760	53.3098	6.7850	3.0	0.86	ENM,FSW,ZLV,WDB	74	116
462	2008-06-15 06:29:27.020	52.8637	4.3617	3.5	2.13	WMH,OTL	75	182
463	2008-06-22 21:06:15.530	53.2477	6.8417	3.0	0.91	WDB,ENM,FSW	98	122
464	2008-06-23 13:52:14.530	53.1088	6.8550	3.0	1.11	ZLV,WDB	60	80
465	2008-07-10 06:57:33.900	53.3505	6.8817	3.0	2.46	ZLV,WDB,VLW,ENV,FSW,ENM,HWF	163	209
466	2008-07-23 20:05:12.970	53.2118	6.6633	3.0	1.24	HWF,ENV,WDB,FSW,ZLV,ENM,VLW	124	141
467	2008-08-05 02:35:51.140	52.7615	6.9083	3.0	1.99	ZLV,WDB,VBG,ENM,FSW,HWF,ENV	12	120
468	2008-08-23 19:49:07.370	53.3298	6.7250	3.0	0.94	ENM,ZLV,HWF,FSW,WDB	119	156
469	2008-08-26 22:55:52.650	52.9490	6.5650	3.0	2.32	HWF,FSW,WDB,VLW,ENM,ZLV,VBG,ENV	123	184
470	2008-09-14 20:32:12.480	53.3307	6.6217	3.0	1.12	FSW,ZLV,HWF,WDB,ENM	124	133
471	2008-09-15 22:26:57.620	53.0535	6.8033	3.0	0.99	ENV,ZLV,VLW,HWF,WDB	71	98
472	2008-09-20 08:45:58.680	53.2380	6.7067	3.0	1.33	ENM,FSW,WDB,ZLV	128	145
473	2008-09-29 10:20:44.810	53.3790	6.6017	3.0	1.83	WDB,HWF,FSW,ZLV,ENM	63	123
474	2008-10-11 08:19:39.900	52.6995	4.3717	3.0	2.65	WMH,OTL	67	99
475	2008-10-26 02:48:50.060	53.2432	6.8050	3.0	1.07	ZLV,HWF,ENM,ENV,VLW,FSW,WDB	79	110
476	2008-10-26 07:49:52.410	52.9445	6.5533	3.0	1.73	WDB,VLW,HWF,ENV,ZLV,FSW,ENM	112	151
477	2008-10-29 16:36:21.820	53.3297	6.7100	3.0	1.38	FSW,WDB,ENM,ZLV,HWF	79	115
478	2008-10-30 05:54:29.080	53.3367	6.7200	3.0	3.22	ENM,FSW,ZLV,HWF,VLW,WDB,VBG,ENV	120	140
479	2008-11-07 16:40:01.270	53.3808	6.7350	3.0	2.16	ENM,WDB,HWF,VBG,ZLV,VLW,FSW,ENV	124	174
480	2008-11-10 10:55:06.900	53.0825	6.7633	3.0	0.66	VLW,HWF,ENV,ZLV,WDB	104	153
481	2008-11-16 22:51:09.670	53.0482	6.7917	3.0	1.21	HWF,WDB,ENV,VLW,ZLV	91	122
482	2008-12-10 03:22:38.900	53.2795	6.8283	3.0	1.09	HWF,ZLV,FSW,WDB,ENM	132	136
483	2008-12-15 20:41:17.080	53.3360	6.6000	3.0	1.54	WDB,ZLV,ENM,HWF,FSW	118	139
484	2008-12-23 15:16:58.840	53.4025	6.7100	3.0	1.43	ZLV,WDB,ENV,ENM,HWF,FSW	121	136
485	2008-12-24 03:27:10.953	53.0648	6.5817	3.0	1.23	FSW,HWF,WDB,ENM,ZLV,ENV	4	128
486	2009-01-01 08:34:39.080	53.0950	6.7183	3.0	1.51	VLW,WDB,ENM,ZLV,ENV,FSW,HWF	92	112
487	2009-01-01 09:35:46.690	53.3295	6.9017	3.0	1.22	ENV,ZLV,FSW,HWF,WDB,ENM	112	93
488	2009-01-01 16:54:46.910	53.3663	6.7717	3.0	1.73	WDB,HWF,ENM,FSW,ZLV,ENV	170	142
489	2009-01-08 01:17:01.760	53.3477	6.7167	3.0	1.66	ENM,VLW,ZLV,WDB,HWF,FSW,ENV	67	114
490	2009-01-09 20:16:58.440	53.3412	6.7133	3.0	1.88	WDB,ENV,VLW,ENM,HWF,FSW,ZLV	119	167
491	2009-01-15 12:41:13.360	53.3388	6.8717	3.0	1.03	FSW,ENM,ZLV,WDB	97	109
492	2009-01-17 06:05:03.640	53.1703	6.7950	3.0	1.15	ENM,ZLV,HWF,WDB,ENV,FSW,VLW	118	139
493	2009-02-01 04:23:24.160	53.3598	6.7400	3.0	2.23	WDB,HWF,ENM,FSW,ZLV,ENV,VBG,VLW	65	173
494	2009-02-03 06:53:52.070	53.3147	6.8750	3.0	1.17	FSW,ZLV,ENM,WDB	101	78
495	2009-02-04 12:23:50.020	53.3760	6.7417	3.0	1.66	ZLV,WDB,FSW,ENM,HWF	95	134
496	2009-02-05 11:56:12.950	53.3275	6.9233	3.0	1.06	ZLV,ENM,WDB,FSW	99	59
497	2009-02-16 09:24:55.580	53.2977	6.8000	3.0	1.42	ZLV,ENM,WDB,FSW,HWF	124	133
498	2009-02-22 11:56:26.650	53.1180	6.6467	3.0	0.76	ZLV,ENV,WDB	55	92
499	2009-02-23 18:03:15.490	53.1315	6.8300	3.0	0.95	HWF,FSW,VLW,ZLV,ENV,WDB	143	114
500	2009-02-26 01:21:49.580	53.1188	6.6500	3.0	0.53	FSW,WDB,HWF,ZLV	174	90
501	2009-02-26 03:03:15.250	53.1183	6.6467	3.0	1.07	HWF,ZLV,FSW,WDB	118	148
502	2009-03-05 23:36:34.620	53.1187	6.6467	3.0	0.78	ZLV,WDB	38	103
503	2009-03-13 14:33:32.820	53.3497	6.9017	3.0	1.21	ENM,FSW,ZLV,WDB	113	144
504	2009-03-14 15:32:16.310	53.1193	6.6517	3.0	1.02	WDB,ENV,ZLV	121	187
505	2009-03-14 15:32:27.700	53.1178	6.6433	3.0	0.98	WDB,ENV,ZLV	132	175
506	2009-03-14 20:10:51.950	53.1160	6.6367	3.0	0.53	ZLV,WDB	75	61
507	2009-03-17 00:06:15.040	53.1215	6.6517	3.0	0.43	ZLV,WDB	124	134
508	2009-03-17 03:34:07.360	53.1202	6.6483	3.0	0.50	ZLV,WDB	52	78
509	2009-03-17 04:38:27.410	53.1188	6.6483	3.0	1.38	ENV,WDB,ENM,FSW,ZLV,HWF,VLW	93	164
510	2009-03-17 06:32:52.220	53.1198	6.6483	3.0	1.12	ZLV,WDB	95	67
511	2009-03-17 16:34:55.070	53.1182	6.6517	3.0	0.50	ZLV,WDB	163	98
512	2009-03-17 18:39:57.720	53.1193	6.6533	3.0	0.53	ZLV,WDB	114	148
513	2009-03-17 18:40:09.260	53.1187	6.6450	3.0	0.59	ZLV,WDB	125	136
514	2009-03-17 19:10:16.550	53.1197	6.6483	3.0	0.93	WDB,ZLV	136	121
515	2009-03-17 19:10:33.600	53.1202	6.6483	3.0	0.93	WDB,ZLV	153	104
516	2009-03-17 19:10:49.310	53.1198	6.6467	3.0	0.93	WDB,ZLV	169	88
517	2009-03-17 19:11:12.380	53.1210	6.6483	3.0	1.01	WDB,ZLV	192	65
518	2009-03-17 19:15:35.800	53.1200	6.6483	3.0	0.96	ZLV,WDB	76	57
519	2009-03-17 19:16:15.040	53.1202	6.6483	3.0	0.96	ZLV,WDB	115	146
520	2009-03-17 19:27:36.410	53.1195	6.6500	3.0	0.68	ZLV,WDB	156	105
521	2009-03-17 19:28:41.320	53.1197	6.6500	3.0	0.68	ZLV,WDB	221	40
522	2009-03-17 21:28:51.490	53.1203	6.6517	3.0	1.06	ZLV,WDB	135	126
523	2009-03-17 22:42:06.790	53.1187	6.6517	3.0	0.79	ZLV,WDB	51	82
524	2009-03-18 14:26:39.470	53.1195	6.6533	3.0	0.86	WDB,ZLV	153	104
525	2009-03-18 18:16:45.080	53.1188	6.6500	3.0	0.85	WDB,ZLV	134	123
526	2009-03-18 18:27:18.770	53.1197	6.6517	3.0	0.64	WDB,ZLV	128	129
527	2009-03-20 21:07:48.860	53.1188	6.6417	3.0	0.52	ZLV,WDB	140	119
528	2009-03-20 21:21:54.820	53.1185	6.6450	3.0	0.59	ZLV,WDB	90	41
529	2009-03-20 21:30:22.620	53.1200	6.6467	3.0	0.48	ZLV,WDB	86	45
530	2009-03-20 21:37:48.460	53.1202	6.6483	3.0	0.59	WDB,ZLV	146	111
531	2009-03-20 22:48:15.160	53.1203	6.6550	3.0	0.37	ZLV,WDB	23	109

Continued on next page

ID	Origin time	Latitude	Longitude	Depth [km]	Magnitude	Stations	Left [s]	Right [s]
532	2009-03-20 22:49:29.960	53.1168	6.6383	3.0	0.45	ZLV,WDB	98	34
533	2009-03-21 04:31:35.700	53.1220	6.6483	3.0	0.16	ZLV,WDB	112	86
534	2009-03-21 05:11:06.510	53.1200	6.6517	3.0	0.51	WDB,ZLV	127	130
535	2009-03-22 00:32:19.110	53.1198	6.6483	3.0	1.22	ZLV,WDB	20	237
536	2009-03-22 00:34:53.490	53.1193	6.6483	3.0	0.61	ZLV,WDB	175	83
537	2009-03-27 02:51:28.160	53.3080	6.8100	3.0	0.96	FSW,WDB,ZLV,ENM	35	95
538	2009-04-14 21:05:25.880	53.3447	6.6800	3.0	2.62	VLW,ZLV,VBG,ENV,ENM,HWF,FSW,WDB	154	176
539	2009-04-14 23:35:02.870	53.3585	6.7800	3.0	0.95	ENM,FSW,WDB	92	79
540	2009-04-16 17:12:15.910	53.3133	6.8450	3.0	2.59	ZLV,VBG,ENV,HWF,ENM,FSW,VLW	91	134
541	2009-04-20 14:42:51.490	53.2962	6.8083	3.0	1.47	WDB,ZLV,ENM	96	125
542	2009-05-01 14:13:01.730	53.2222	6.7200	3.0	1.20	FSW,WDB,HWF,ENM,ZLV	95	123
543	2009-05-04 11:31:16.560	53.3563	6.7817	3.0	1.81	HWF,WDB,ENM,ZLV,FSW	66	130
544	2009-05-07 01:20:23.540	53.3788	6.7783	3.0	1.37	FSW,ZLV,ENM,HWF,WDB	92	41
545	2009-05-07 03:42:12.640	53.3157	6.7283	3.0	1.59	HWF,ZLV,ENM,WDB,FSW	82	111
546	2009-05-07 13:14:42.560	53.2530	6.7233	3.0	1.25	ENM,WDB,ZLV,FSW,HWF	170	127
547	2009-05-08 05:23:11.950	53.3538	6.7617	3.0	3.00	VBG,ENV,ENM,ZLV,WDB,HWF,FSW	113	153
548	2009-05-08 15:54:22.870	53.1417	6.7150	3.0	0.91	HWF,WDB,ENM,ZLV,FSW	110	99
549	2009-05-22 01:40:29.530	53.0760	6.8350	3.0	1.34	HWF,ENV,FSW,VLW,ZLV,WDB	145	115
550	2009-05-26 00:07:59.580	53.3017	6.9300	3.0	1.27	WDB,ZLV,FSW	100	31
551	2009-05-26 11:00:36.740	53.3138	6.9283	3.0	1.34	ZLV,FSW,WDB	79	103
552	2009-06-01 02:32:25.490	53.2302	6.8783	3.0	0.88	ZLV,FSW,WDB	62	68
553	2009-06-15 15:32:50.850	53.2865	6.8133	3.0	1.05	ZLV,FSW,WDB	46	92
554	2009-07-05 10:42:46.260	53.3075	6.7550	3.0	1.79	WDB,ENM,VLW,HWF,ZLV,ENV,FSW	116	109
555	2009-07-05 18:52:42.270	53.2257	6.8350	3.0	1.22	VLW,ENV,FSW,HWF,ENM,ZLV,WDB	166	104
556	2009-07-14 16:11:14.140	52.7725	4.3083	3.0	2.67	WMH,OTL	40	227
557	2009-07-22 00:00:00.110	53.2903	6.7650	3.0	1.67	ZLV,VLW,ENM,FSW	4	128
558	2009-08-19 01:49:38.130	53.2315	6.6317	3.0	0.67	ENM,WDB,FSW,ZLV	54	78
559	2009-09-14 00:32:51.390	53.2778	6.8450	3.0	1.32	ZLV,FSW,WDB,ENM	56	77
560	2009-09-29 02:23:10.190	53.3138	6.8017	3.0	1.55	ENV,FSW,ENM,ZLV,HWF,WDB,VLW	19	114
561	2009-11-02 02:00:05.650	52.7898	6.8633	3.0	1.40	VBG,HWF,ZLV,VLW,ENV,WDB	43	91
562	2009-11-18 05:17:49.390	53.1453	6.7483	3.0	1.63	WDB,VLW,ZLV,FSW,HWF,ENV	127	131
563	2009-11-19 01:09:30.840	53.0708	6.8167	3.5	1.10	HWF,ENV,VLW,ENM,WDB,ZLV,FSW	79	53
564	2009-11-19 13:20:09.420	52.9718	6.5883	3.0	0.85	VLW,HWF,VBG,ENV	141	169
565	2009-11-20 09:27:32.460	53.3208	6.7467	3.0	1.22	ENM,FSW,ZLV,WDB	125	132
566	2009-11-26 12:54:14.030	52.8917	6.1133	3.0	2.81	WMH,FSW,ENM,HWF,OTL,ZLV,PPB,VBG,VLW,WDB	105	169
567	2009-12-02 08:53:31.220	53.2912	6.8333	3.0	1.14	WDB,ZLV,ENM,FSW	132	140
568	2009-12-04 04:12:32.140	53.2842	6.7433	3.0	2.34	FSW,WDB,VBG,HWF,ENM,VLW,ZLV	53	80
569	2009-12-07 00:24:59.870	53.4512	6.9233	3.0	1.32	ENM,FSW,WDB	94	37
570	2009-12-21 04:55:28.140	53.2237	6.7433	3.0	1.49	WDB,FSW,ZLV,HWF,VLW	69	63
571	2009-12-23 18:38:25.410	53.3095	6.7600	3.0	1.53	WDB,ZLV,FSW,VLW,VBG,HWF	79	129
572	2009-12-25 23:37:52.170	53.2272	6.7500	3.0	0.72	WDB,HWF,FSW,ZLV	120	130
573	2010-01-09 12:31:12.380	53.3670	6.6650	3.0	1.68	HWF,FSW,VLW,ZLV,WDB	115	142
574	2010-01-14 17:12:22.650	53.2927	6.8167	3.0	1.18	WDB,FSW,ZLV	98	114
575	2010-02-11 07:14:12.600	53.0837	6.7667	3.0	0.31	WDB,ZLV	46	88
576	2010-02-17 15:55:01.980	53.1922	6.7917	3.0	1.16	FSW,WDB,HWF,ZLV	130	178
577	2010-02-19 23:12:51.580	53.2877	6.8017	3.0	1.80	VLW,WDB,HWF,ZLV,FSW	171	162
578	2010-03-04 19:59:57.890	53.3422	6.7917	3.0	1.40	FSW,ZLV,WDB	95	100
579	2010-03-31 15:15:02.770	53.1903	6.7767	3.0	2.37	WDB,HWF,FSW,VLW,VBG	124	146
580	2010-04-03 11:50:56.760	53.3457	6.6583	3.0	1.44	WDB,FSW	10	122
581	2010-04-25 00:46:00.400	53.3178	6.8000	3.0	1.56	HWF,WDB,FSW	77	56
582	2010-04-25 13:13:17.170	53.1575	6.8500	3.0	1.02	WDB,FSW,VLW	23	126
583	2010-05-03 09:26:16.070	53.3870	6.8100	3.0	2.31	VLW,HWF,VBG	132	125
584	2010-05-05 03:38:03.030	53.4045	6.7750	3.0	1.60	VLW,HWF	31	99
585	2010-05-07 08:26:35.780	53.4907	6.6167	3.0	2.50	HWF,VLW	92	93
586	2010-05-08 23:36:07.210	53.2782	6.8650	3.0	1.00	HWF,VLW	107	150
587	2010-05-09 17:05:09.550	53.2472	6.9267	3.0	1.70	HWF,VLW	72	114
588	2010-05-30 18:58:36.120	53.2383	6.6783	3.0	1.50	HWF	101	28
589	2010-05-30 18:58:57.990	53.2383	6.6783	3.0	1.20	HWF	122	7
590	2010-06-09 19:19:22.460	53.1818	6.7750	3.0	2.02	HWF	68	61
591	2010-06-10 19:57:35.180	53.2257	6.6517	3.0	1.14	HWF	57	72
592	2010-06-21 00:40:07.480	53.2495	6.7450	3.0	1.30	HWF,VLW	108	24
593	2010-06-21 04:02:58.420	53.2180	6.6200	3.0	1.50	HWF,VLW	119	141
594	2010-06-21 08:06:03.700	53.0742	6.8350	3.0	1.70	HWF,VLW	97	113
595	2010-07-24 00:46:43.620	53.2803	6.7350	3.0	1.80	HWF	119	138
596	2010-08-14 07:43:20.250	53.4028	6.7033	3.0	2.50	HWF,VLW	55	111

B.2 Borehole data availability at all stations and levels

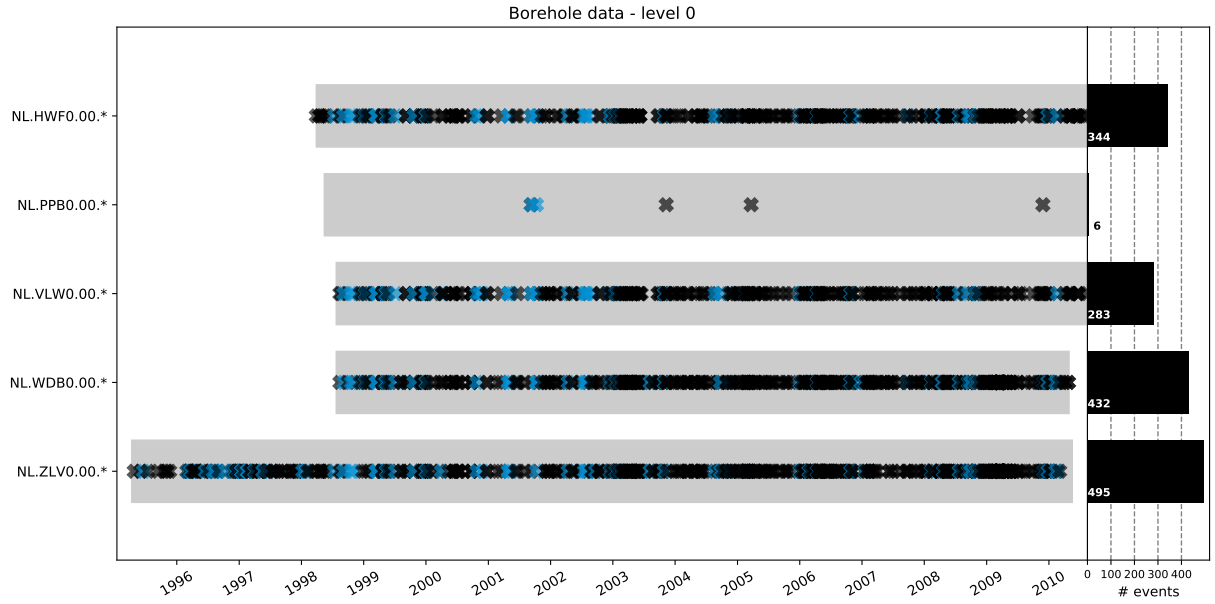

FIGURE B.1: Overview of borehole triggered data (level 0). Grey rectangles represent the time span in which stations were operational. Crosses symbolise events for which waveform data are available (blue: events outside the Groningen field, black: within the field). The histogram on the right summarises the number of events recorded at each station.

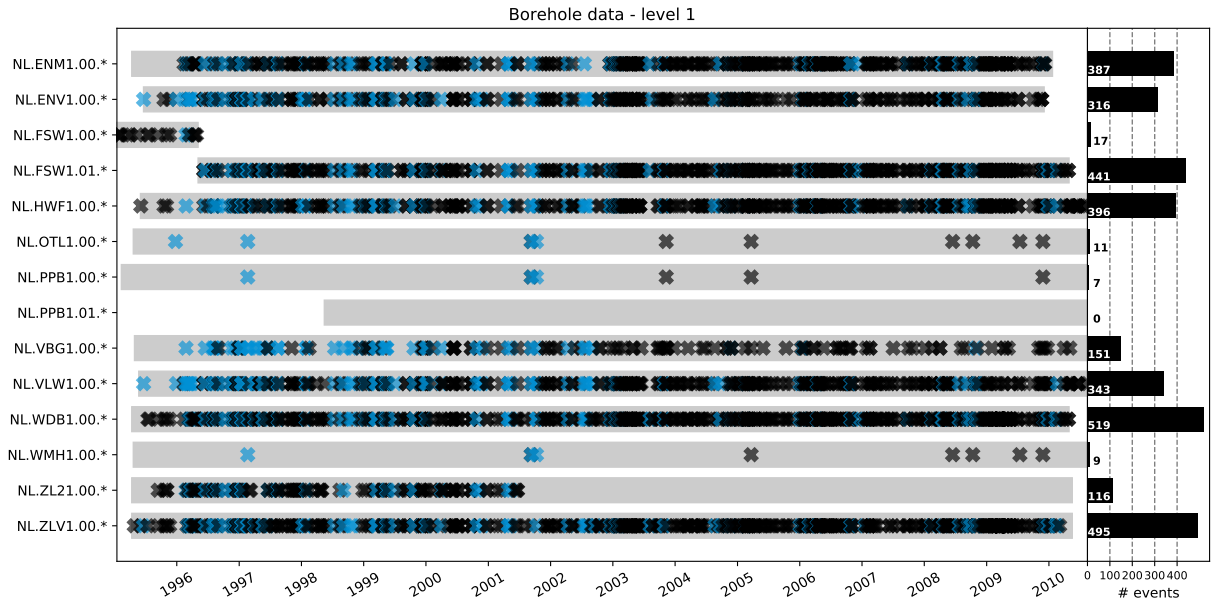

FIGURE B.2: Same as Fig. B.1 for level 1.

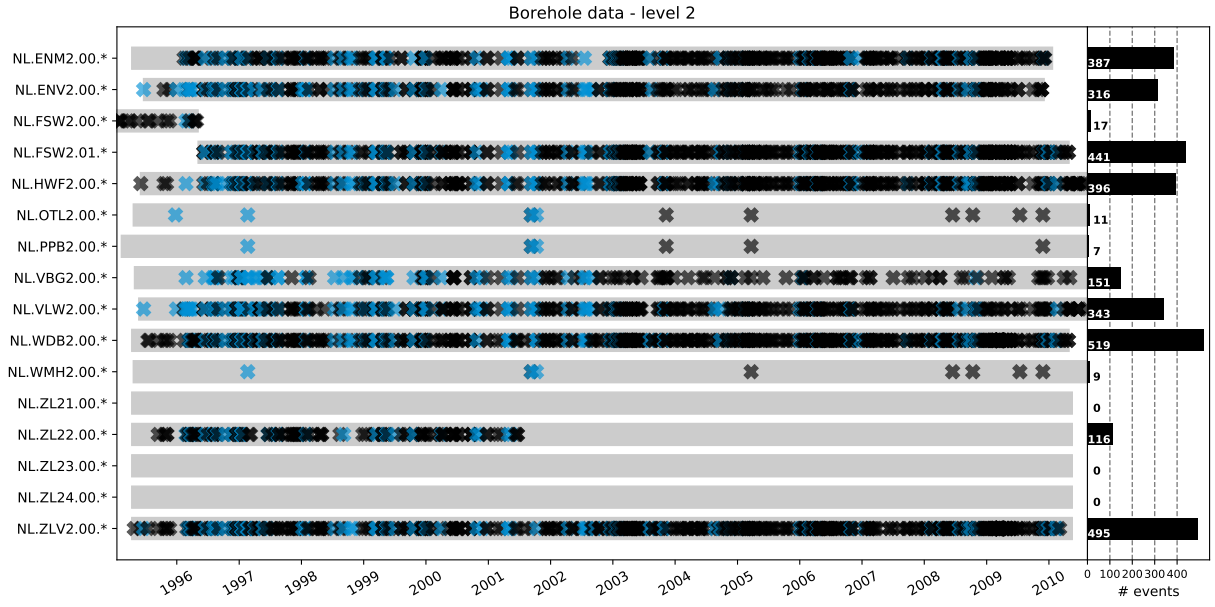

FIGURE B.3: Same as Fig. B.1 for level 2.

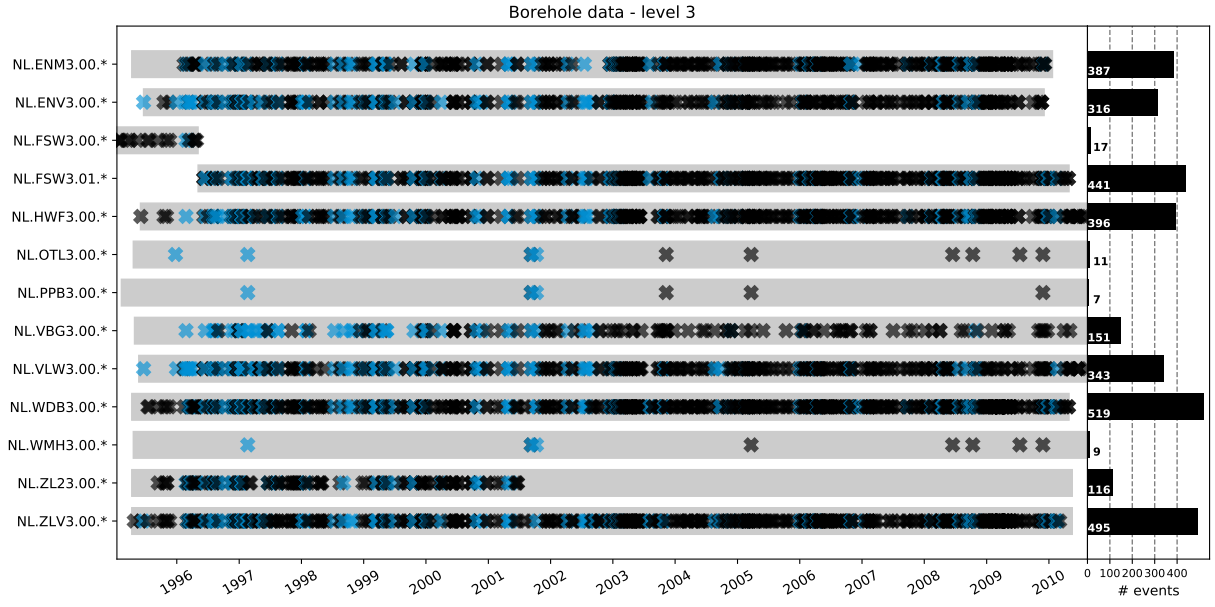

FIGURE B.4: Same as Fig. B.1 for level 3.

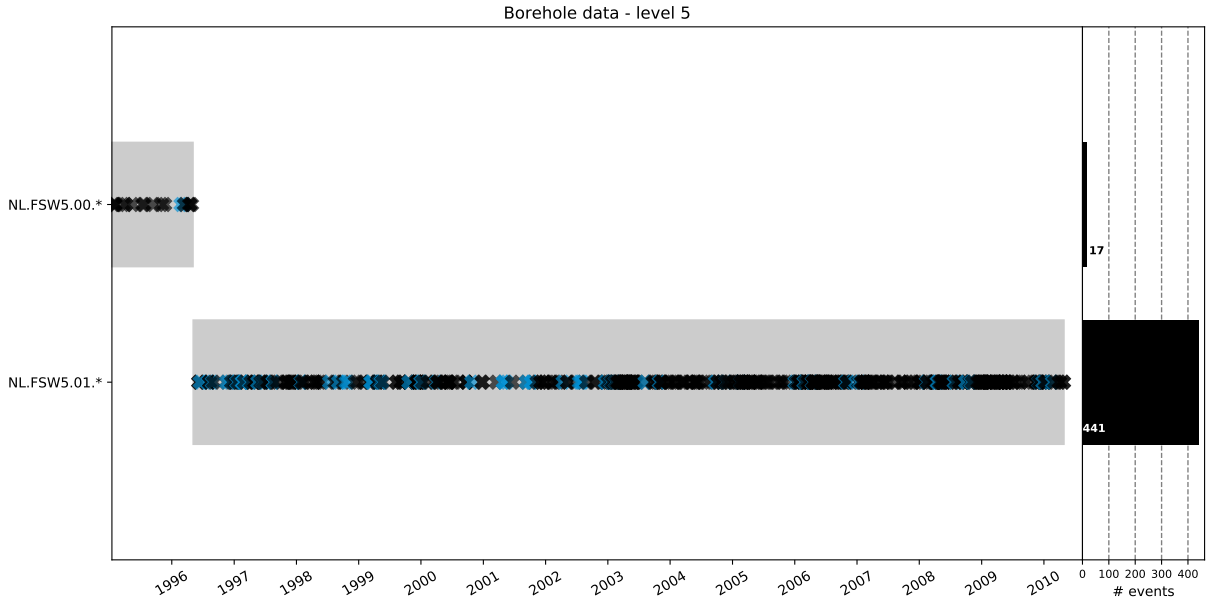

FIGURE B.5: Same as Fig. B.1 for level 5.

B.3 Borehole station metadata

TABLE B.2: Same as Table 2.2 for ENV.

Name	Channel	Installation date	Removal date	Latitude	Longitude	Depth [m]	Elevation [m]	Fs [Hz]	Azimuth [°]	Dip [°]
ENV1	HHN	1995-06-20	2009-12-04	52.8944	6.6337	50	17	120	322	0
	HHE	1995-06-20	2009-12-04	52.8944	6.6337	50	17	120	52	0
	HHZ	1995-06-20	2009-12-04	52.8944	6.6337	50	17	120	0	-90
ENV2	HHN	1995-06-20	2009-12-04	52.8944	6.6337	100	17	120	337	0
	HHE	1995-06-20	2009-12-04	52.8944	6.6337	100	17	120	67	0
	HHZ	1995-06-20	2009-12-04	52.8944	6.6337	100	17	120	0	-90
ENV3	HHN	1995-06-20	2009-12-04	52.8944	6.6337	150	17	120	207	0
	HHE	1995-06-20	2009-12-04	52.8944	6.6337	150	17	120	297	0
	HHZ	1995-06-20	2009-12-04	52.8944	6.6337	150	17	120	0	-90
ENV4	HHN	1995-06-20	2009-12-04	52.8944	6.6337	200	17	120	311	0
	HHE	1995-06-20	2009-12-04	52.8944	6.6337	200	17	120	41	0
	HHZ	1995-06-20	2009-12-04	52.8944	6.6337	200	17	120	0	-90

TABLE B.3: Same as Table 2.2 for FSW.

Name	Channel	Installation date	Removal date	Latitude	Longitude	Depth [m]	Elevation [m]	Fs [Hz]	Azimuth [°]	Dip [°]
FSW1	HHN	1992-07-22	1996-05-05	53.2135	7.1195	0	1	121.12	158	0
	HHE	1992-07-22	1996-05-05	53.2135	7.1195	0	1	121.12	248	0
	HHZ	1992-07-22	1996-05-05	53.2135	7.1195	0	1	121.12	0	-90
FSW2	HHN	1992-07-22	1996-05-05	53.2135	7.1195	75	1	121.12	204	0
	HHE	1992-07-22	1996-05-05	53.2135	7.1195	75	1	121.12	294	0
	HHZ	1992-07-22	1996-05-05	53.2135	7.1195	75	1	121.12	0	-90
FSW3	HHN	1992-07-22	1996-05-05	53.2135	7.1195	150	1	121.12	11	0
	HHE	1992-07-22	1996-05-05	53.2135	7.1195	150	1	121.12	101	0
	HHZ	1992-07-22	1996-05-05	53.2135	7.1195	150	1	121.12	0	-90
FSW4	HHN	1992-07-22	1996-05-05	53.2135	7.1195	225	1	121.12	214	0
	HHE	1992-07-22	1996-05-05	53.2135	7.1195	225	1	121.12	304	0
	HHZ	1992-07-22	1996-05-05	53.2135	7.1195	225	1	121.12	0	-90
FSW5	HHN	1992-07-22	1996-05-05	53.2135	7.1195	300	1	121.12	278	0
	HHE	1992-07-22	1996-05-05	53.2135	7.1195	300	1	121.12	8	0
	HHZ	1992-07-22	1996-05-05	53.2135	7.1195	300	1	121.12	0	-90
FSW1	HHN	1996-05-05	2010-04-29	53.2135	7.1195	0	1	120.00	158	0
	HHE	1996-05-05	2010-04-29	53.2135	7.1195	0	1	120.00	248	0
	HHZ	1996-05-05	2010-04-29	53.2135	7.1195	0	1	120.00	0	-90
FSW2	HHN	1996-05-05	2010-04-29	53.2135	7.1195	75	1	120.00	204	0
	HHE	1996-05-05	2010-04-29	53.2135	7.1195	75	1	120.00	294	0
	HHZ	1996-05-05	2010-04-29	53.2135	7.1195	75	1	120.00	0	-90
FSW3	HHN	1996-05-05	2010-04-29	53.2135	7.1195	150	1	120.00	11	0
	HHE	1996-05-05	2010-04-29	53.2135	7.1195	150	1	120.00	101	0
	HHZ	1996-05-05	2010-04-29	53.2135	7.1195	150	1	120.00	0	-90
FSW4	HHN	1996-05-05	2010-04-29	53.2135	7.1195	225	1	120.00	214	0
	HHE	1996-05-05	2010-04-29	53.2135	7.1195	225	1	120.00	304	0
	HHZ	1996-05-05	2010-04-29	53.2135	7.1195	225	1	120.00	0	-90
FSW5	HHN	1996-05-05	2010-04-29	53.2135	7.1195	300	1	120.00	278	0
	HHE	1996-05-05	2010-04-29	53.2135	7.1195	300	1	120.00	8	0
	HHZ	1996-05-05	2010-04-29	53.2135	7.1195	300	1	120.00	0	-90

TABLE B.4: Same as Table 2.2 for HWF.

Name	Channel	Installation date	Removal date	Latitude	Longitude	Depth [m]	Elevation [m]	Fs [Hz]	Azimuth [°]	Dip [°]
HWF0	HHN	1998-03-29	2010-11-24	53.071	6.3512	0	7	120	0	0
	HHE	1998-03-29	2010-11-24	53.071	6.3512	0	7	120	90	0
	HHZ	1998-03-29	2010-11-24	53.071	6.3512	0	7	120	0	-90
HWF1	HHN	1995-06-02	2010-11-24	53.071	6.3512	50	7	120	166	0
	HHE	1995-06-02	2010-11-24	53.071	6.3512	50	7	120	256	0
	HHZ	1995-06-02	2010-11-24	53.071	6.3512	50	7	120	0	-90
HWF2	HHN	1995-06-02	2010-11-24	53.071	6.3512	100	7	120	257	0
	HHE	1995-06-02	2010-11-24	53.071	6.3512	100	7	120	347	0
	HHZ	1995-06-02	2010-11-24	53.071	6.3512	100	7	120	0	-90
HWF3	HHN	1995-06-02	2010-11-24	53.071	6.3512	150	7	120	342	0
	HHE	1995-06-02	2010-11-24	53.071	6.3512	150	7	120	72	0
	HHZ	1995-06-02	2010-11-24	53.071	6.3512	150	7	120	0	-90
HWF4	HHN	1995-06-02	2010-11-24	53.071	6.3512	200	7	120	199	0
	HHE	1995-06-02	2010-11-24	53.071	6.3512	200	7	120	289	0
	HHZ	1995-06-02	2010-11-24	53.071	6.3512	200	7	120	0	-90

TABLE B.5: Same as Table 2.2 for OTL.

Name	Channel	Installation date	Removal date	Latitude	Longitude	Depth [m]	Elevation [m]	Fs [Hz]	Azimuth [°]	Dip [°]
OTL1	HHN	1995-04-21	2010-10-11	52.6289	4.8227	50	-4	120	89	0
	HHE	1995-04-21	2010-10-11	52.6289	4.8227	50	-4	120	179	0
	HHZ	1995-04-21	2010-10-11	52.6289	4.8227	50	-4	120	0	-90
OTL2	HHN	1995-04-21	2010-10-11	52.6289	4.8227	100	-4	120	191	0
	HHE	1995-04-21	2010-10-11	52.6289	4.8227	100	-4	120	281	0
	HHZ	1995-04-21	2010-10-11	52.6289	4.8227	100	-4	120	0	-90
OTL3	HHN	1995-04-21	2010-10-11	52.6289	4.8227	150	-4	120	325	0
	HHE	1995-04-21	2010-10-11	52.6289	4.8227	150	-4	120	55	0
	HHZ	1995-04-21	2010-10-11	52.6289	4.8227	150	-4	120	0	-90
OTL4	HHN	1995-04-21	2010-10-11	52.6289	4.8227	200	-4	120	115	0
	HHE	1995-04-21	2010-10-11	52.6289	4.8227	200	-4	120	205	0
	HHZ	1995-04-21	2010-10-11	52.6289	4.8227	200	-4	120	0	-90

TABLE B.6: Same as Table 2.2 for PPB.

Name	Channel	Installation date	Removal date	Latitude	Longitude	Depth [m]	Elevation [m]	Fs [Hz]	Azimuth [°]	Dip [°]
PPB0	HHN	1998-05-15	2010-10-16	52.6526	4.67	0	1	120	0	0
	HHE	1998-05-15	2010-10-16	52.6526	4.67	0	1	120	90	0
	HHZ	1998-05-15	2010-10-16	52.6526	4.67	0	1	120	0	-90
PPB1	HHN	1995-02-10	2010-10-16	52.6526	4.67	15	1	120	355	0
	HHE	1995-02-10	2010-10-16	52.6526	4.67	15	1	120	85	0
	HHZ	1995-02-10	2010-10-16	52.6526	4.67	15	1	120	0	-90
PPB2	HHN	1995-02-10	2010-10-16	52.6526	4.67	90	1	120	135	0
	HHE	1995-02-10	2010-10-16	52.6526	4.67	90	1	120	225	0
	HHZ	1995-02-10	2010-10-16	52.6526	4.67	90	1	120	0	-90
PPB3	HHN	1995-02-10	2010-10-16	52.6526	4.67	165	1	120	276	0
	HHE	1995-02-10	2010-10-16	52.6526	4.67	165	1	120	6	0
	HHZ	1995-02-10	2010-10-16	52.6526	4.67	165	1	120	0	-90
PPB4	HHN	1995-02-10	2010-10-16	52.6526	4.67	240	1	120	116	0
	HHE	1995-02-10	2010-10-16	52.6526	4.67	240	1	120	206	0
	HHZ	1995-02-10	2010-10-16	52.6526	4.67	240	1	120	0	-90

TABLE B.7: Same as Table 2.2 for VBG.

Name	Channel	Installation date	Removal date	Latitude	Longitude	Depth [m]	Elevation [m]	Fs [Hz]	Azimuth [°]	Dip [°]
VBG1	HHN	1995-04-28	2010-09-01	52.544	6.6693	42	11	120	340	0
	HHE	1995-04-28	2010-09-01	52.544	6.6693	42	11	120	70	0
	HHZ	1995-04-28	2010-09-01	52.544	6.6693	42	11	120	0	-90
VBG2	HHN	1995-04-28	2010-09-01	52.544	6.6693	92	11	120	294	0
	HHE	1995-04-28	2010-09-01	52.544	6.6693	92	11	120	24	0
	HHZ	1995-04-28	2010-09-01	52.544	6.6693	92	11	120	0	-90
VBG3	HHN	1995-04-28	2010-09-01	52.544	6.6693	142	11	120	104	0
	HHE	1995-04-28	2010-09-01	52.544	6.6693	142	11	120	194	0
	HHZ	1995-04-28	2010-09-01	52.544	6.6693	142	11	120	0	-90
VBG4	HHN	1995-04-28	2010-09-01	52.544	6.6693	192	11	120	90	0
	HHE	1995-04-28	2010-09-01	52.544	6.6693	192	11	120	180	0
	HHZ	1995-04-28	2010-09-01	52.544	6.6693	192	11	120	0	-90

TABLE B.8: Same as Table 2.2 for VLW.

Name	Channel	Installation date	Removal date	Latitude	Longitude	Depth [m]	Elevation [m]	Fs [Hz]	Azimuth [°]	Dip [°]
VLW0	HHN	1998-07-24	2010-10-29	52.9682	7.0972	0	7	120	0	0
	HHE	1998-07-24	2010-10-29	52.9682	7.0972	0	7	120	90	0
	HHZ	1998-07-24	2010-10-29	52.9682	7.0972	0	7	120	0	-90
VLW1	HHN	1995-05-23	2010-10-29	52.9682	7.0972	50	7	120	202	0
	HHE	1995-05-23	2010-10-29	52.9682	7.0972	50	7	120	292	0
	HHZ	1995-05-23	2010-10-29	52.9682	7.0972	50	7	120	0	-90
VLW2	HHN	1995-05-23	2010-10-29	52.9682	7.0972	100	7	120	252	0
	HHE	1995-05-23	2010-10-29	52.9682	7.0972	100	7	120	342	0
	HHZ	1995-05-23	2010-10-29	52.9682	7.0972	100	7	120	0	-90
VLW3	HHN	1995-05-23	2010-10-29	52.9682	7.0972	150	7	120	123	0
	HHE	1995-05-23	2010-10-29	52.9682	7.0972	150	7	120	213	0
	HHZ	1995-05-23	2010-10-29	52.9682	7.0972	150	7	120	0	-90
VLW4	HHN	1995-05-23	2010-10-29	52.9682	7.0972	200	7	120	89	0
	HHE	1995-05-23	2010-10-29	52.9682	7.0972	200	7	120	179	0
	HHZ	1995-05-23	2010-10-29	52.9682	7.0972	200	7	120	0	-90

TABLE B.9: Same as Table 2.2 for WDB.

Name	Channel	Installation date	Removal date	Latitude	Longitude	Depth [m]	Elevation [m]	Fs [Hz]	Azimuth [°]	Dip [°]
WDB0	HHN	1998-07-24	2010-04-29	53.2083	6.7355	0	-2	120	0	0
	HHE	1998-07-24	2010-04-29	53.2083	6.7355	0	-2	120	90	0
	HHZ	1998-07-24	2010-04-29	53.2083	6.7355	0	-2	120	0	-90
WDB1	HHN	1995-04-12	2010-04-29	53.2083	6.7355	47	-2	120	94	0
	HHE	1995-04-12	2010-04-29	53.2083	6.7355	47	-2	120	184	0
	HHZ	1995-04-12	2010-04-29	53.2083	6.7355	47	-2	120	0	-90
WDB2	HHN	1995-04-12	2010-04-29	53.2083	6.7355	97	-2	120	232	0
	HHE	1995-04-12	2010-04-29	53.2083	6.7355	97	-2	120	322	0
	HHZ	1995-04-12	2010-04-29	53.2083	6.7355	97	-2	120	0	-90
WDB3	HHN	1995-04-12	2010-04-29	53.2083	6.7355	147	-2	120	131	0
	HHE	1995-04-12	2010-04-29	53.2083	6.7355	147	-2	120	221	0
	HHZ	1995-04-12	2010-04-29	53.2083	6.7355	147	-2	120	0	-90
WDB4	HHN	1995-04-12	2010-04-29	53.2083	6.7355	197	-2	120	250	0
	HHE	1995-04-12	2010-04-29	53.2083	6.7355	197	-2	120	340	0
	HHZ	1995-04-12	2010-04-29	53.2083	6.7355	197	-2	120	0	-90

TABLE B.10: Same as Table 2.2 for WMH.

Name	Channel	Installation date	Removal date	Latitude	Longitude	Depth [m]	Elevation [m]	Fs [Hz]	Azimuth [°]	Dip [°]
WMH1	HHN	1995-04-21	2010-10-11	52.7096	4.7498	50	-1	120	260	0
	HHE	1995-04-21	2010-10-11	52.7096	4.7498	50	-1	120	350	0
	HHZ	1995-04-21	2010-10-11	52.7096	4.7498	50	-1	120	0	-90
WMH2	HHN	1995-04-21	2010-10-11	52.7096	4.7498	100	-1	120	9	0
	HHE	1995-04-21	2010-10-11	52.7096	4.7498	100	-1	120	99	0
	HHZ	1995-04-21	2010-10-11	52.7096	4.7498	100	-1	120	0	-90
WMH3	HHN	1995-04-21	2010-10-11	52.7096	4.7498	150	-1	120	280	0
	HHE	1995-04-21	2010-10-11	52.7096	4.7498	150	-1	120	10	0
	HHZ	1995-04-21	2010-10-11	52.7096	4.7498	150	-1	120	0	-90
WMH4	HHN	1995-04-21	2010-10-11	52.7096	4.7498	200	-1	120	210	0
	HHE	1995-04-21	2010-10-11	52.7096	4.7498	200	-1	120	300	0
	HHZ	1995-04-21	2010-10-11	52.7096	4.7498	200	-1	120	0	-90

TABLE B.11: Same as Table 2.2 for ZL2.

Name	Channel	Installation date	Removal date	Latitude	Longitude	Depth [m]	Elevation [m]	Fs [Hz]	Azimuth [°]	Dip [°]
ZL21	HHN	1995-04-12	2009-04-10	53.0921	6.7533	25	2	120	25	0
	HHE	1995-04-12	2009-04-10	53.0921	6.7533	25	2	120	115	0
	HHZ	1995-04-12	2009-04-10	53.0921	6.7533	25	2	120	0	-90
ZL22	HHN	1995-04-12	2009-04-10	53.0921	6.7533	75	2	120	350	0
	HHE	1995-04-12	2009-04-10	53.0921	6.7533	75	2	120	80	0
	HHZ	1995-04-12	2009-04-10	53.0921	6.7533	75	2	120	0	-90
ZL23	HHN	1995-04-12	2009-04-10	53.0921	6.7533	125	2	120	160	0
	HHE	1995-04-12	2009-04-10	53.0921	6.7533	125	2	120	250	0
	HHZ	1995-04-12	2009-04-10	53.0921	6.7533	125	2	120	0	-90
ZL24	HHN	1995-04-12	2009-04-10	53.0921	6.7533	175	2	120	44	0
	HHE	1995-04-12	2009-04-10	53.0921	6.7533	175	2	120	134	0
	HHZ	1995-04-12	2009-04-10	53.0921	6.7533	175	2	120	0	-90

TABLE B.12: Same as Table 2.2 for ZLV.

Name	Channel	Installation date	Removal date	Latitude	Longitude	Depth [m]	Elevation [m]	Fs [Hz]	Azimuth [°]	Dip [°]
ZLV0	HHN	1996-02-15	2010-05-18	53.0921	6.7533	0	2	120	0	0
	HHE	1996-02-15	2010-05-18	53.0921	6.7533	0	2	120	90	0
	HHZ	1996-02-15	2010-05-18	53.0921	6.7533	0	2	120	0	-90
ZLV1	HHN	1995-04-12	2010-05-18	53.0921	6.7533	50	2	120	64	0
	HHE	1995-04-12	2010-05-18	53.0921	6.7533	50	2	120	154	0
	HHZ	1995-04-12	2010-05-18	53.0921	6.7533	50	2	120	0	-90
ZLV2	HHN	1995-04-12	2010-05-18	53.0921	6.7533	100	2	120	133	0
	HHE	1995-04-12	2010-05-18	53.0921	6.7533	100	2	120	223	0
	HHZ	1995-04-12	2010-05-18	53.0921	6.7533	100	2	120	0	-90
ZLV3	HHN	1995-04-12	2010-05-18	53.0921	6.7533	150	2	120	222	0
	HHE	1995-04-12	2010-05-18	53.0921	6.7533	150	2	120	312	0
	HHZ	1995-04-12	2010-05-18	53.0921	6.7533	150	2	120	0	-90
ZLV4	HHN	1995-04-12	2010-05-18	53.0921	6.7533	200	2	120	130	0
	HHE	1995-04-12	2010-05-18	53.0921	6.7533	200	2	120	220	0
	HHZ	1995-04-12	2010-05-18	53.0921	6.7533	200	2	120	0	-90

B.4 Borehole orientation

B.4.1 Vertical component

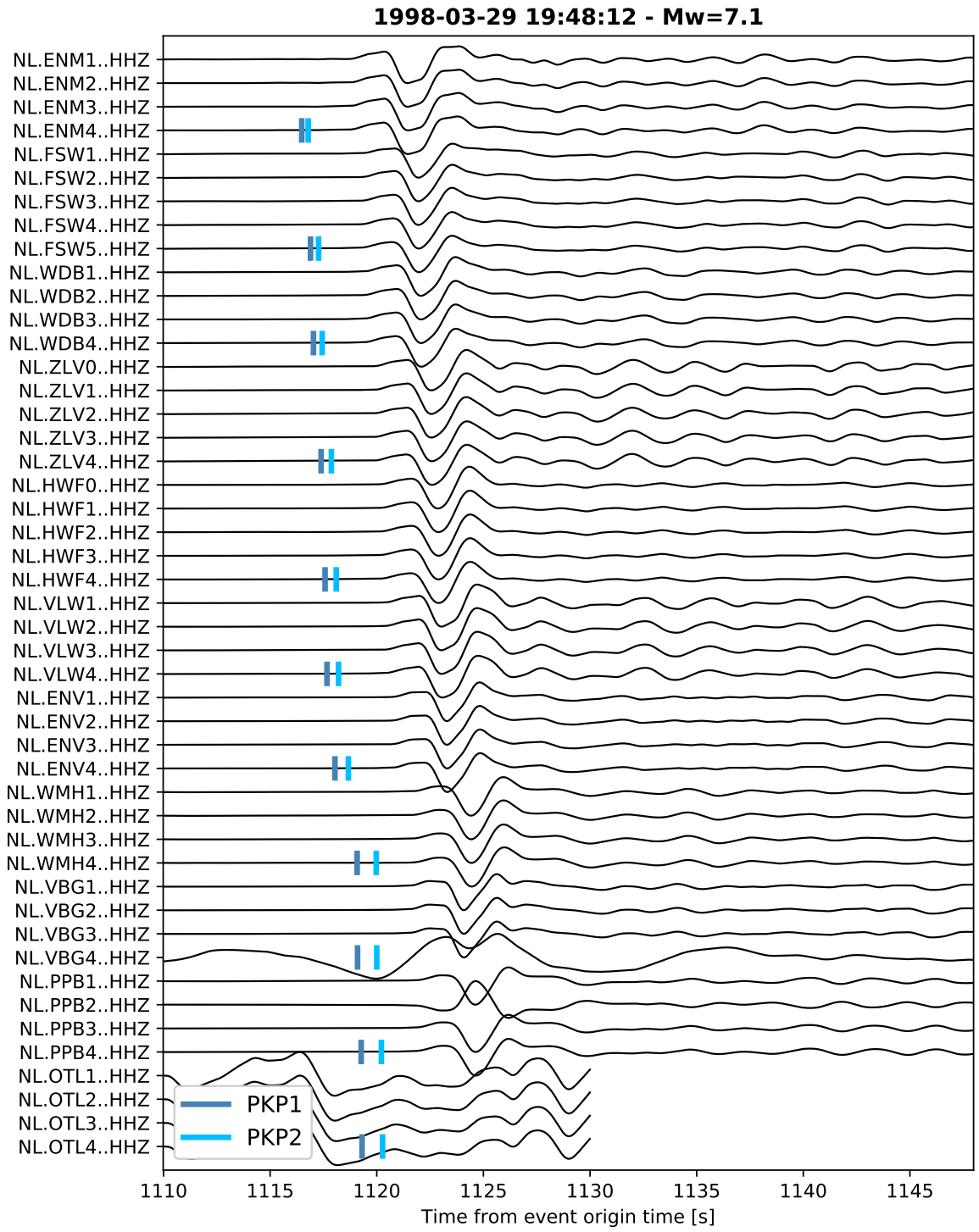

FIGURE B.6: Vertical component waveforms recorded on each level of every borehole station for the 1998 M_w 7.1 Fiji earthquake and filtered between 0.05 and 0.8 Hz. Blue vertical bars represent the theoretical arrival times of the PKP-phases using the iasp91 1D velocity model (Kennett and Engdahl, 1991). Traces have been sorted by decreasing distance to the source from top to bottom.

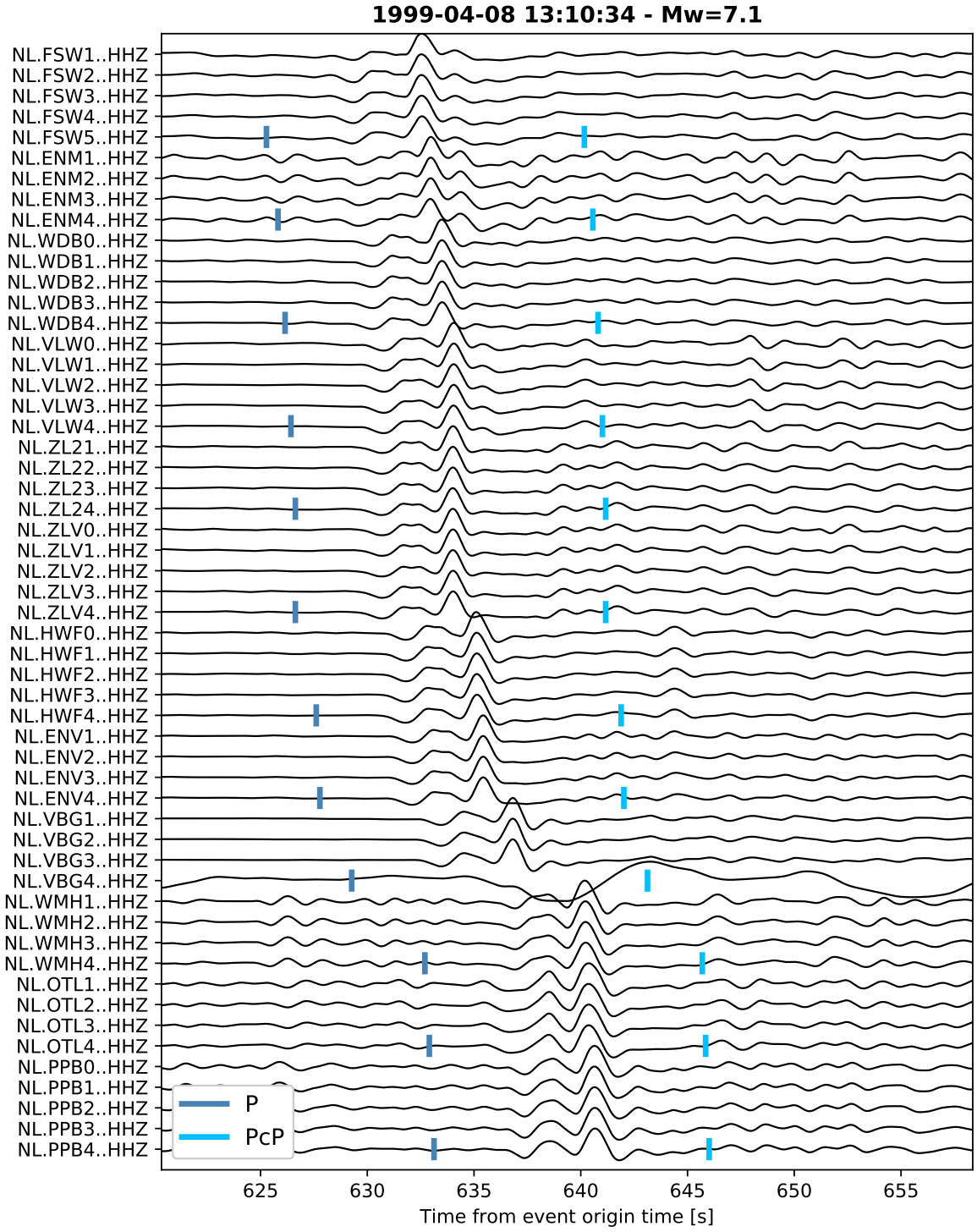

FIGURE B.7: Same as Fig. B.6 for the 1999 M_w 7.1 China earthquake.

B.4.2 Horizontal components

Results

TABLE B.13: Individual borehole sensor orientation results. ID is the event ID (see Tab. B.1). $_L$ is the event magnitude. d is the event-station distance. θ is the orientation angle resulting from the semi-automated approach. θ_{diff} is the difference to the angle stored in the station XML file and is coloured when it exceeds 25° (the darker the larger the difference). The offset angle is measured between max(R·Z) and min(|T|). Larger offsets (>30°) are coloured (the darker, the larger the difference). The next-two-last column indicates the particle motion linearity. SNR is the signal-to-noise ratio computed on the vertical component around the P-wave onset. Linearity and SNR columns are coloured depending on their values (the darker, the smaller). Stations marked with an asterisk are surface sensors that have not been oriented previously. Rows marked by a cross correspond to examples shown in Figs. B.18-B.29.

Station	ID	Origin time	$_L$	d [km]	θ [°]	θ_{diff} [°]	Offset [°]	Linearity	SNR
ENM1	107	1998-02-15 07:24:16.420	2.6	20.2	146	-24	70	5.0	224.1
	166	2000-06-12 15:48:23.010	2.6	18.8	320	161	46	5.3	47.2
	275	2003-10-24 01:52:41.160	3.0	24.1	139	-17	44	3.1	187.4
	278	2003-11-10 00:22:38.030	3.0	16.6	142	-20	7	6.9	369.2
x	280	2003-11-16 20:04:11.480	2.7	16.2	137	-14	53	6.8	407.2
	391	2006-08-08 09:49:23.380	2.5	16.3	135	-13	81	9.4	141.4
ENM2	107	1998-02-15 07:24:16.420	2.6	20.2	186	-9	17	3.0	284.5
	166	2000-06-12 15:48:23.010	2.6	18.8	190	-13	13	3.9	72.7
	275	2003-10-24 01:52:41.160	3.0	24.1	187	-10	39	4.1	210.3
	278	2003-11-10 00:22:38.030	3.0	16.6	175	1	3	5.8	597.9
	280	2003-11-16 20:04:11.480	2.7	16.2	181	-3	12	5.9	456.7
	391	2006-08-08 09:49:23.380	2.5	16.3	179	-2	21	4.1	149.3
	538	2009-04-14 21:05:25.880	2.6	14.9	162	15	5	25.0	396.3
	547	2009-05-08 05:23:11.950	3.0	19.5	173	4	12	6.3	356.8
ENM3	107	1998-02-15 07:24:16.420	2.6	20.2	265	-101	19	2.7	313.9
	166	2000-06-12 15:48:23.010	2.6	18.8	189	-25	2	2.1	98.5
	278	2003-11-10 00:22:38.030	3.0	16.6	161	2	37	4.6	478.9
	280	2003-11-16 20:04:11.480	2.7	16.2	303	-138	65	1.5	742.9
	297	2004-06-21 23:32:02.760	2.8	51.8	110	54	35	3.0	53.5
	391	2006-08-08 09:49:23.380	2.5	16.3	262	-98	24	1.8	214.2
	411	2007-02-17 01:41:14.010	2.6	24.8	105	59	23	7.1	71.2
	538	2009-04-14 21:05:25.880	2.6	14.9	153	11	8	9.8	481.5
	540	2009-04-16 17:12:15.910	2.6	26.3	311	-147	68	1.9	141.5
	547	2009-05-08 05:23:11.950	3.0	19.5	181	-16	5	1.9	406.5
ENM4	107	1998-02-15 07:24:16.420	2.6	20.2	125	-34	15	1.9	623.6
	275	2003-10-24 01:52:41.160	3.0	24.1	104	-13	0	4.3	476.2
	278	2003-11-10 00:22:38.030	3.0	16.6	90	0	4	4.7	753.0
	280	2003-11-16 20:04:11.480	2.7	16.2	91	0	1	2.4	644.3
	297	2004-06-21 23:32:02.760	2.8	51.8	68	23	6	3.5	77.1
	391	2006-08-08 09:49:23.380	2.5	16.3	104	-13	1	1.5	236.6
	411	2007-02-17 01:41:14.010	2.6	24.8	36	55	1	14.7	82.0
	538	2009-04-14 21:05:25.880	2.6	14.9	76	15	5	8.6	595.4
	540	2009-04-16 17:12:15.910	2.6	26.3	109	-18	17	1.3	214.7
	547	2009-05-08 05:23:11.950	3.0	19.5	83	8	2	6.1	600.6
ENV1	58	1996-12-28 18:16:56.580	2.7	28.4	307	15	5	11.1	79.1
	66	1997-02-19 21:53:50.810	3.4	28.1	327	-5	80	5.1	114.0
	103	1998-01-28 21:33:03.840	2.7	28.3	301	20	72	3.2	62.7
	115	1998-07-14 12:12:02.230	3.3	29.1	303	19	64	5.1	85.3
	175	2000-10-25 18:10:34.790	3.2	29.0	312	9	56	14.0	263.4
	278	2003-11-10 00:22:38.030	3.0	48.2	334	-11	7	4.0	67.3
	346	2005-10-12 16:06:42.530	2.5	14.5	323	0	46	2.6	75.8
	350	2006-01-10 23:41:06.140	2.6	8.0	318	4	4	10.4	309.9
ENV2	58	1996-12-28 18:16:56.580	2.7	28.4	317	20	6	6.9	94.7
	103	1998-01-28 21:33:03.840	2.7	28.3	38	-61	39	4.5	89.8
	115	1998-07-14 12:12:02.230	3.3	29.1	316	21	32	2.0	126.5
	154	1999-12-31 11:00:55.330	2.8	28.7	327	9	3	5.9	82.9
	175	2000-10-25 18:10:34.790	3.2	29.0	328	8	36	15.6	368.4
	275	2003-10-24 01:52:41.160	3.0	45.9	355	-18	55	4.1	65.4
x	346	2005-10-12 16:06:42.530	2.5	14.5	320	17	4	4.9	137.9
	350	2006-01-10 23:41:06.140	2.6	8.0	331	6	2	2.1	520.1
	411	2007-02-17 01:41:14.010	2.6	37.4	334	2	8	42.6	29.2

Continued on next page

Station	ID	Origin time	L	d [km]	θ [°]	θ_{diff} [°]	Offset [°]	Linearity	SNR
	547	2009-05-08 05:23:11.950	3.0	51.9	166	171	23	5.4	27.7
ENV3	25	1996-03-12 12:13:48.170	2.6	29.4	209	-1	0	2.1	27.4
	58	1996-12-28 18:16:56.580	2.7	28.4	204	3	5	2.5	68.3
	66	1997-02-19 21:53:50.810	3.4	28.1	215	-8	6	3.8	358.5
	103	1998-01-28 21:33:03.840	2.7	28.3	212	-5	7	5.4	104.8
	107	1998-02-15 07:24:16.420	2.6	52.2	206	0	1	5.4	38.5
	115	1998-07-14 12:12:02.230	3.3	29.1	205	2	3	2.8	227.2
	154	1999-12-31 11:00:55.330	2.8	28.7	207	0	13	3.0	116.4
	175	2000-10-25 18:10:34.790	3.2	29.0	206	0	1	5.7	585.6
	278	2003-11-10 00:22:38.030	3.0	48.2	204	3	17	16.5	114.4
	346	2005-10-12 16:06:42.530	2.5	14.5	204	3	0	1.8	237.4
	350	2006-01-10 23:41:06.140	2.6	8.0	206	1	1	17.9	270.7
	547	2009-05-08 05:23:11.950	3.0	51.9	213	-5	29	22.6	34.6
ENV4	25	1996-03-12 12:13:48.170	2.6	29.4	303	8	0	2.2	30.1
	58	1996-12-28 18:16:56.580	2.7	28.4	292	19	8	2.2	145.4
	66	1997-02-19 21:53:50.810	3.4	28.1	306	4	4	5.7	397.5
	103	1998-01-28 21:33:03.840	2.7	28.3	298	12	9	4.1	132.7
	107	1998-02-15 07:24:16.420	2.6	52.2	298	12	6	6.3	30.5
	115	1998-07-14 12:12:02.230	3.3	29.1	298	13	0	6.4	259.2
	154	1999-12-31 11:00:55.330	2.8	28.7	302	8	1	6.0	146.8
	175	2000-10-25 18:10:34.790	3.2	29.0	311	0	7	11.1	725.5
	275	2003-10-24 01:52:41.160	3.0	45.9	310	0	6	5.2	81.8
	346	2005-10-12 16:06:42.530	2.5	14.5	292	19	27	2.0	220.6
	390	2006-08-08 05:04:00.050	3.5	51.0	306	5	8	7.5	195.4
FSW1	107	1998-02-15 07:24:16.420	2.6	28.0	91	67	2	13.8	93.7
x	278	2003-11-10 00:22:38.030	3.0	31.3	240	-82	16	15.5	172.9
	280	2003-11-16 20:04:11.480	2.7	31.4	253	-95	23	3.9	154.0
	350	2006-01-10 23:41:06.140	2.6	46.6	292	-134	19	3.1	41.6
	391	2006-08-08 09:49:23.380	2.5	31.5	288	-130	7	2.4	45.8
	411	2007-02-17 01:41:14.010	2.6	27.9	346	172	68	1.3	49.0
	478	2008-10-30 05:54:29.080	3.2	30.0	332	-174	0	11.9	156.2
	538	2009-04-14 21:05:25.880	2.6	32.8	167	-9	28	9.6	63.9
	540	2009-04-16 17:12:15.910	2.6	21.4	330	-172	9	3.4	313.3
	547	2009-05-08 05:23:11.950	3.0	28.6	332	-174	6	3.9	70.6
	566	2009-11-26 12:54:14.030	2.8	76.5	291	-133	8	1.7	34.8
FSW2	58	1996-12-28 18:16:56.580	2.7	42.6	210	-5	17	9.8	58.5
	66	1997-02-19 21:53:50.810	3.4	42.8	183	20	1	1.7	77.7
	103	1998-01-28 21:33:03.840	2.7	42.7	194	10	1	5.1	41.2
	107	1998-02-15 07:24:16.420	2.6	28.0	202	1	0	75.9	181.1
	115	1998-07-14 12:12:02.230	3.3	42.7	198	6	29	5.0	67.2
	166	2000-06-12 15:48:23.010	2.6	28.9	23	-179	15	3.3	157.1
	273	2003-09-27 13:57:54.150	2.7	32.0	198	6	7	7.2	47.6
	278	2003-11-10 00:22:38.030	3.0	31.3	202	1	1	1.2	218.5
	280	2003-11-16 20:04:11.480	2.7	31.4	204	0	6	1.8	165.8
	297	2004-06-21 23:32:02.760	2.8	47.6	231	-26	31	1.1	185.5
	391	2006-08-08 09:49:23.380	2.5	31.5	208	-3	2	1.5	40.9
	411	2007-02-17 01:41:14.010	2.6	27.9	28	175	39	34.7	80.4
	478	2008-10-30 05:54:29.080	3.2	30.0	202	1	22	10.5	124.5
	538	2009-04-14 21:05:25.880	2.6	32.8	31	172	37	2.0	57.1
	540	2009-04-16 17:12:15.910	2.6	21.4	202	1	1	14.8	197.7
	547	2009-05-08 05:23:11.950	3.0	28.6	203	0	26	3.1	89.3
	566	2009-11-26 12:54:14.030	2.8	76.5	204	0	5	6.3	31.6
FSW3	25	1996-03-12 12:13:48.170	2.6	42.1	27	-16	20	8.7	27.9
	66	1997-02-19 21:53:50.810	3.4	42.8	19	-8	10	7.1	46.5
	103	1998-01-28 21:33:03.840	2.7	42.7	16	-4	0	3.3	55.0
	107	1998-02-15 07:24:16.420	2.6	28.0	9	1	1	184.7	181.6
	115	1998-07-14 12:12:02.230	3.3	42.7	23	-11	0	9.8	70.8
	166	2000-06-12 15:48:23.010	2.6	28.9	9	1	3	12.3	262.1
	190	2001-09-09 06:58:12.520	3.5	173.6	40	-28	3	5.2	35.9
	191	2001-09-10 04:30:15.430	3.2	173.7	26	-14	8	2.9	45.8
	273	2003-09-27 13:57:54.150	2.7	32.0	2	9	5	11.6	49.6
	278	2003-11-10 00:22:38.030	3.0	31.3	19	-8	0	2.0	308.1
	280	2003-11-16 20:04:11.480	2.7	31.4	21	-10	4	2.0	152.5
	297	2004-06-21 23:32:02.760	2.8	47.6	18	-6	6	12.3	150.5
	350	2006-01-10 23:41:06.140	2.6	46.6	22	-10	0	10.0	28.2
	391	2006-08-08 09:49:23.380	2.5	31.5	14	-2	11	3.0	44.2
	411	2007-02-17 01:41:14.010	2.6	27.9	19	-8	4	4.3	61.4
	478	2008-10-30 05:54:29.080	3.2	30.0	6	4	0	23.7	89.2
	538	2009-04-14 21:05:25.880	2.6	32.8	12	-1	11	1.8	51.3
	540	2009-04-16 17:12:15.910	2.6	21.4	15	-4	12	6.1	162.8
	547	2009-05-08 05:23:11.950	3.0	28.6	14	-3	11	2.4	71.5
	566	2009-11-26 12:54:14.030	2.8	76.5	23	-11	1	2.0	32.2
FSW4	25	1996-03-12 12:13:48.170	2.6	42.1	223	-9	21	3.6	38.6
	66	1997-02-19 21:53:50.810	3.4	42.8	214	0	3	26.6	31.8
	103	1998-01-28 21:33:03.840	2.7	42.7	205	9	0	10.0	59.4
	107	1998-02-15 07:24:16.420	2.6	28.0	211	2	1	4.7	191.4
	115	1998-07-14 12:12:02.230	3.3	42.7	216	-1	3	34.8	98.5

Continued on next page

Station	ID	Origin time	L	d [km]	θ [°]	θ_{diff} [°]	Offset [°]	Linearity	SNR
	166	2000-06-12 15:48:23.010	2.6	28.9	211	2	3	2.2	283.4
	175	2000-10-25 18:10:34.790	3.2	42.8	213	0	1	40.5	143.9
	190	2001-09-09 06:58:12.520	3.5	173.6	172	42	0	7.2	40.1
	273	2003-09-27 13:57:54.150	2.7	32.0	209	5	2	1.2	97.0
	278	2003-11-10 00:22:38.030	3.0	31.3	206	7	0	1.7	327.7
	280	2003-11-16 20:04:11.480	2.7	31.4	200	13	0	16.8	186.9
	297	2004-06-21 23:32:02.760	2.8	47.6	208	6	16	11.4	147.2
	391	2006-08-08 09:49:23.380	2.5	31.5	201	13	1	5.9	66.8
	411	2007-02-17 01:41:14.010	2.6	27.9	186	27	2	2.8	49.8
	478	2008-10-30 05:54:29.080	3.2	30.0	208	5	0	3.3	121.4
	540	2009-04-16 17:12:15.910	2.6	21.4	210	3	0	1.3	227.4
	566	2009-11-26 12:54:14.030	2.8	76.5	204	10	0	3.6	30.7
FSW5	66	1997-02-19 21:53:50.810	3.4	42.8	291	-13	0	4.6	28.1
	103	1998-01-28 21:33:03.840	2.7	42.7	281	-2	0	2.9	48.6
	107	1998-02-15 07:24:16.420	2.6	28.0	281	-3	8	10.5	161.5
	115	1998-07-14 12:12:02.230	3.3	42.7	286	-7	1	9.7	124.5
	154	1999-12-31 11:00:55.330	2.8	42.4	324	-46	7	13.1	85.7
	166	2000-06-12 15:48:23.010	2.6	28.9	282	-4	4	12.4	259.3
	175	2000-10-25 18:10:34.790	3.2	42.8	281	-3	1	14.0	154.6
	190	2001-09-09 06:58:12.520	3.5	173.6	290	-11	2	34.4	32.5
	191	2001-09-10 04:30:15.430	3.2	173.7	300	-21	1	10.5	37.0
	273	2003-09-27 13:57:54.150	2.7	32.0	279	0	3	11.3	121.6
	278	2003-11-10 00:22:38.030	3.0	31.3	288	-10	5	2.1	424.4
	280	2003-11-16 20:04:11.480	2.7	31.4	286	-8	2	3.2	206.6
x	297	2004-06-21 23:32:02.760	2.8	47.6	288	-9	0	113.6	156.9
	350	2006-01-10 23:41:06.140	2.6	46.6	285	-6	0	63.0	25.5
	391	2006-08-08 09:49:23.380	2.5	31.5	284	-5	3	6.3	68.5
	411	2007-02-17 01:41:14.010	2.6	27.9	292	-14	3	12.9	74.4
	478	2008-10-30 05:54:29.080	3.2	30.0	278	0	5	14.8	131.9
	538	2009-04-14 21:05:25.880	2.6	32.8	284	-6	12	3.6	89.2
	540	2009-04-16 17:12:15.910	2.6	21.4	283	-5	0	83.4	296.2
	547	2009-05-08 05:23:11.950	3.0	28.6	285	-7	1	24.2	121.5
	566	2009-11-26 12:54:14.030	2.8	76.5	283	-4	1	10.1	43.0
HWF0*	346	2005-10-12 16:06:42.530	2.5	13.8	172	-172	8	4.3	352.7
	411	2007-02-17 01:41:14.010	2.6	29.3	151	-150	0	2.6	70.0
HWF1	175	2000-10-25 18:10:34.790	3.2	54.1	156	10	32	14.1	57.3
	278	2003-11-10 00:22:38.030	3.0	36.3	171	-4	0	29.1	200.7
	280	2003-11-16 20:04:11.480	2.7	38.4	168	-1	46	23.3	83.8
	297	2004-06-21 23:32:02.760	2.8	20.3	152	13	8	9.6	222.8
	346	2005-10-12 16:06:42.530	2.5	13.8	146	19	29	3.1	92.1
	390	2006-08-08 05:04:00.050	3.5	38.8	166	0	22	30.3	322.3
	411	2007-02-17 01:41:14.010	2.6	29.3	171	-4	2	34.3	86.9
	478	2008-10-30 05:54:29.080	3.2	38.5	166	0	5	23.1	198.1
	538	2009-04-14 21:05:25.880	2.6	37.6	173	-6	28	16.1	84.3
	547	2009-05-08 05:23:11.950	3.0	41.8	170	-4	6	13.6	25.8
HWF2	175	2000-10-25 18:10:34.790	3.2	54.1	252	5	5	5.3	57.6
	273	2003-09-27 13:57:54.150	2.7	38.5	274	-16	13	5.5	31.3
	278	2003-11-10 00:22:38.030	3.0	36.3	266	-8	5	48.6	222.0
	280	2003-11-16 20:04:11.480	2.7	38.4	271	-13	10	5.6	70.1
	297	2004-06-21 23:32:02.760	2.8	20.3	247	9	3	30.0	235.2
	346	2005-10-12 16:06:42.530	2.5	13.8	243	13	8	2.8	128.5
	350	2006-01-10 23:41:06.140	2.6	19.6	238	19	10	5.3	140.6
	390	2006-08-08 05:04:00.050	3.5	38.8	271	-13	4	9.4	307.4
	411	2007-02-17 01:41:14.010	2.6	29.3	267	-9	1	56.0	90.3
	478	2008-10-30 05:54:29.080	3.2	38.5	266	-8	4	30.4	193.1
	538	2009-04-14 21:05:25.880	2.6	37.6	275	-17	16	14.6	65.2
HWF3	107	1998-02-15 07:24:16.420	2.6	42.5	356	-13	6	13.1	31.6
	175	2000-10-25 18:10:34.790	3.2	54.1	328	14	0	7.8	79.2
	273	2003-09-27 13:57:54.150	2.7	38.5	354	-11	3	9.2	29.2
	275	2003-10-24 01:52:41.160	3.0	38.6	346	-3	0	82.1	108.1
	278	2003-11-10 00:22:38.030	3.0	36.3	345	-2	5	46.7	234.6
	280	2003-11-16 20:04:11.480	2.7	38.4	351	-8	6	21.9	68.5
	297	2004-06-21 23:32:02.760	2.8	20.3	320	21	4	1.9	359.9
	346	2005-10-12 16:06:42.530	2.5	13.8	322	19	7	6.0	156.9
	350	2006-01-10 23:41:06.140	2.6	19.6	329	13	67	4.3	168.6
	390	2006-08-08 05:04:00.050	3.5	38.8	350	-7	0	30.1	256.1
	411	2007-02-17 01:41:14.010	2.6	29.3	349	-6	1	20.0	139.3
	478	2008-10-30 05:54:29.080	3.2	38.5	346	-3	3	46.6	179.2
	538	2009-04-14 21:05:25.880	2.6	37.6	349	-6	12	15.2	102.0
HWF4	107	1998-02-15 07:24:16.420	2.6	42.5	221	-21	0	2.3	40.4
	166	2000-06-12 15:48:23.010	2.6	39.7	195	3	3	6.0	31.7
	273	2003-09-27 13:57:54.150	2.7	38.5	205	-5	6	7.4	37.6
	275	2003-10-24 01:52:41.160	3.0	38.6	197	2	0	69.9	140.2
	278	2003-11-10 00:22:38.030	3.0	36.3	207	-7	2	16.4	227.2
x	280	2003-11-16 20:04:11.480	2.7	38.4	202	-2	7	5.0	102.2
	297	2004-06-21 23:32:02.760	2.8	20.3	182	16	0	59.8	341.4
	346	2005-10-12 16:06:42.530	2.5	13.8	183	15	1	44.8	151.5

Continued on next page

Station	ID	Origin time	L	d [km]	θ [°]	θ_{diff} [°]	Offset [°]	Linearity	SNR
	350	2006-01-10 23:41:06.140	2.6	19.6	183	16	9	14.3	191.5
	390	2006-08-08 05:04:00.050	3.5	38.8	209	-9	3	6.3	289.2
	411	2007-02-17 01:41:14.010	2.6	29.3	201	-1	1	31.6	122.4
	478	2008-10-30 05:54:29.080	3.2	38.5	204	-4	4	5.8	231.5
	538	2009-04-14 21:05:25.880	2.6	37.6	208	-8	15	3.6	92.5
	547	2009-05-08 05:23:11.950	3.0	41.8	200	-1	2	11.4	46.7
OTL1	192	2001-10-10 06:41:09.360	2.7	13.2	80	8	5	7.7	112.2
OTL2	192	2001-10-10 06:41:09.360	2.7	13.2	199	-8	0	2.6	104.1
	474	2008-10-11 08:19:39.900	2.6	31.5	184	6	8	9.4	30.1
OTL3	192	2001-10-10 06:41:09.360	2.7	13.2	344	-19	1	42.3	98.7
OTL4	192	2001-10-10 06:41:09.360	2.7	13.2	107	7	7	2.9	216.5
	474	2008-10-11 08:19:39.900	2.6	31.5	103	11	0	1.3	37.7
VBG1	66	1997-02-19 21:53:50.810	3.4	40.7	329	10	89	15.5	43.6
	175	2000-10-25 18:10:34.790	3.2	41.2	312	27	14	2.0	51.9
	297	2004-06-21 23:32:02.760	2.8	45.1	169	170	8	7.1	31.0
VBG2	58	1996-12-28 18:16:56.580	2.7	41.1	287	6	38	4.2	38.1
	66	1997-02-19 21:53:50.810	3.4	40.7	286	7	5	14.7	71.6
	175	2000-10-25 18:10:34.790	3.2	41.2	281	12	7	11.6	83.9
	297	2004-06-21 23:32:02.760	2.8	45.1	279	14	39	12.8	56.8
VBG3	58	1996-12-28 18:16:56.580	2.7	41.1	105	-1	1	39.5	44.0
x	66	1997-02-19 21:53:50.810	3.4	40.7	97	6	2	54.3	56.9
	103	1998-01-28 21:33:03.840	2.7	40.9	96	7	41	9.7	28.1
	107	1998-02-15 07:24:16.420	2.6	90.7	90	13	16	1.7	26.3
	115	1998-07-14 12:12:02.230	3.3	41.3	100	3	7	15.7	27.4
	175	2000-10-25 18:10:34.790	3.2	41.2	99	4	0	39.3	80.7
	278	2003-11-10 00:22:38.030	3.0	87.0	88	16	2	1.9	44.8
	297	2004-06-21 23:32:02.760	2.8	45.1	276	-172	27	20.6	56.9
	390	2006-08-08 05:04:00.050	3.5	89.8	98	5	23	5.7	83.2
VBG4	154	1999-12-31 11:00:55.330	2.8	41.4	89	0	0	87.5	38.5
	166	2000-06-12 15:48:23.010	2.6	88.8	59	30	3	18.1	31.0
	278	2003-11-10 00:22:38.030	3.0	87.0	73	17	8	18.7	74.7
VLW0*	154	1999-12-31 11:00:55.330	2.8	15.2	292	68	3	2.0	2144.6
	297	2004-06-21 23:32:02.760	2.8	35.7	350	9	40	1.1	154.8
VLW1	9	1995-06-20 08:59:40.120	2.7	15.8	199	3	82	1.2	64.0
	25	1996-03-12 12:13:48.170	2.6	14.8	347	-144	3	5.5	108.4
	58	1996-12-28 18:16:56.580	2.7	15.4	25	177	8	1.6	317.6
	103	1998-01-28 21:33:03.840	2.7	15.6	176	26	14	5.9	370.0
	154	1999-12-31 11:00:55.330	2.8	15.2	191	11	3	2.3	418.8
	278	2003-11-10 00:22:38.030	3.0	48.2	49	152	6	3.1	29.8
	297	2004-06-21 23:32:02.760	2.8	35.7	174	27	5	1.3	136.4
VLW2	9	1995-06-20 08:59:40.120	2.7	15.8	251	1	8	7.4	85.6
	25	1996-03-12 12:13:48.170	2.6	14.8	252	0	9	21.2	168.3
	58	1996-12-28 18:16:56.580	2.7	15.4	250	2	2	107.0	446.3
	103	1998-01-28 21:33:03.840	2.7	15.6	262	-9	1	16.8	585.0
	154	1999-12-31 11:00:55.330	2.8	15.2	259	-6	2	28.6	757.3
	278	2003-11-10 00:22:38.030	3.0	48.2	224	27	60	2.4	39.1
	297	2004-06-21 23:32:02.760	2.8	35.7	243	8	3	14.8	169.3
VLW3	9	1995-06-20 08:59:40.120	2.7	15.8	118	5	3	3.5	108.1
	25	1996-03-12 12:13:48.170	2.6	14.8	123	0	0	64.0	167.4
	58	1996-12-28 18:16:56.580	2.7	15.4	122	1	1	47.3	458.3
	103	1998-01-28 21:33:03.840	2.7	15.6	125	-1	1	35.3	512.5
	154	1999-12-31 11:00:55.330	2.8	15.2	127	-3	0	83.3	795.2
VLW4	9	1995-06-20 08:59:40.120	2.7	15.8	79	10	1	14.2	124.1
	25	1996-03-12 12:13:48.170	2.6	14.8	83	6	1	26.4	212.3
	58	1996-12-28 18:16:56.580	2.7	15.4	82	7	0	72.4	546.9
	103	1998-01-28 21:33:03.840	2.7	15.6	80	9	0	25.7	442.1
	154	1999-12-31 11:00:55.330	2.8	15.2	84	5	1	34.5	749.5
	278	2003-11-10 00:22:38.030	3.0	48.2	70	18	10	2.8	71.6
x	297	2004-06-21 23:32:02.760	2.8	35.7	77	11	2	8.0	191.1
	350	2006-01-10 23:41:06.140	2.6	35.4	63	26	3	9.2	34.4
	390	2006-08-08 05:04:00.050	3.5	50.3	78	11	2	6.6	114.0
WDB0*	273	2003-09-27 13:57:54.150	2.7	15.8	111	-110	19	4.8	271.8
	280	2003-11-16 20:04:11.480	2.7	15.2	181	178	12	2.1	368.8
	391	2006-08-08 09:49:23.380	2.5	15.8	342	17	13	1.4	147.4
	538	2009-04-14 21:05:25.880	2.6	15.6	185	174	1	3.0	317.9
	547	2009-05-08 05:23:11.950	3.0	16.3	197	162	1	3.2	200.7
WDB1	58	1996-12-28 18:16:56.580	2.7	46.5	316	138	27	1.6	27.6
	166	2000-06-12 15:48:23.010	2.6	14.7	89	5	14	1.1	119.0
	273	2003-09-27 13:57:54.150	2.7	15.8	85	9	27	1.5	139.7
	280	2003-11-16 20:04:11.480	2.7	15.2	85	8	15	1.7	233.5
	297	2004-06-21 23:32:02.760	2.8	31.5	127	-32	11	4.7	165.1
	391	2006-08-08 09:49:23.380	2.5	15.8	79	14	6	1.4	65.6
	538	2009-04-14 21:05:25.880	2.6	15.6	87	6	19	3.2	284.7
	547	2009-05-08 05:23:11.950	3.0	16.3	89	4	12	1.9	252.9
WDB2	66	1997-02-19 21:53:50.810	3.4	46.6	245	-13	11	2.1	50.0
	107	1998-02-15 07:24:16.420	2.6	16.6	210	22	6	10.7	227.6
	166	2000-06-12 15:48:23.010	2.6	14.7	209	23	0	7.1	152.9

Continued on next page

Station	ID	Origin time	L	d [km]	θ [°]	θ_{diff} [°]	Offset [°]	Linearity	SNR
	175	2000-10-25 18:10:34.790	3.2	47.0	252	-20	5	2.6	52.6
	273	2003-09-27 13:57:54.150	2.7	15.8	208	24	25	4.2	176.3
	280	2003-11-16 20:04:11.480	2.7	15.2	195	36	17	2.9	395.9
	297	2004-06-21 23:32:02.760	2.8	31.5	257	-24	4	10.7	167.6
	350	2006-01-10 23:41:06.140	2.6	30.2	260	-28	5	2.7	122.3
	391	2006-08-08 09:49:23.380	2.5	15.8	188	43	1	1.7	116.5
	538	2009-04-14 21:05:25.880	2.6	15.6	194	37	22	3.3	338.4
	547	2009-05-08 05:23:11.950	3.0	16.3	208	23	1	15.3	292.8
WDB3	58	1996-12-28 18:16:56.580	2.7	46.5	212	-80	24	1.9	35.3
	66	1997-02-19 21:53:50.810	3.4	46.6	173	-42	10	3.8	76.1
WDB4	66	1997-02-19 21:53:50.810	3.4	46.6	258	-8	21	2.1	86.1
	107	1998-02-15 07:24:16.420	2.6	16.6	228	22	1	27.8	246.8
	115	1998-07-14 12:12:02.230	3.3	47.0	279	-29	5	32.7	33.4
	154	1999-12-31 11:00:55.330	2.8	46.6	268	-18	1	6.3	27.3
	166	2000-06-12 15:48:23.010	2.6	14.7	226	24	3	25.0	248.0
	175	2000-10-25 18:10:34.790	3.2	47.0	274	-24	2	17.6	59.2
x	273	2003-09-27 13:57:54.150	2.7	15.8	220	30	0	83.0	207.5
	280	2003-11-16 20:04:11.480	2.7	15.2	221	28	4	63.5	340.5
	391	2006-08-08 09:49:23.380	2.5	15.8	225	24	1	28.4	111.8
	538	2009-04-14 21:05:25.880	2.6	15.6	216	33	2	36.9	391.1
	547	2009-05-08 05:23:11.950	3.0	16.3	232	17	1	39.9	320.5
WMH2	474	2008-10-11 08:19:39.900	2.6	25.6	350	18	9	3.6	33.0
WMH3	474	2008-10-11 08:19:39.900	2.6	25.6	282	-2	3	5.2	28.9
WMH4	474	2008-10-11 08:19:39.900	2.6	25.6	221	-11	23	12.0	40.5
ZL21	103	1998-01-28 21:33:03.840	2.7	34.8	179	-154	87	3.9	78.6
	166	2000-06-12 15:48:23.010	2.6	27.6	12	12	1	3.8	49.0
ZL22	103	1998-01-28 21:33:03.840	2.7	34.8	1	-11	8	5.2	110.0
	107	1998-02-15 07:24:16.420	2.6	29.4	350	0	11	5.3	54.5
	166	2000-06-12 15:48:23.010	2.6	27.6	353	-3	14	2.8	62.3
	175	2000-10-25 18:10:34.790	3.2	35.3	1	-11	12	8.5	179.0
ZL23	25	1996-03-12 12:13:48.170	2.6	35.0	158	1	17	1.3	30.2
	58	1996-12-28 18:16:56.580	2.7	34.7	172	-11	3	4.7	111.3
	103	1998-01-28 21:33:03.840	2.7	34.8	174	-14	11	2.9	89.2
x	107	1998-02-15 07:24:16.420	2.6	29.4	157	3	2	58.8	67.8
	166	2000-06-12 15:48:23.010	2.6	27.6	163	-3	14	3.3	83.1
	175	2000-10-25 18:10:34.790	3.2	35.3	170	-10	19	10.5	172.4
ZL24	58	1996-12-28 18:16:56.580	2.7	34.7	56	-11	9	1.2	80.2
	107	1998-02-15 07:24:16.420	2.6	29.4	30	14	4	13.9	102.7
ZLV0*	115	1998-07-14 12:12:02.230	3.3	35.3	174	-174	15	3.2	69.7
	166	2000-06-12 15:48:23.010	2.6	27.6	193	166	17	4.4	56.5
	273	2003-09-27 13:57:54.150	2.7	28.7	186	173	13	2.3	25.2
	280	2003-11-16 20:04:11.480	2.7	28.2	192	168	21	7.3	150.9
	297	2004-06-21 23:32:02.760	2.8	20.7	253	107	2	4.6	475.4
	390	2006-08-08 05:04:00.050	3.5	29.0	173	-173	0	17.7	301.9
	411	2007-02-17 01:41:14.010	2.6	15.4	167	-167	3	1.6	410.6
	478	2008-10-30 05:54:29.080	3.2	27.3	175	-175	0	1.6	211.5
	538	2009-04-14 21:05:25.880	2.6	28.6	172	-172	1	9.0	62.1
	547	2009-05-08 05:23:11.950	3.0	29.2	181	178	0	2.0	67.3
ZLV1	58	1996-12-28 18:16:56.580	2.7	34.7	278	146	58	5.9	103.3
	66	1997-02-19 21:53:50.810	3.4	34.7	96	-31	56	10.7	160.5
	115	1998-07-14 12:12:02.230	3.3	35.3	90	-26	81	10.5	87.0
	154	1999-12-31 11:00:55.330	2.8	34.8	87	-23	16	11.3	41.1
	166	2000-06-12 15:48:23.010	2.6	27.6	250	173	71	5.1	60.3
	273	2003-09-27 13:57:54.150	2.7	28.7	69	-5	80	5.3	31.7
	275	2003-10-24 01:52:41.160	3.0	22.7	70	-6	45	11.0	303.9
	280	2003-11-16 20:04:11.480	2.7	28.2	71	-6	7	17.1	67.6
	297	2004-06-21 23:32:02.760	2.8	20.7	74	-9	27	27.4	314.4
	411	2007-02-17 01:41:14.010	2.6	15.4	72	-8	14	2.7	208.6
	478	2008-10-30 05:54:29.080	3.2	27.3	75	-11	16	3.5	173.4
	538	2009-04-14 21:05:25.880	2.6	28.6	249	174	70	8.9	75.1
	547	2009-05-08 05:23:11.950	3.0	29.2	72	-8	30	5.7	68.9
	566	2009-11-26 12:54:14.030	2.8	48.5	72	-8	48	5.9	80.3
ZLV2	58	1996-12-28 18:16:56.580	2.7	34.7	345	148	7	5.3	135.6
	107	1998-02-15 07:24:16.420	2.6	29.4	130	3	1	13.6	67.2
	115	1998-07-14 12:12:02.230	3.3	35.3	334	158	3	3.4	108.4
	154	1999-12-31 11:00:55.330	2.8	34.8	158	-25	57	3.9	60.7
	166	2000-06-12 15:48:23.010	2.6	27.6	151	-18	13	3.5	101.6
	175	2000-10-25 18:10:34.790	3.2	35.3	331	161	78	2.8	172.1
	273	2003-09-27 13:57:54.150	2.7	28.7	158	-25	7	3.5	68.0
	275	2003-10-24 01:52:41.160	3.0	22.7	147	-14	24	6.3	457.5
	280	2003-11-16 20:04:11.480	2.7	28.2	165	-31	5	3.0	228.1
	297	2004-06-21 23:32:02.760	2.8	20.7	38	95	15	1.3	475.2
	346	2005-10-12 16:06:42.530	2.5	24.9	325	168	75	1.3	75.4
	350	2006-01-10 23:41:06.140	2.6	19.5	360	133	51	1.9	331.6
	390	2006-08-08 05:04:00.050	3.5	29.0	165	-32	8	1.8	731.8
	391	2006-08-08 09:49:23.380	2.5	28.8	166	-32	9	2.9	42.2
	411	2007-02-17 01:41:14.010	2.6	15.4	148	-15	7	7.4	822.5

Continued on next page

Station	ID	Origin time	L	d [km]	θ [°]	θ_{diff} [°]	Offset [°]	Linearity	SNR
	478	2008-10-30 05:54:29.080	3.2	27.3	148	-15	1	15.9	475.3
	538	2009-04-14 21:05:25.880	2.6	28.6	164	-31	8	1.6	92.6
	540	2009-04-16 17:12:15.910	2.6	25.4	137	-4	8	16.7	151.0
	547	2009-05-08 05:23:11.950	3.0	29.2	144	-11	7	10.4	193.8
	566	2009-11-26 12:54:14.030	2.8	48.5	54	78	15	1.5	214.6
ZLV3	25	1996-03-12 12:13:48.170	2.6	35.0	266	-44	5	3.1	27.0
	103	1998-01-28 21:33:03.840	2.7	34.8	234	-12	2	1.9	77.1
	107	1998-02-15 07:24:16.420	2.6	29.4	223	0	12	10.9	81.9
	115	1998-07-14 12:12:02.230	3.3	35.3	243	-21	3	6.2	96.7
	154	1999-12-31 11:00:55.330	2.8	34.8	245	-23	6	6.1	68.8
	166	2000-06-12 15:48:23.010	2.6	27.6	217	4	9	8.0	98.8
	273	2003-09-27 13:57:54.150	2.7	28.7	218	3	1	79.1	62.5
	275	2003-10-24 01:52:41.160	3.0	22.7	210	11	1	13.8	551.2
	280	2003-11-16 20:04:11.480	2.7	28.2	218	4	0	221.7	233.6
	297	2004-06-21 23:32:02.760	2.8	20.7	235	-12	13	17.9	423.5
	346	2005-10-12 16:06:42.530	2.5	24.9	47	175	72	2.2	56.0
	350	2006-01-10 23:41:06.140	2.6	19.5	234	-11	21	6.0	312.0
	390	2006-08-08 05:04:00.050	3.5	29.0	220	1	8	91.5	478.6
	391	2006-08-08 09:49:23.380	2.5	28.8	218	4	10	15.8	35.4
	411	2007-02-17 01:41:14.010	2.6	15.4	225	-3	7	10.4	869.4
	478	2008-10-30 05:54:29.080	3.2	27.3	221	0	1	42.1	392.6
	538	2009-04-14 21:05:25.880	2.6	28.6	219	2	0	183.3	100.2
	540	2009-04-16 17:12:15.910	2.6	25.4	209	12	2	5.9	101.0
	547	2009-05-08 05:23:11.950	3.0	29.2	219	2	0	31.8	119.2
	566	2009-11-26 12:54:14.030	2.8	48.5	232	-10	65	2.3	157.7
ZLV4	103	1998-01-28 21:33:03.840	2.7	34.8	154	-24	2	2.8	75.5
	107	1998-02-15 07:24:16.420	2.6	29.4	122	8	1	23.3	96.8
	115	1998-07-14 12:12:02.230	3.3	35.3	151	-21	2	4.2	126.6
	154	1999-12-31 11:00:55.330	2.8	34.8	137	-7	8	2.4	60.3
	166	2000-06-12 15:48:23.010	2.6	27.6	124	5	1	19.8	58.1
	175	2000-10-25 18:10:34.790	3.2	35.3	149	-19	2	1.9	171.2
	273	2003-09-27 13:57:54.150	2.7	28.7	125	4	1	70.8	91.2
	275	2003-10-24 01:52:41.160	3.0	22.7	124	5	0	102.8	697.8
x	280	2003-11-16 20:04:11.480	2.7	28.2	126	4	1	133.0	252.5
	297	2004-06-21 23:32:02.760	2.8	20.7	140	-9	3	5.7	502.5
	346	2005-10-12 16:06:42.530	2.5	24.9	121	9	10	5.3	56.6
	350	2006-01-10 23:41:06.140	2.6	19.5	137	-6	18	3.3	485.2
	390	2006-08-08 05:04:00.050	3.5	29.0	127	2	3	71.0	562.8
	391	2006-08-08 09:49:23.380	2.5	28.8	132	-1	4	9.4	36.4
	411	2007-02-17 01:41:14.010	2.6	15.4	121	8	3	64.3	1150.0
	478	2008-10-30 05:54:29.080	3.2	27.3	126	3	0	110.9	364.2
	538	2009-04-14 21:05:25.880	2.6	28.6	129	0	1	21.9	105.5
	540	2009-04-16 17:12:15.910	2.6	25.4	118	11	4	5.0	109.5
	547	2009-05-08 05:23:11.950	3.0	29.2	128	1	0	82.5	145.8
	566	2009-11-26 12:54:14.030	2.8	48.5	135	-5	58	7.8	150.2

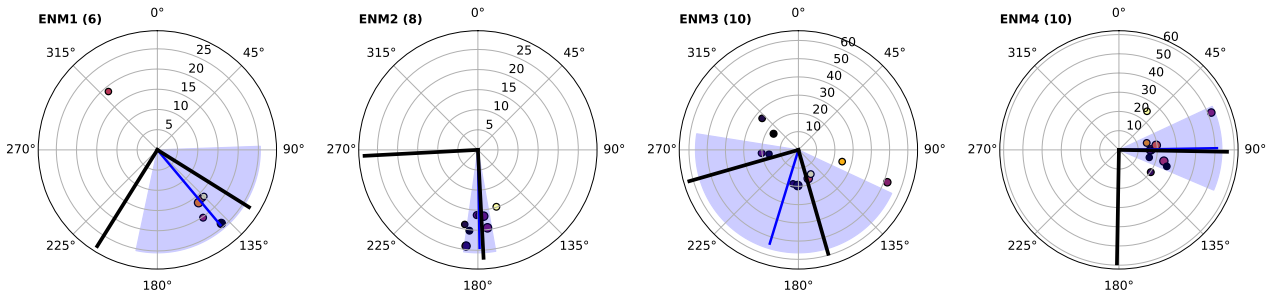

FIGURE B.8: Orientation results for all levels of station ENM. The number of measurements contributing to the mean solution (blue line) is indicated in parentheses. Angles stored in the StationXML file are represented by the two black lines. Individual results are shown as circles with colour depending on the linearity of the particle motion in the horizontal plane (see e.g. Fig. 3.13) and size being proportional to event magnitude, plotted as function of the event-station distance in km (radial axis). Blue-shaded areas symbolise standard deviations.

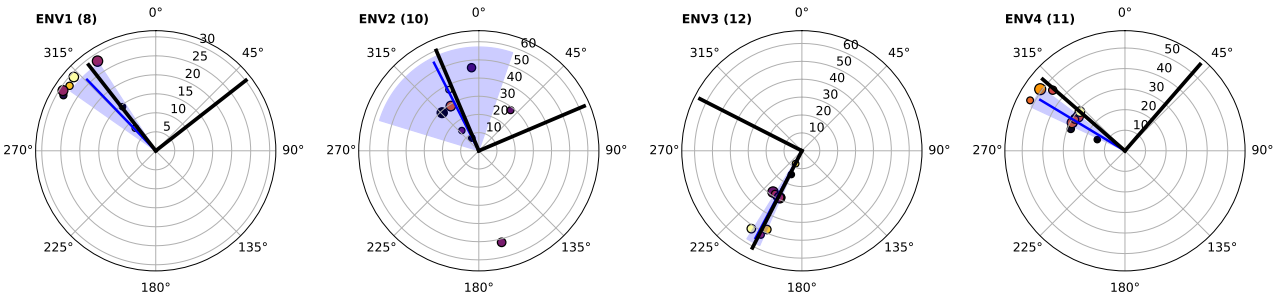

FIGURE B.9: Same as Fig. B.8 for ENV borehole station.

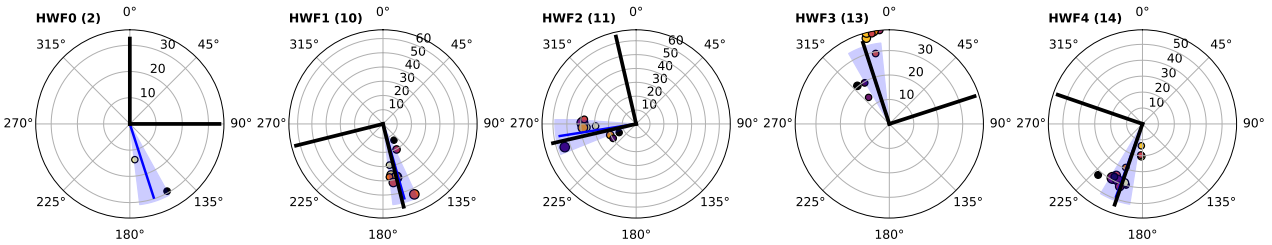

FIGURE B.10: Same as Fig. B.8 for HWF borehole station.

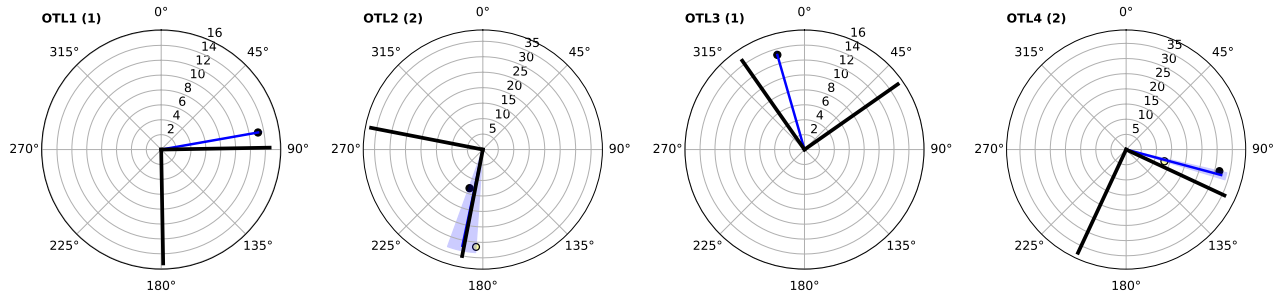

FIGURE B.11: Same as Fig. B.8 for OTL borehole station.

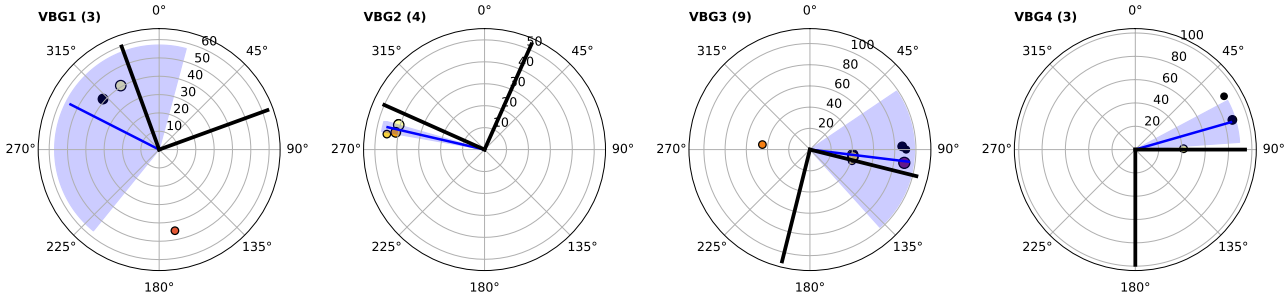

FIGURE B.12: Same as Fig. B.8 for VBG borehole station.

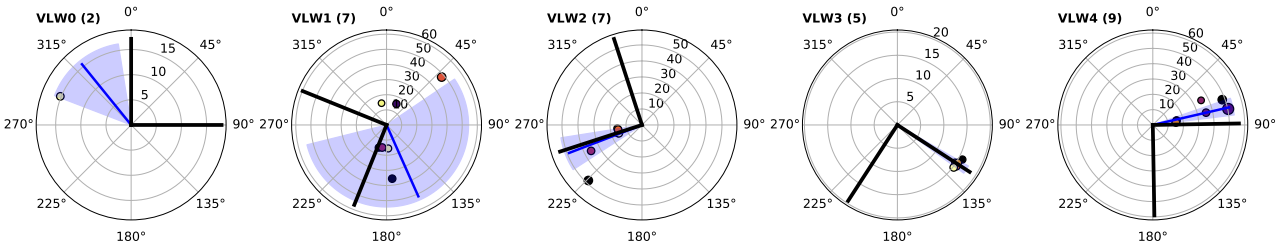

FIGURE B.13: Same as Fig. B.8 for VLW borehole station.

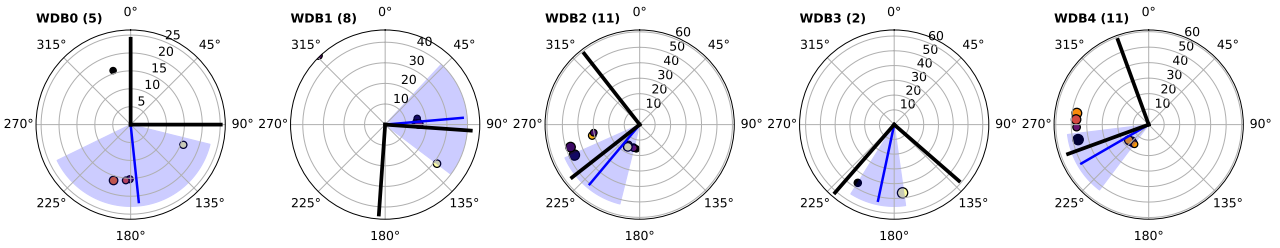

FIGURE B.14: Same as Fig. B.8 for WDB borehole station.

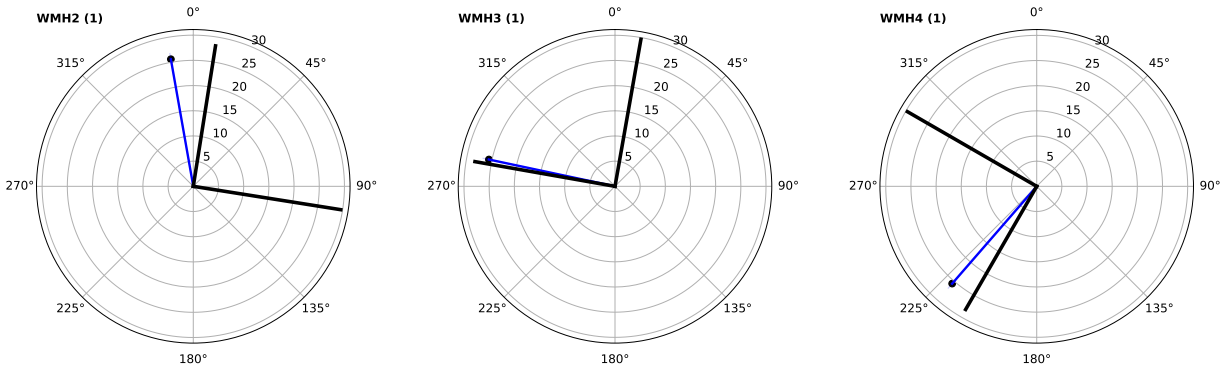

FIGURE B.15: Same as Fig. B.8 for WMH borehole station.

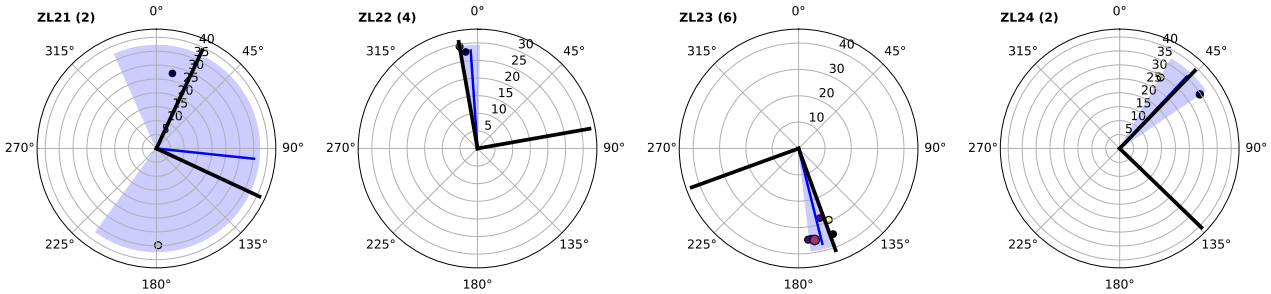

FIGURE B.16: Same as Fig. B.8 for ZL2 borehole station.

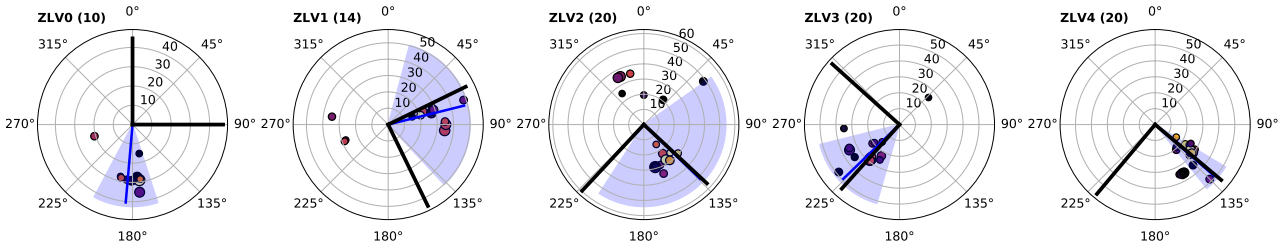

FIGURE B.17: Same as Fig. B.8 for ZLV borehole station.

Examples

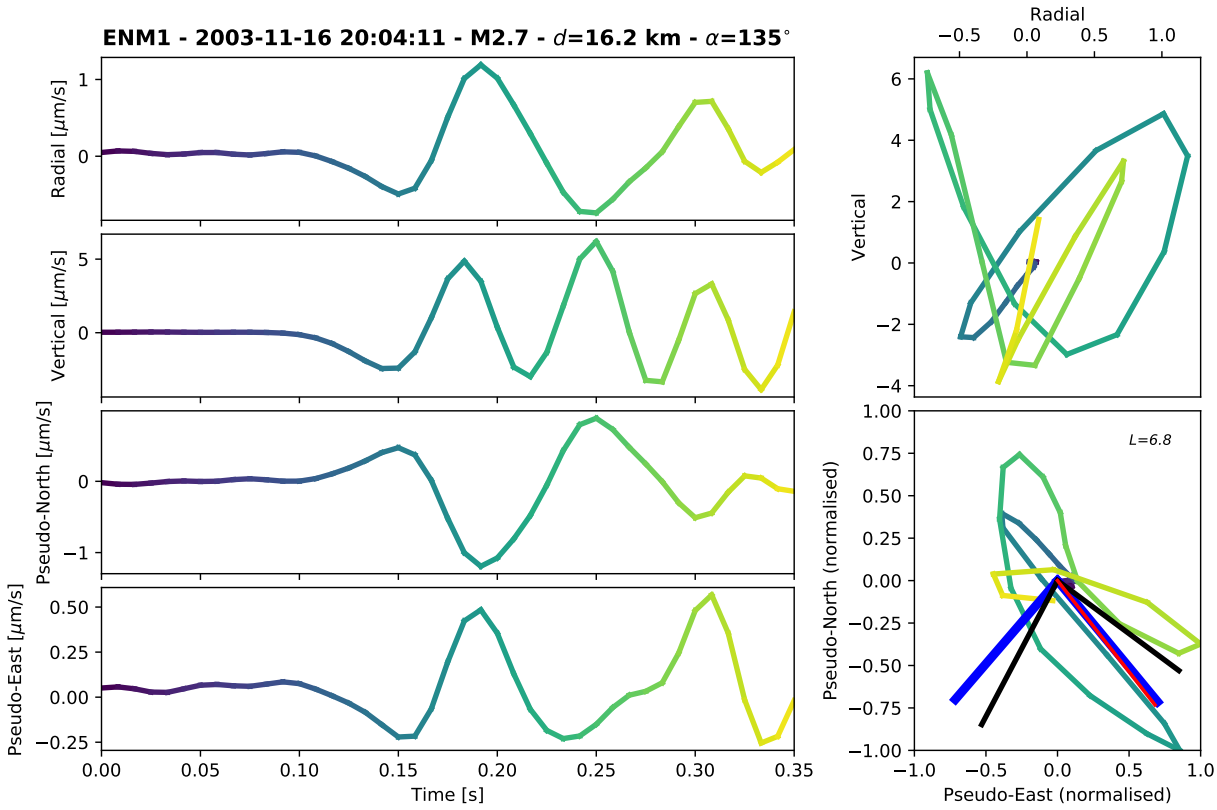

FIGURE B.18: Waveforms and hodograms for radial, vertical, pseudo-north and pseudo-east component of an event recorded on ENM1. On the bottom right plot, the blue lines are the results of our orientation analysis; the black lines are the angles stored in the StationXML file and the red line points towards the principal direction of the particle motion in the horizontal plane. The linearity, defined as the ratio of the largest over the smallest eigenvalue, is indicated on the top right corner.

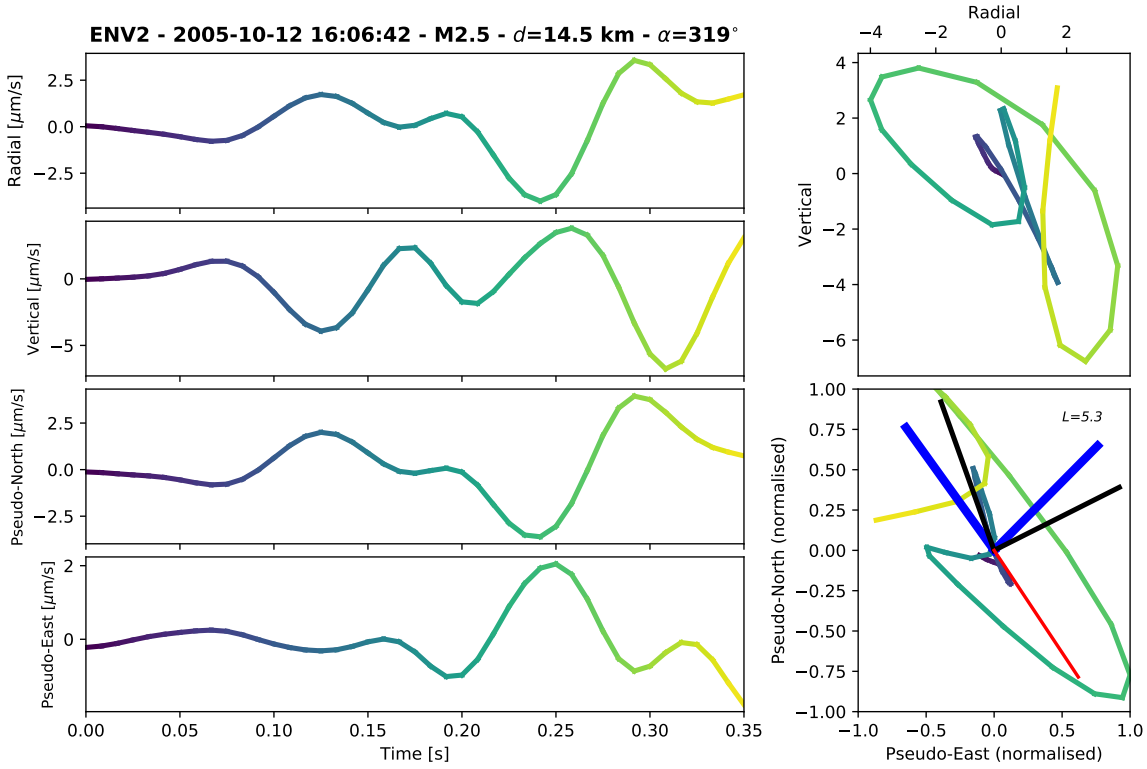

FIGURE B.19: Same as Fig. B.18 for ENV2.

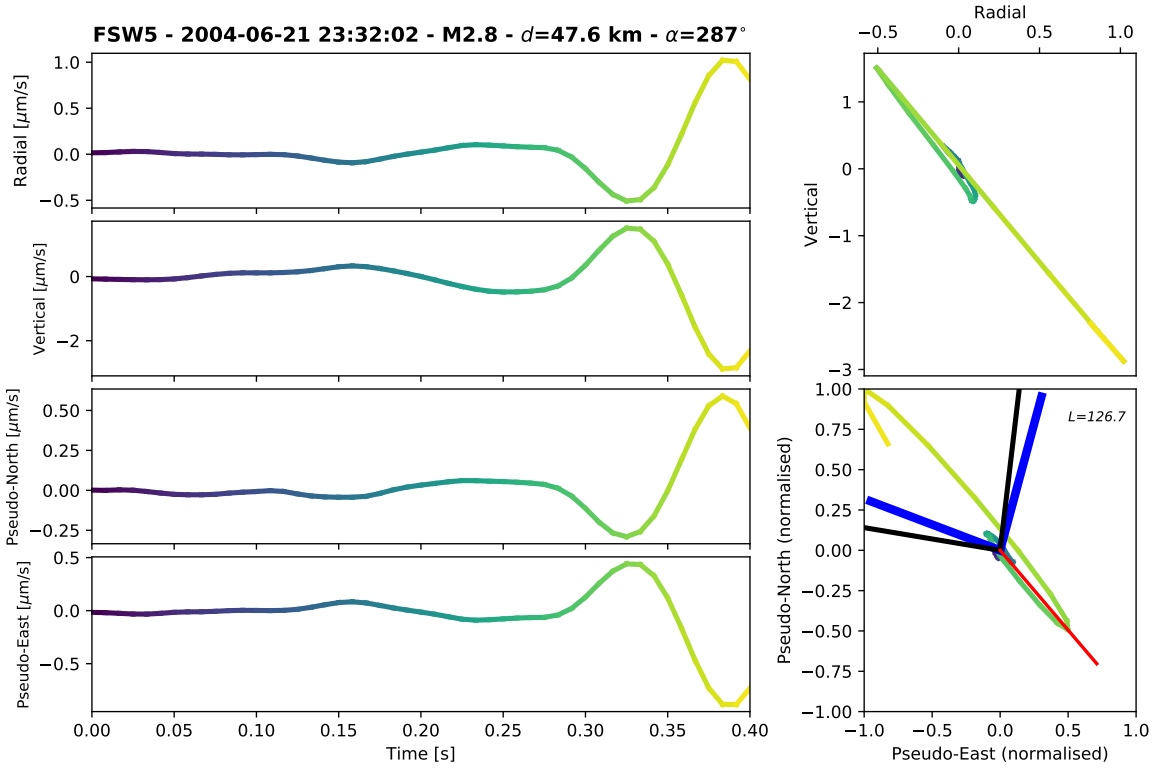

FIGURE B.20: Same as Fig. B.18 for FSW5.

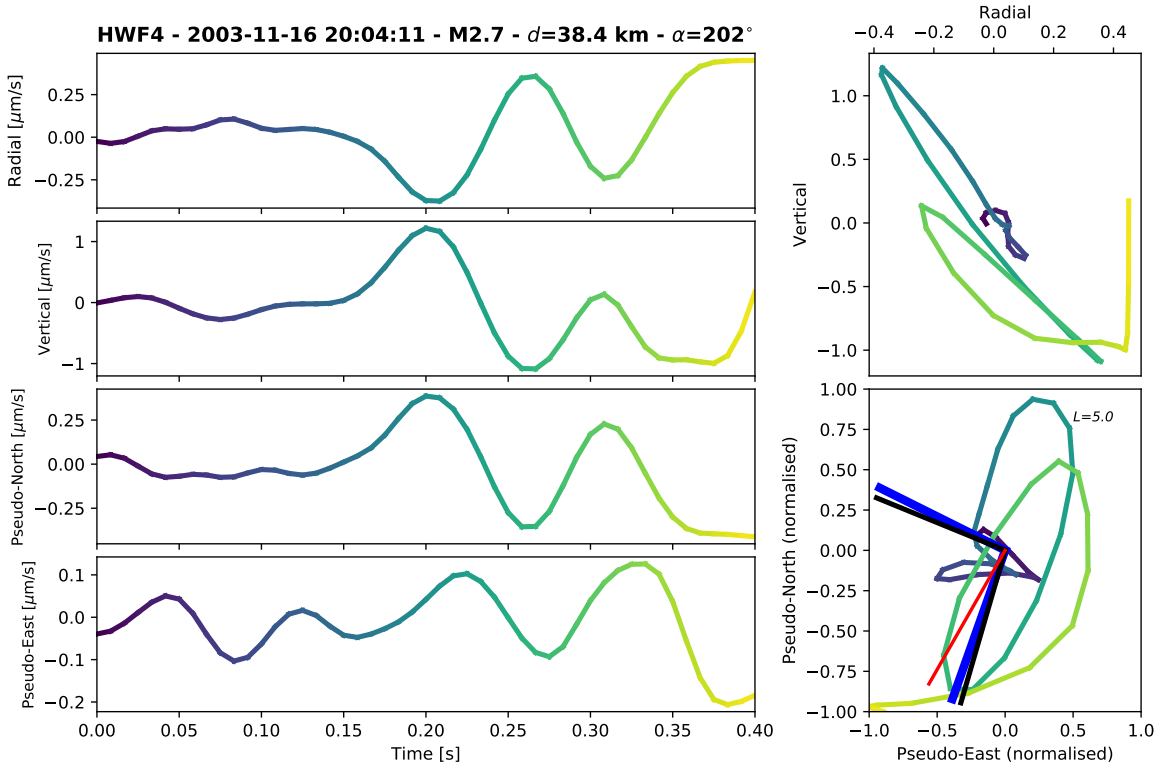

FIGURE B.21: Same as Fig. B.18 for HWF4.

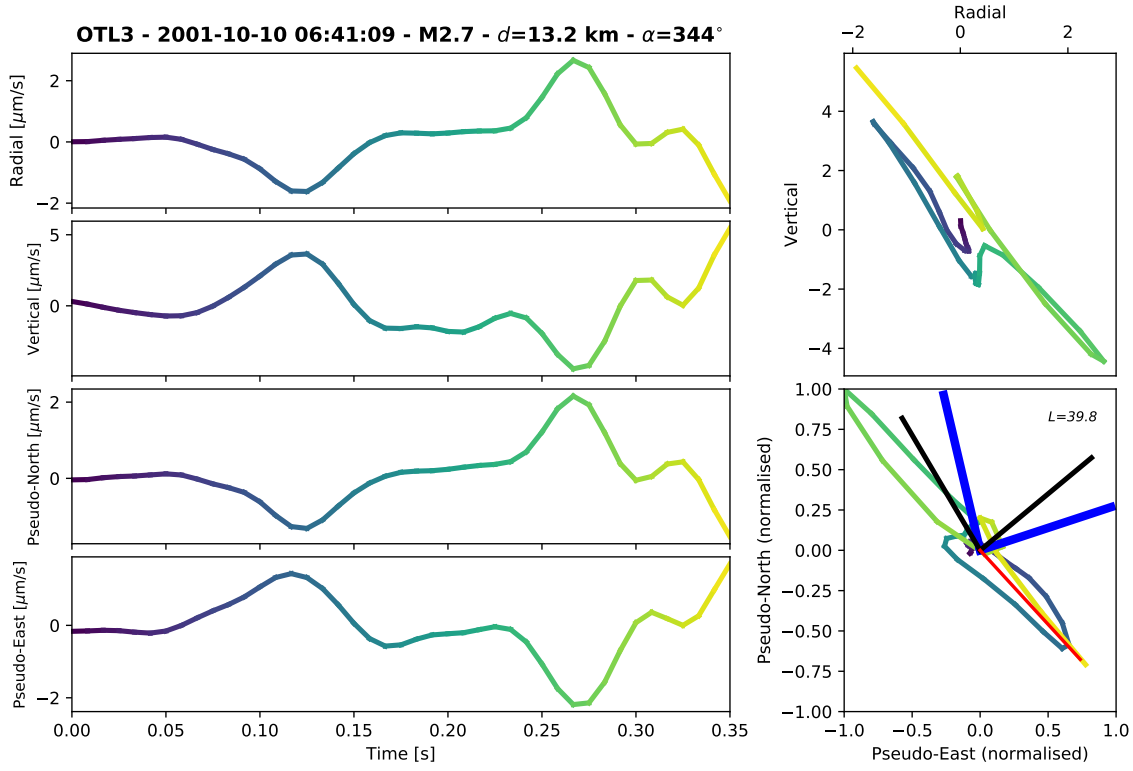

FIGURE B.22: Same as Fig. B.18 for OTL3.

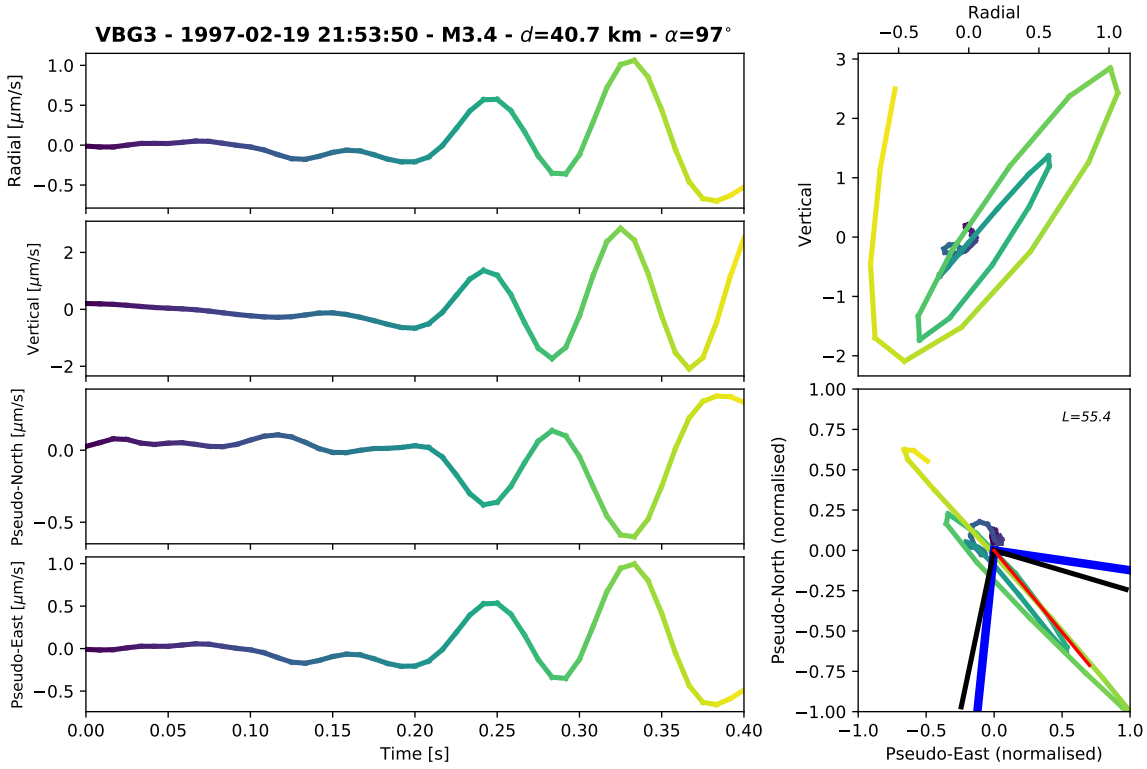

FIGURE B.23: Same as Fig. B.18 for VBG3.

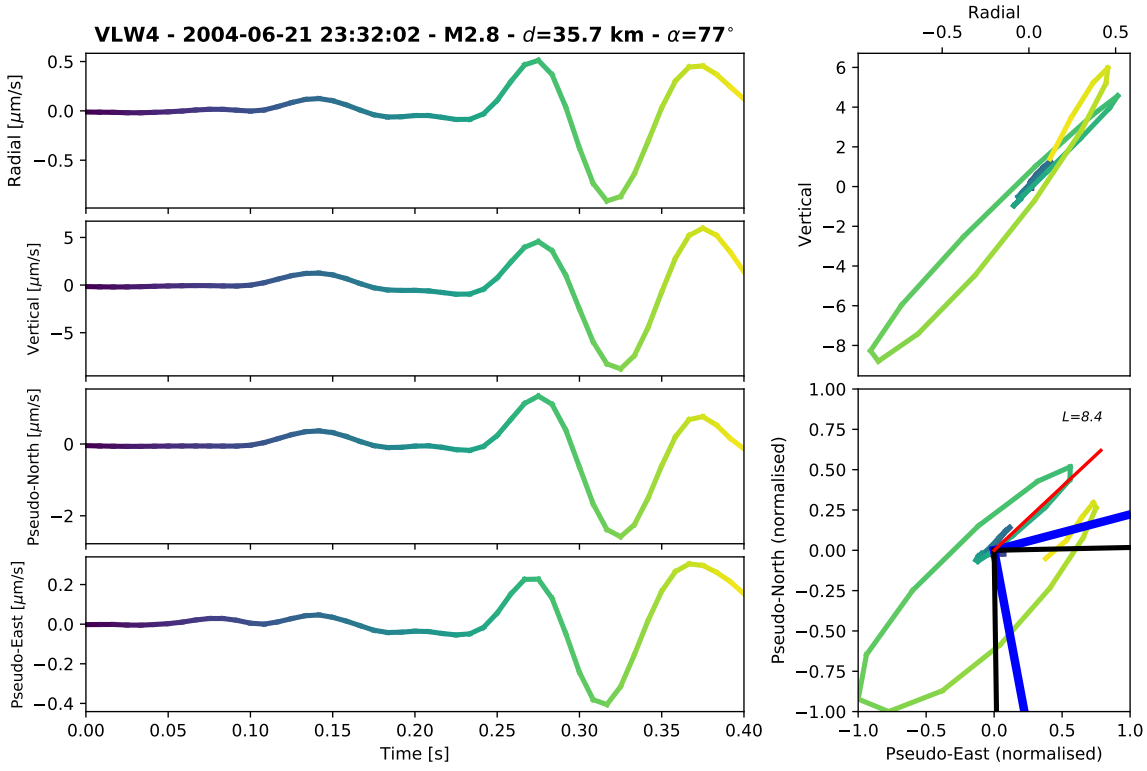

FIGURE B.24: Same as Fig. B.18 for VLW4.

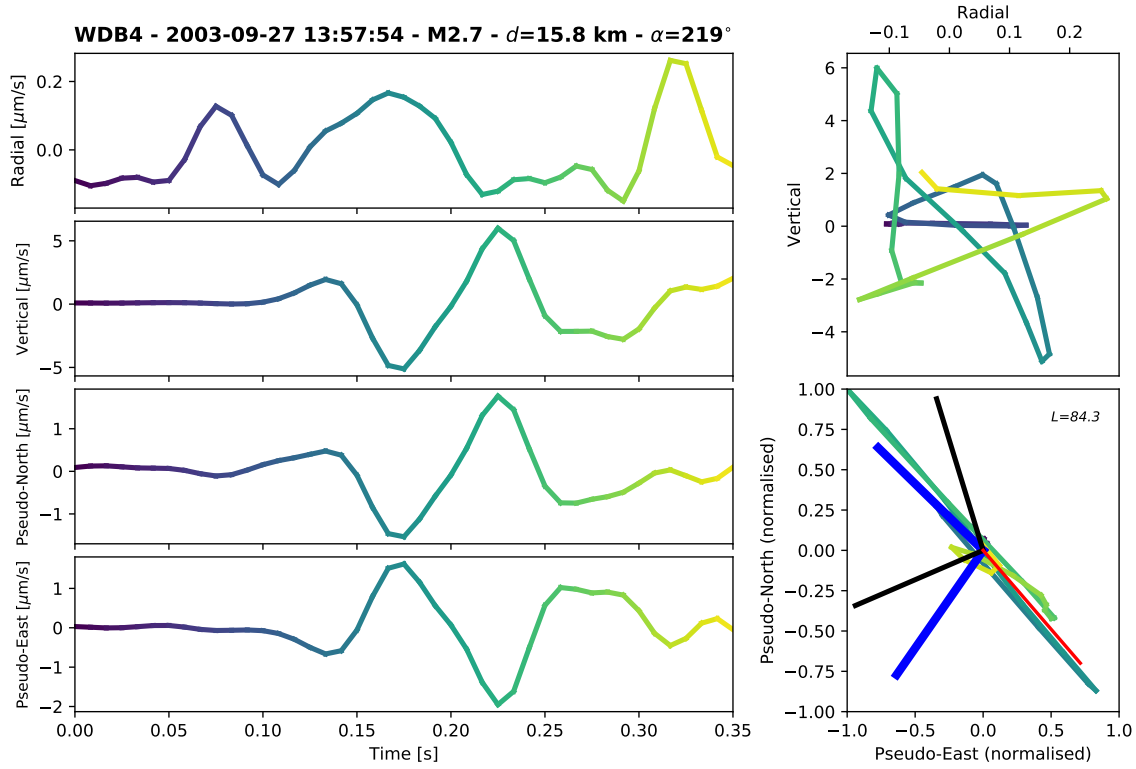

FIGURE B.25: Same as Fig. B.18 for WDB4.

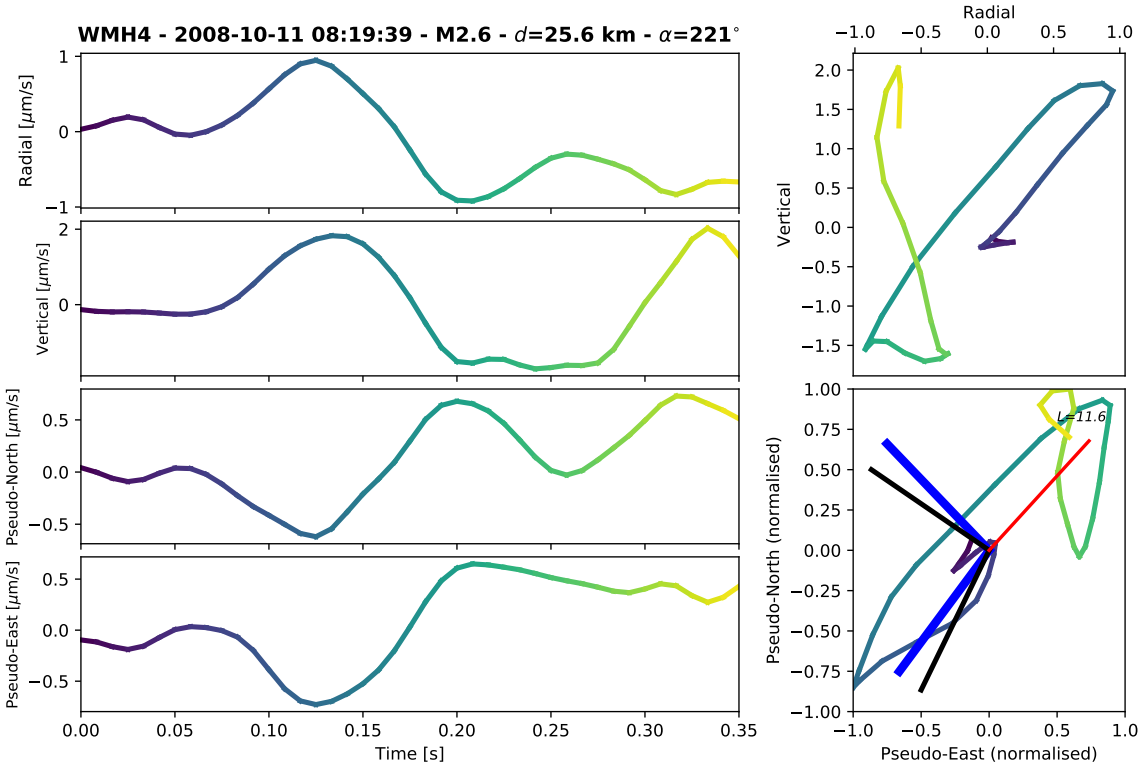

FIGURE B.26: Same as Fig. B.18 for WMH4.

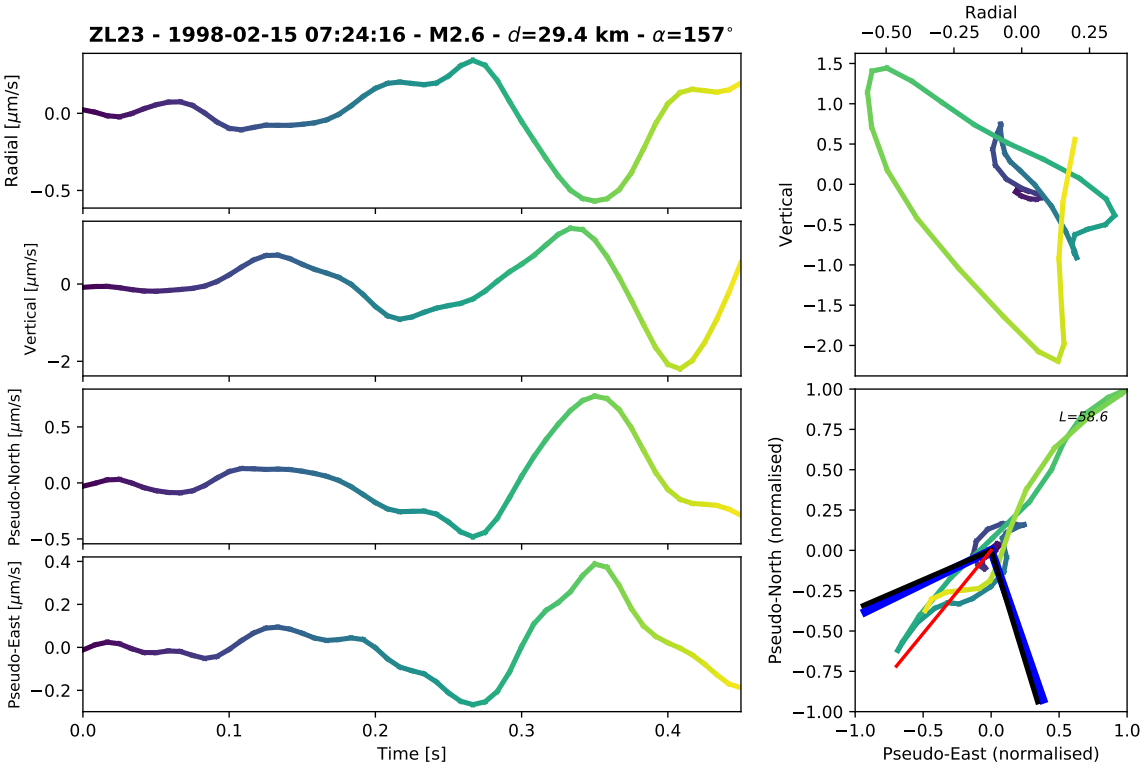

FIGURE B.27: Same as Fig. B.18 for ZL23.

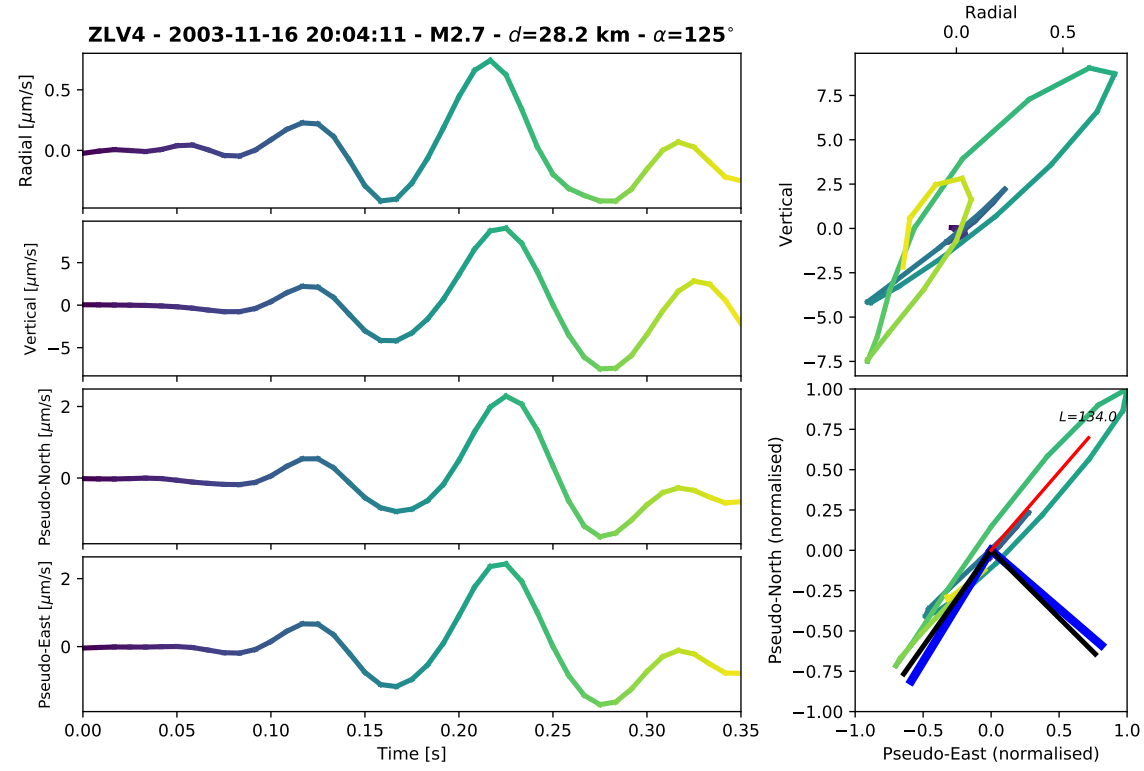

FIGURE B.28: Same as Fig. B.18 for ZLV4.

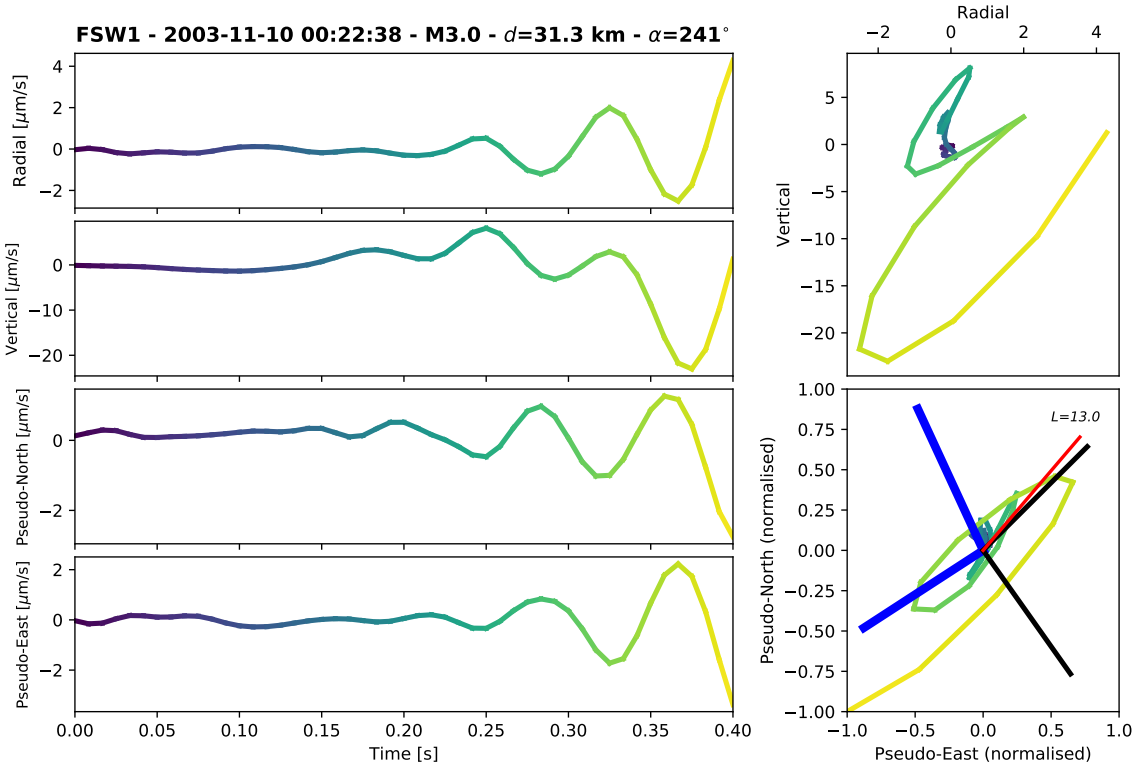

FIGURE B.29: Same as Fig. B.18 for FSW1. In this example, our results differ by about 180° from the XML file angles.

B.5 Borehole overview of malfunctioning components

The figures shown in this section are based on the Appendices F and G of Dost et al. (2022). Grey colour indicates functional components, while red indicates potentially erroneous amplitudes. Red crosses represent specific events, which are reported as suspicious throughout the same report (section 5.2.4 on borehole amplitudes in Dost et al., 2022). Orange lines correspond to reported damages to the DCF receiver (Appendix F in Dost et al., 2022).

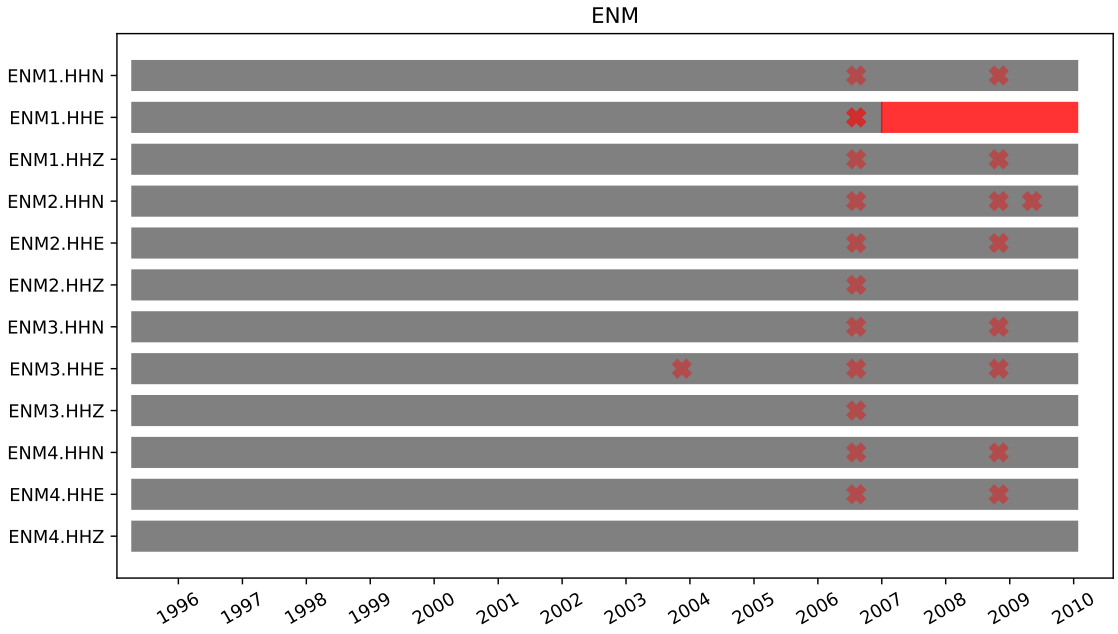

FIGURE B.30: Borehole station ENM

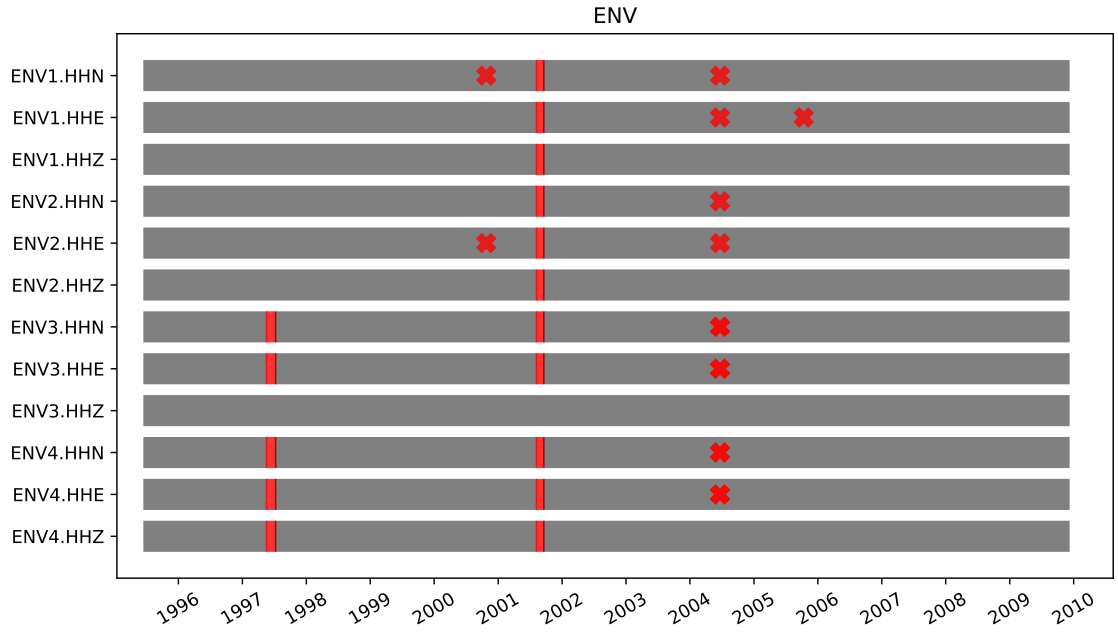

FIGURE B.31: Borehole station ENV

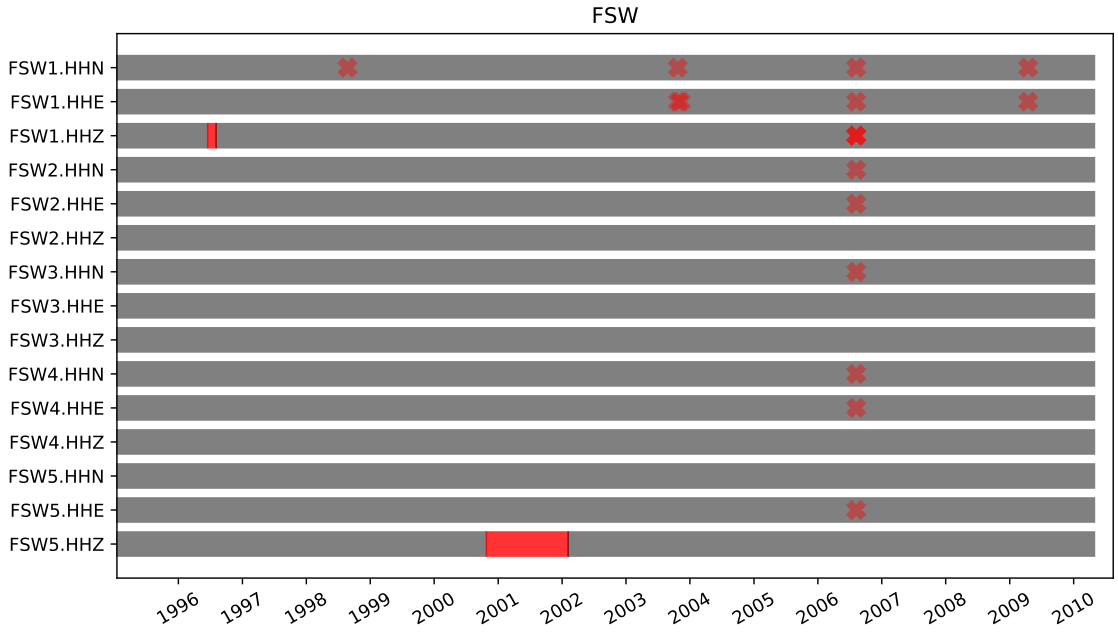

FIGURE B.32: Borehole station FSW

FIGURE B.33: Borehole station HWF

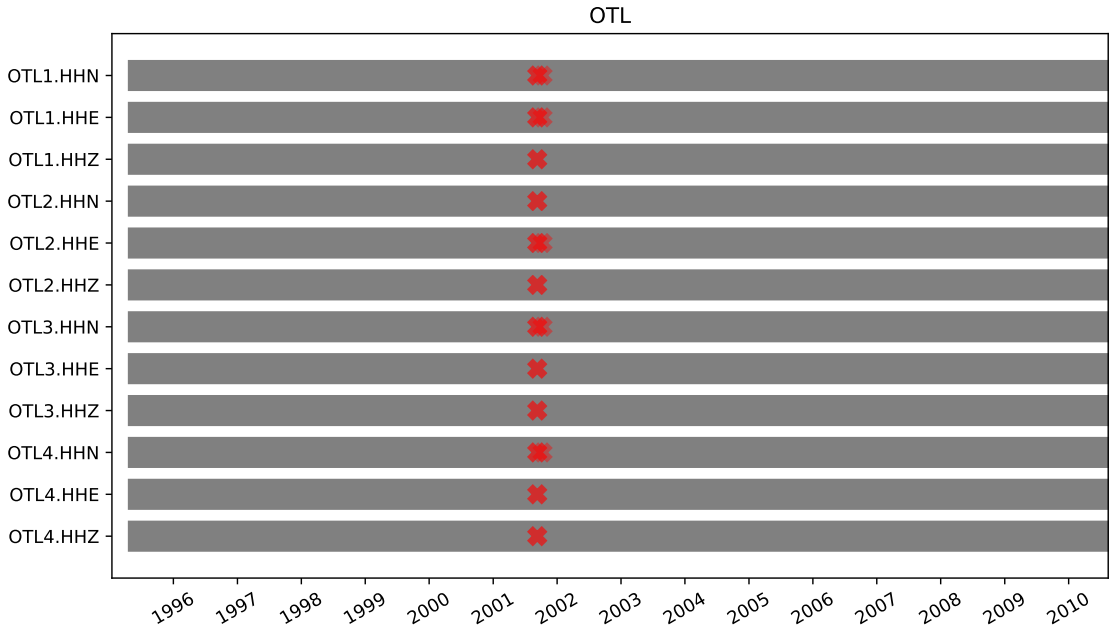

FIGURE B.34: Borehole station OTL

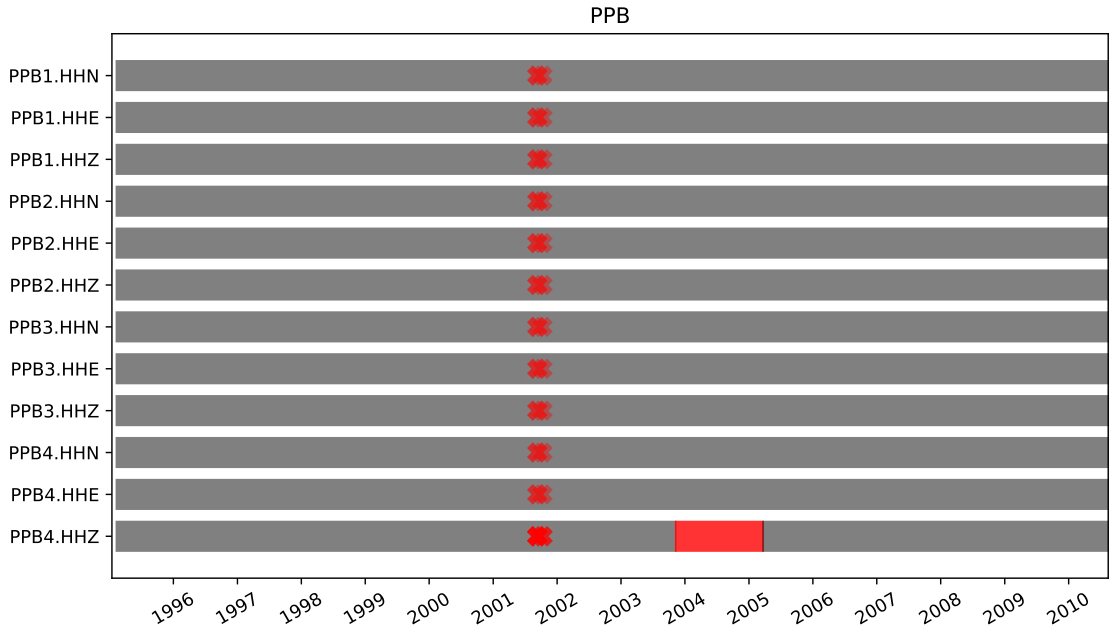

FIGURE B.35: Borehole station PPB

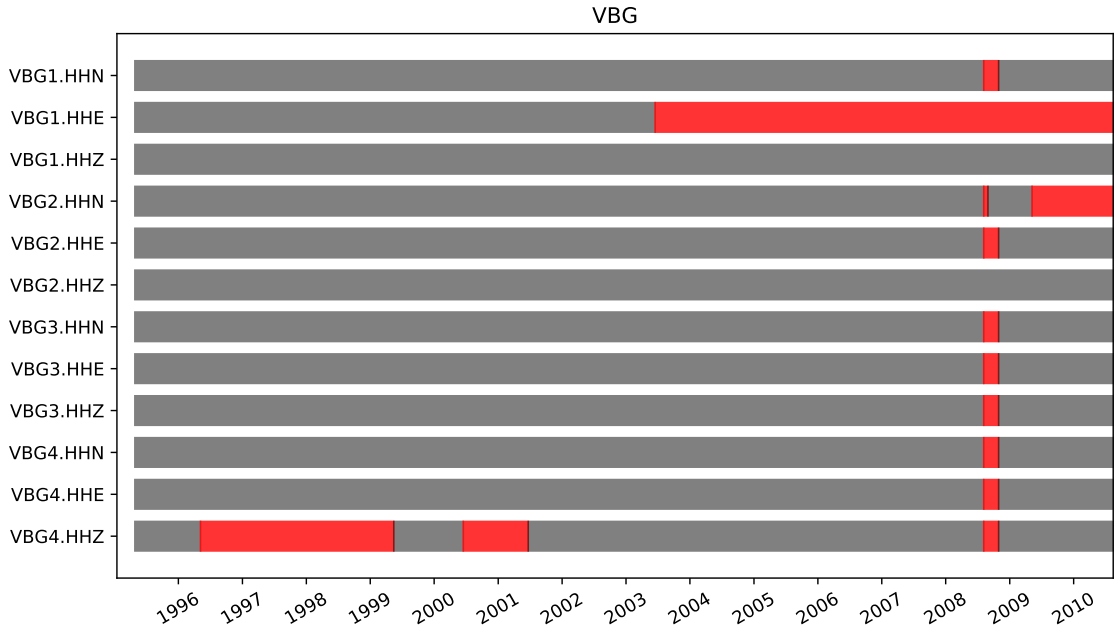

FIGURE B.36: Borehole station VBG

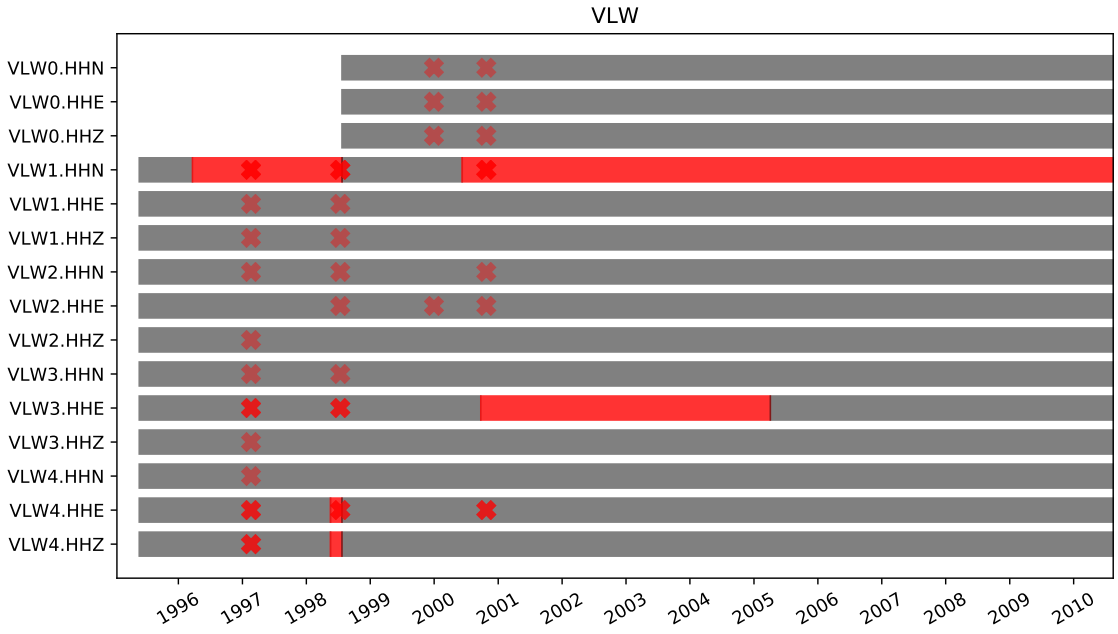

FIGURE B.37: Borehole station VLW

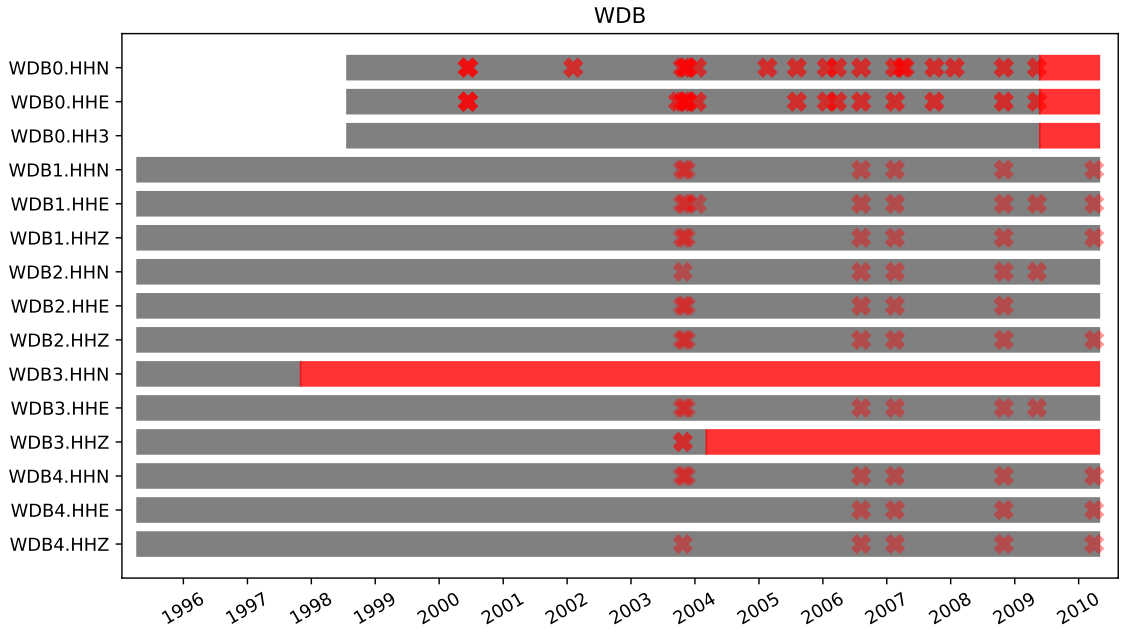

FIGURE B.38: Borehole station WDB

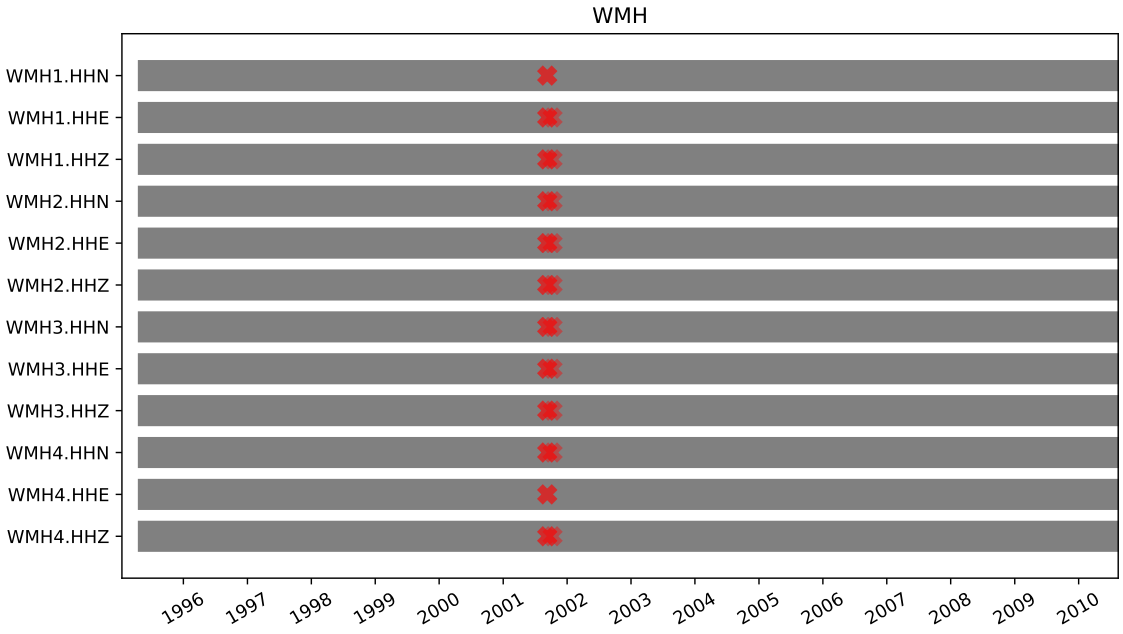

FIGURE B.39: Borehole station WMH

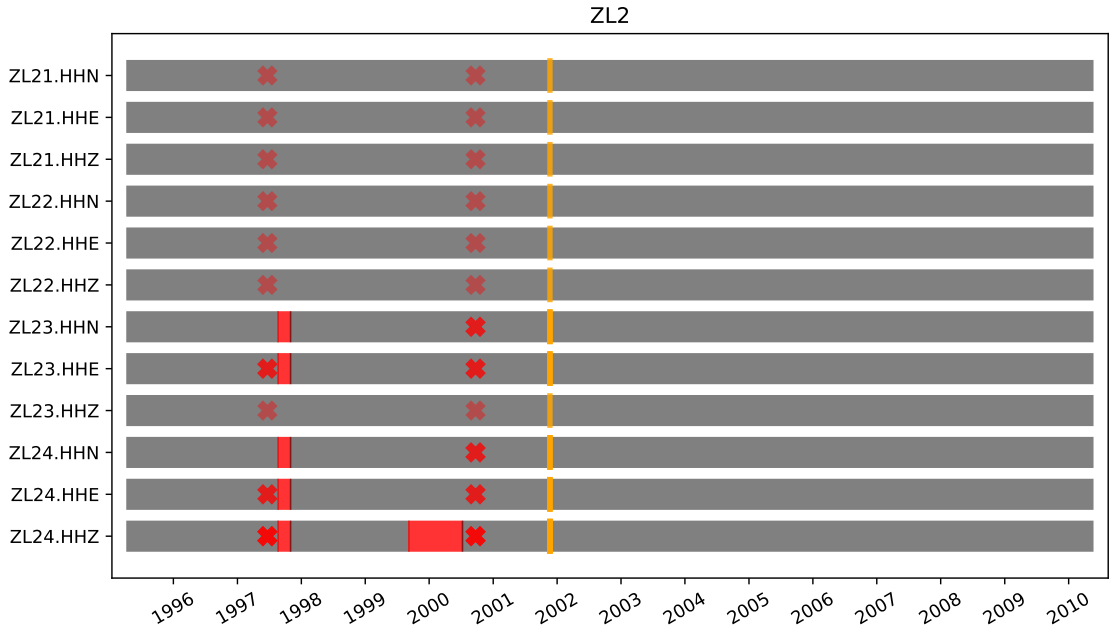

FIGURE B.40: Borehole station ZL2

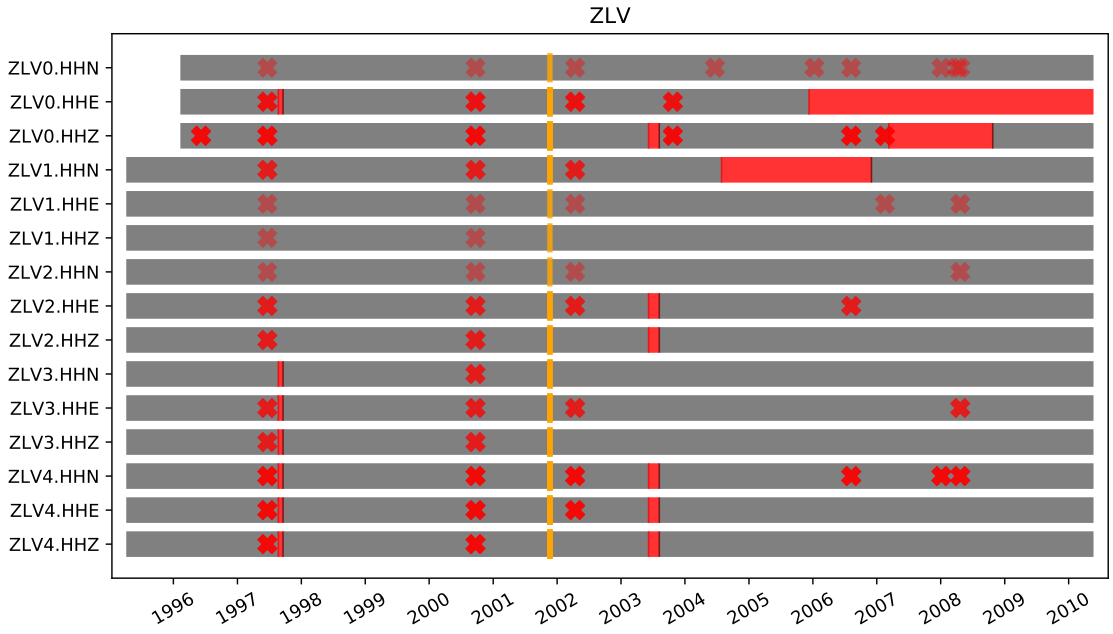

FIGURE B.41: Borehole station ZLV

B.6 Borehole maximum amplitudes as a function of distance at all stations and levels

Each figure shows the absolute maximum amplitude measured on each individual record (by station, level and component).

Data were instrument-corrected, rotated into the ray coordinate system (R-T-Z) and bandpass-filtered in the frequency range from 2 to 50 Hz.

Circles are coloured by event origin time and their size is proportional to event magnitude.

In addition, saturated records and malfunctioning components as reported in section 5.2.4 and appendices F & G of Dost et al. (2022) are highlighted as red- and white-bordered circles, respectively.

Events belonging to files containing multiple events are symbolised by white crosses. Since the extraction of the maximum amplitude was performed automatically, the maximum amplitude corresponds to the one measured for the largest event within the file.

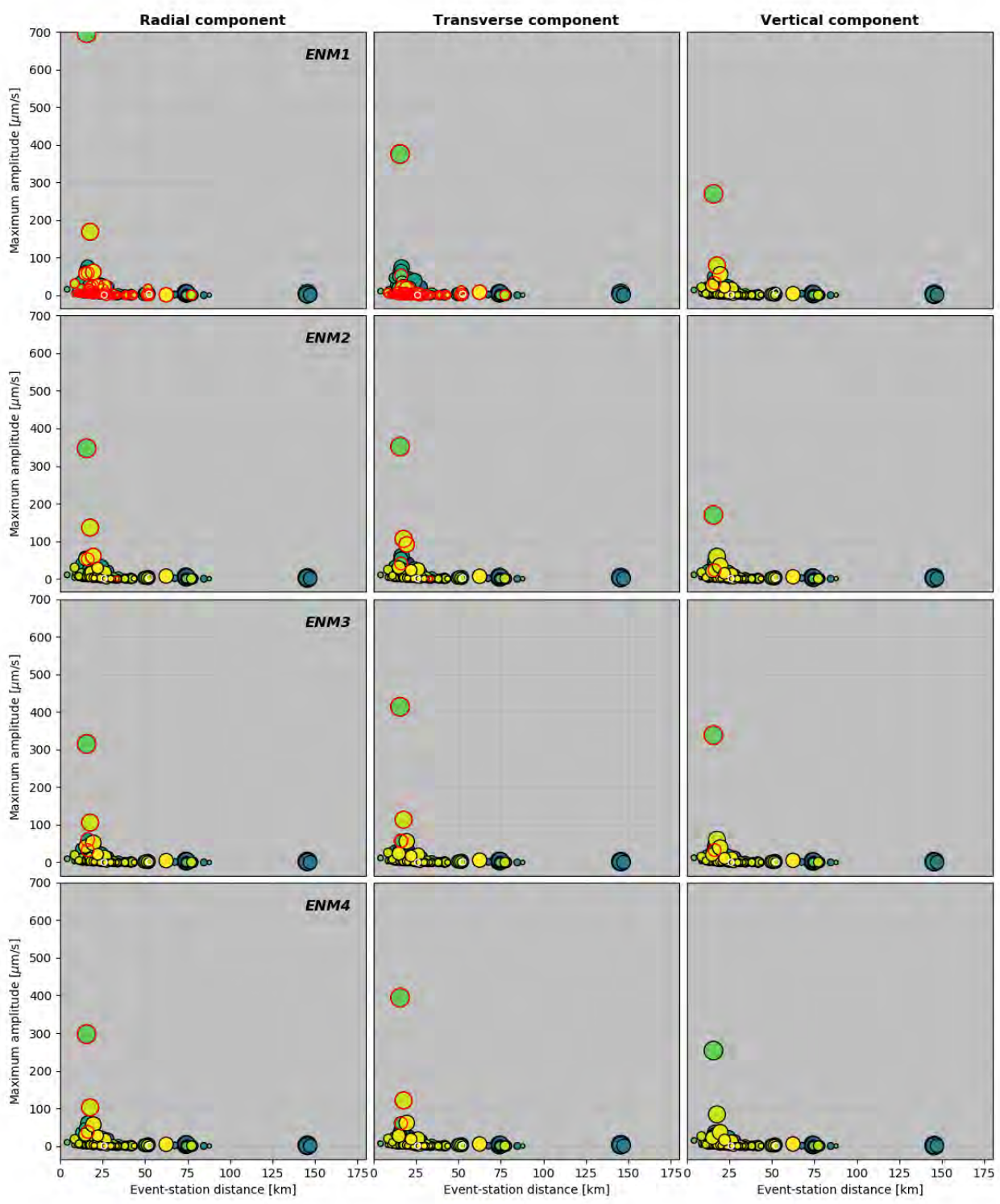

FIGURE B.42: Borehole station ENM: columns correspond to radial, transversal and vertical component, rows to levels 1 to 4

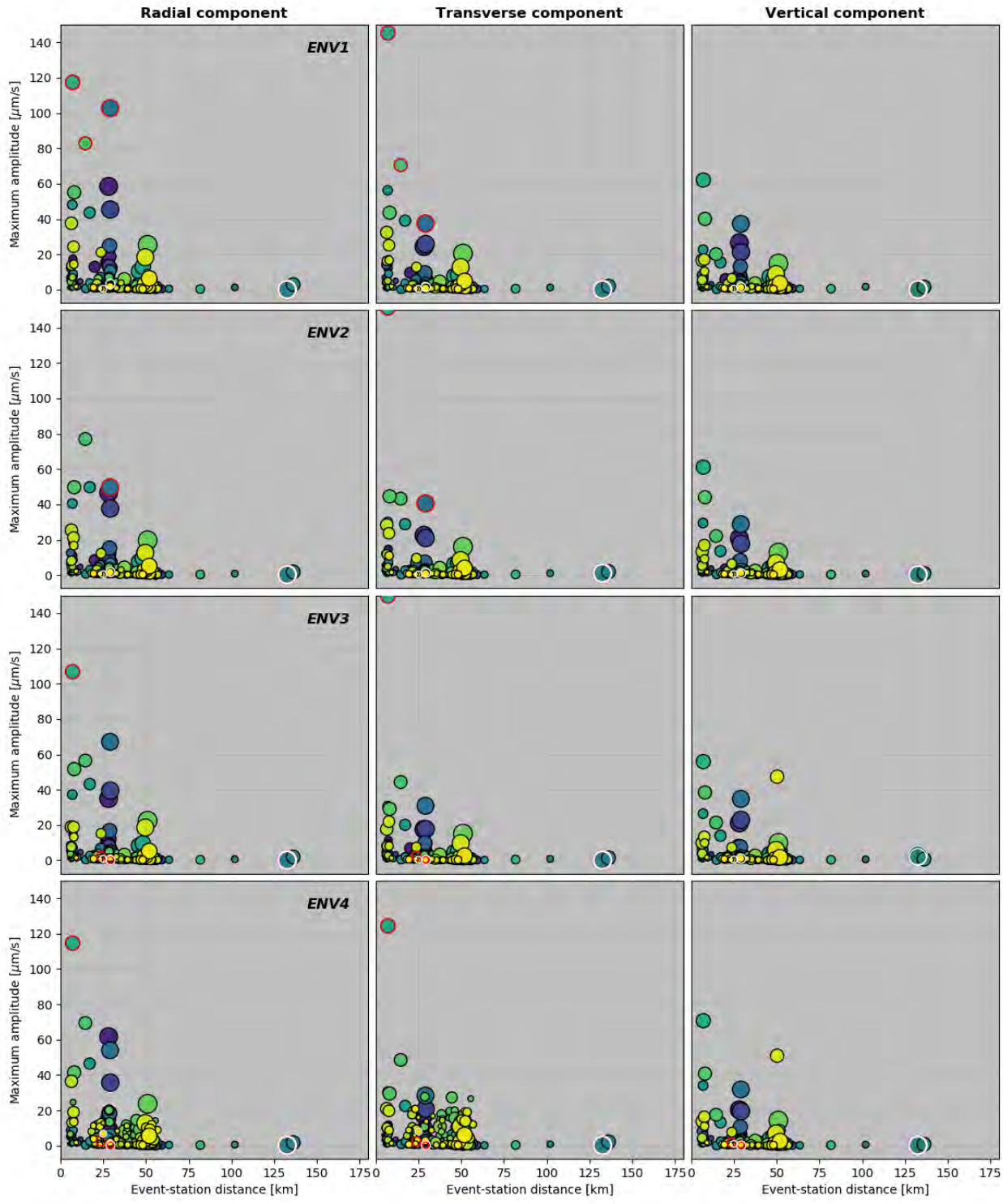

FIGURE B.43: Borehole station ENV: columns correspond to radial, transversal and vertical component, rows to levels 1 to 4

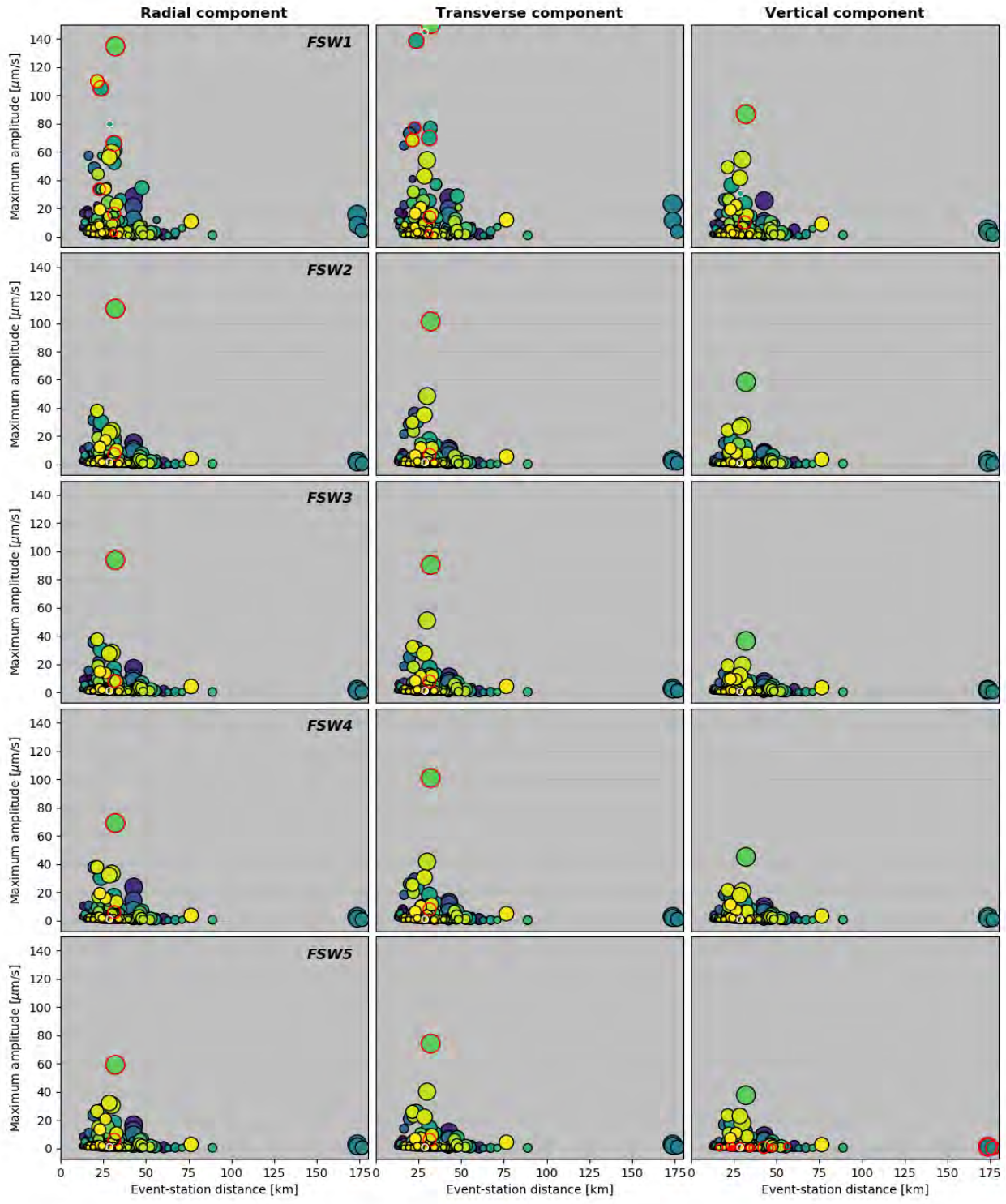

FIGURE B.44: Borehole station FSW: columns correspond to radial, transversal and vertical component, rows to levels 1 to 5

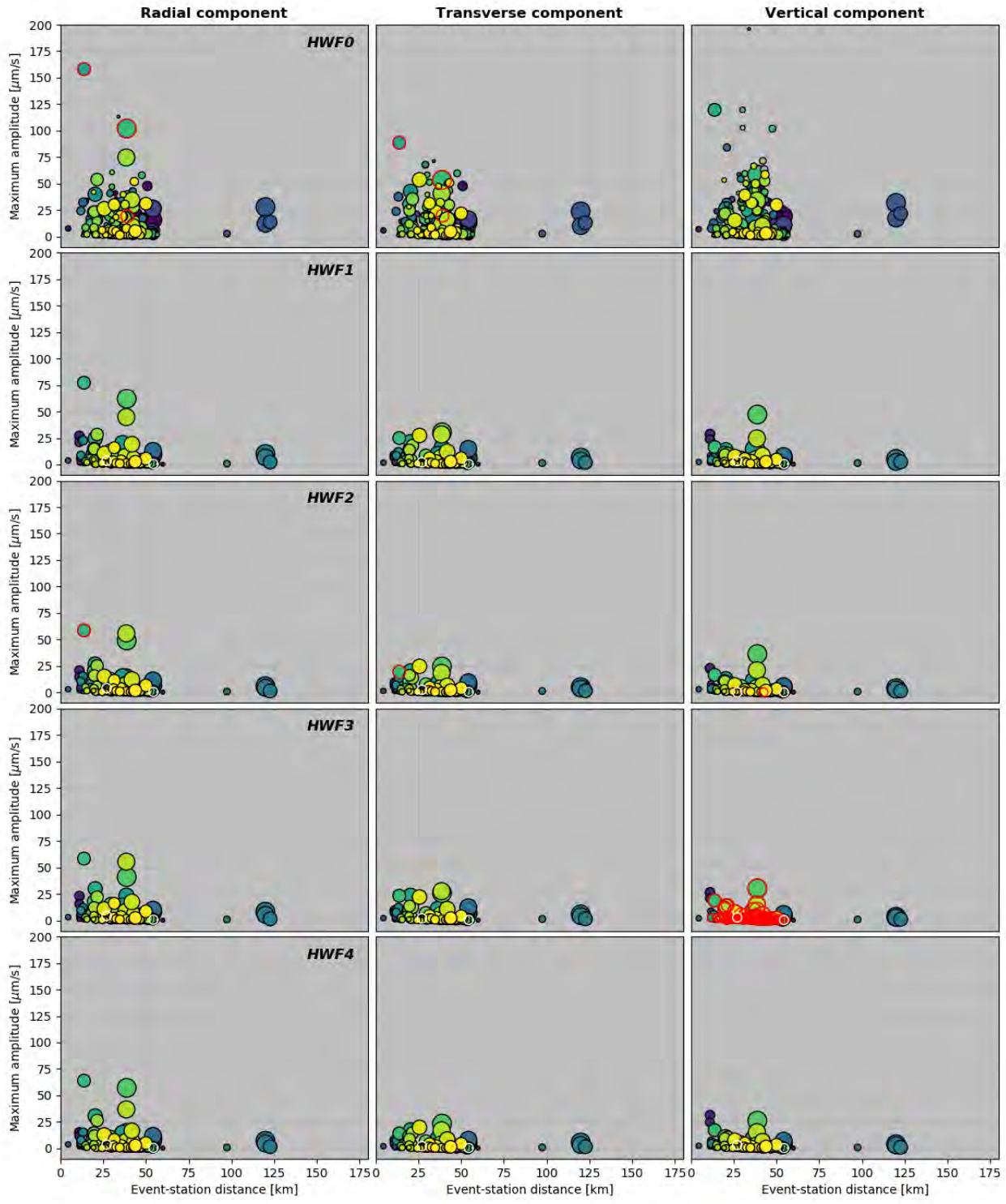

FIGURE B.45: Borehole station HWF: columns correspond to radial, transversal and vertical component, rows to levels 0 to 4

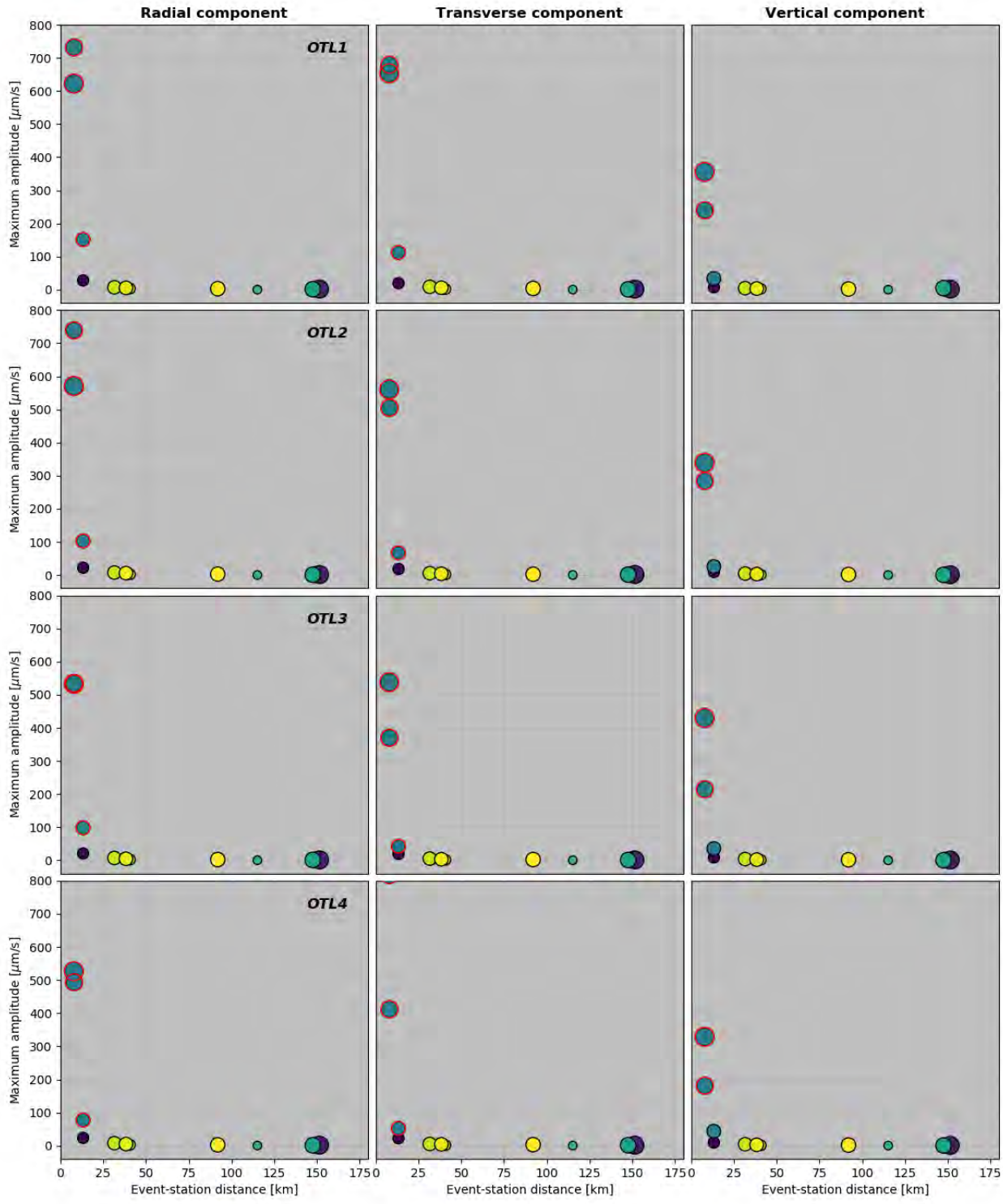

FIGURE B.46: Borehole station OTL: columns correspond to radial, transversal and vertical component, rows to levels 1 to 4

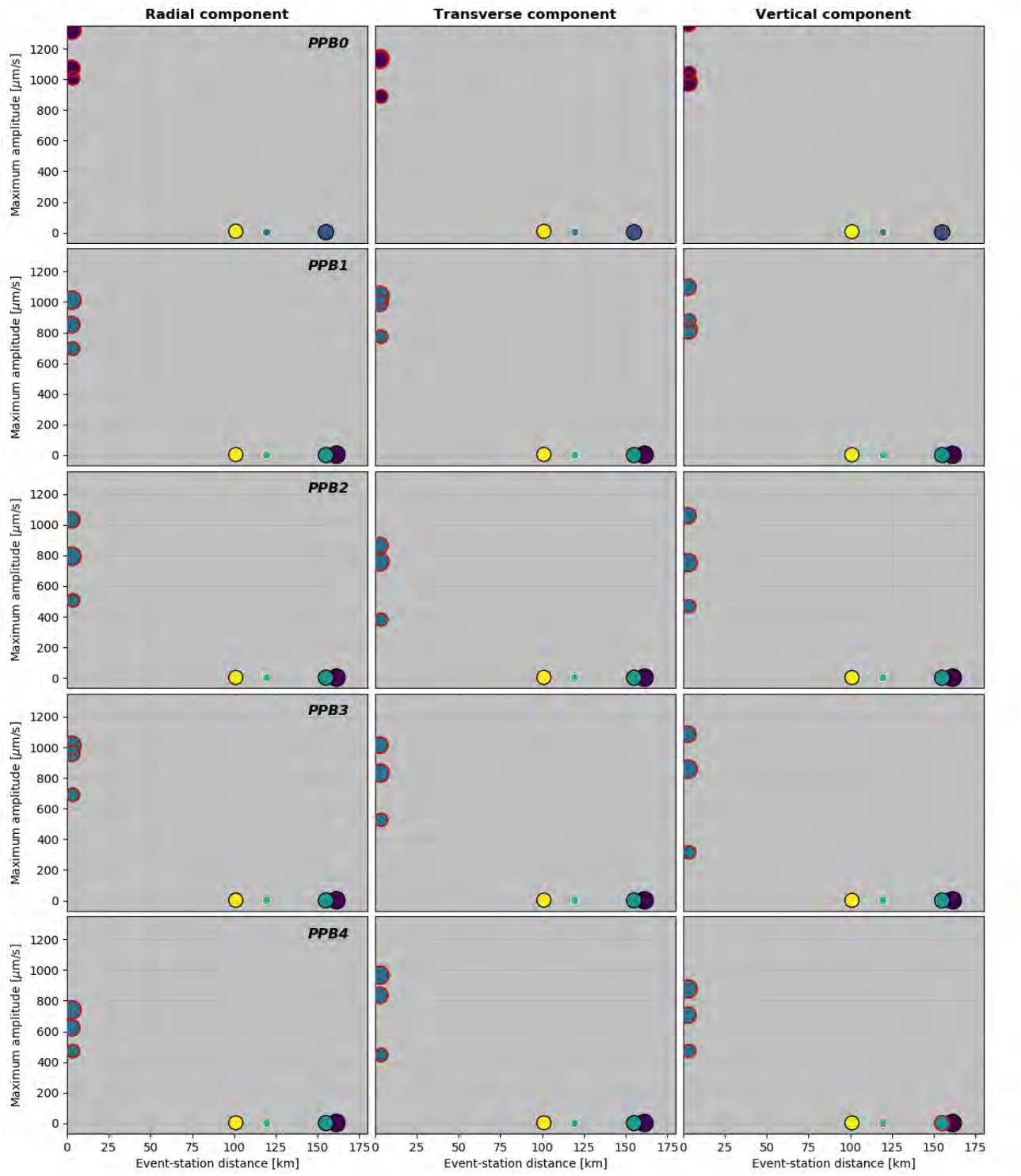

FIGURE B.47: Borehole station PPB: columns correspond to radial, transversal and vertical component, rows to levels 0 to 4

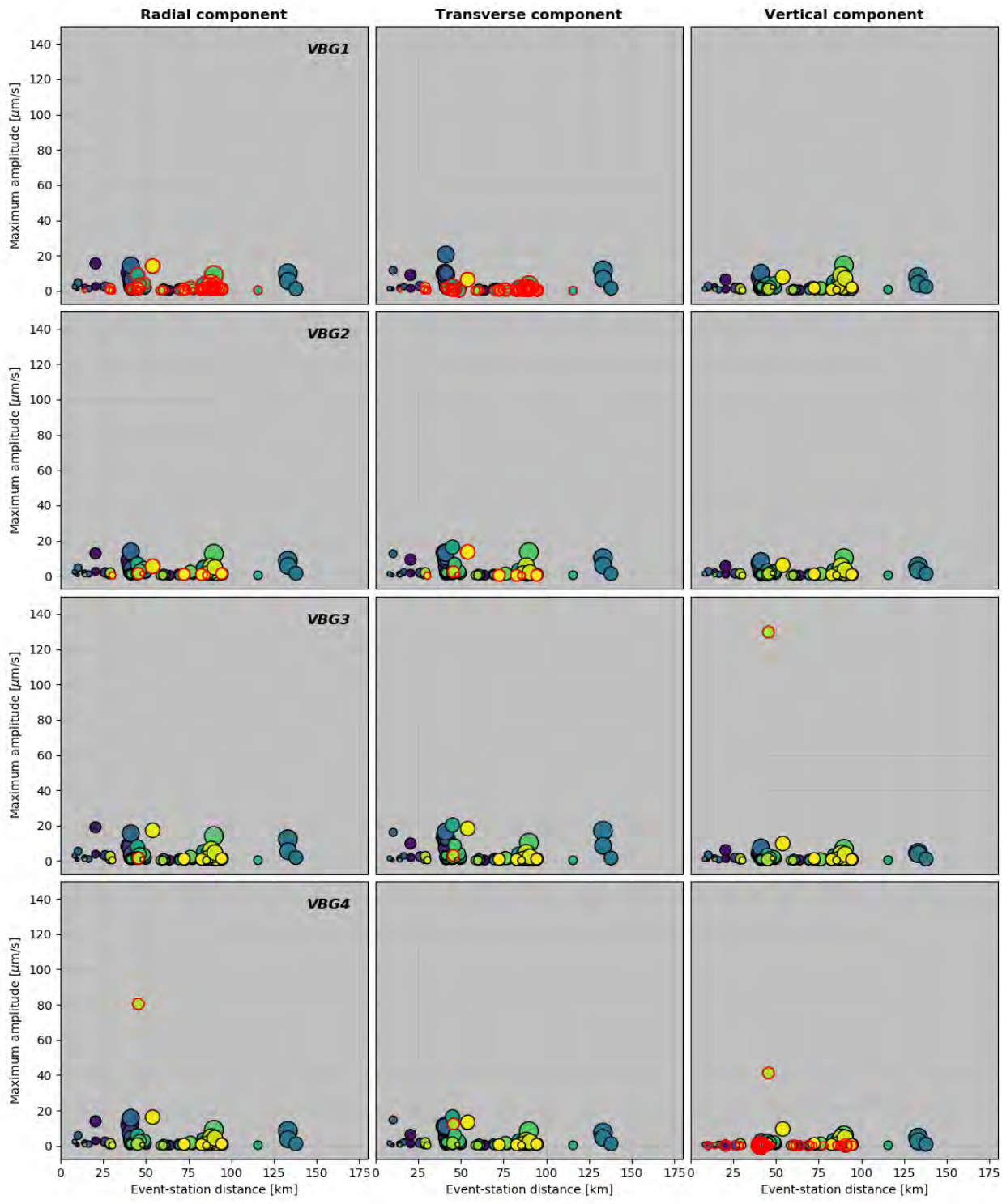

FIGURE B.48: Borehole station VBG: columns correspond to radial, transversal and vertical component, rows to levels 1 to 4

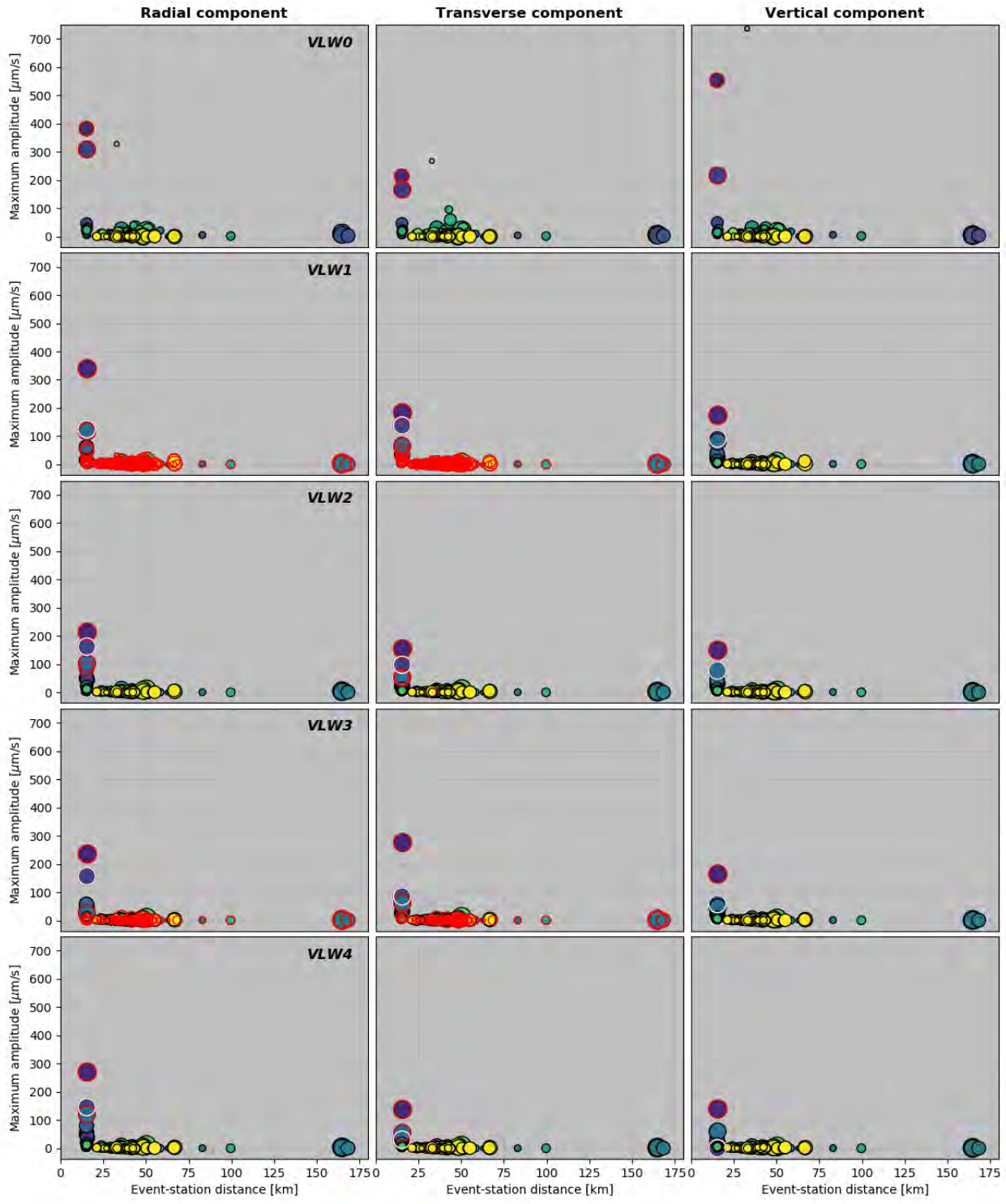

FIGURE B.49: Borehole station VLW: columns correspond to radial, transversal and vertical component, rows to levels 0 to 4

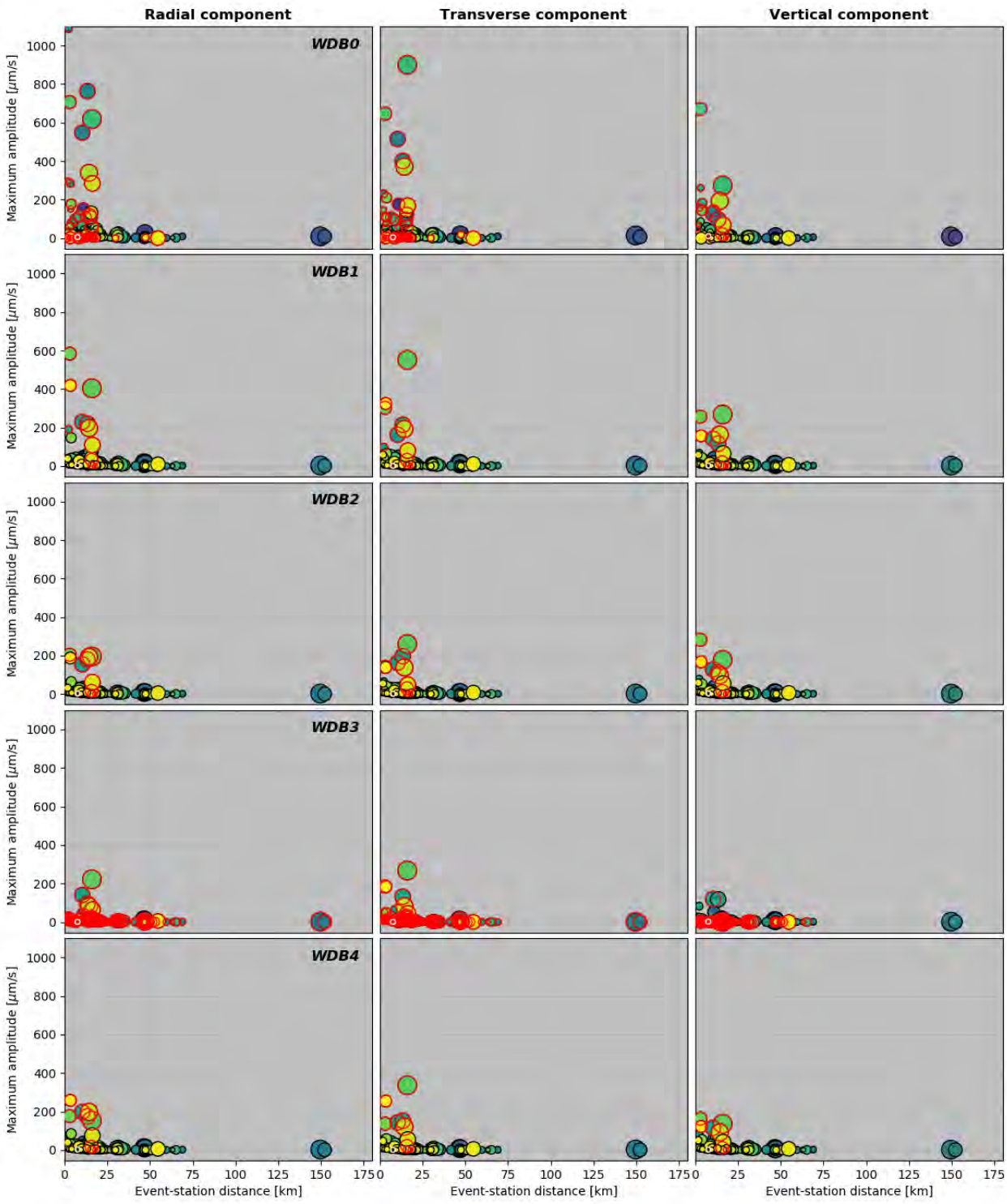

FIGURE B.50: Borehole station WDB: columns correspond to radial, transversal and vertical component, rows to levels 0 to 4

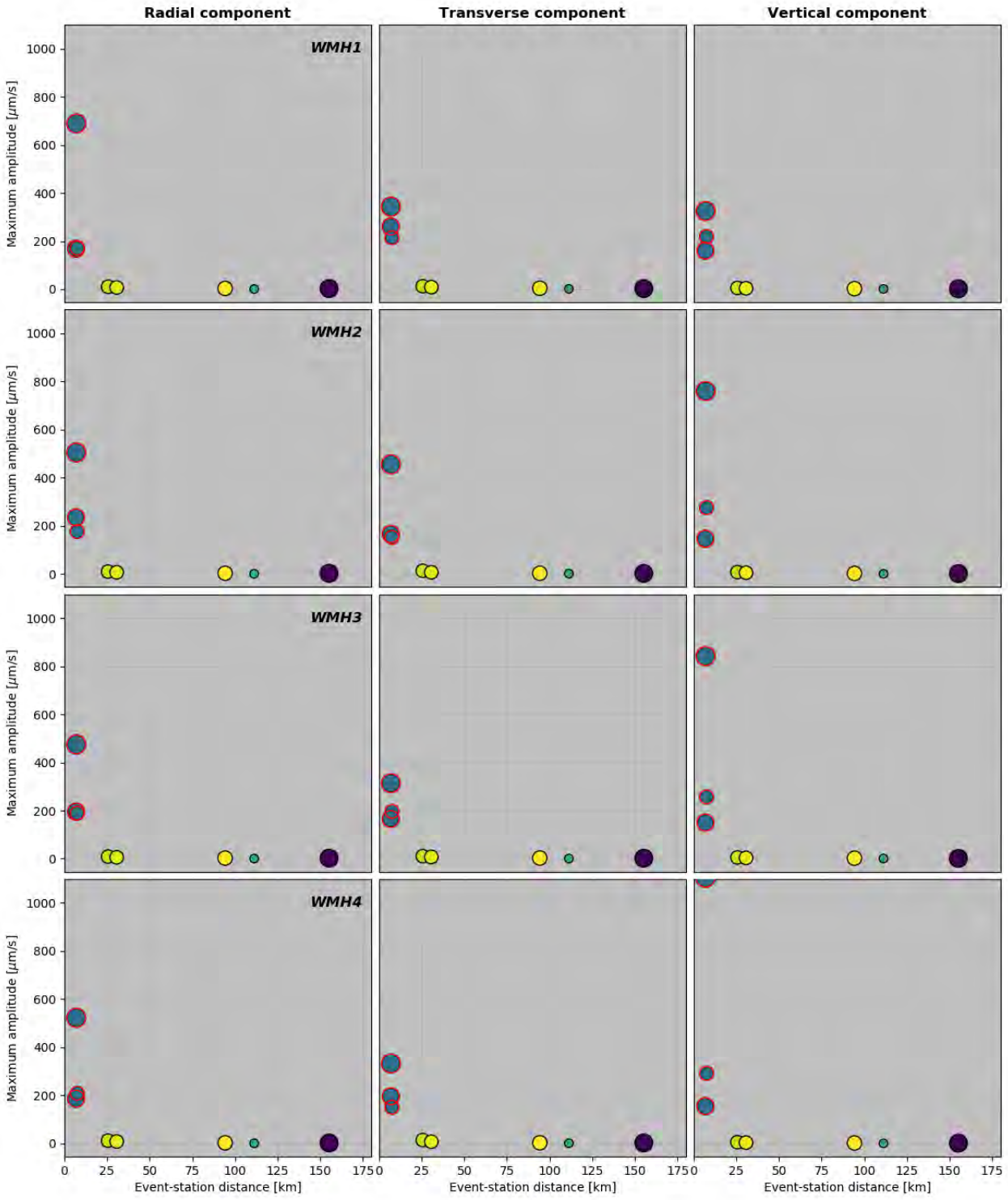

FIGURE B.51: Borehole station WMH: columns correspond to radial, transversal and vertical component, rows to levels 1 to 4

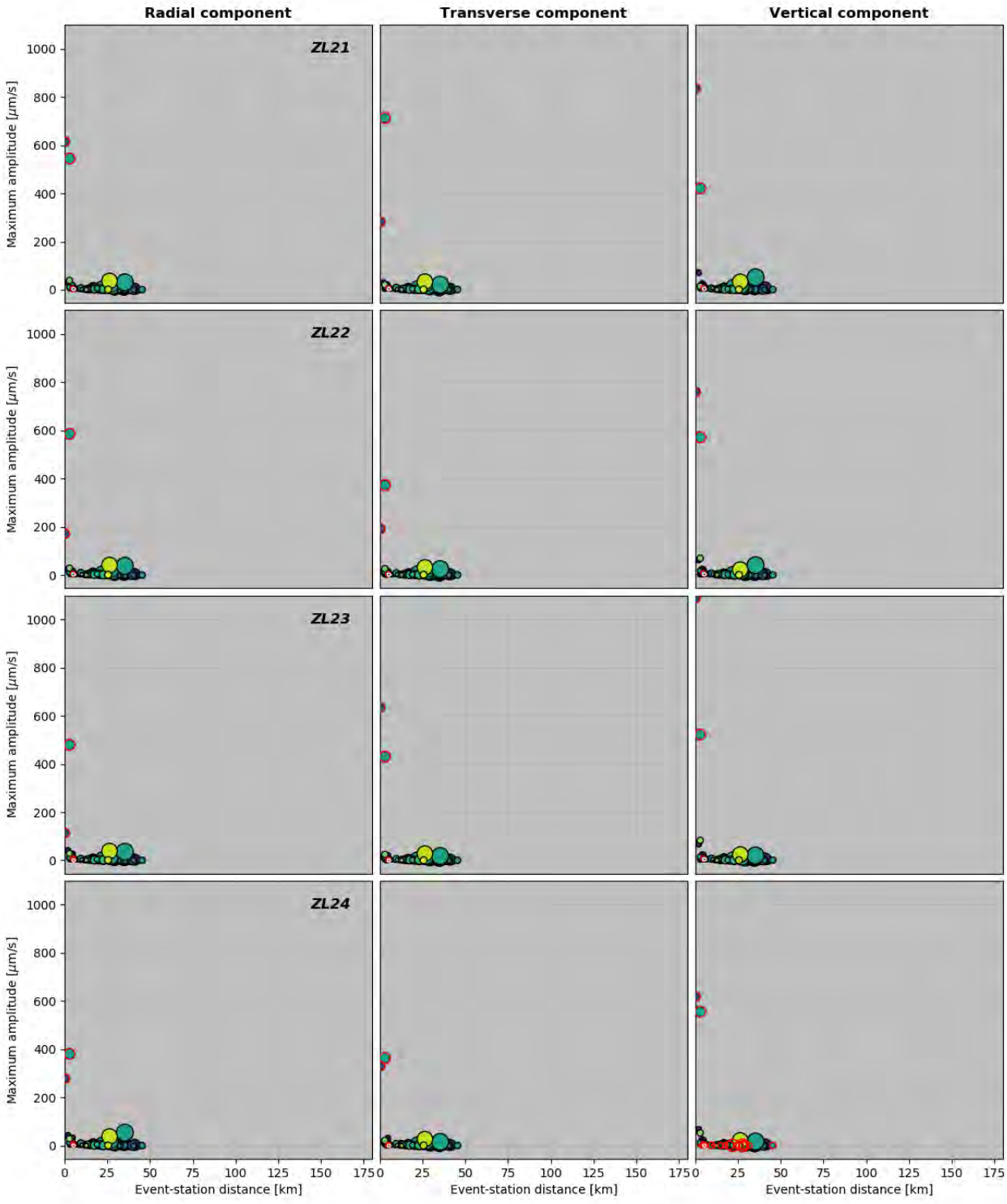

FIGURE B.52: Borehole station ZL2: columns correspond to radial, transversal and vertical component, rows to levels 1 to 4

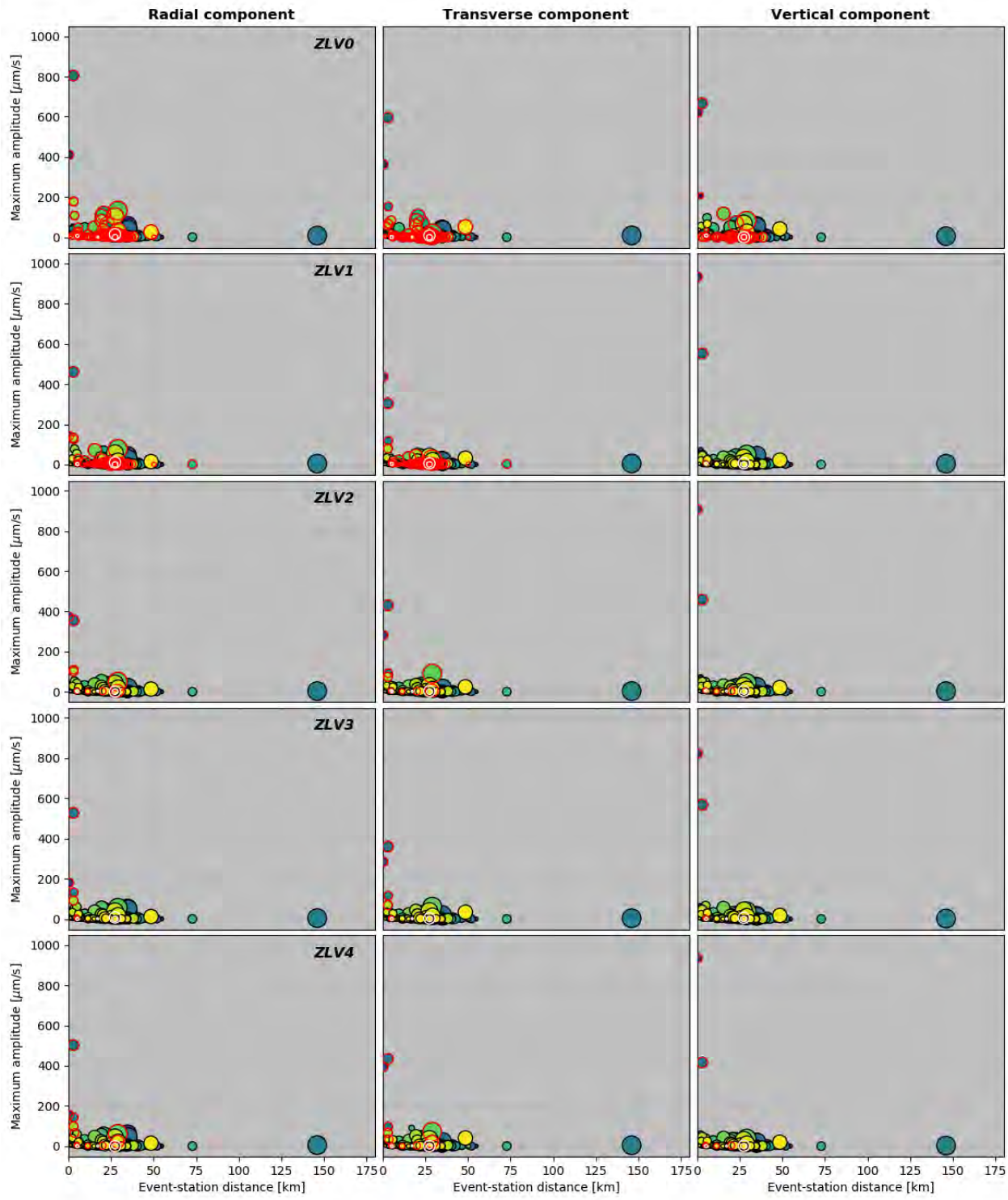

FIGURE B.53: Borehole station ZLV: columns correspond to radial, transversal and vertical component, rows to levels 0 to 4

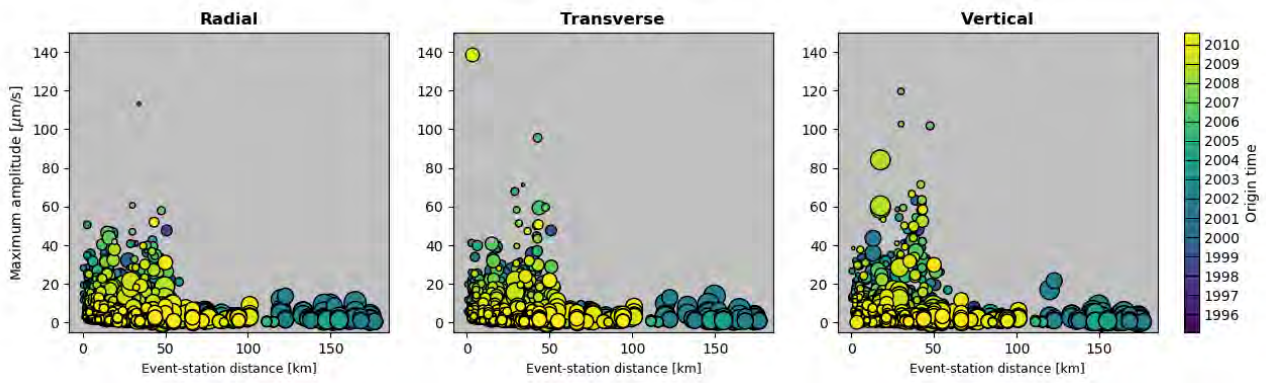

FIGURE B.54: Maximum amplitudes in μm/s as a function of distance for all records on (a) the radial, (b) the transverse and (c) the vertical components after saturated and malfunctioning records were removed.

B.7 Borehole RMS amplitudes as a function of time at all stations and levels

Each figure shows the RMS amplitudes measured on each individual record (by station, level and component) over time.

Data were instrument-corrected and bandpass-filtered in the frequency range from 2 to 50 Hz. Data are not rotated, therefore we refer to the horizontal components as pseudo-North and pseudo-East.

Circles are coloured by event origin time and their size is proportional to the noise window length, which was automatically selected from the start of the record to 0.1 s before the theoretical P-wave arrival time.

In addition, saturated records and malfunctioning components as reported in section 5.2.4 and appendices F & G of Dost et al. (2022) are highlighted as red- and white-bordered circles, respectively.

Events belonging to files containing multiple events are symbolised by white crosses. Since the extraction of the RMS amplitude was performed automatically, the RMS amplitude of the second event in the file will fall within the time span of the first event. For that reason, it might be biased and abnormally high.

Horizontal dashed lines represent the 95% percentile of RMS amplitudes, the threshold above which outliers can be defined.

B.7.1 Results

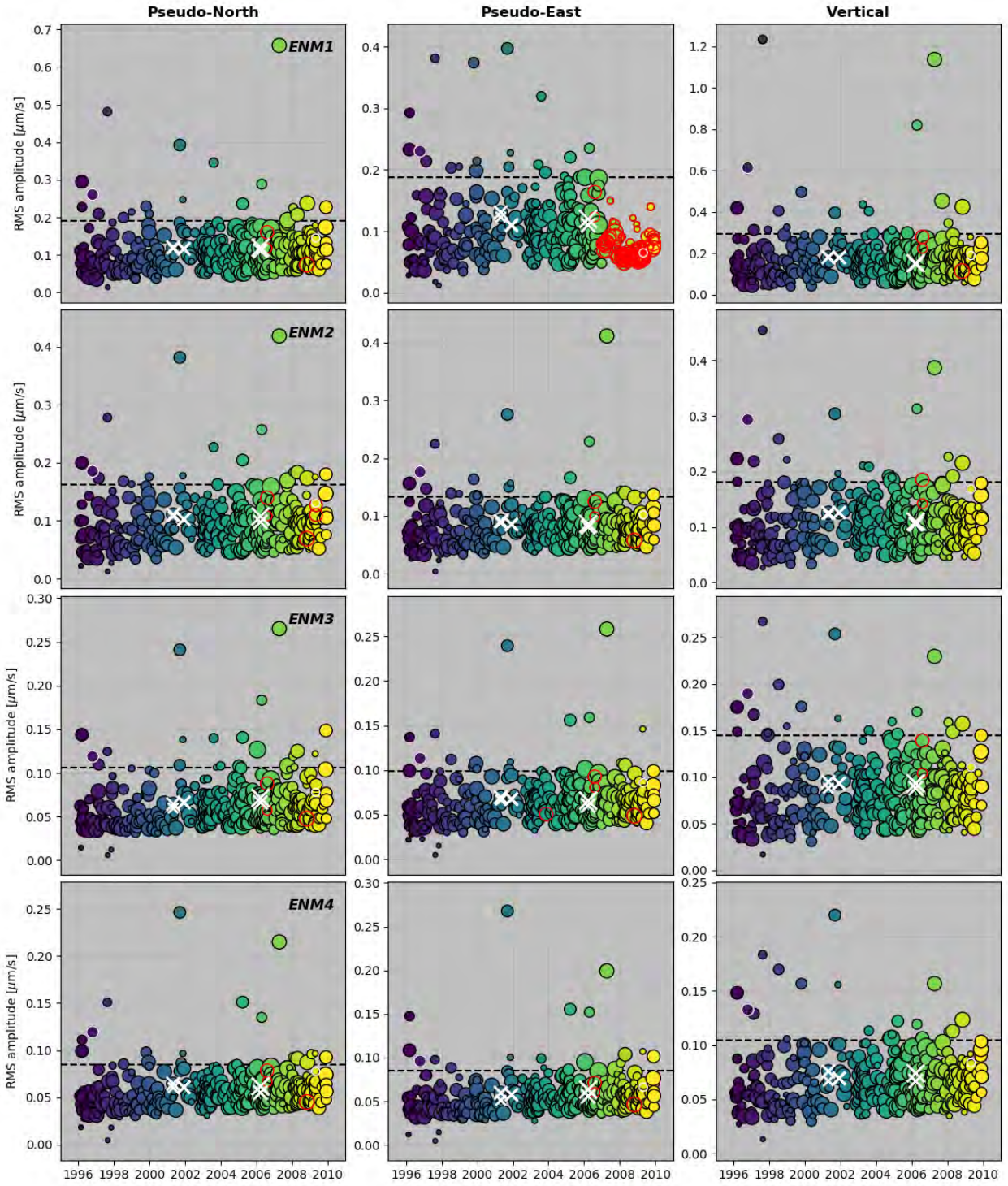

FIGURE B.55: Borehole station ENM: columns correspond to pseudo-North, pseudo-East and vertical components, rows to levels 1 to 4

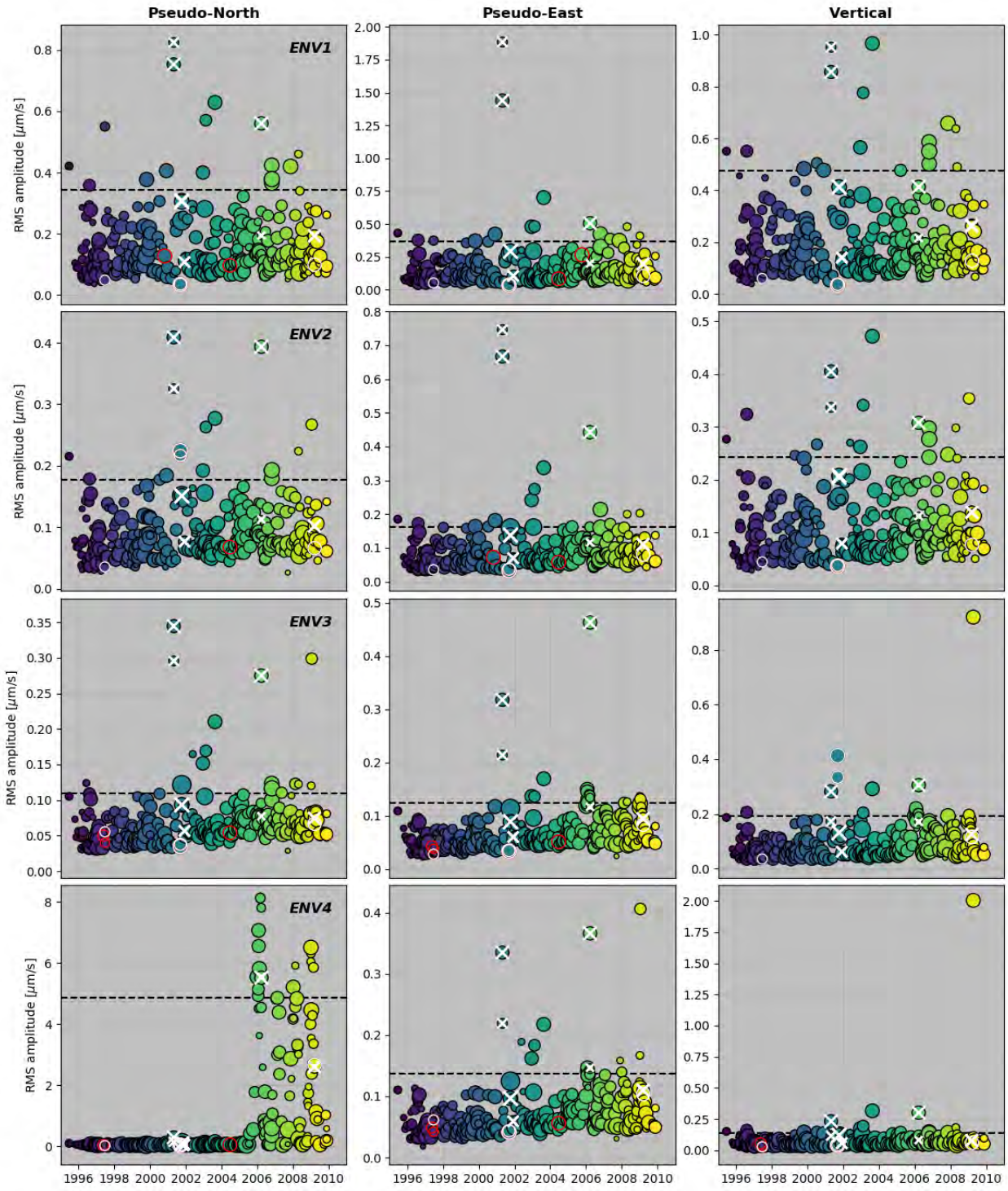

FIGURE B.56: Borehole station ENV: columns correspond to pseudo-North, pseudo-East and vertical components, rows to levels 1 to 4

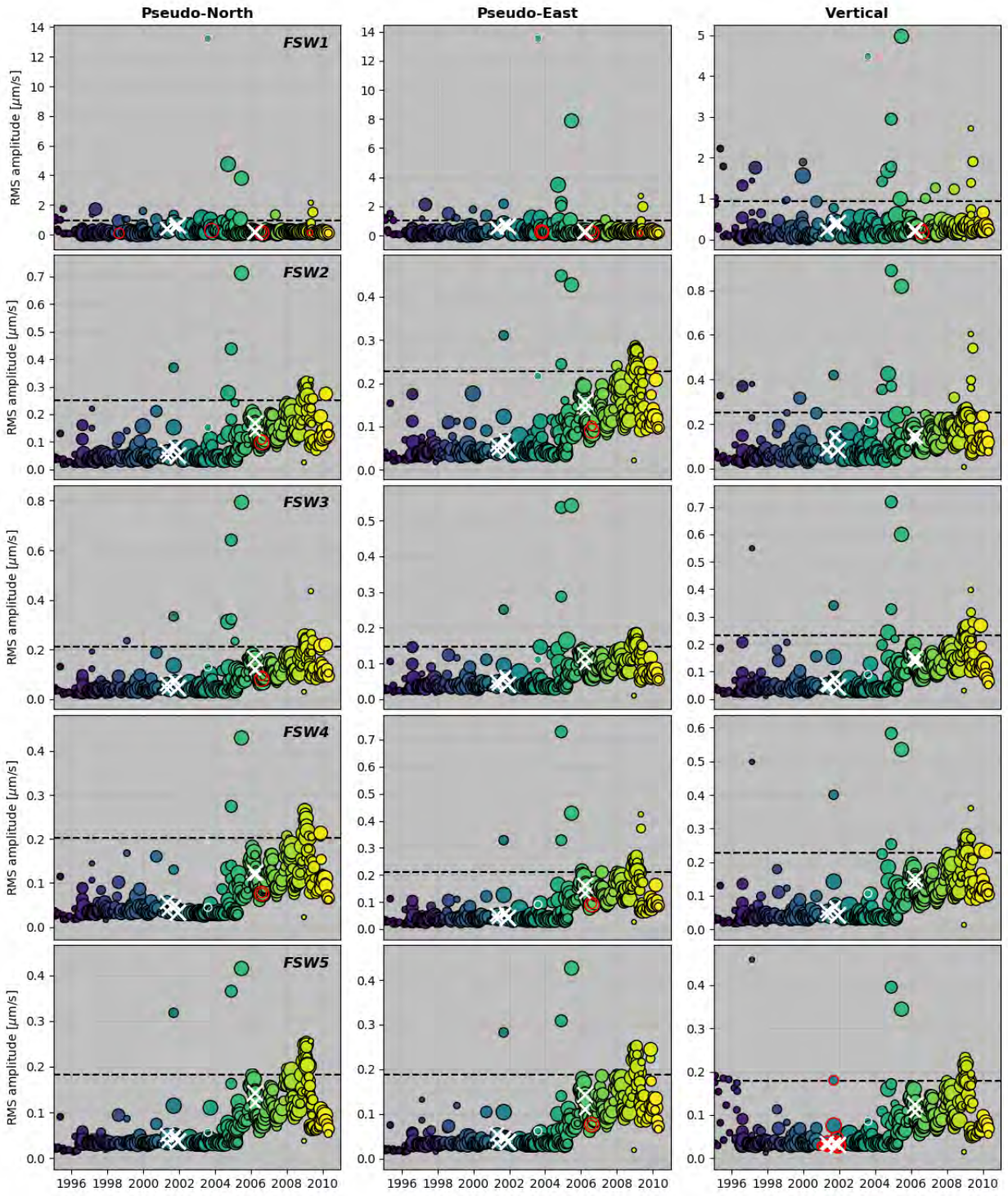

FIGURE B.57: Borehole station FSW: columns correspond to pseudo-North, pseudo-East and vertical components, rows to levels 1 to 5

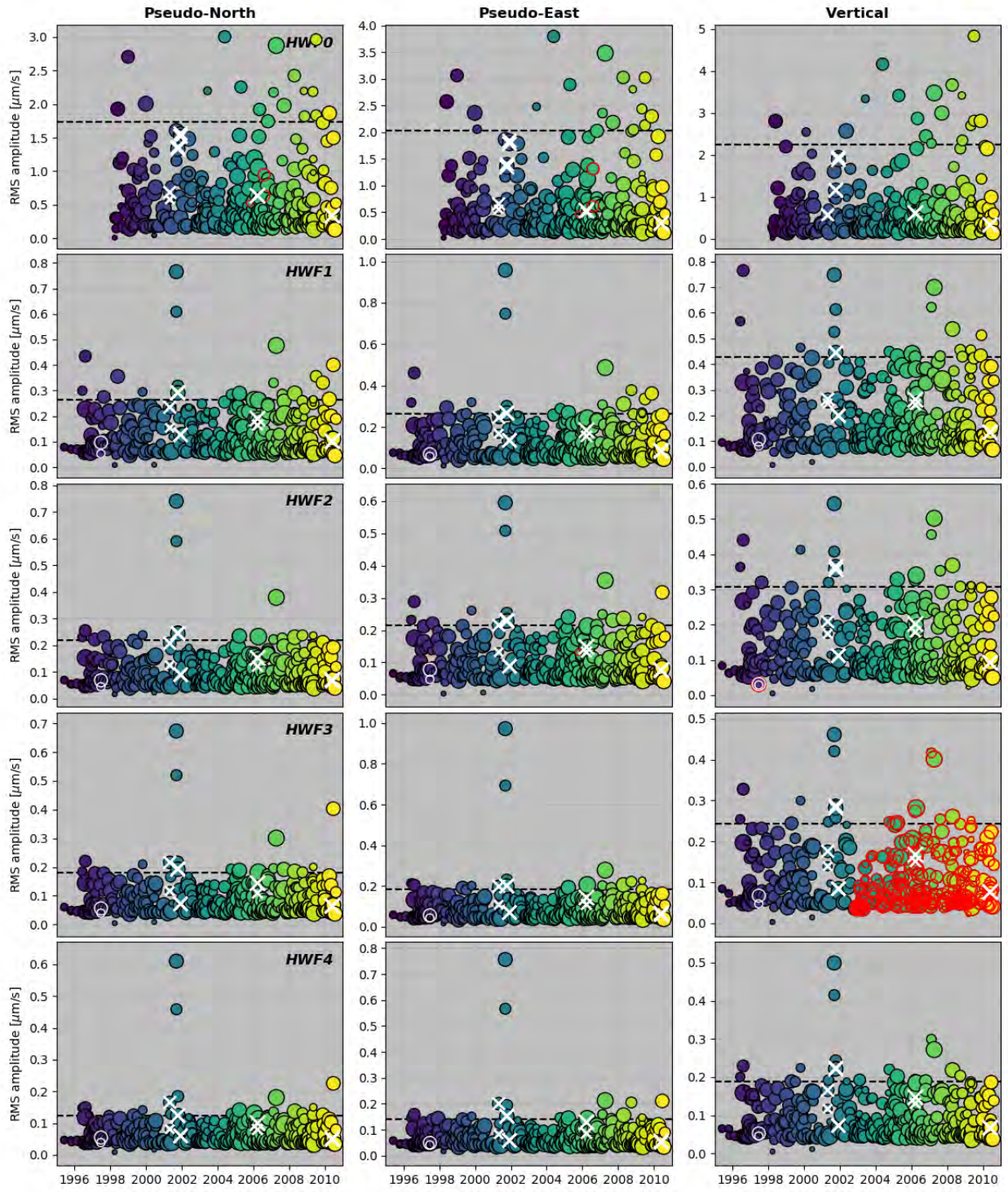

FIGURE B.58: Borehole station HWF: columns correspond to pseudo-North, pseudo-East and vertical components, rows to levels 0 to 4

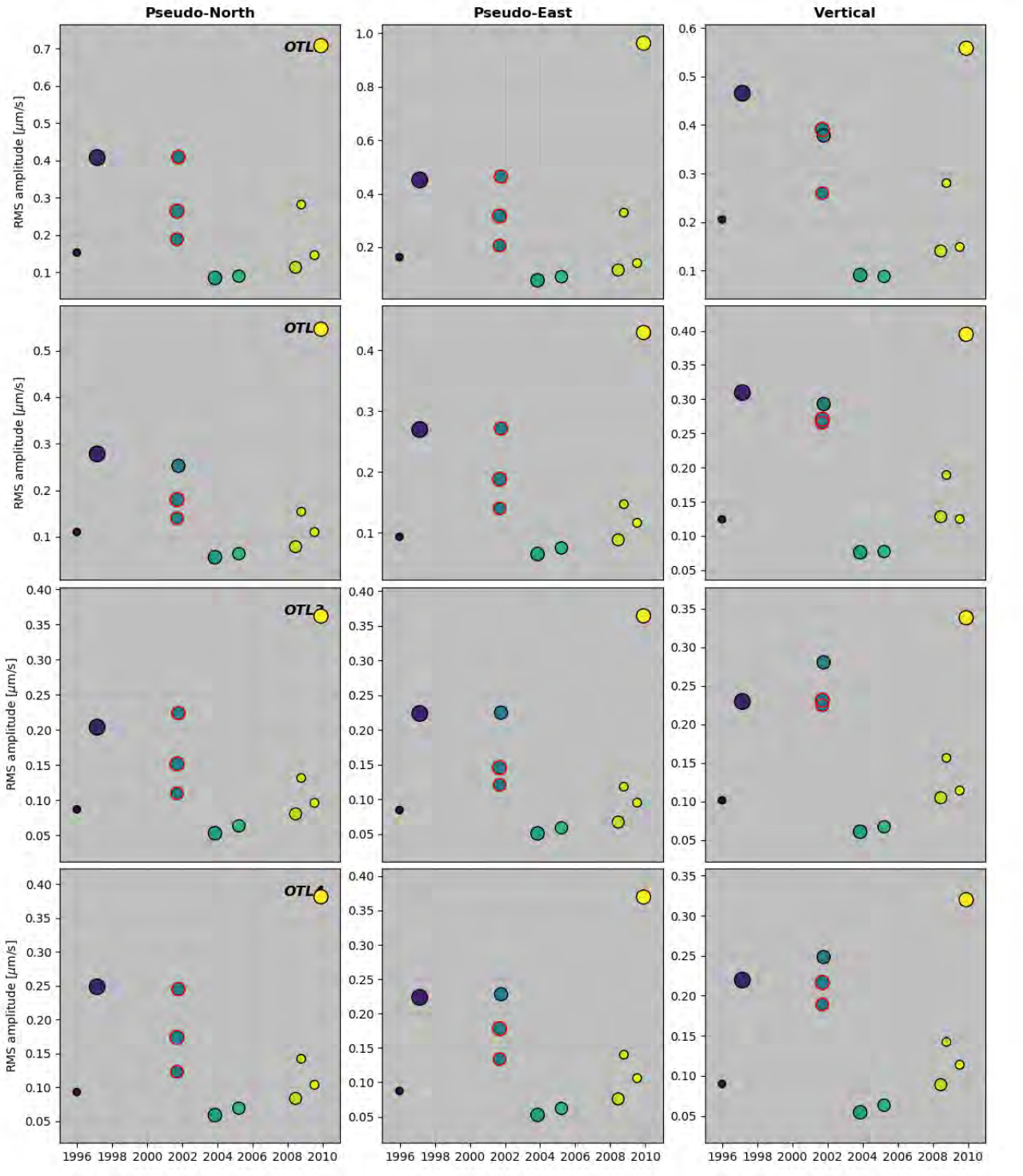

FIGURE B.59: Borehole station OTL: columns correspond to pseudo-North, pseudo-East and vertical components, rows to levels 1 to 4

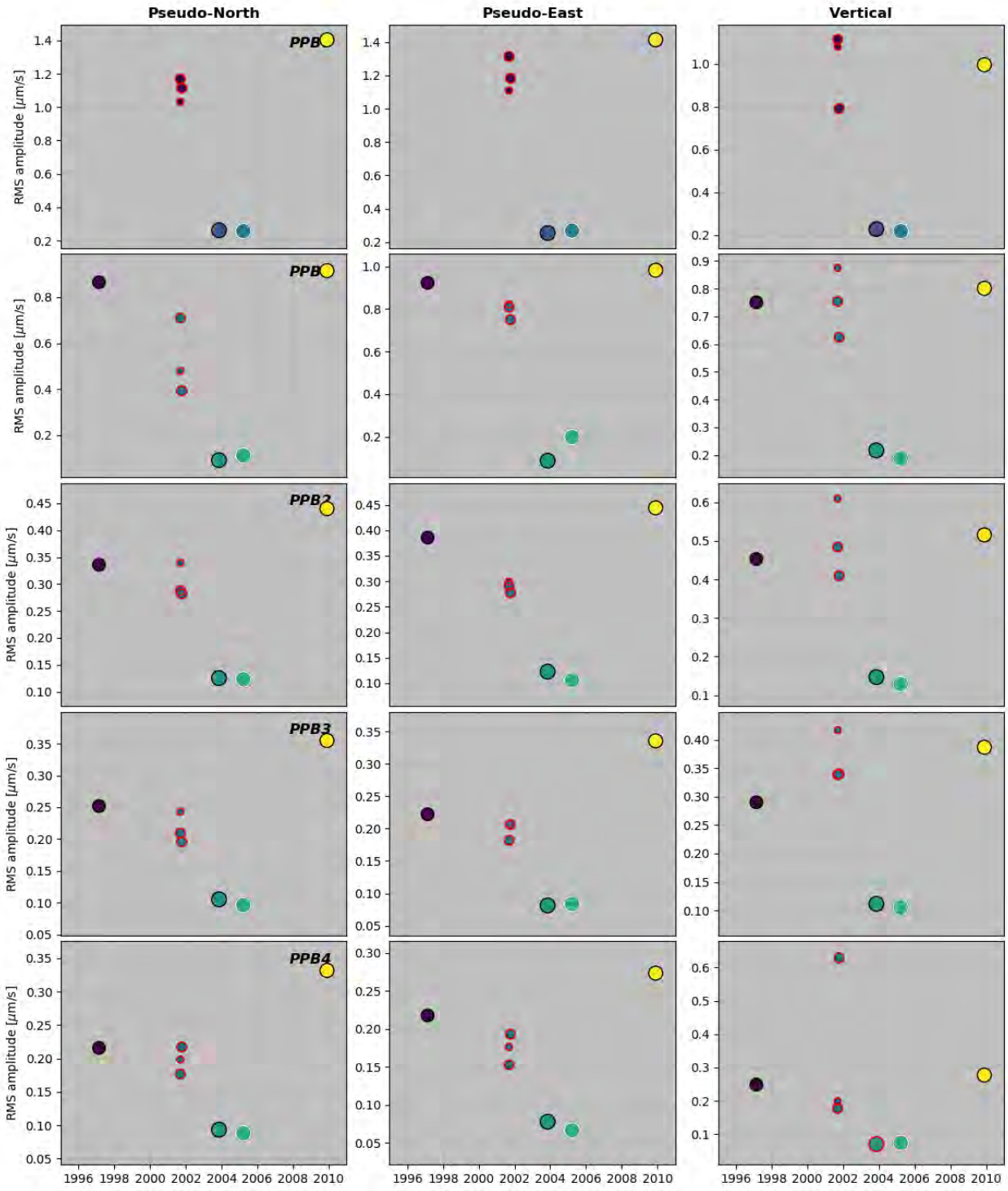

FIGURE B.60: Borehole station PPB: columns correspond to pseudo-North, pseudo-East and vertical components, rows to levels 0 to 4

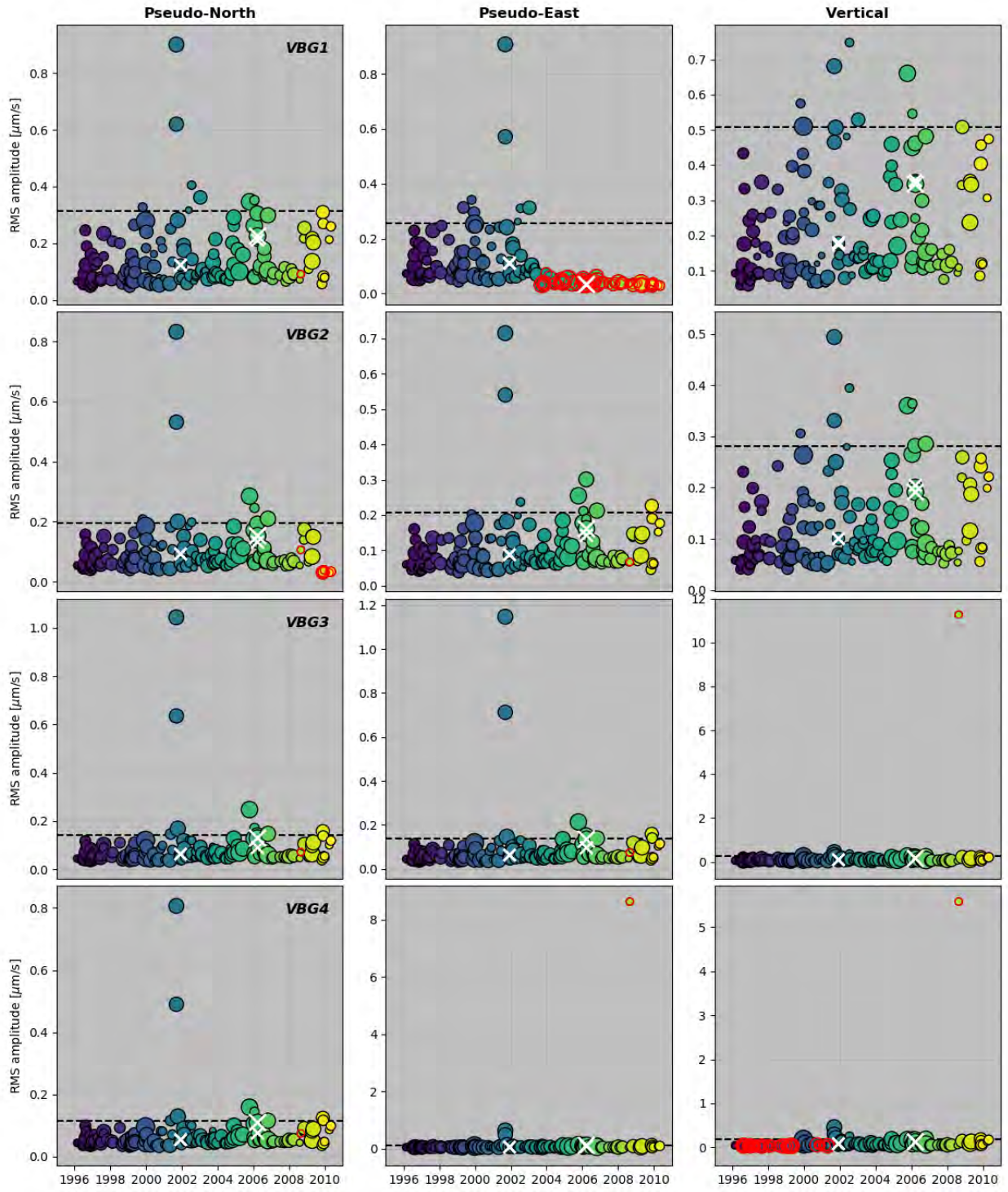

FIGURE B.61: Borehole station VBG: columns correspond to pseudo-North, pseudo-East and vertical components, rows to levels 1 to 4

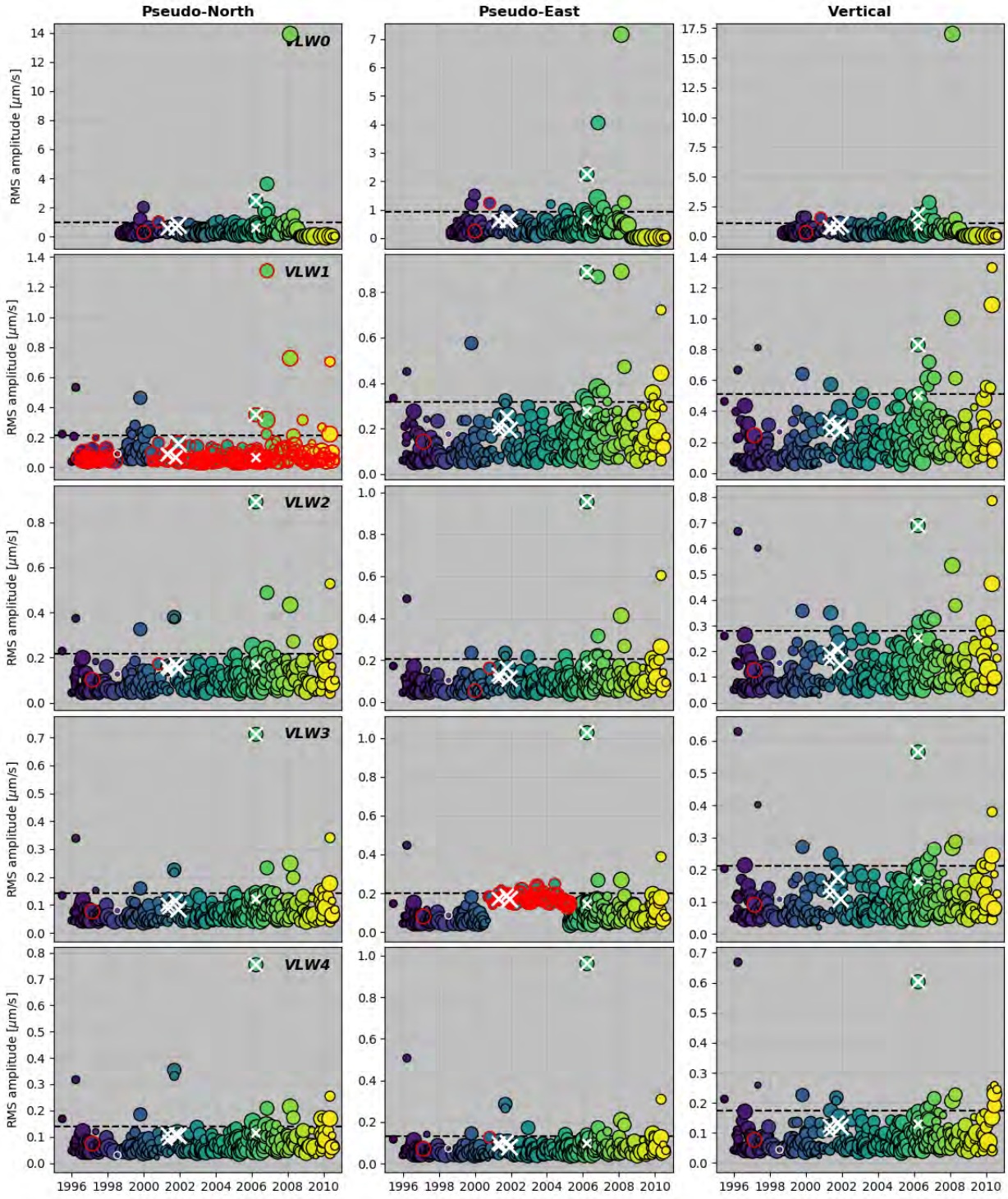

FIGURE B.62: Borehole station VLW: columns correspond to pseudo-North, pseudo-East and vertical components, rows to levels 0 to 4

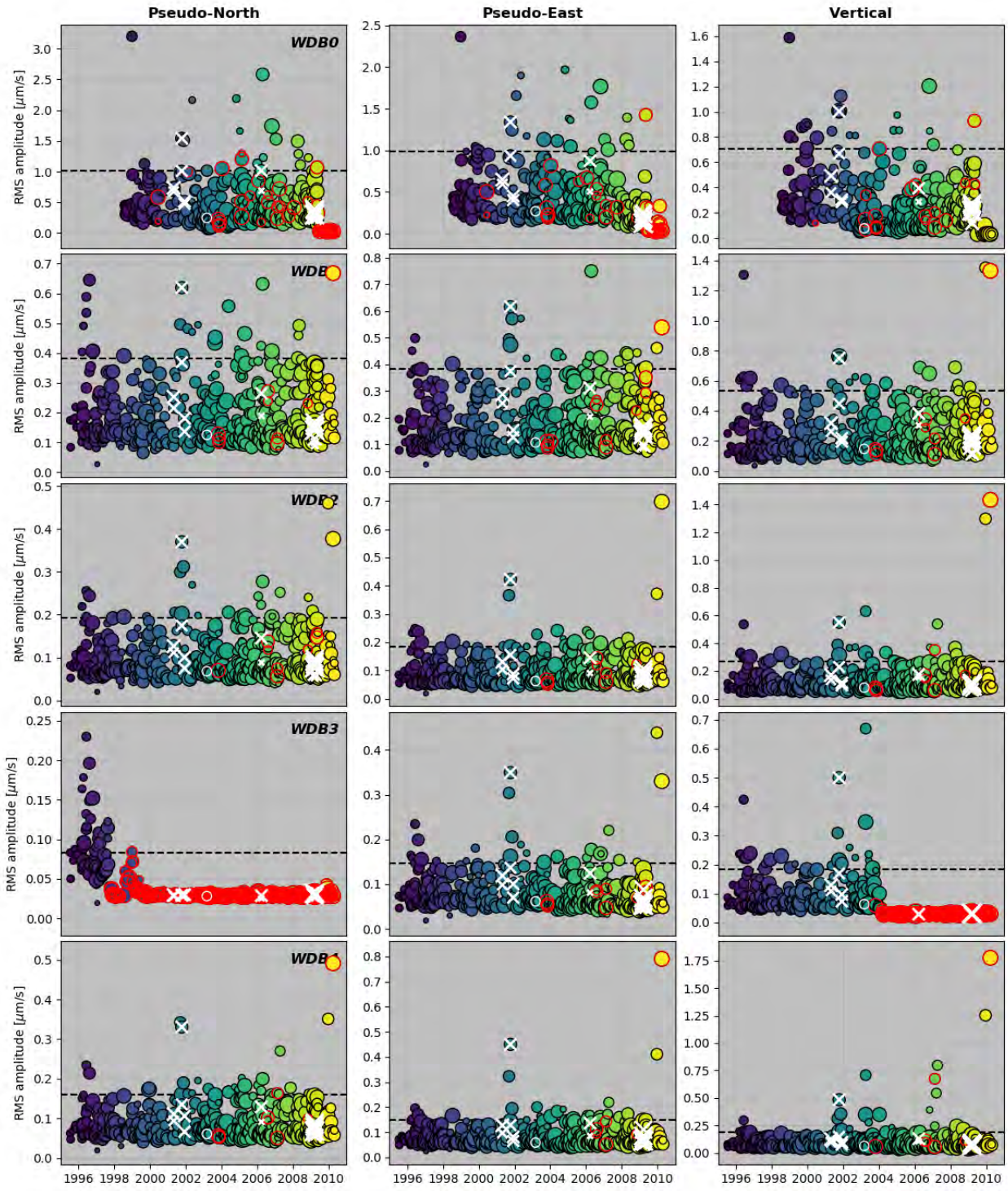

FIGURE B.63: Borehole station WDB: columns correspond to pseudo-North, pseudo-East and vertical components, rows to levels 0 to 4

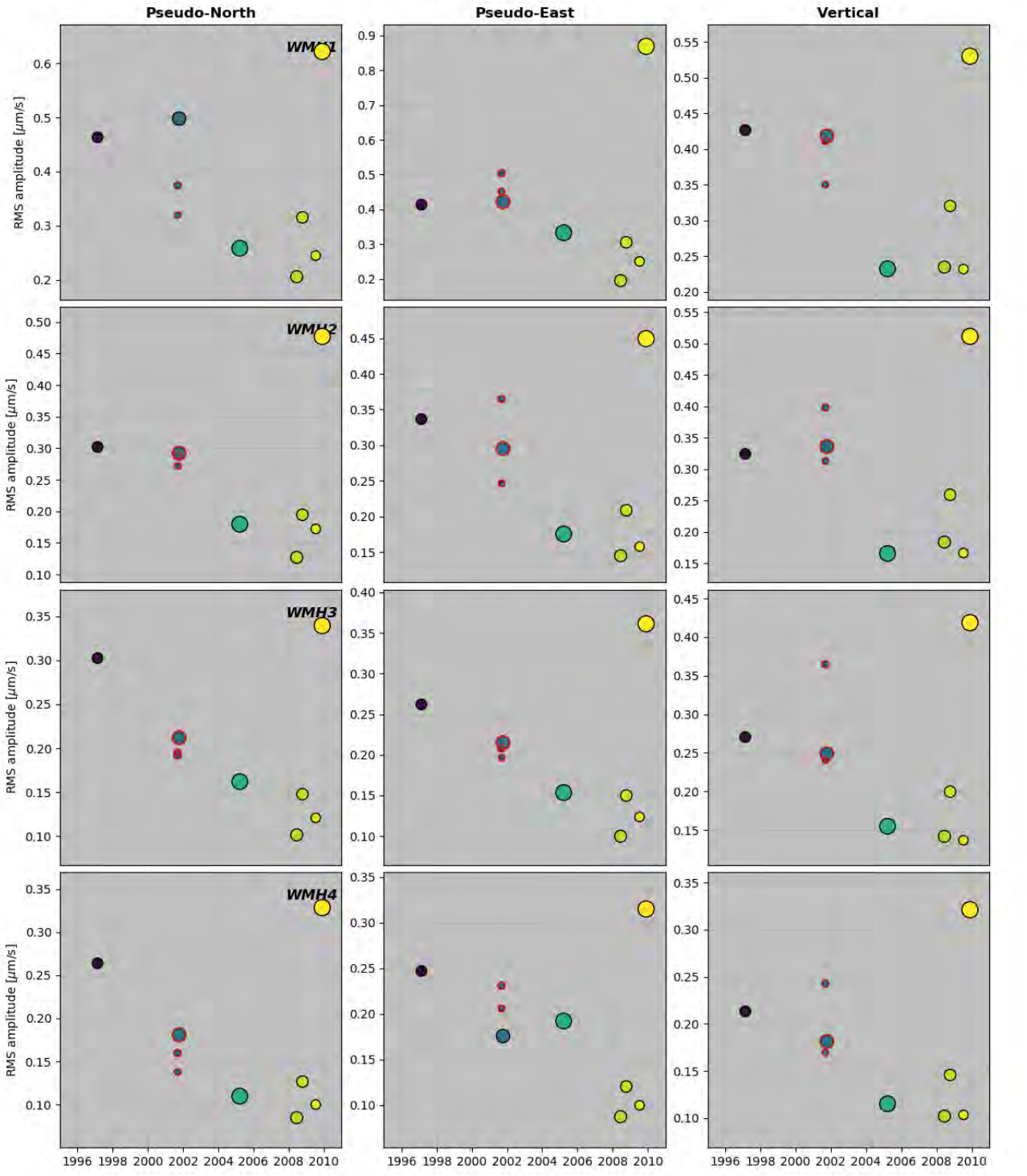

FIGURE B.64: Borehole station WMH: columns correspond to pseudo-North, pseudo-East and vertical components, rows to levels 1 to 4

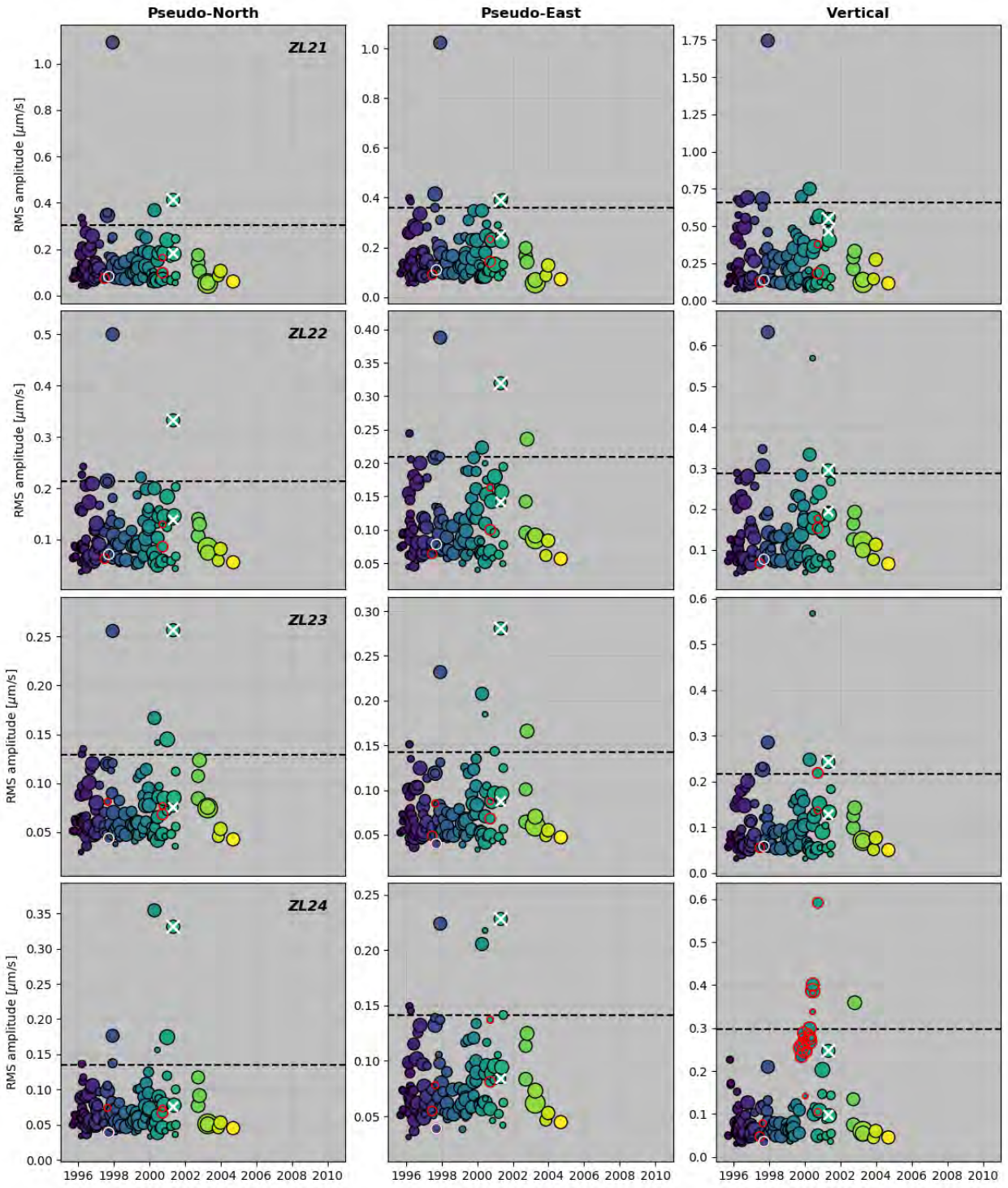

FIGURE B.65: Borehole station ZL2: columns correspond to pseudo-North, pseudo-East and vertical components, rows to levels 1 to 4

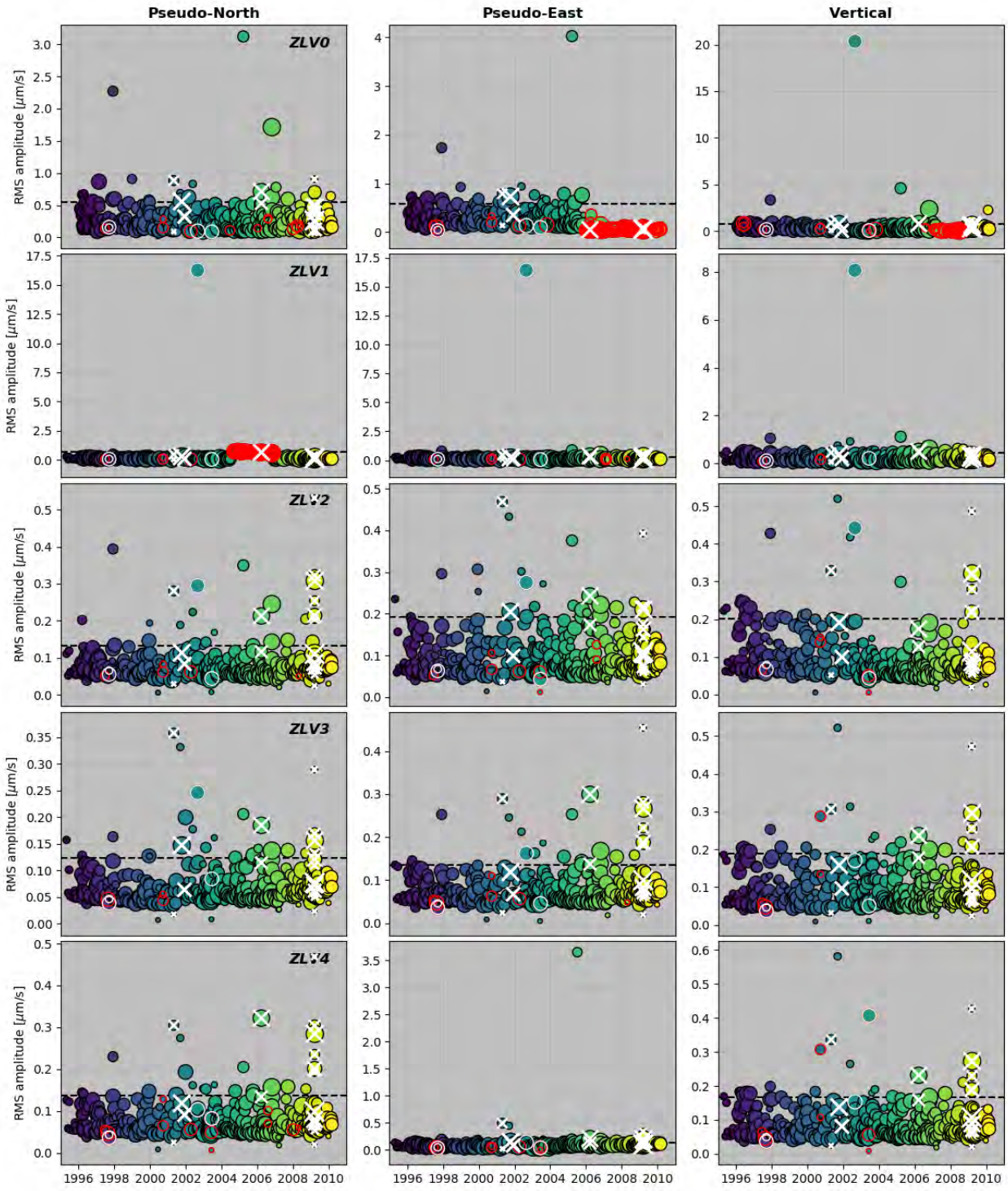

FIGURE B.66: Borehole station ZLV: columns correspond to pseudo-North, pseudo-East and vertical components, rows to levels 0 to 4

B.7.2 Examples of outliers

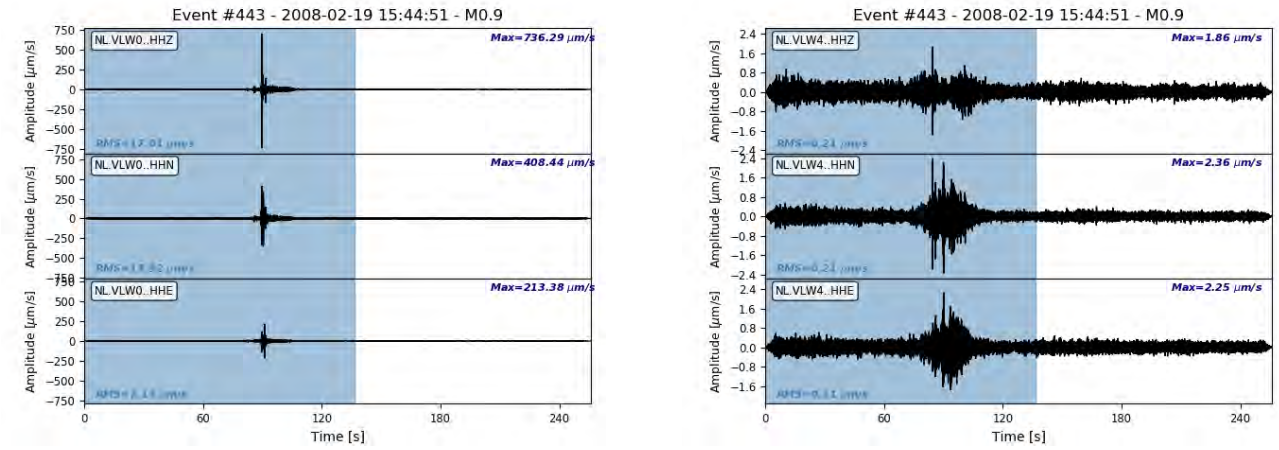

(a) VLW0 (b) VLW4

FIGURE B.67: Three-component records of the 19th February, 2008 event recorded on VLW. Time on the x-axis represents seconds from the record start time. The blue-shaded area corresponds to the window used to compute the RMS amplitude and includes a very strong signal, which occurs before the event origin time. Since its amplitude increases on shallower geophones, it suggests that the signal originates from the surface.

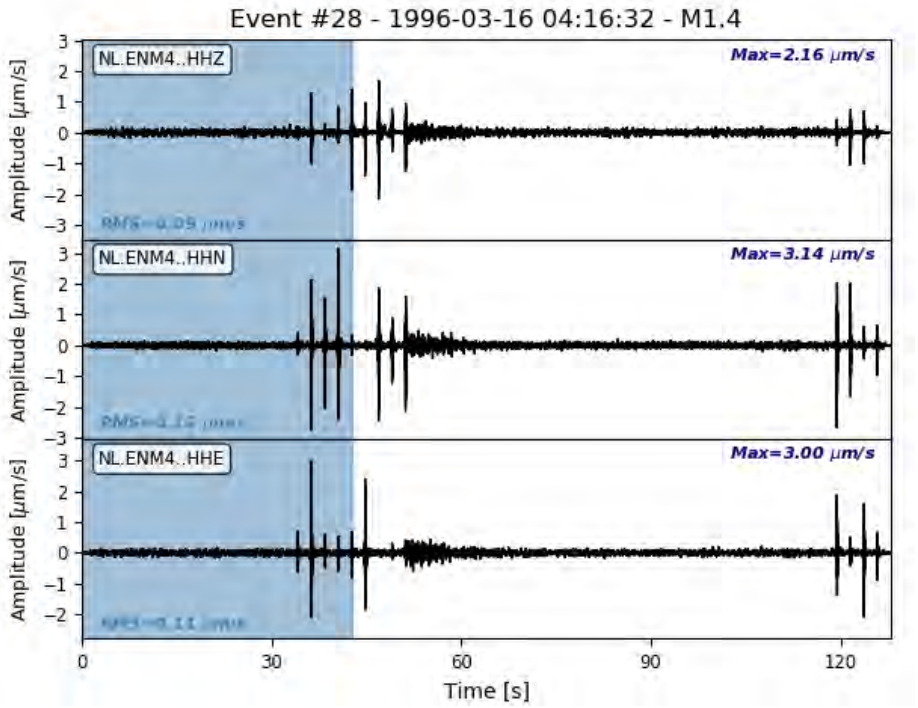

FIGURE B.68: Three-component waveform records of the 16th March, 1996 event recorded on ENM4. The blue-shaded area represents the window within which the RMS amplitude has been measured.

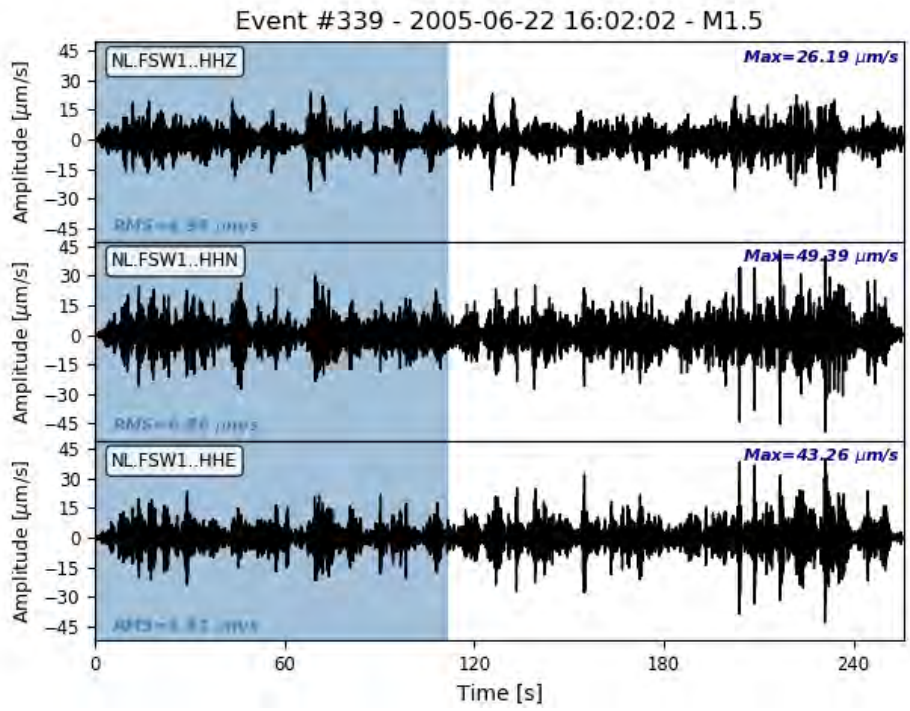

FIGURE B.69: Three-component waveform records of the 22nd June, 2005 event recorded on FSW1. The blue-shaded area represents the window within which the RMS amplitude has been measured.

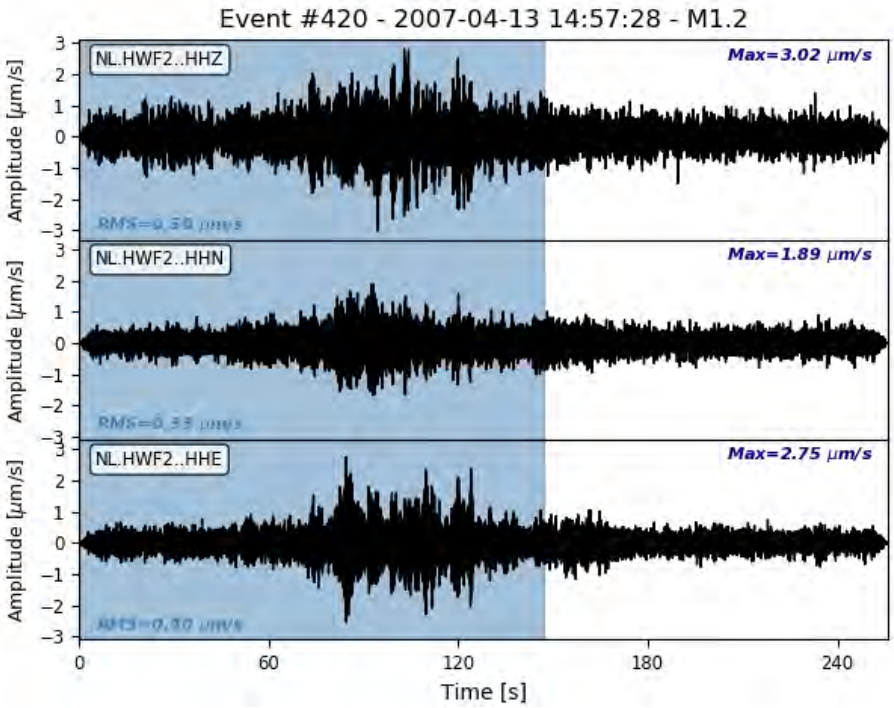

FIGURE B.70: Three-component waveform records of the 13th April, 2007 event recorded on HWF2. The blue-shaded area represents the window within which the RMS amplitude has been measured.

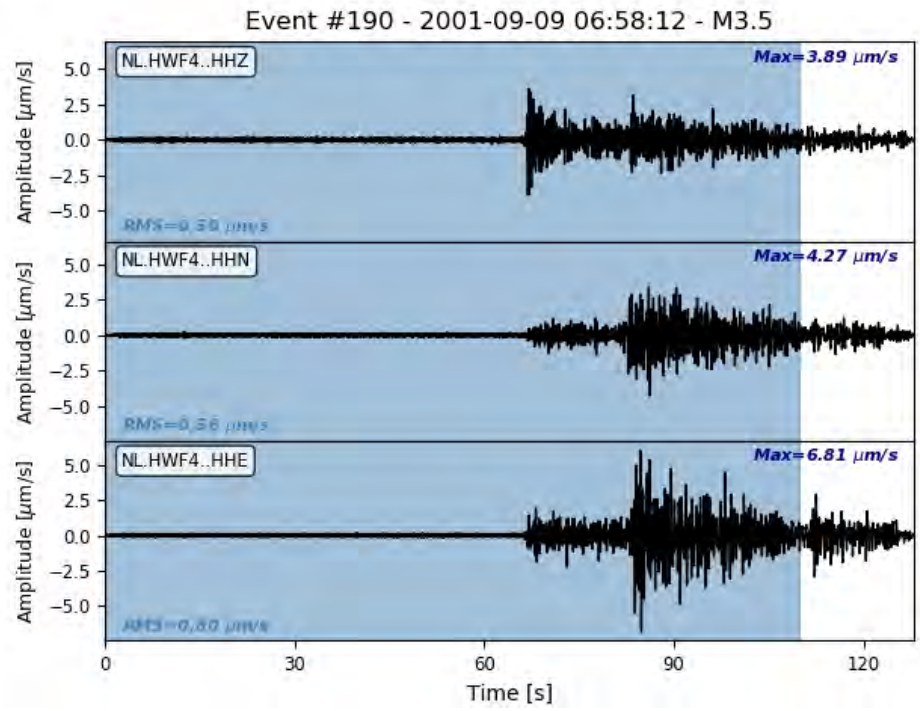

FIGURE B.71: Three-component waveform records of the 9th September, 2001 event recorded on HWF4. The blue-shaded area represents the window within which the RMS amplitude has been measured.

B.7.3 Results without outliers

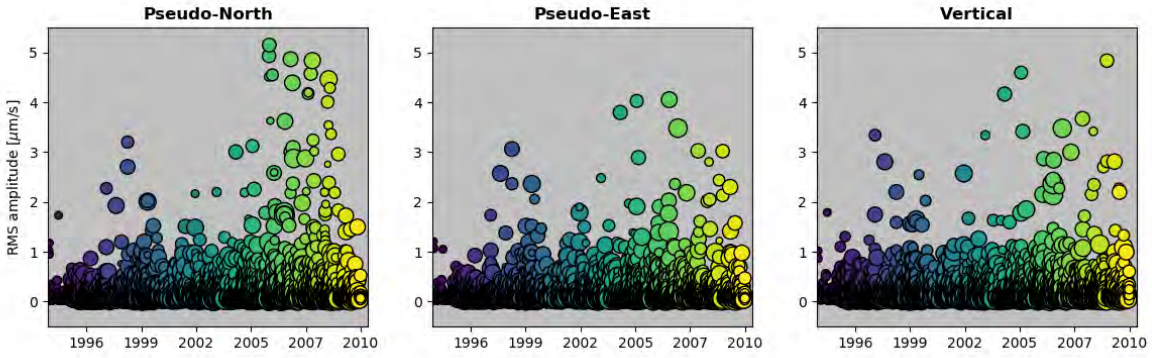

FIGURE B.72: RMS amplitudes in μm/s as a function of time for all records on the (a) pseudo-North, (b) pseudo-East and (c) vertical components. Circles are coloured by event origin time and their size is scaled by RMS window lengths. Outliers were removed.

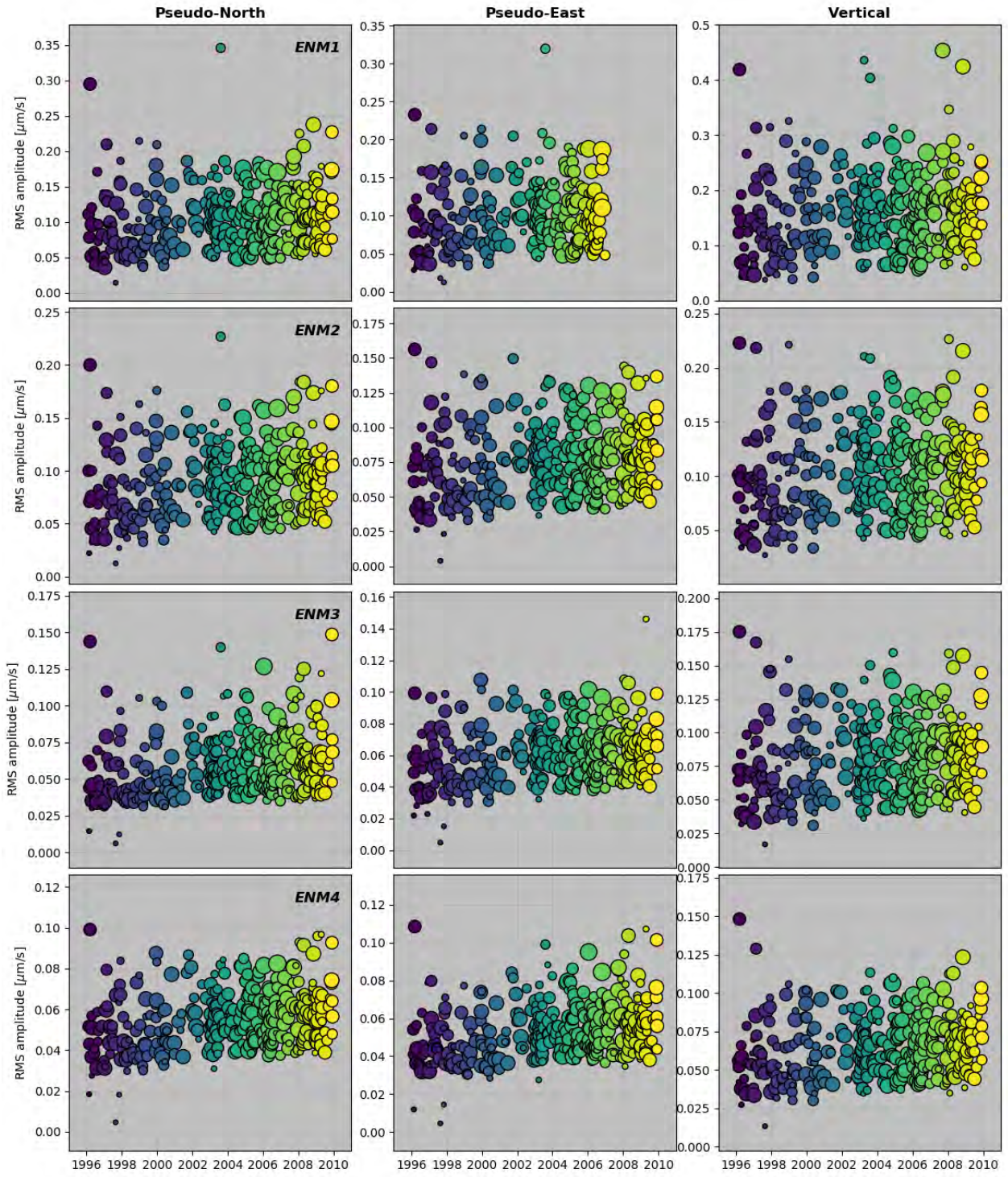

FIGURE B.73: ENM - outliers removed

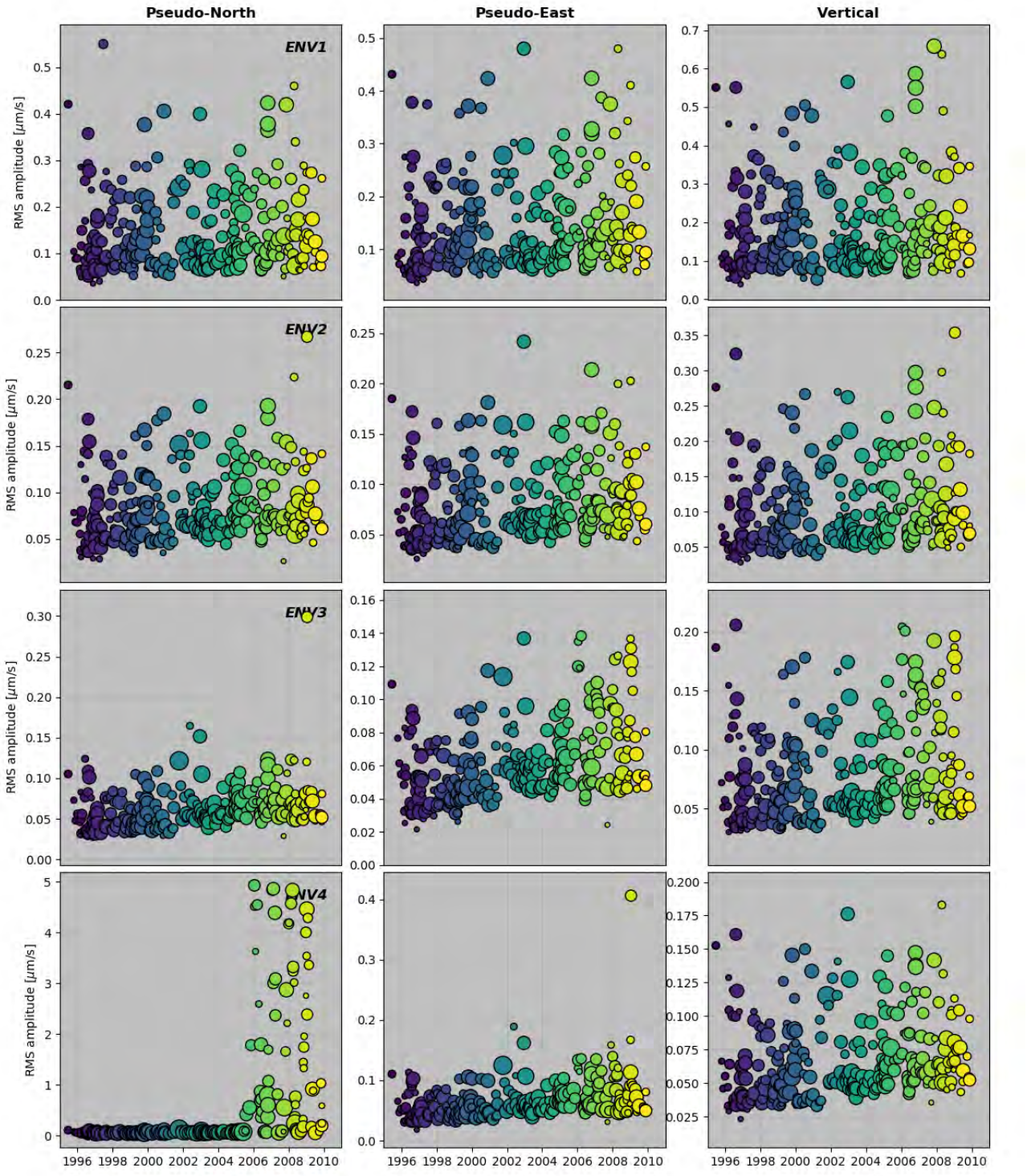

FIGURE B.74: ENV - outliers removed

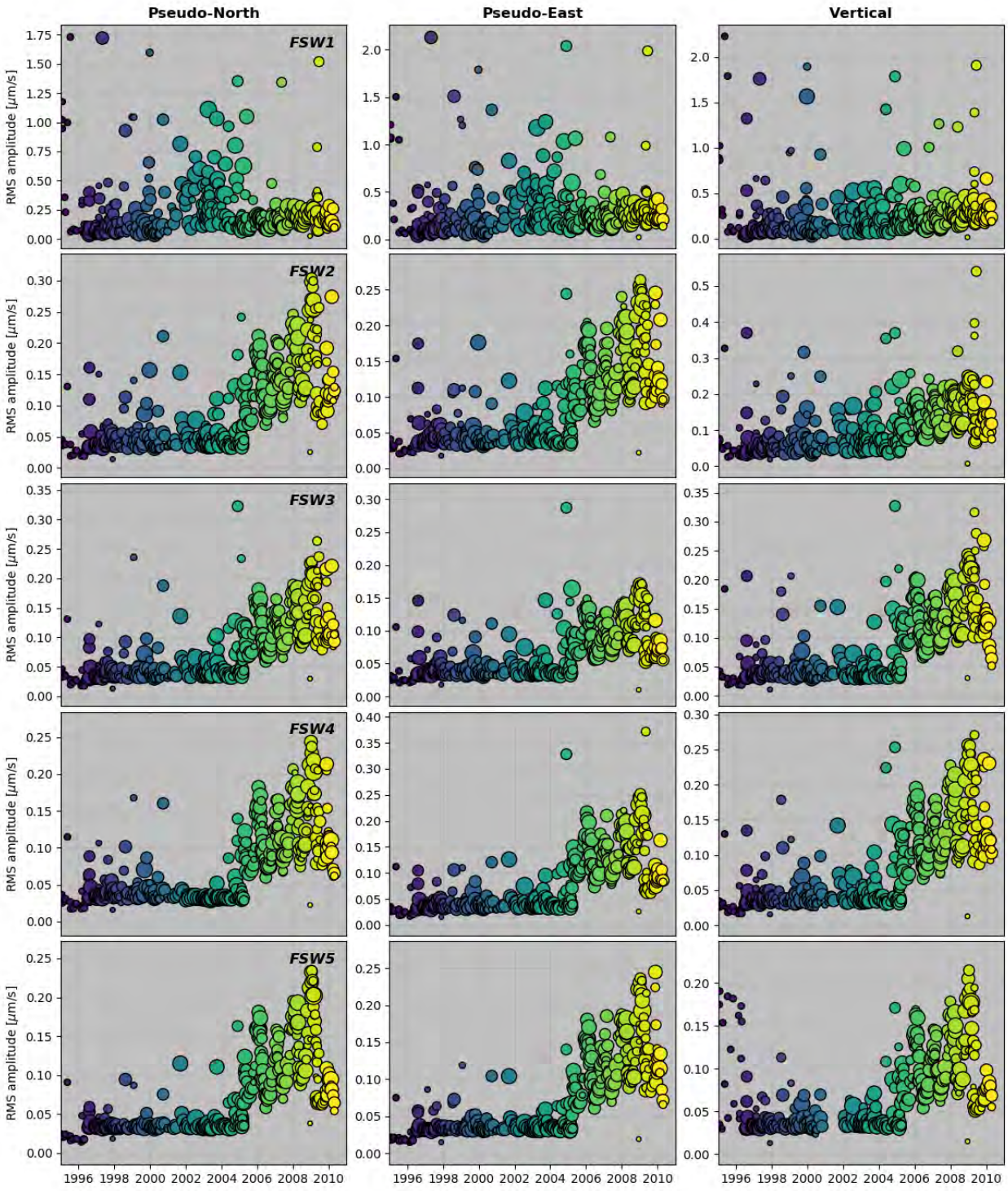

FIGURE B.75: FSW - outliers removed

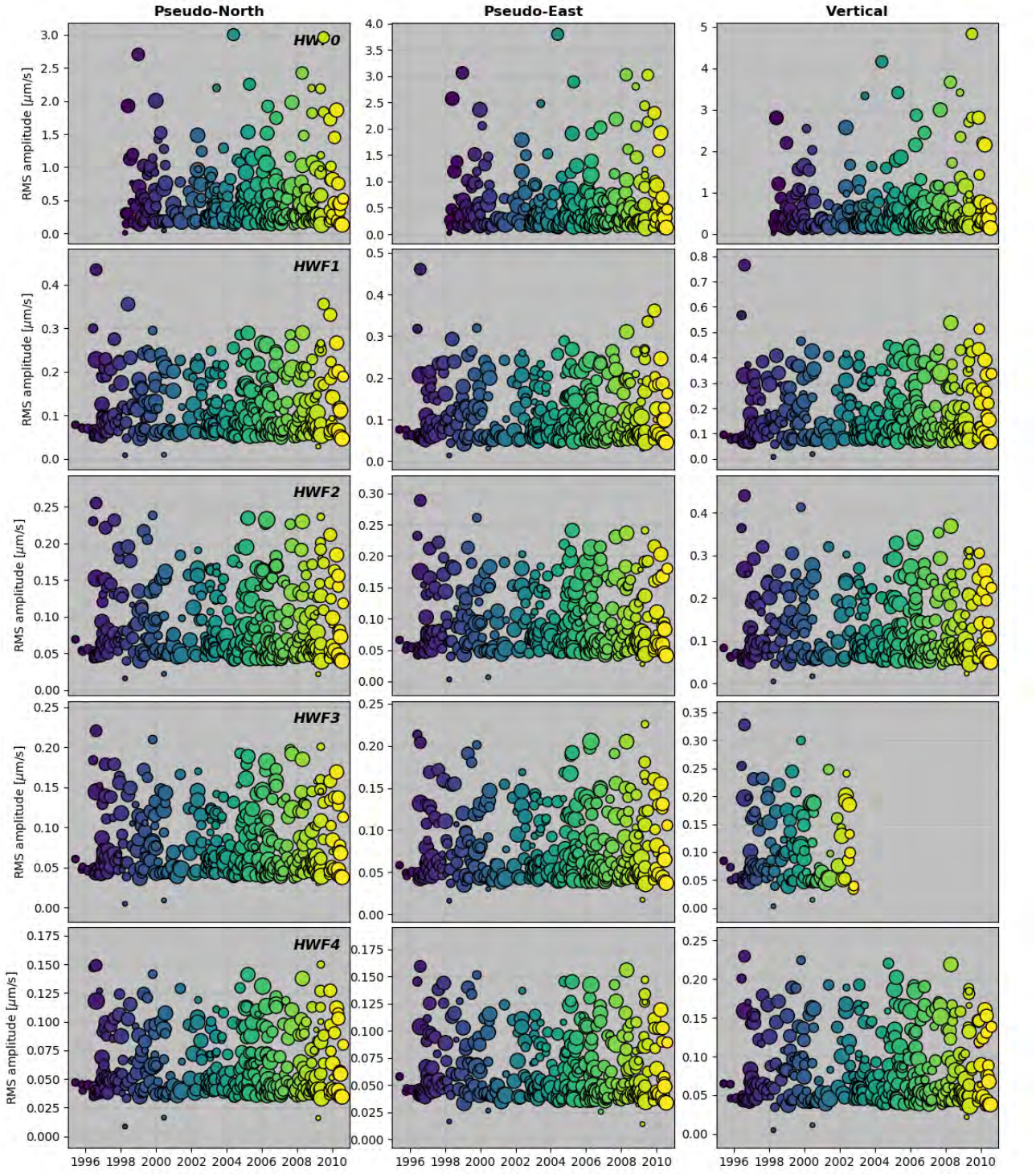

FIGURE B.76: HWF - outliers removed

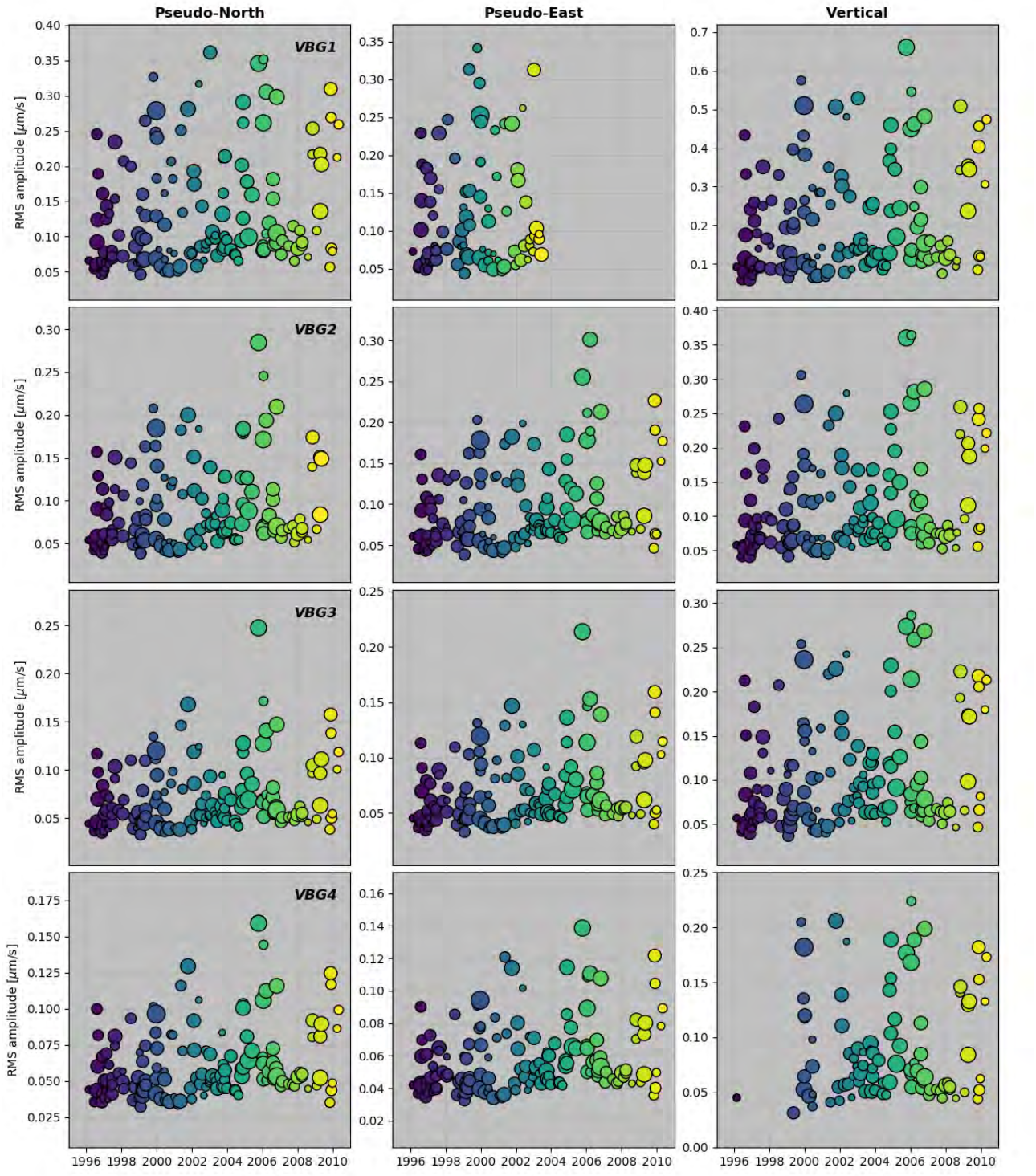

FIGURE B.77: VBG - outliers removed

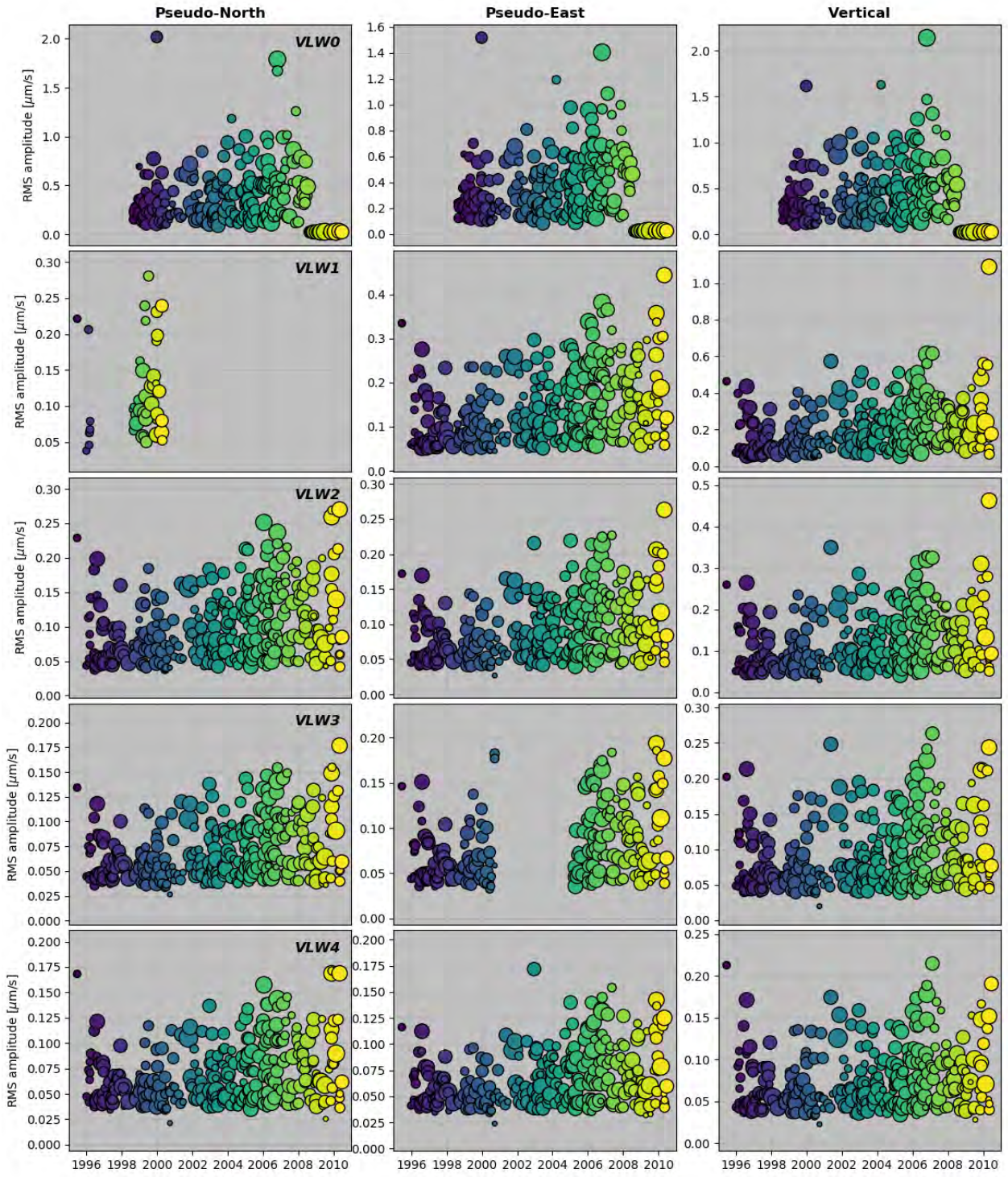

FIGURE B.78: VLW - outliers removed

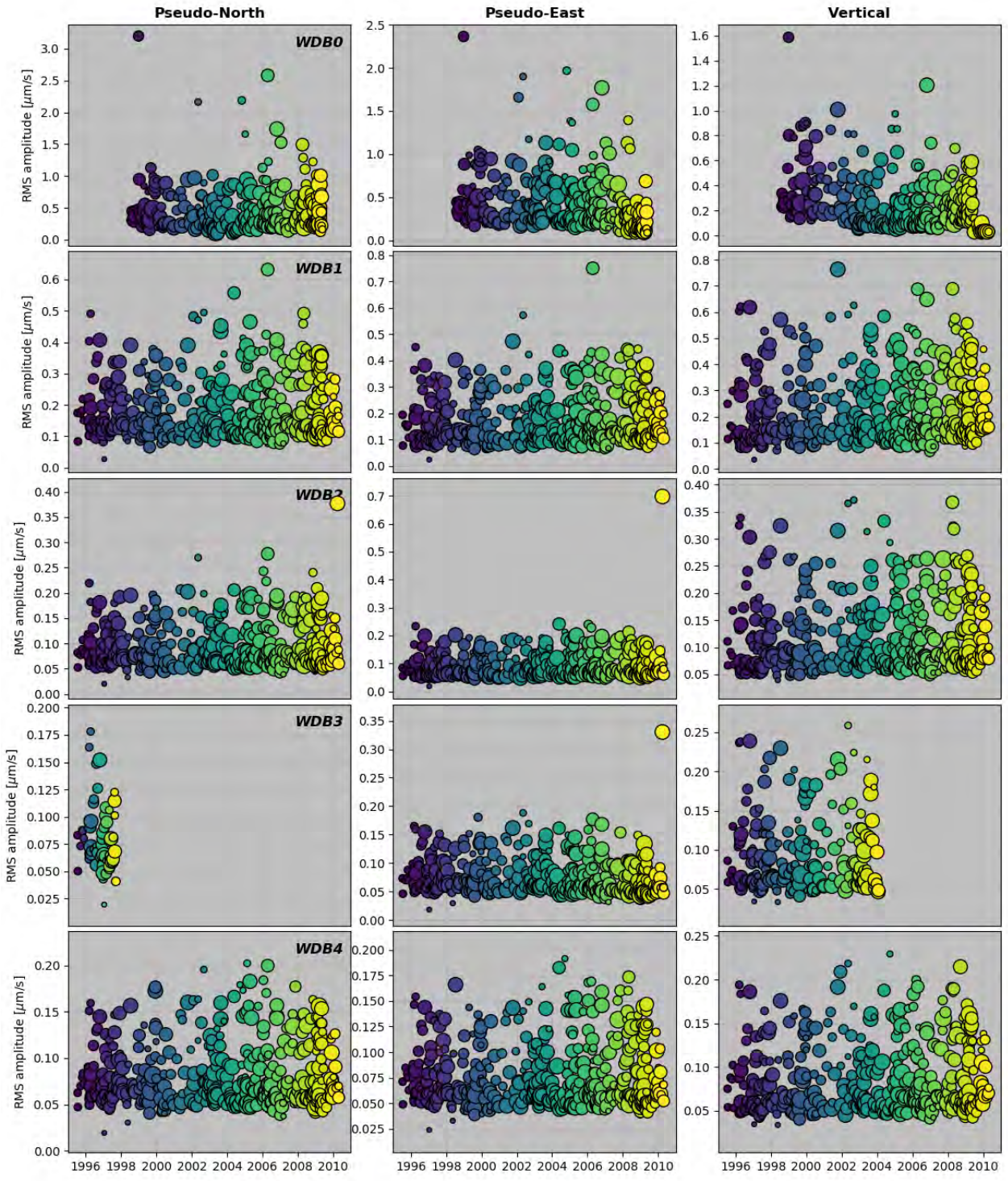

FIGURE B.79: WDB - outliers removed

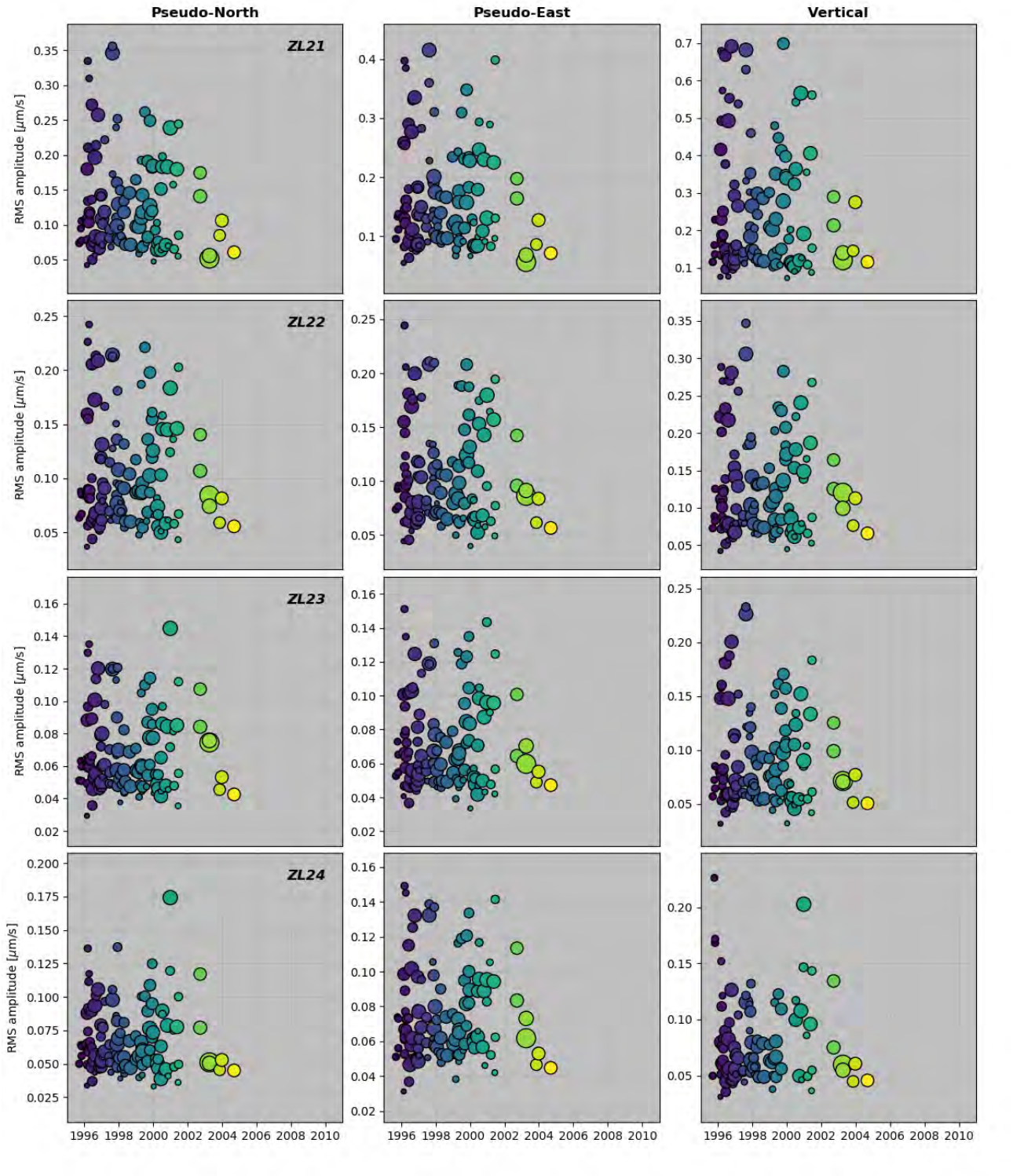

FIGURE B.80: ZL2 - outliers removed

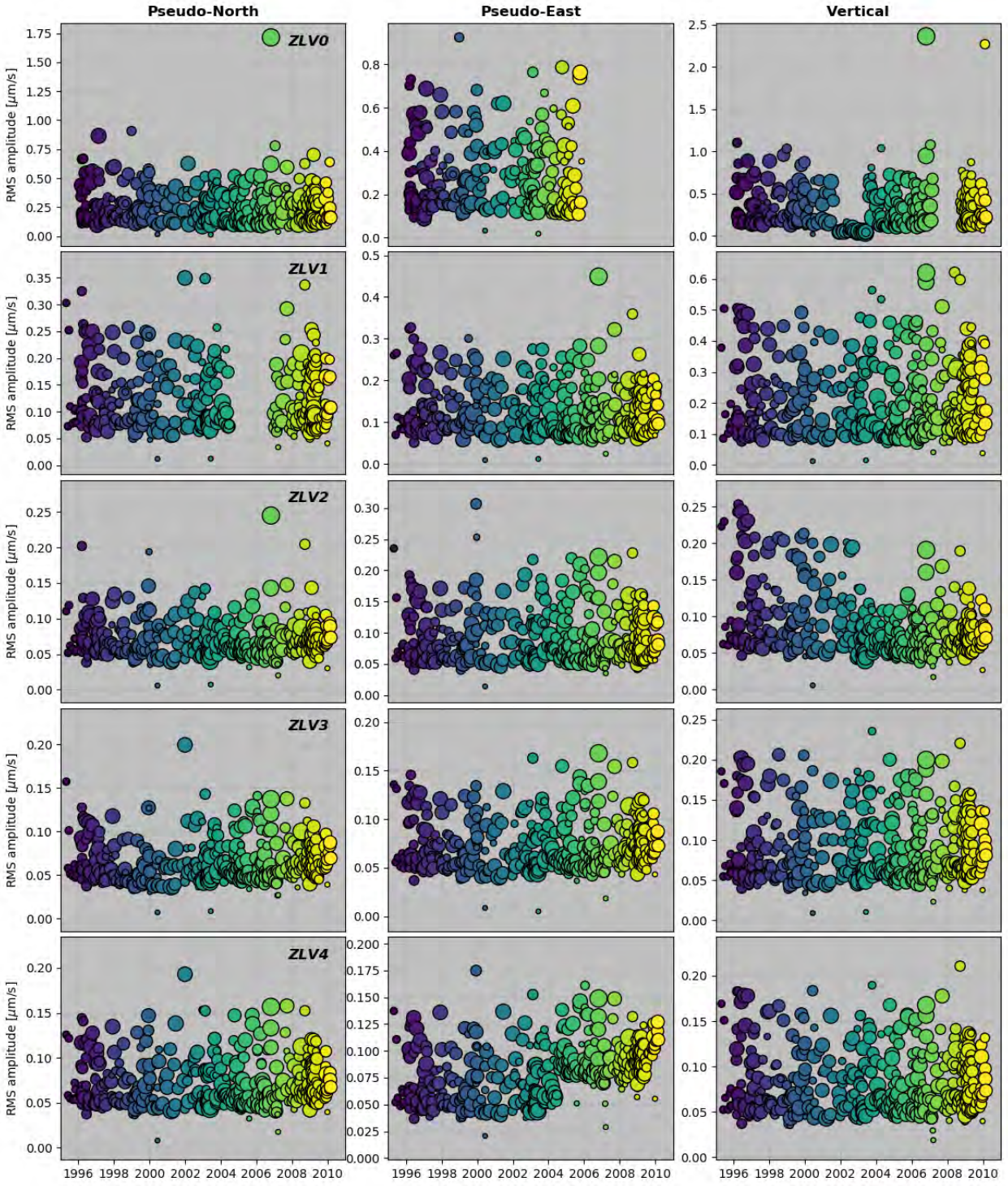

FIGURE B.81: ZLV - outliers removed

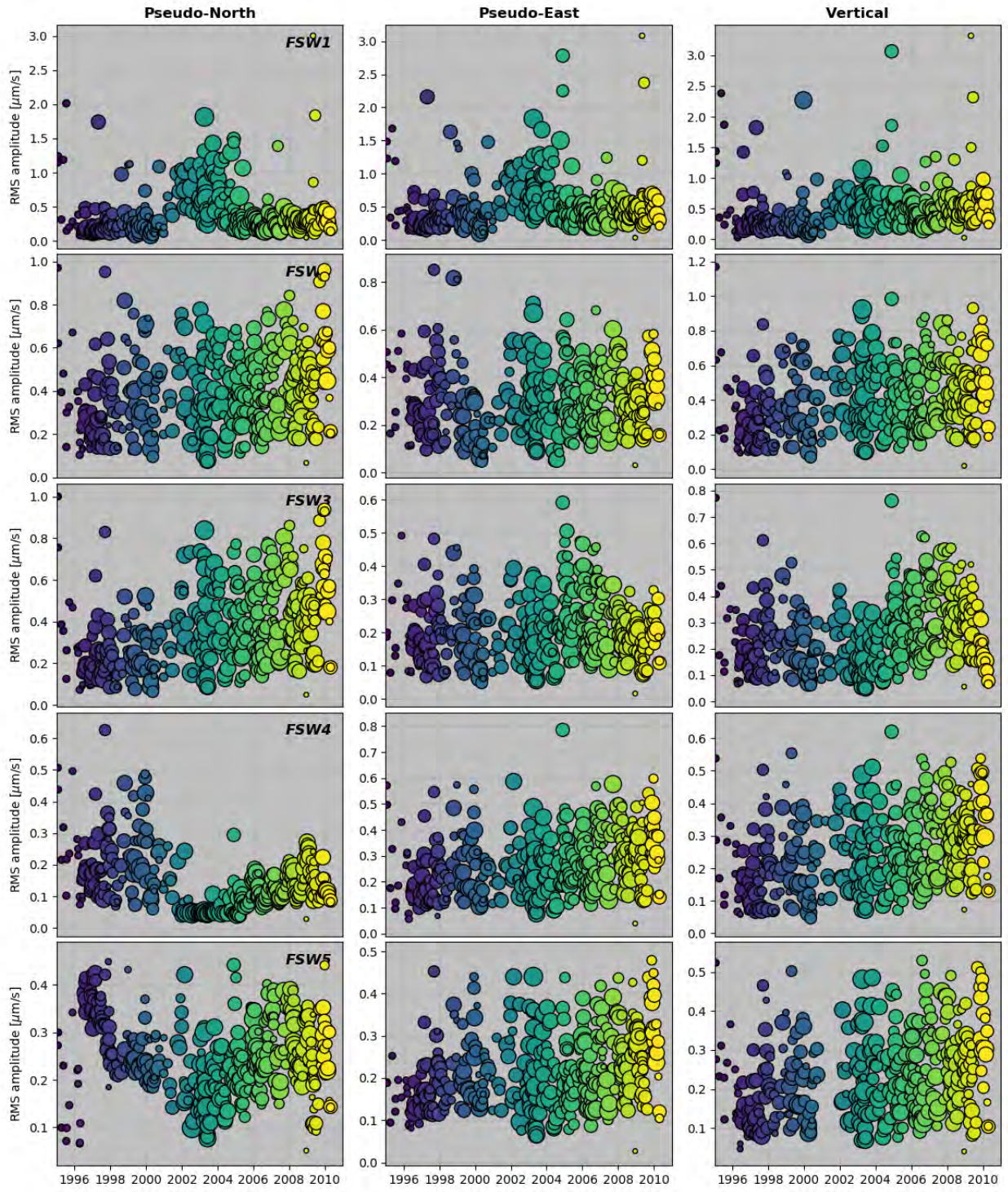

FIGURE B.82: FSW - unfiltered data - outliers removed. To be compared to Fig. B.75.

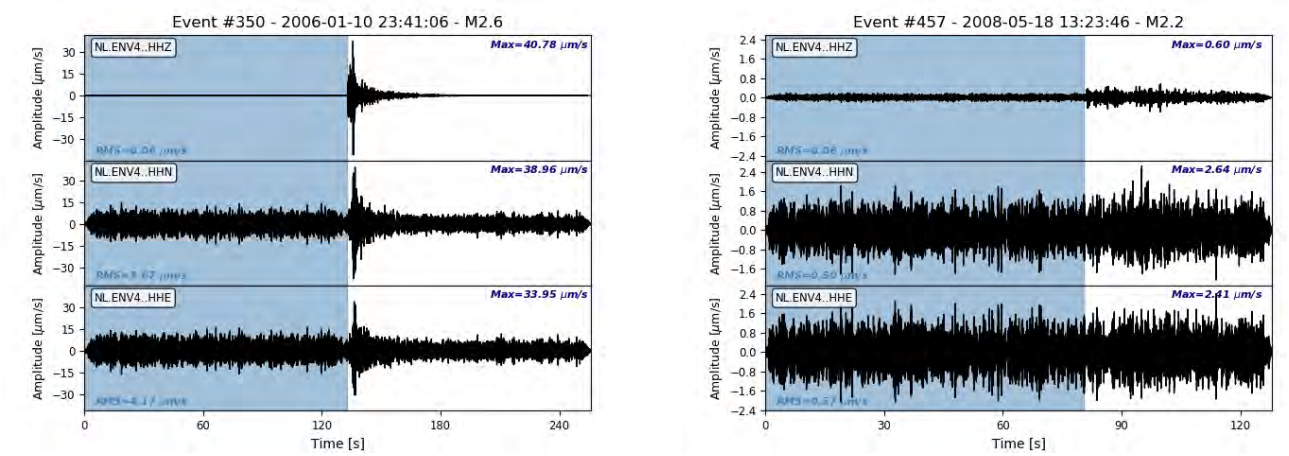

(a) (b)

FIGURE B.83: Two examples of records where the noise level on the horizontal components of ENV4 is significantly higher than on the vertical component. The blue-shaded area represents the window that was used to compute the RMS amplitude.

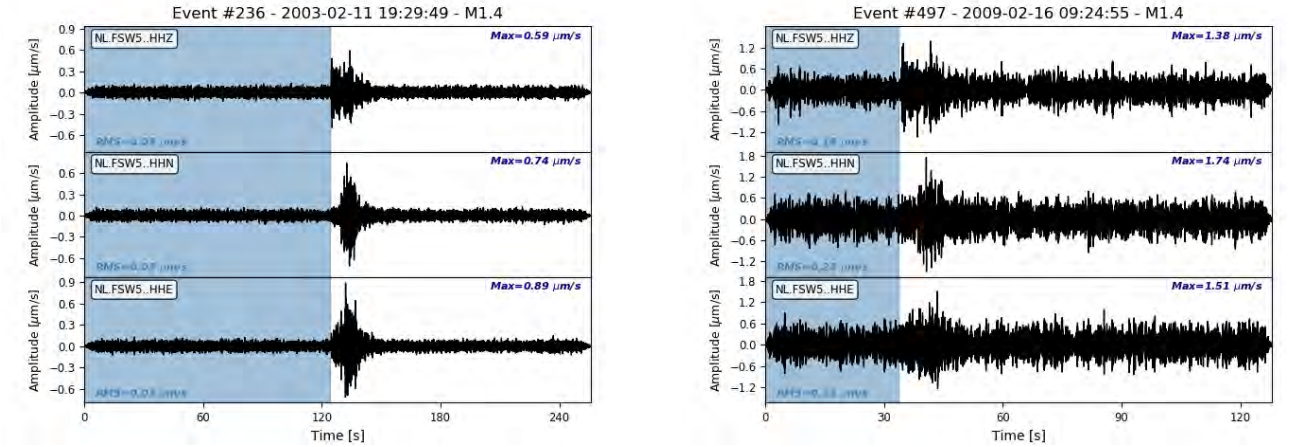

(a) Example of records before 2005 (b) Example of records after 2005

FIGURE B.84: Two examples of records for which the noise level on all components of FSW5 is significantly higher after 2005. The blue-shaded area represents the window that was used to compute the RMS amplitude.

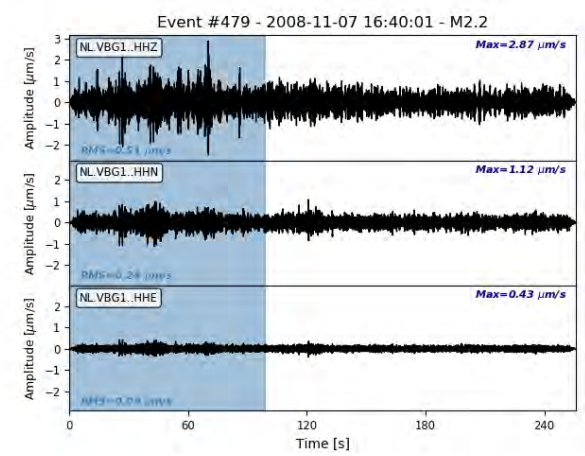

(a) Example of lower amplitude on the East component of VBG1.

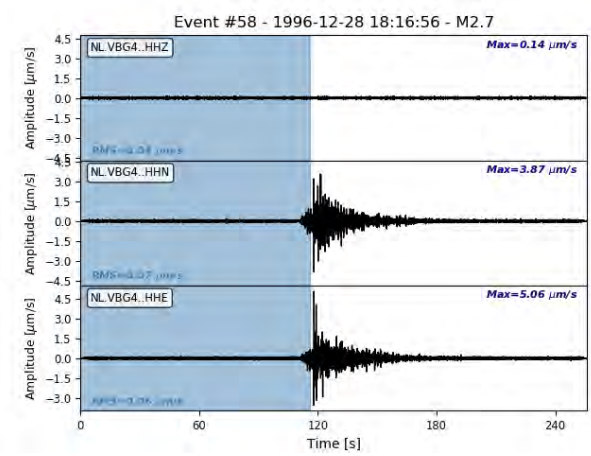

(b) Example of lower amplitude on the vertical component of VBG4.

FIGURE B.85: Blue-shaded areas represent the window used to compute RMS amplitudes.

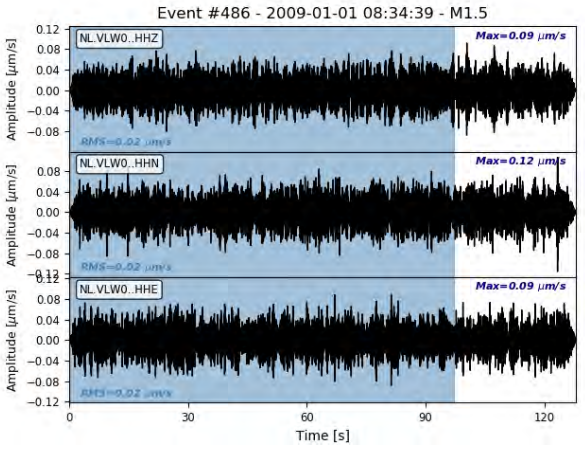

(a) 1st January, 2009 event of VLW0.

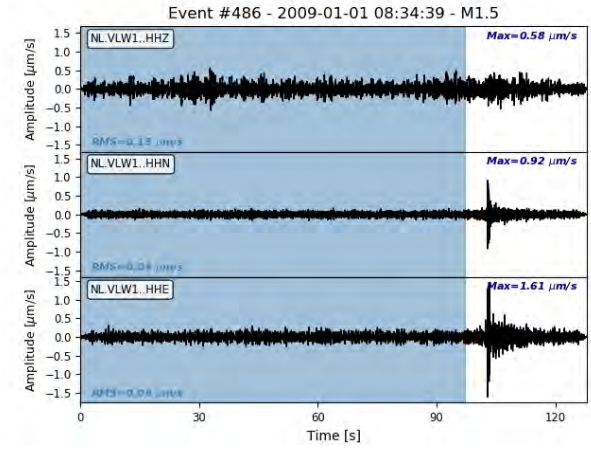

(b) 1st January, 2009 event of VLW1.

FIGURE B.86: Illustration of malfunctioning components of VLW0 as of 2008. Records of the same event on (a) VLW0 and (b) VLW1: the event is not visible on VLW0. Blue-shaded areas represent the window used to compute RMS amplitudes.

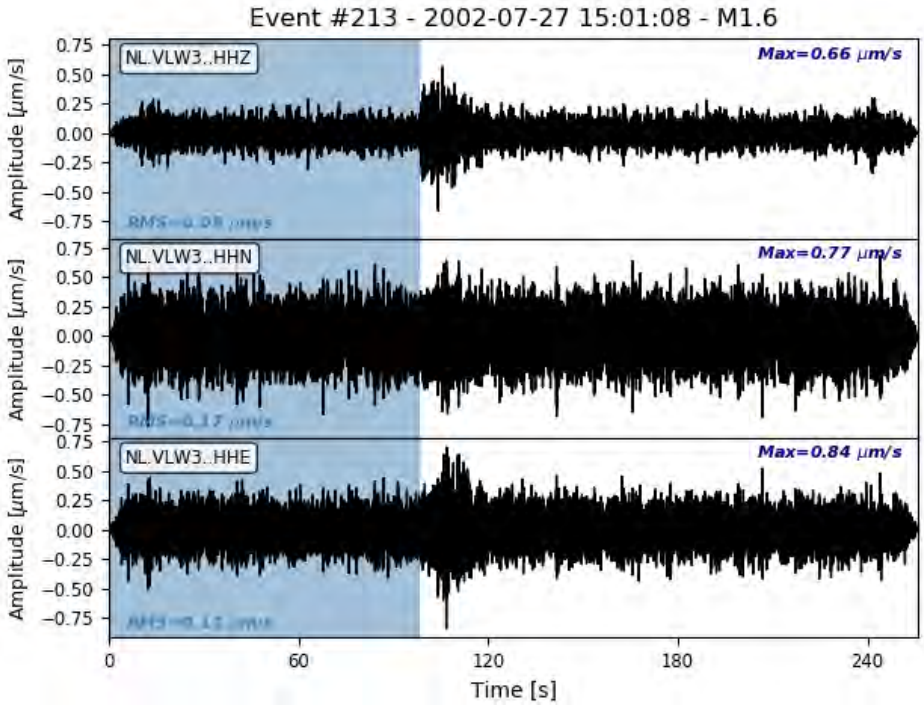

FIGURE B.87: Example of abnormally high amplitudes on the horizontal components of VLW3 in the period 2001-2005. The blue-shaded area represents the window in which the RMS amplitude was measured.

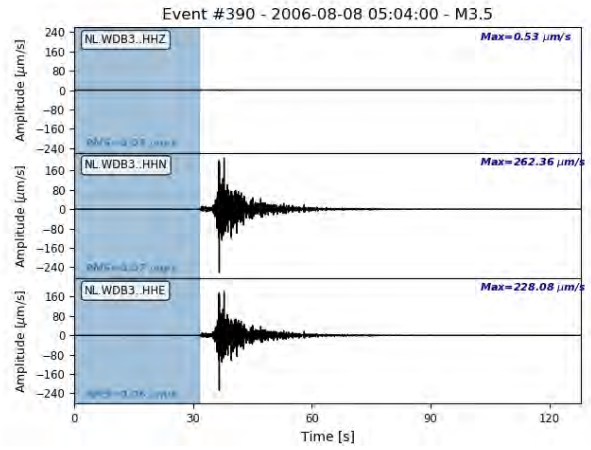

(a) Example of malfunctioning vertical component of WDB3 in 2004.

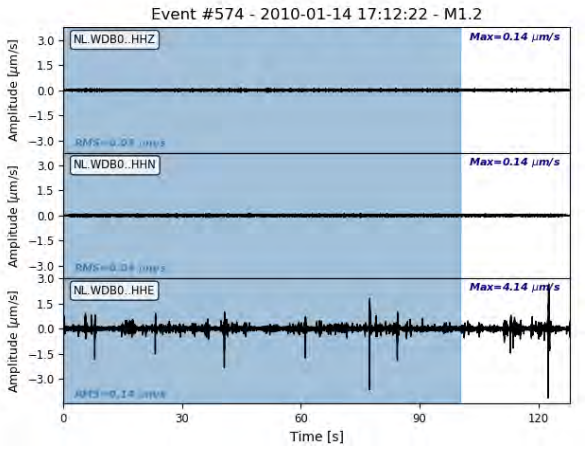

(b) Example of malfunctioning WDB0 sensor in 2010 (all components affected).

FIGURE B.88: Illustration of malfunctioning components of WDB. Blue-shaded areas represent the window used to compute RMS amplitudes.

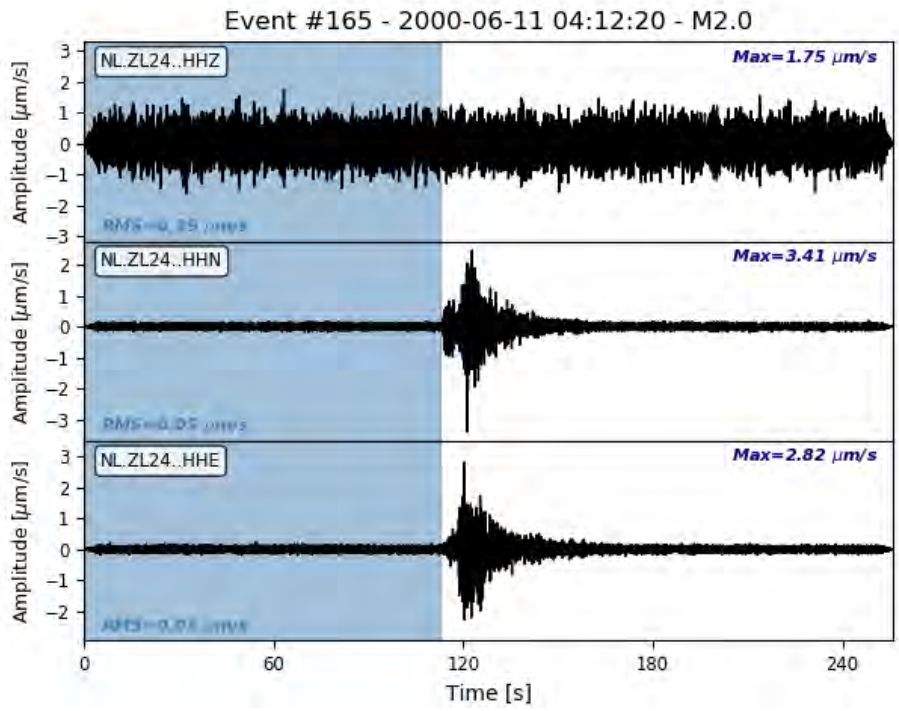

FIGURE B.89: Three-component waveform records of the 11th June, 2000 event on ZL24. The blue-shaded area represents the window in which the RMS amplitude was measured. The vertical component is clearly malfunctioning.

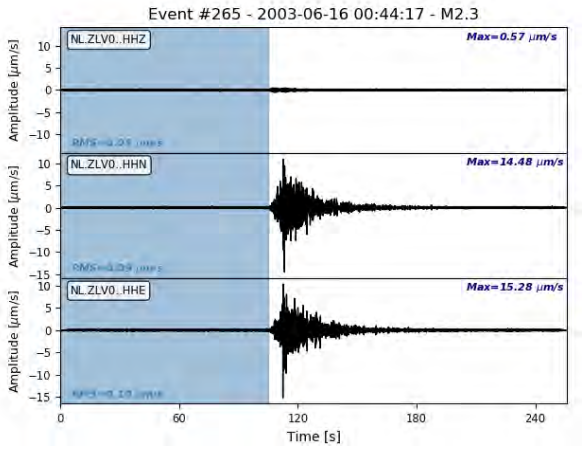

(a) Example of malfunctioning vertical component of ZLV0 in 2003.

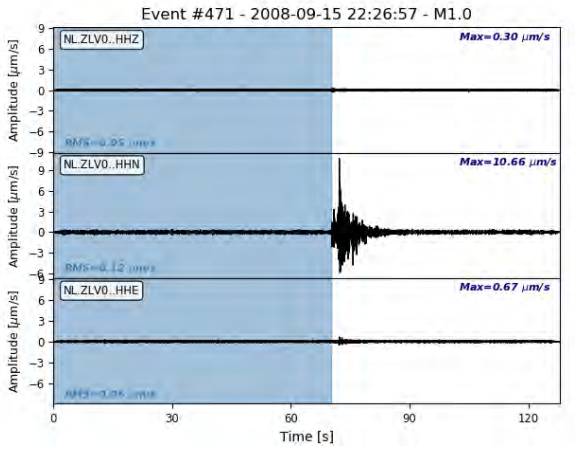

(b) Example of malfunctioning vertical and East components of ZLV0 in 2008.

FIGURE B.90: Illustration of malfunctioning components of WDB. Blue-shaded areas represent the window used to compute RMS amplitudes.

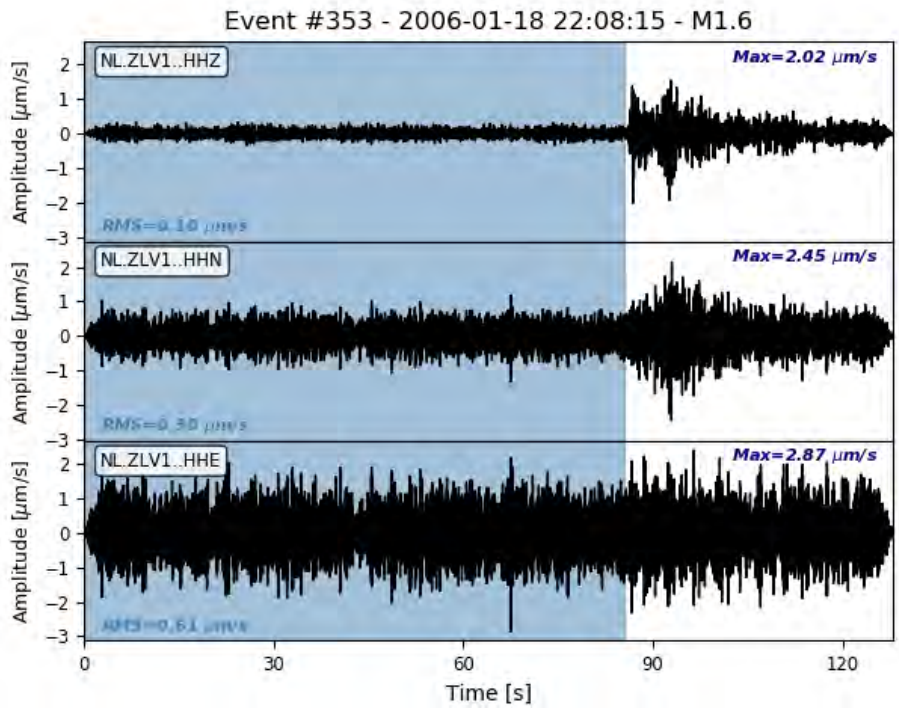

FIGURE B.91: Example of abnormally high amplitudes on the horizontal components of ZLV1 in the period 2005-2007. The blue-shaded area represents the window within which the RMS amplitude has been measured.

B.8 Borehole timing

TABLE B.14: List of 161 borehole records with timing irregularities exceeding one sample. Second and minute flags express the number of samples differing from the theoretical second and minute marks, respectively. The flag on spurious pulses is a boolean indicating whether irregular pulses were detected.

Event time	Station	Second flag	Minute flag	Spurious
1996-02-29 08:07:34	ZLV	7	-8	True
1996-03-06 09:20:50	ZLV	24	25	True
1996-03-12 18:34:12	ZLV	2	-3	True
1996-03-16 04:16:32	ENM	0	119	True
1996-06-07 04:20:56	ENV	0	2	True
1996-06-16 02:53:27	VBG	14	-15	True
1996-08-04 00:42:17	VBG	4	5	True
1996-08-04 00:42:17	HWF	13	-14	True
1996-08-06 13:38:27	HWF	3	-4	True
1996-08-06 13:38:27	ZLV	3	4	True
1996-11-17 04:59:52	ENV	0	2038	True
1996-12-28 00:54:08	ZLV	2	-3	True
1996-12-28 00:54:08	ZL2	48	49	True
1997-01-08 01:20:54	ZL2	3	-4	True
1997-03-08 14:29:04	ZL2	10	-11	True
1997-04-01 00:34:19	HWF	8	-9	True
1997-04-01 00:34:19	FSW	0	2	True
1997-05-04 02:42:39	WDB	19	-20	True
1997-05-04 02:42:39	ZLV	2	-3	True
1997-05-04 04:29:09	WDB	24	25	True
1997-06-19 23:19:25	WDB	6	7	True
1997-06-19 23:19:25	ZL2	3	-4	True
1997-08-18 04:42:28	ENM	0	7199	True
1997-08-18 04:42:28	HWF	44	-45	True
1997-08-18 05:17:32	VBG	-4	3	True
1997-08-23 00:01:56	ZL2	0	239	True
1997-08-23 19:39:35	WDB	0	2	True
1998-02-05 21:11:49	ZLV	2	-3	True

Continued on next page

Event time	Station	Second flag	Minute flag	Spurious
1998-04-19 08:00:12	ZL2	2	3	True
1998-04-19 15:32:35	ZLV	6	-7	True
1998-04-19 15:32:35	ZL2	31	-32	True
1998-04-30 01:08:41	ZLV	2	-3	True
1998-05-30 09:43:15	WDB	0	2	True
1998-07-14 12:12:02	ENV	2	3	True
1998-07-14 12:12:02	WDB	29	-30	True
1998-11-01 17:48:29	ENV	3	-4	True
1999-08-10 23:24:18	WDB	8	9	True
2000-05-16 01:11:14	HWF	3	-4	False
2000-06-09 17:03:47	HWF	3	-4	True
2000-07-06 23:09:56	HWF	4	5	True
2000-07-10 15:05:49	HWF	10	-11	True
2000-07-13 08:41:52	HWF	34	-35	True
2000-09-22 20:52:06	HWF	20	21	True
2000-09-23 03:47:47	HWF	12	13	True
2000-10-25 18:10:34	HWF	26	-27	True
2001-06-21 03:50:49	ENM	0	2	True
2001-08-07 17:09:01	ZLV	-34	87	True
2001-09-09 06:58:12	HWF	9	-10	True
2001-10-10 06:41:09	VBG	6	-7	True
2002-05-22 13:38:13	ENV	0	2	True
2002-08-29 21:13:22	WDB	2	-3	True
2002-08-29 21:13:22	ZLV	0	2	True
2002-09-05 00:00:21	ENV	0	2	True
2002-09-06 06:07:05	WDB	21	-22	True
2003-02-11 19:29:49	VLW	0	2	True
2003-08-20 08:46:14	ENV	-59	62	True
2003-08-20 08:46:14	WDB	8	-9	False
2003-08-25 04:24:55	WDB	11	-12	True
2003-09-22 17:50:11	ENV	31	32	True
2003-09-27 13:57:54	ENM	31	-32	True
2003-10-24 01:52:41	ENM	20	21	True
2003-10-29 14:30:09	WDB	3	-4	True
2003-11-10 02:40:55	ENM	2	-3	True
2003-11-10 02:40:55	ENV	2	-3	True
2003-12-26 10:09:58	ENM	26	-27	True
2003-12-29 13:09:59	ENM	4	-5	True
2004-01-24 13:53:44	ENM	12	13	True
2004-01-30 11:47:40	ENM	2	-3	True
2004-03-21 17:05:44	ENM	18	-19	True
2004-03-26 02:32:45	ENM	34	-35	True
2004-04-30 22:12:43	ENM	56	-57	True
2004-08-21 01:06:32	ENM	5	6	True
2004-08-21 01:06:32	ZLV	1	2	True
2004-08-21 01:06:32	ENV	6	7	True
2004-09-22 12:44:33	ENM	2	-3	False
2004-10-30 11:40:52	FSW	14	-15	True
2004-10-31 17:27:21	ENM	9	-10	True
2004-11-13 12:15:57	ENM	11	-12	True
2004-11-24 18:18:57	ENM	0	2	True
2004-11-25 14:25:54	ENM	2	-3	True
2004-11-25 14:25:54	FSW	2	-3	True
2004-11-26 06:58:01	ENM	2	-3	True
2004-11-26 06:58:01	FSW	5	-6	True
2004-12-16 21:14:30	ENM	3	-4	True
2005-01-17 00:00:55	ZLV	56	1023	False
2005-01-17 00:00:55	FSW	30	-31	True
2005-01-17 00:00:55	WDB	-3	118	True
2005-02-08 13:20:33	FSW	34	35	True
2005-02-16 10:46:17	ENM	19	-20	True
2005-02-16 10:46:17	FSW	37	-38	True
2005-02-18 11:26:29	VLW	0	2	True
2005-02-18 11:26:29	ENM	12	13	True
2005-02-18 11:26:29	FSW	45	46	True
2005-02-18 12:55:46	ENM	17	-18	True
2005-02-18 12:55:46	FSW	54	-55	True
2005-02-18 18:49:25	FSW	16	-17	True
2005-02-18 22:05:52	FSW	16	-17	True
2005-02-18 22:05:52	ENM	2	-3	True
2005-03-08 23:00:58	ENM	22	-23	True
2005-03-08 23:00:58	WDB	-3	118	True
2005-03-10 02:04:39	FSW	3	-4	True
2005-03-21 10:58:33	FSW	42	-43	True
2005-03-21 23:21:19	FSW	4	-5	True
2005-04-02 23:21:08	ENM	15	-16	True
2005-04-02 23:21:08	FSW	36	-37	True
2005-06-22 16:02:02	ENV	20	-21	True

Continued on next page

Event time	Station	Second flag	Minute flag	Spurious
2006-01-02 12:00:45	FSW	4	5	True
2006-01-10 23:41:06	ENV	0	2	True
2006-01-20 20:22:50	FSW	2	-3	True
2006-01-23 11:17:39	FSW	2	-3	True
2006-01-28 03:00:42	FSW	0	2	True
2006-03-04 04:32:33	FSW	2	-3	True
2006-08-26 22:41:18	VBG	13	-14	True
2006-10-15 20:18:00	FSW	2	-3	False
2007-02-04 04:47:35	FSW	0	2	True
2007-02-17 01:41:14	FSW	43	44	True
2007-03-03 06:43:33	FSW	9	10	True
2007-03-21 23:04:36	FSW	35	36	True
2007-06-09 20:07:33	VLW	40	-41	False
2007-06-09 20:07:33	WDB	5	-6	True
2007-06-09 20:07:33	ENM	11	-12	True
2007-06-09 20:07:33	ENV	4	-5	True
2007-06-10 17:27:40	ENV	2	-3	True
2007-06-10 17:27:40	VLW	2	-3	True
2007-06-10 17:27:40	WDB	2	-3	True
2007-06-10 17:27:40	ZLV	3	-4	True
2007-06-23 02:01:45	FSW	0	2	True
2007-11-13 10:26:05	FSW	2	-3	True
2008-04-07 04:32:22	FSW	9	10	True
2008-05-18 13:23:46	FSW	0	2	True
2008-10-29 16:36:21	ENM	2	3	True
2008-10-30 05:54:29	ENM	5	-6	True
2008-11-07 16:40:01	VBG	0	2	True
2008-11-07 16:40:01	FSW	0	2	True
2008-12-15 20:41:17	ENM	5	-6	True
2009-01-01 08:34:39	ENM	7	-8	True
2009-01-01 08:34:39	FSW	2	-3	True
2009-01-01 09:35:46	ENM	10	11	True
2009-01-08 01:17:01	ENM	2	-3	True
2009-01-15 12:41:13	ENM	16	-17	True
2009-01-15 12:41:13	FSW	48	49	True
2009-02-03 06:53:52	FSW	0	2	True
2009-02-04 12:23:50	FSW	49	50	True
2009-02-04 12:23:50	ENM	10	-11	True
2009-02-05 11:56:12	ENM	15	-16	True
2009-02-16 09:24:55	ENM	11	-12	True
2009-02-16 09:24:55	FSW	0	2	True
2009-02-26 03:03:15	FSW	0	2	True
2009-03-13 14:33:32	ENM	40	41	True
2009-03-14 15:32:16	ENV	3	4	True
2009-03-14 15:32:16	ENV	3	4	True
2009-03-27 02:51:28	ENM	20	21	True
2009-03-27 02:51:28	FSW	0	2	True
2009-04-16 17:12:15	ENM	38	-39	True
2009-07-22 00:00:00	FSW	2	3	True
2009-07-22 00:00:00	ZLV	5	-6	True
2009-11-26 12:54:14	ENM	0	2	True
2010-02-17 15:55:01	HWF	15	-16	True
2010-03-04 19:59:57	FSW	39	-40	True
2010-04-03 11:50:56	FSW	26	-27	True
2010-04-25 00:46:00	FSW	2	-3	True
2010-04-25 13:13:17	FSW	27	28	True

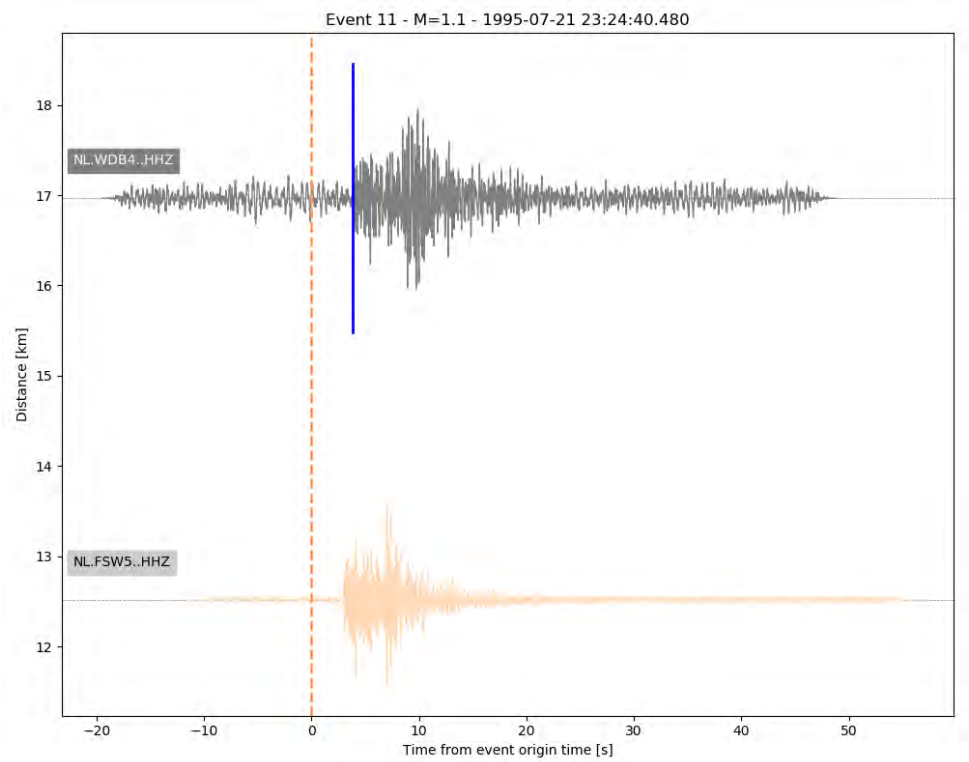

FIGURE B.92: Vertical component waveforms for the 21st July, 1995 event recorded on the 4th borehole level sorted according to the event-station distances. Data have been instrument-corrected and filtered between 2 and 50 Hz. The event origin time is symbolised by the vertical orange dashed line. P-wave arrival times (if available) are plotted as vertical blue bars. Traces are coloured following the colour code described in the text. The DCF signal corresponding to station WDB4 is shown in Fig. 3.17e.

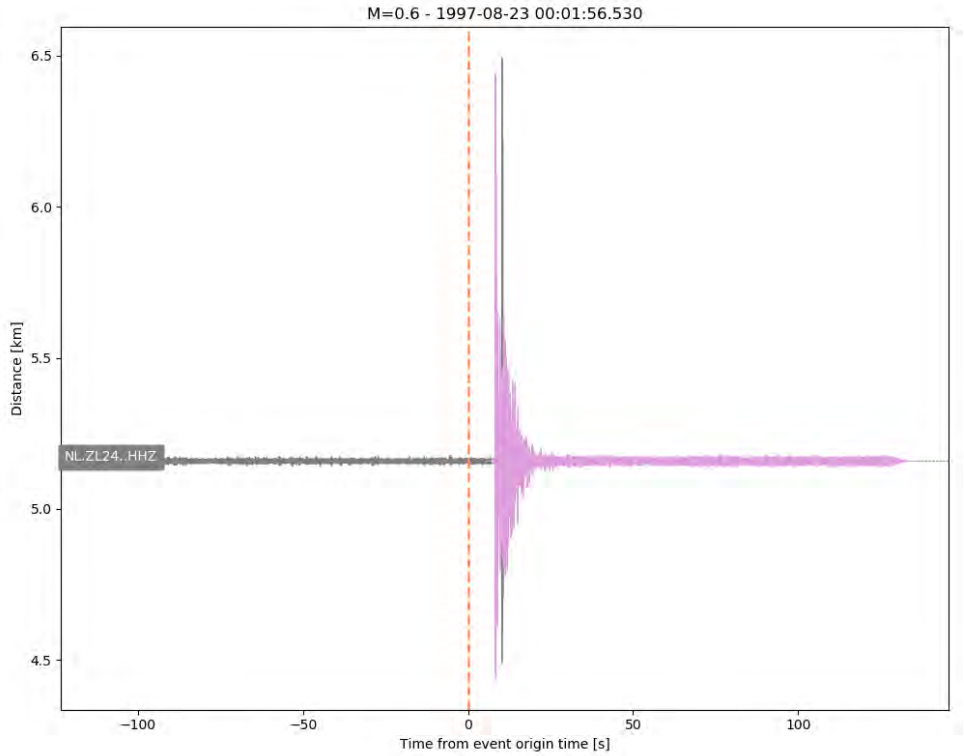

FIGURE B.93: Same as Fig. B.92 for the 23rd August, 1997 event. The DCF signal corresponding to station ZL2 is shown in Fig. 3.17c.

Report Number: 21-002	Confidential: X Unlimited:	External: X Internal:	NORSAR Project No.: 10201
Title:	Quality control for the publication of offline data by KNMI (KEM-11)		
Client:	Staatstoezicht op de Mijnen, Netherlands		
Project manager:	5.1.2.e		
Authors/prepared by:	5.1.2.e		
Submitted to:	Staatstoezicht op de Mijnen, Netherlands		
Contract reference:			
Archive reference:			
Approved by: Project manager: Quality control:	Name: 5.1.2.e 5.1.2.e	Signature: 5.1.2.e 5.1.2.e	Date: 24.10.2022 24.10.2022

NORSAR

info@norsar.no
www.norsar.no